Realisation of the Use of Computational Model as Part of TKA Surgical Planning

by

Willy Theodore

Thesis

Submitted to Flinders University

for the degree of

Doctor of Philosophy

College of Science and Engineering

August 2019

CONTENTS

Summary

Total Knee Arthroplasty (TKA), despite being a highly successful medical operation when measured in terms longevity, has a recurrent problem of patient dissatisfaction and complications in the range of 15-20%. Patient satisfaction is known to be a complex multifactorial issue with factors such as implant component position, pain relief, functionality or stability after surgery, patient expectation, other co-morbidities, experience of healthcare delivery. These factors can be largely grouped into surgical factors, patient factors and patient management factors. With the extensive variation between patients, clinicians need tools to help them triage patients, helping them make decision what resources needed to treat individual patient to achieve the best possible outcome for the patient while minimizing the healthcare cost. Surgical planning is one key aspect that can help clinicians better choose options for surgery.

Joint dynamics has been shown to influence clinical outcomes and is a result of complex interactions between the implant component design, component alignment, and patient specific anatomic characteristics. The relationship between these factors is not well understood and computational modelling is a scalable technique compared to other functional techniques that allow the study of both surgical and patient factors impact on joint dynamics following TKA. A computational model needs to have the right balance between complexity and practicality to be used in clinical setting.

This thesis presented a series of studies towards the development of a low-cost knee computational model that could be used to predict the clinical outcome of TKA on knee dynamics in clinical setting. The first half of this thesis discussed the development and validation technique used for the model. New registration techniques were developed to ensure the definition of reference frames between in-vitro and in-silico environment during validation is consistent. This was often overlooked in previous computational model validation studies. The computational model developed was able to complete a simulation cycle within few minutes while achieving great agreement with experimental data.

The second half of this thesis explored new non-invasive techniques to incorporate subject specific ligament properties into the developed model. Stress radiographs were used as surrogate of the load-displacement response of the knee and ligament properties were optimized to match the response. A wide variation in optimized parameters between subjects and ligaments were seen however its effects to the model dynamics is not yet well understood.

Lastly, this thesis discussed the work involved in realising the use of developed computational model as medical device. The low-cost knee computational model developed in this thesis was successfully registered as medical device and has been used in clinical setting. The model has been used to analyse approximately 1,800 post-operative complications and over 3,000 TKA pre-operative planning. In conclusion, with the right balance between complexity and practicality, it is possible to use computational modelling as part of TKA surgical planning.

Declaration

I certify that this thesis does not incorporate without acknowledgment any material previously submitted for a degree or diploma in any university; and that to the best of my knowledge and belief it does not contain any material previously published or written by another person except where due reference is made in the text.

Signed 

Date 09-Apr-2019

Acknowledgements

Firstly, I would like to express my sincere gratitude to my advisor Prof. Mark Taylor for the continuous support of my PhD study and related research, for his patience, motivation, and immense knowledge. Your guidance helped me to find balance between my competing professional commitments and research work. I could not have imagined having a better advisor and mentor for my PhD study. I would also like to thank Flinders University and its helpful staff for all the guidance and support provided to external research student.

My sincere thanks also go to Brad Miles and Bede O'Connor for the time, ideas and funding that have gone into my PhD work. You have always been there when I need extra motivation to keep me going. Your vision in marrying the academia and commercial reality to improve patient quality of life has led the completion of this PhD and its application in clinical setting.

Thank you to every Orthopaedic surgeon I have ever had the honour of working with and learning from. The clinical insights provided are tremendous to keep this PhD clinically relevant. A special thank you to David Liu, David Dickison, Jonathan Bare, Stephen McMahon, Justin Roe, Brett Fritsch, Michael Solomon, Richard Boyle, David Parker, and Andrew Shimmin. Your willingness to try new ideas and sacrifice time for discussion has been humbling to witness.

Thank you to Scripps Biomechanical lab and Cleveland clinic Biomechanical lab for the support of the experimental studies. Your patience and willingness for back-and-forth iteration is fundamental in setting the ground work for this thesis.

Thank you to all of my colleagues, past and present at 360 Knee Systems and Optimized Ortho throughout the years. Special mentions to Joe Little, Joshua Twiggs, Andy Li, Kevin Wong, Edgar Wakelin, and linda Tran for the insights and encouragements, but also for the hard question which incented me to widen my research from various perspectives.

Last but not the least, I would like to thank my family. Words cannot express how grateful I am to my parents for their mental support. Thank you to my brothers, Andri and Ricky for the constant support.

Introduction

The knee is one of the most complex joints in the body, it has the important function of providing support and mobility during standing and gait. It has a role in almost all daily activities and hence, susceptible to failure particularly degenerative joint diseases like osteoarthritis.

When a knee has lost functionality due to trauma and/or disease, it may require to be managed by means of Total Knee Arthroplasty (TKA). Due to worldwide aging population, the use of TKA has increased steadily every year, especially in individuals younger than 65 years of age [1]. The aim of TKA is to provide substantial relief from pain and functional improvement in patients with arthritis. Although, TKA is considered one of the most successful operations, there are still complications and around 20% of patients are dissatisfied with their outcome. [2]. Furthermore, due to a lack of standardisation and validity of adequate outcome measures, it is difficult to determine which elements before, during and after surgery; and throughout the rehabilitation process affect the outcomes of TKA. However, with the evolution of patient centred care, technological advances in hardware and software, there is an opportunity to combine clinical and biomechanical data collected prior, during and after surgery with computational modelling and data analytics to find patterns or combinations of factors that affect outcomes of TKA. Clinical and biomechanical data include radiography imaging, knee joint assessment, subjective scores, implant geometry used, soft tissue state, patient co-morbidities and mental state. Understanding the combination of these factors may provide insights to improve patient management from surgical planning to rehabilitation programs and, as a consequence, the overall outcome for each individual patient.

This thesis aimed to present a series of studies towards the development of a computational model that intended to be used as part of surgical planning tool to help clinicians triage patient treatments. This includes the development and validation of a patient specific TKA computational model and a

clinical approach to quantify patient specific ligament characteristics that can be incorporated in the model. This thesis will follow the structure outlined below.

Chapter 1: Literature review - presents the literature review of the anatomy, physiology and relevant pathology of the knee joint, the surgical options for intervention and existing computational modelling technique for TKA.

Chapter 2: **Variability in Static Alignment and Kinematics for Kinematically Aligned TKA** – This chapter presents the development of a simplified computational model of the knee replicating a mechanical simulator and its ability to differentiate simulated kinematics between mechanically and kinematically aligned components. This chapter shows the potentials of simplified computational model can be used as part of surgical planning. Kinematic and mechanical alignments captured in this chapter are only used as generalisations of the alignment philosophies the surgeon would normally follow. The aim of this chapter is to show the potential of simplified computational models to differentiate kinematics characteristics of different component alignments. This does not indicate the model is limited to only simulate mechanical and kinematic alignment.

Chapter 3: Accurate Determination of Post-operative 3D Component Positioning in Total Knee Arthroplasty: The AURORA Protocol – Following from chapter 2, it was later realised there was inconsistency in registration technique used to transform the experimental outputs to computational model reference frame in model validation. This chapter describes a new technique to measure post-operative component position from Computed Tomography (CT). The technique developed involves registering both implant and preoperative bone 3D CT segmented models to a postoperative CT reference frame. Doing so allowed for a more accurate definition of component placement in all 3 planes, going beyond what 2D radiography can provide. While not the primary author of this paper, my contribution to the publication includes the conception of the registration technique, development of the step-by-step instructions, designed and supervised the reproducibility study. In addition, I assisted in writing and reviewing the manuscript. I contributed 70% to the research design, 50% on

data collection and 50% of manuscript preparation and review. Permission from the primary author has been provided.

Chapter 4: A Technique for Accurate Kinematic Validation of a Low-cost Subject Specific TKA Model – While previous chapter described registration technique to measure post-operative component placement, this chapter extends the technique to register experimental outputs from a mechanical simulator to the reference frame of a computational model. In the first validation attempt, it was realised that different landmark definition was used to compare the experimental kinematics and simulated kinematics. This was also found in previously published computational validation studies. This chapter presents the application of the registration technique to transform experimental outputs from a mechanical simulator to computational model reference frame which allows identical landmark definition to be used for kinematics comparison.

Chapter 5: Use of Stressed Radiographs to Characterise Multiplanar Knee Laxity – Previous chapter showed validation of a low-cost knee computational model utilising ligament properties reported in literature. The computational model developed was able to distinguish individual specimen kinematic characteristics well in early and mid-flexion but not so well in deep flexion, when the soft tissue envelope is more active. Previous published computational knee models have conducted experimental studies to calibrate subject specific ligament properties. However, the method was invasive and cannot be replicated in clinical setting. This chapter investigates the use of stress radiograph to quantify subject's knee laxity as a surrogate for displacement and applied load data. The subject's knee was stressed at different positions and the laxity was quantified using 3D-2D registration technique.

Chapter 6: **Estimation of Subject Specific Ligament Properties from Non-Invasive Laxity Data -** a novel technique was developed to quantify subject specific ligament parameters from clinical laxity data processed in chapter 5. Using the known position and load from stressed radiographs, an optimization model was developed to derive ligament free length given the boundary conditions from stressed

radiographs. The resultant strains and simulated kinematics were compared between generic and subject specific ligament parameters.

Chapter 7: **General discussion** – The added value and limitations of previous chapters are discussed, and future work is suggested for realising the use of computational model as part of surgical planning.

Chapter 1

Anatomy of the knee

The knee joint is one of the most complex and largest synovial joints in the body (i.e. the joint is enclosed in a fibrous capsule, containing synovial fluid). Although often referred to as a 'ginglymus' (simple hinge) joint, it is in fact a complex multi-condylar joint, with 12 degrees of freedom, including the patellofemoral joint, and two distinct tibiofemoral articulations (both medial and lateral condyles). It is therefore considered to have three 'compartments', and in this sense a 'total' knee replacement may be referred to as a 'tri-compartmental' knee replacement.

The knee is also one of the most heavily loaded joints in the body and this can be attributed to various mechanical factors [3]. Due to its position between the femur and the tibia, the knee is subjected to high contact forces and moments, making it prone to injury. Also, as the knee is a joint with nonconforming surfaces, which accounts for its large range of mobility, and the loads are distributed over relatively small contact areas generating high stresses [3, 4]. Due to the incongruency of the joint, the knee is inherently unstable and relies on the passive contribution of ligaments and the active contribution of muscles for stability [4].

Image removed due to copyright restriction.

Figure 1.1. Sagittal cross-section (left) & posterior view (right) of the knee [5].

Bony Anatomy

The knee joint consists of four bones, the femur, tibia, fibula and patella [4]. The relative position of these bones is shown in Figure 1.1. The femur and tibia articulate together directly (two convex condyles on the distal epiphysis of the femur articulate with the superior surface of the proximal tibial condyles), thus forming the tibiofemoral joint. The patella, also known as the kneecap, is the largest sesamoid bone in the body whose main function is to increase the leverage of moment arm during knee extension [3]. It articulates with the anterior groove of the distal femur forming the patellofemoral joint. The area of the bones where contact occurs is covered with a layer of articular cartilage, a collagen-based soft-tissue which provides impact-damping and reduces joint friction [3, 4].

Menisci

Knee meniscus are crescent shaped pads of load bearing cartilaginous tissue, presents on both tibiofemoral condyles [3]. The main role of the menisci is to protect the articular cartilage from excessive pressure. Most of the direct tibiofemoral contact is eliminated while the surface contact of

the joint is increased thus reducing contact stress. Menisci are also considered as shock-absorbing structures that protect the articular surfaces of the bone [4]. The menisci are located over the lateral and medial condyles of the tibia, connected posteriorly by a transverse ligament, and to both the femur and tibia by additional ligamentous attachments [4].

Synovial Membrane

The articulating region is enclosed by a synovial membrane, containing the synovial fluid which assists in lowering joint friction and providing fluid ingress for nutrient supply to the cartilage [4].

Fibrous Capsule

An extensive fibrous capsule surrounds the entire joint, blending with the surrounding tendons and ligaments, providing additional protection and soft-tissue restraint [4].

Tendons and Ligaments

The patella is embedded within a tendinous link between the tibial tuberosity (on the anterior aspect of the proximal tibia), and the different muscles which form the quadriceps group. The (inferior) tendinous link between the tibia and patella is called the patellar ligament (PL), while the (superior) link between the patella and the quadriceps muscles is the quadriceps tendon (QT) [6]. Embedded within this tendinous link, the patella provides increased leverage for the quadriceps muscles; in deeper flexion angles the quadriceps wraps over the anterior surface of the distal femur (quadriceps 'wrapping') [6]. The patella, articulating in the patellar groove on the anterior aspect of the distal femur, controls the line of action of the quad muscle forces, and by increasing the moment arm, increases the magnitude of the extension moment which the quadriceps can generate at the knee [3, 6].

The knee is stabilised by four main ligaments (Figure 1.1): two cruciates (anterior and posterior) and two collaterals (medial and lateral), abbreviated ACL, PCL, MCL and LCL respectively [6].

The MCL lies somewhat posteriorly on the medial side of the joint and is attached to the medial epicondyle of the femur superiorly and the medial tibial condyle, and medial surface of the tibial shaft. The MCL is composed of two parts: the superficial and the deep portions [6]. LCL is a rounded cord-like ligament on the lateral side of the knee joint. It is attached to the lateral epicondyle of the femur and the fibula [6]. Both collateral ligaments are responsible for the transverse stability of the knee during extension by preventing side to side movements of the tibia and the femur relative to one another. They also prevent lift-off of the femur in varus-valgus tilt [3, 6].

The ACL is attached to the medial aspect of the anterior intercondylar area of the tibia, between the attachment sites of the anterior horns of the lateral and medial menisci. It passes posterosuperiorly and laterally attaches to the lateral condyle of the femur on its posteromedial surface [3, 4]. The PCL is shorter and stronger than the ACL. It is attached to the posterior intercondylar fossa of the tibia posterior to the attachments of the posterior horns of both of the menisci [4]. The PCL passes anterosuperiorly and medially to attach to the anterior aspect of the lateral surface of the medial femoral condyle. The cruciate ligaments are essential ligaments that prevent anterior-posterior displacement of the tibia relative to the femur [4]. They cross one another and form an “X” when viewed from the anterior-posterior and medial-lateral aspects of the knee joint.

Muscle groups

The most notable muscles are those responsible for sagittal-plane knee flexion (the hamstrings: biceps femoris, semimembranosus & semitendinosus) and extension (the quadriceps: rectus femoris and the vastus muscle group: v.mediales v.intermedius and v.laterales) [4]. In reality, there is of course always an interdependence between the role of different muscle groups during different activities, and the full musculature of the lower limb must be considered as a single system for dynamic analysis.

Biomechanics of the Knee

Knee Alignment

Lower limb alignment depends on the exact anatomy of the femur, tibia, hip, knee and ankle and can be illustrated using simple straight lines to represent different joint axes [4]. Since, this analysis is two-dimensional, it allows representation of radiographic alignment seen in the frontal and sagittal planes.

Mechanical and anatomic axes

The mechanical axis of the tibio-femoral joint is defined as the line connecting the centre of the proximal joint to the centre of the distal joint whereas the anatomic axis is defined as the mid-diaphyseal line of that bone [4].

The mechanical axis of the femur is defined by the hip centre and femoral centre. The femoral centre is defined as the deepest point of the intercondylar notch [6, 7]. The femoral anatomic axis intersects the knee joint line generally more medial to the knee joint centre, in the vicinity of the medial tibial spine. When extended proximally, it usually passes through the piriformis fossa just medial to the greater trochanter medial cortex [7]. The angle between the femoral mechanical and anatomic axes is 7°±2° (see Figure 1.2) [8].

On the other hand, the mechanical and anatomic axis of the tibia are nearly the same. They are parallel to each other with the anatomic axis is normally a few millimetres medial to the mechanical axis [7]. The mechanical axis is defined by a line that connects centre of tibia spine to ankle centre (Figure 1.3). Ankle centre is usually defined as the midpoint of the medial and lateral malleolus, which are the medial and lateral most prominence points on the ankle [7].

Image removed due to copyright restriction.

Figure 1.2. Mechanical and anatomic axis of femur [7].

Image removed due to copyright restriction.

Figure 1.3. Mechanical and anatomic axis of tibia [7].

Malalignment

Ideal alignment refers to colinearity of the three points, three points, the hip centre, the femoral centre and the ankle center. Thus, malalignment refers to the loss of colinearity of the hip, knee and ankle in the frontal plane outside the native range. The native range is typically 4±4° with male tending to be in varus while female are in valgus [9]. Varus deformity can be caused by tibial varus deformity,

femoral varus deformity, lateral joint laxity and/or loss of medial cartilage and depressed medial tibial plateau. Similarly, valgus deformity can be caused by tibial or femoral valgus deformity, medial joint laxity and/or loss of lateral cartilage and depressed lateral tibia plateau (Figure 1.4).

Image removed due to copyright restriction.

Figure 1.4. (a) Varus deformity. Depressed medial tibial plateau. (b) Valgus deformity. Depressed lateral tibial plateau (from [7]).

Mechanical alignment (MA) is one of the most common implant positioning target for total knee arthroplasty (TKA). Its primary aim of is to restore the mechanical axis of the limb to neutral (within a ±3° range) as it is believed to be the most important factor for the durability of the implant. However, a number of patients may indeed exist for whom their native anatomy is not neutral. For instance, patients with so called “constitutional varus“ knees have always had varus alignment since reaching skeletal maturity. Bellemans et al [10] studied a cohort of 250 asymptomatic adult volunteers between 20 and 27 years old. They found as high as 32% of males and 17% of females had constitutional varus

knees with a natural mechanical alignment more than or equal to 3° varus. This shows the variability in natural alignment exists amongst individuals. Therefore, one should question that zero-degree mechanical alignment should be the goal in every patient undergoing TKA.

Motion of the Tibio-femoral joint

Due to the configuration and interaction of the three knee joint bones (femur, tibia and patella), the knee joint can potentially have twelve degrees-of freedom (DOF), 6 DOF from tibio-femoral joint and 6 DOF from patella-femoral joint. In this section, motion of tibio-femoral joint will be discussed. Flexion-extension (F-E) is by far the most visually apparent rotational motion; however considerable internal-external (I-E) and varus-valgus (V-V) rotation are also possible. The translational motions are less apparent, although several millimetres of anterior-posterior (A-P) and medial-lateral (M-L) displacement are possible, and condylar 'lift-off' may result in slight compression-distraction (C-D) displacements. A number of specific issues related to knee kinematics are briefly outlined below:

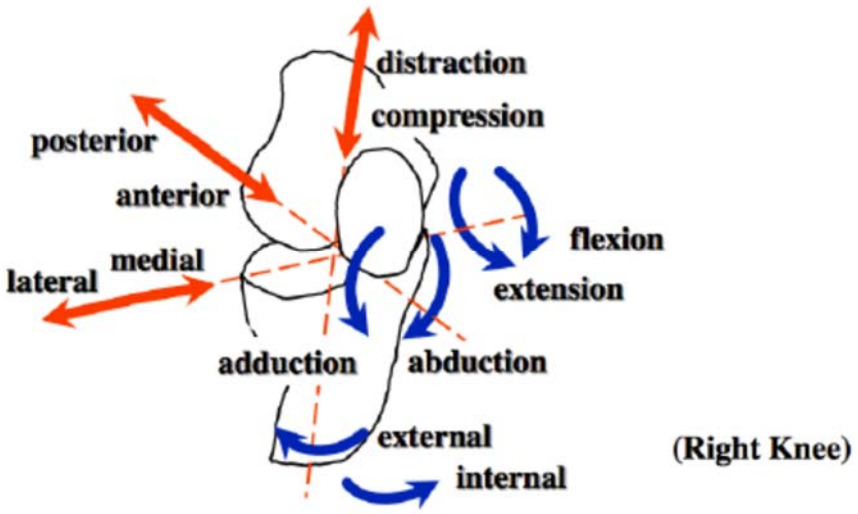

Figure 1.5. Six degrees of freedom of the knee.

Range of Motion of the Knee

Due to inter-patient variability, it is difficult to define a 'typical' range of motion (ROM) for the knee joint. In addition, magnitude of the loads applied to the knee affect the degree of motion of the knee.

Consequently, this has led to a distinction being made between the 'active' and 'passive' ROM (abbreviated AROM and PROM respectively) - i.e. whether the motion is made under the subject's own muscle action, or whether external manipulation is used to achieve the motion. Clinically, AROM is reported to be on average ~130°, decreasing with age. PROM is higher, typically ~160°, again decreasing with age [11, 12]. Flexion angles over 90°, and especially those beyond 120°, are often referred to as 'deep flexion' (not required for general ambulatory activities, but required for some kneeling & squatting everyday activities, such as gardening, domestic cleaning or kneeling prayer). Facilitating this 'deep flexion' ROM is a key goal for TKA designs.

Knee Locking and Screw Home Mechanism

There are several effects combined to improve the stability of the knee whilst stationary. The distal radius of the femoral condyle is larger than the posterior radius, thus increasing conformity in full flexion. For normal subjects, the line of action of body-weight is slightly anterior to the tibiofemoral contact when in full knee extension, tending to maintain the knee in extension. This is accompanied by an internal rotation of the femur relative to the tibia, causing the surrounding soft tissues to tighten, resulting in a higher degree of stability. This 'locked' stance state is released when the popliteal muscle contracts, causing the femur to rotate externally relative to the tibia and so reducing the soft tissue constraint prior to the knee flexing (see Figure 1.6) [13]. This mechanism for increasing stability in full extension is often referred to as the 'screw home' effect [14].

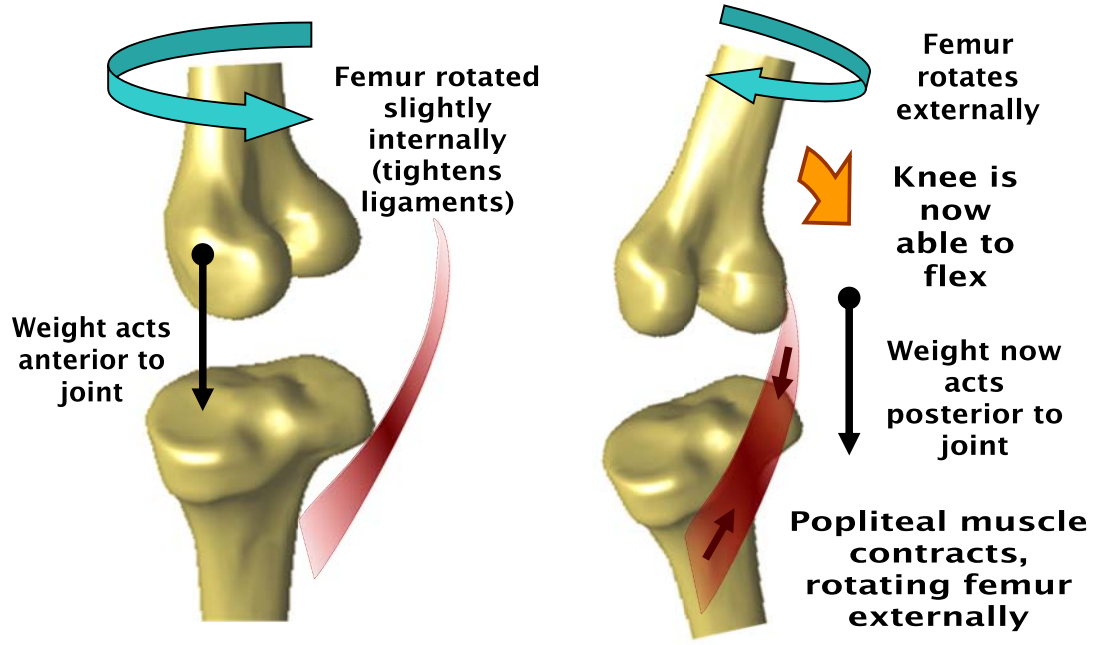

Figure 1.6. (Left) Knee is locked in screw home position and is released in flexion (Right).

Femoral Rollback

Femoral rollback is defined as posterior movement of the femur relative to the tibia as the knee flexes (Figure 1.7). Both the femoral axis of rotation and the tibiofemoral contact point are predicted to move posteriorly as flexion increases, according to these simple rigid-linkage predictions. The concept became the subject of some debate within the orthopaedic research community, with studies both confirming and refuting the femoral rollback phenomenon. However, recent fluoroscopy studies have shown that the medial condyle hardly moves posteriorly whereas the lateral condyle moved backwards by rolling and sliding [15]. Another fluoroscopy study [16] revealed that the rollback during active loading (i.e. when the knee is subject to large muscle loads during daily activities) is much more variable [17]. Finally, it is important to distinguish between the movement of the two bones (defined by hard anatomical landmarks), and the movement of the contact point between the bones; it is possible to have 'paradoxical' motion of the contact point relative to the motion of the two bones [19, 20].

Image removed due to copyright restriction.

Figure 1.7. simple 2-D representation of femoral rollback concept [21].

Medial Pivot

It is widely reported that the femur tends to rotate externally as the knee flexes (i.e. the tibia rotates internally relative to the femur) [22]. This, coupled with the hypothesised posterior motion of the femur during femoral rollback, would result in a combination of rotation and translation about the long axis of the bones, which could equivalently be represented by a single rotation (with no corresponding translation) about a 'virtual' pivot point shifted towards the medial condyle (see Figure 1.8). Note that the 'medial pivot' concept is dependent upon the 'femoral rollback' assumption, and so the caveats associated with that concept apply equally to the medial pivot hypothesis. If paradoxical motion occurs, the virtual pivot will not be medially-shifted. Once again, inter-subject variability is considerable, and there is no single 'correct' description of the medial pivot effect; however it is widely reported within the literature [22]. A recent cadaver study by Victor et al [23] reported that medial pivot behaviour is clearly seen under passive loading conditions but minimised as the knee is loaded during squatting motion. This suggests that medial pivot behaviour is driven by the morphology of the tibia and femoral condyle [23, 24].

Moreover, characteristics of knee motion can change dramatically depending on the axes used to describe them [25, 26]. For example, Li et al [26] studied knee kinematics characteristics during step-up activity using fluoroscopic imaging. They described the knee motion using three definitions (Transepicondylar axis, geometric centre axis, and condylar contact points). They found kinematics reported using Transepicondylar axis and condylar contact points projections was similar. However, when geometric centre axis was used, the femoral condyle motion pattern was dramatically different. The lateral condyle shifted posteriorly throughout the step-up activity instead of shifting anteriorly when described with other 2 definitions.

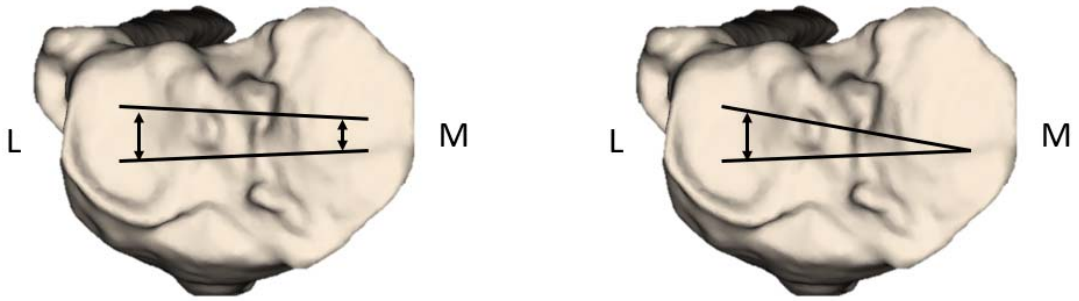

Figure 1.8. The medial pivot concept. (Left) Femur rotates and translates relative to tibia as knee flexes. (Right) Femur pivot at tibia medial plateau center as knee flexes.

Reference to Describe Knee Motion

The multiple degrees of freedom and complex motions at the knee mean that kinematics can be complex, so kinematics must be defined clearly and reported consistently to avoid ambiguity or confusion. An important and widely-adopted method was proposed by Grood & Suntay [27]. In this cylindrical-axis co-ordinate system, the sequence in which the different rotations and translations are applied does not alter the final position & orientation (i.e. the system is sequence-independent; this is an important advantage over e.g. the Euler co-ordinate system); see Figure 1.9 . The femur and tibia are considered as two cylinders with their own axes. These two cylinders is linked by a perpendicular

axis, referred to as floating axis. This floating axis is used to calculate the coronal alignment of the leg and is dependent on the position of the femur relative to the tibia.

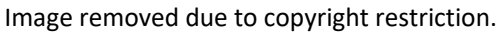

Figure 1.9. Grood and Suntay coordinate system [27].

Kinematics VS Kinetics

For common activities of daily living (ADL) types, knee mechanics can be recorded or estimated by various methods, including clinical motion analysis using video recording (or, more recently, fluoroscopy studies – e.g. ([28]) & force plates (for external joint reaction forces), coupled with optimization algorithms (based on inverse dynamics methods) and/or EMG data (for internal joint contact forces). Rarely, more 'invasive' assessment methods have also been used; e.g. markers with traction pins were fixed directly into the bone.

Often-cited examples of these studies are the early work by Morrison [29] for ambulatory gait, and Andriacchi et al [30] for stair climbing. More recently, telemetric measurements using prosthetics with embedded sensors have provided direct in-vivo data to compare with the theoretical results of earlier investigators; first for the hip joint (as pioneered in the early 1990's by Bergmann et al [31], and

subsequently for the knee, since the late 1990's (notably studies by Taylor et al [32, 33] for a distal femoral implant, Kaufman et al [34], Kutzner et al [35] and most recently D'Lima et al [36, 37] for an instrumented tibial tray).

Before the mechanics of gait are discussed, it is important to distinguish the concept of kinematics and kinetics. Kinematics is a study of geometry motion. It describes the bodies' motion without reference to the forces (the cause of motion or generated due to the motion). Meanwhile, kinetics is a study of the relationship between the motions of the bodies and its causes (forces and torques). For example, the flexion at the knee is the most apparent kinematics feature whereas the forces introduced by the extensor mechanism to flex the knee is part of the kinetics. Kinematics and kinetics of tibio-femoral joint will be discussed in this section.

In addition, in kinetics it is important to make a clear distinction between the internal forces acting between the contacting joint condylar surfaces (often termed joint contact force, or JCF), and the external resultant forces experienced by the whole limb segments (termed joint reaction force, or JRF). By necessity of Newtonian mechanics, the static magnitude of the external JRF will be of the same order as the subject's bodyweight (BW), (although dynamic external forces can exceed 1BW due to accelerating/decelerating forces in locomotion). The internal JCF can be much higher however even under static conditions (often several times BW), since antagonistic muscular co-contraction (necessary to stabilise the joint) are considerable. Internal joint forces include ligament force and patellar force. The patella bone acts as the level arm of the knee extensor mechanism and the force exerted on patella is described as the resultant force of quadriceps and patellar tendon force [21]. Flexion of the knee increases patellar force. Therefore, the joint reaction force that opposes the patellar force increases with knee flexion and can reach up to seven to eight times of body weight in high load activity such as squatting [21, 38]. On the other hand, ligament force acts as stabilizer for the knee to balance against the external resultant forces [39]. Direct measurements of ligament forces in human tissue is currently impracticable [39]. Typically, studies of ligament forces are calculated

using computer and mathematical model [39, 40]. The ligament forces are calculated as summation of internal joint forces needed to oppose external joint reaction force [39]. The soft tissue mechanics that affects ligament force are described in the next few sections. To summarise, the muscles and ligaments work together to create a summation of knee internal joint forces that opposes the external joint reaction force.

Mechanics of Normal Gait

Walking/gait is the most prevalent activity of daily living (ADL). Consequently, the analysis of gait has received considerable attention in the literature and therefore the mechanics of normal gait will be discussed further in this section.

Knee flexion

Knee flexion/extension during gait is the most apparent kinematic feature of this joint. Briefly, during initial contact the knee joint is flexed at around 10°; the next step in the gait cycle is termed "loading response" which occurs roughly during the first 15% of the gait cycle, where the knee further flexions around 20°; between 15% and 40% of the gait cycle is the mid-stance period where the knee extends to around 10° flexion; roughly between 40% and 60% of the gait cycle is terminal stance and pre-swing where the knee starts flexing in preparation for the swing phase of gait; at around 60% occurs toe-off and the swing phase of gait starts; in mid-swing, the knee reaches maximum peak flexion of around 60° aiding towards toe clearance, after which the knee starts extending in preparation for initial contact [41]. Figure 1.10 shows a typical knee flexion/extension signal.

Image removed due to copyright restriction.

Figure 1.10. Typical knee flexion in normal gait [42].

Joint Contact Force

Since 1970, researchers have used gait analysis and mathematical models to estimate the contact forces during gait. Morrison et al [29] calculated the joint contact forces of gait of 2 – 4 BW while other studies reported up to 3BW [43] and up to 7BW [44]. This variation could be due to differences in the mathematical model used in the calculation. To overcome this uncertainties, telemeterised implants were developed to measure the joint contact forces in vivo. Recent studies by Kutzner et al [35], they reported peak forces in gait of 261% BW Figure 1.11 which were smaller than those determined analytically.

During gait, the lower limb alternately supports the weight of the body. At first approximation, the knee should bear a high load in stance phase and a low load in the swing phase. Loading in swing phase is not 'zero' due to the passive restrained provided by soft tissues and antagonistic muscle action. Antagonistic co-contraction of the muscles around the knee means that JCFs are higher than corresponding JRFs. Table 1.1 shows the peak joint contact force and internal-external torque for different activities from a telemeterised implants study [35]. It is important to note that one of the main limitations with telemeterised implants is that they only measure axial force or a joint force

without discriminating among medial and lateral force. Also, there is no telemeterised implant for the patella currently present in literature.

Image removed due to copyright restriction.

Figure 1.11. Load patterns for walking, adopted from [35]. HS: heel strike; CTO: contralateral toe off; CHS: contralateral heel strike.

Table 1.1. Joint contact forces from telemeterised study [35].

Activity	Resultant peak Forces %BW	Resultant external torque %BWm
Two-legged stance	107	-0.3
Sitting down	225	0.2
Standing up	246	0.3
Knee bend	253	0.1
One legged stance	259	0.3
Level walking	261	0.5
Ascending stairs	316	0.4
Descending stairs	346	0.3

Internal-External (I-E) motion

I-E kinematics and kinetics are an important characteristic of normal gait and cannot be neglected. It helps establish favourable trunk orientation for the proceeding step. Since the stance foot is fixed on the ground, the I-E moment to twist the trunk must be generated across the lower limb. As illustrated

in Figure 1.12, the trunk will experience external moment in the stance phase. To counterbalance, the reaction moment must be an internal moment. Therefore, the femur will experience external moment whereas the tibia will experience internal moment. From telemeterised study, the maximum I-E moment was highest during walking (0.5 BWm), refer to Table 1.1 [35].

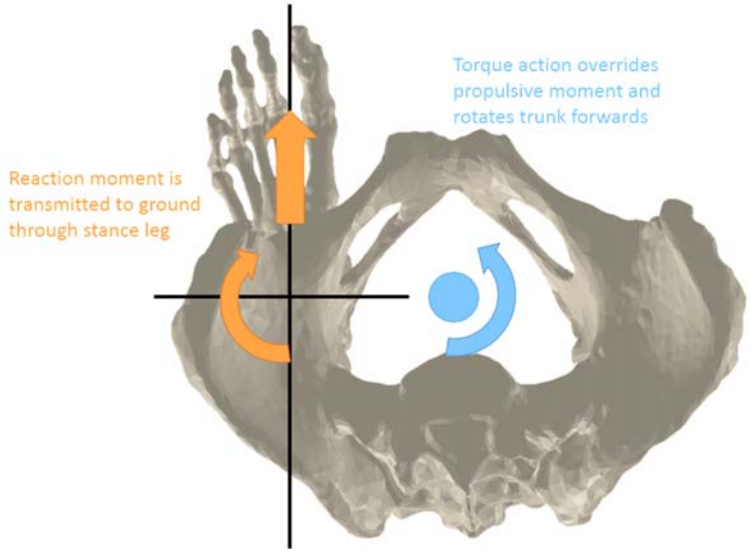

Figure 1.12. Torque is acting externally on the trunk and tibia counterbalance with internal moment.

Anterior-Posterior (A-P) motion

A-P motion is important to maintain knee stability. Recent studies using MRI revealed that the medial condyle hardly moved posteriorly whereas the lateral condyle moved backwards by rolling and sliding [45]. The medial articulating surface radius are larger compared to the lateral's and hence the tendency of the roll back of the lateral condyle [46]. During knee flexion at 60° (maximum during gait), in vivo studies [47] shown the femoral condyle can move back up to 5mm. From telemeterised study, the A-P force are shown to be negligible compared to axial force under daily activities [35].

Passive Vs Active load

It is important to acknowledged that the knee behave differently under passive and active load. Studies reported that in general knee had more rotation and translation under passive loading compared to active loading [23]. In active loading where the hamstring and quadriceps are loaded,

the rotation and translation during motion decreased [23, 48]. Li et al [48] observed the tibia rotation relative to femur reduced by up to 30% when the knee is actively loaded.

Mechanics of Soft Tissue

Ligaments of the knee are innervated and play an important proprioceptive role during kinematic and kinetic conditions [49-53]. They are complex multi-bundle structures, with different origins and insertions, different mechanical properties between bundles and a non-linear behaviour [54] (Figure 1.13).

Image removed due to copyright restriction.

Figure 1.13. Stress-strain curve showing the pattern of ligament deformation observed during a uniaxial tensile test [54].

In the relaxed state of the ligament, collagen fibres are stress-free and are arranged in wavy and crimped-shaped patterns. In the first region of the curve, a very low force is required to achieve finite deformation of the individual fibres without stretching them.

The second region, generally called the toe-region, is upwardly concave. In this part of the curve, the tissue is elongated with a small increase in loads as the collagen fibres are straightened out. As loading continues, the stiffness of the tissue increases, and progressively greater force is required to produce

equivalent amounts of elongation. The end of the toe region has been reported to have a strain value of between 1.5 and 4 % [55, 56].

The third region, which is more or less linear, corresponds to a phase where the collagen fibres are straightened, and the stiffness of the tissue is roughly constant.

Then if the elongation of the tissue sample is pursued until a critical value, sequential failure of the most stressed fibre bundles initiates [57]. This phenomenon is accompanied by small force reductions that can sometimes be observed in the loading curves for both tendons and ligaments. When the ultimate tensile strength of the specimen is reached, complete failure occurs rapidly, and the tissue can carry less load until full failure. Various studies have demonstrated that ligament properties vary considerably between different subjects [58], and that the precise configuration of ligament bundles is important in determining the overall ligament behaviour [59].

Soft tissue model in computational modelling

Numerical methods have been used for decades in describing ligament behaviour. One dimensional line elements such as springs, trusses and beams are frequently used to model the mechanical behaviour of ligaments. In other words, the ligaments can be described using some form of non-linear spring equation. Trent and colleagues were one of the first groups to estimate the stiffness and initial strain of a spring model experimentally in 1976 [60] as reported by Wismans in 1980 [61]. In this model, the mechanical response of the ligament is usually described by three distinct regions, with zero compression during ligament shortening, and a tensile response with an initial toe region and a final linear region [62]. Model developed by Blankevoort et al [62] is one of the most often used spring models. There are other 1D models that includes mechanical properties like Young's modulus [63, 64], but they are less used as with this approach. It is more useful to describe the ligament properties using stiffness constant.

Alternatively, ligament geometries can be modelled as 2D or 3D structures. This approach can facilitate the ligament wrapping effect using surface-to-surface and enables analysis of regional biomechanical response but is more computational expensive. Moreover, the mathematical description of the material properties in the 2D or 3D continuum models remain challenging [65, 66]. An advantage of using 1D spring to describe ligament model in computational modelling is that they are computationally inexpensive and the possibility to exactly replicate ligaments non-linear force-elongation curves from experimental test [67].

Galbusera et al [67] published a review on ligament models and properties used previous computational modelling studies. Although there are studies perform experimental test to determine ligament properties, most studies are still referencing old studies for spring model properties. This could be due to the complexity of experimental protocols and variability between different subjects, particularly the age of donor and/or pathologies that might have affected ligament mechanical behaviour. As shown by Galbusera et al [67] ligament properties for 1D non-linear spring model from Blankevoort study [62] were referenced the most, followed by Rahman et al [68]. The properties reported in previous studies are shown on Table 1.2 and Table 1.3.

Table 1.2. Ligament properties reported by Blankevoort and Huiskes. k is the linear stiffness and ε_r is the reference strain for the joint in extension [62]. ***Negative strain indicates the ligament is longer (laxer) in the reference state compared to the state when the ligament length is measured.***

ligament	ligament bundle	stiffness (k) [N]	reference strain (ε_r)
anterior cruciate	anterior	5000	0.06
	posterior	5000	0.1
posterior cruciate	anterior	9000	-0.24
	posterior	9000	-0.03
lateral collateral	anterior	2000	-0.25
	posterior	2000	0.08
	superior	2000	-0.05
medial collateral	anterior	2750	0.04
	posterior	2750	0.03
	inferior	2750	0.04

Table 1.3. Ligament properties reported by Abdel Rahman et al [68]. The study used different spring equation from Blankevoort.

ligament	ligament bundle	stiffness (K1) [N/mm]	stiffness (K2) [N/mm^2]	reference strain (ε_r)
anterior cruciate	anterior	83.15	22.48	0.000
	posterior	83.15	26.27	0.051
posterior cruciate	anterior	125.0	31.26	1.004
	posterior	60.0	19.29	1.05
lateral collateral		72.22	10.0	1.05
medial collateral	anterior	91.25	10.0	0.94
	oblique	27.86	5.0	1.031
	deep	27.07	5.0	1.049

Knee Joint Pathology

As one of the heavy loaded joints in the body, the knee joint is prone to failure. The main cause of knee failure is arthritis, of which the most common form is osteoarthritis (OA). This is a localised degenerative condition generally associated with old age and overuse of the joint – essentially, natural 'wear and tear' of the cartilage. When this happens, the bones of the joints rub more closely against one another. The rubbing results in pain, swelling, stiffness and decreased ability to move; effectively causing loss of joint functionality and impairing quality of life. Risk factors for knee OA include systemic factors such as obesity, increasing age, female gender and family history; joint-specific factors such as malalignment (leading to abnormal loading) and previous knee injury (particularly anterior cruciate ligament (ACL) and meniscal injury) also pay an important role [69-71] . Its incidence has increased markedly over recent years as a result of the ageing population and the prevalence of risk factors, principally obesity [72].

The second common form of arthritis is rheumatoid arthritis (RA). This is a progressive disease in which the immune system triggers inflammation of the synovial fluid, causing destruction of the joint soft tissues. Rheumatoid arthritis generally begins to cause problems at an earlier age than OA, and is systemic, often affecting multiple joints. Other cause of knee failure is trauma.

Treatments Options

There is no cure for arthritis but there are a number of treatments that my help relieve the pain and disability it can cause.

Non-surgical treatments for knee OA

Almost everyone will eventually develop some degree of osteoarthritis. In its initial stage of diagnosis, few non-surgical treatments are available such as lifestyle modifications, physical therapy, assistive remedies and medications.

Surgical treatments

Partial or total joint replacement/arthroplasty is generally the last resort when non-surgical treatments are unsuccessful. There are range of possible surgical options, depending on the degree of joint deterioration [73]. The bullet-list below outline the options, with the earlier options being most conservative, and therefore being preferable, where possible.

- Tissue resection: For younger patients, it may not be appropriate to use an implant at first, instead resecting the natural knee tissues, e.g. *meniscectomy*, where the damaged meniscal cartilage is partially or totally removed, and *osteotomy*, where a portion of bone is removed to better distribute loads across the knee [73].

- Interpositional spacers: where only the meniscus is damaged, a conservative option is an interpositional spacer, to replace the worn cartilage (so preventing bone-on-bone articulation) without any resection of bone stock [73].

- Bone osteotomy: tibia osteotomy can be performed in early stage of osteoarthritis. The tibia bone is effectively cut in order to realign the joint (lateral closed wedge for varus deformity and medial closed wedge for valgus deformity) and off load the affected cartilage. Femoral osteotomy can be performed too although it is less common [73].

- Hemiarthroplasty: hemiarthroplasty replaces only the articulating surface of *one* bone, e.g. a tibial hemiarthroplasty may replace only one of the tibial condyles, with an anatomically representative resurfacing implant [73].

- Unicompartmental & bi-lateral arthroplasty: When damage is limited to one condyle a popular option is to use a *unicompartmental* knee replacement (UKR) – this does require limited resection of both the femur and tibia but leaves sufficient bone stock for subsequent revision to a full TKA if needed. In some cases, separate UKR implants can be used for the medial and lateral condyles (called *bi-lateral* arthroplasty), allowing the intercondylar region and associated cruciate ligaments to be entirely retained. Early clinical data shows UKR has a higher revision rate than TKR [74], and some concerns remain over whether UKR can accelerate contra-lateral condyle degradation [75]; however this is based on early experiences, and results will potentially improve as the technique is more widely practised. Nonetheless UKR is an attractive option, since despite any shortcomings in longevity it is generally easier to revise from a UKR to a TKA, than to revise a TKA [73]. However, UKR surgery may be more complicated compared to TKA surgery.

- Total Knee Arthroplasty (TKA): TKA is the last solution for the end stage osteoarthritis. TKA involves resection of considerable bone stock, including at least part of intercondylar region of both the femur and tibia. TKA consists of at least three components, femoral component, tibial component, tibia insert to replicate the natural meniscus. TKA may or may not include patellar resurfacing, depending on the patellofemoral joint deterioration and surgeon's clinical judgement [73].

Total Knee Arthroplasty

Total knee arthroplasty is the last recourse for the treatment of joint disease. According to Papas and colleagues, in their paper "The History of Total Knee Arthroplasty" they traced back the first attempts for TKA in 1890 in Germany where surgeons implanted ivory components within the bone along with

other materials and describe the evolution of implants and TKA procedures from the 1950s to current times [76]. According to 2017 Australian Joint Registry [1], there is 52,836 TKA procedures performed in 2016, 2.8% increased from 2015 and 139.8% from 2003. The most common diagnosis for TKA was osteoarthritis (97.4%) and in the last decade the number of TKA is increasing due to aging population. Figure 1.14 shows the proportion of TKA patients by age group. In comparison, the United Kingdom national joint registry reported 90,938 TKA procedures performed in 2017 [77] while the Swedish joint registry reported 13,689 TKA procedures in 2017 [78].

Image removed due to copyright restriction.

Figure 1.14. Primary Total Knee Replacement by age [1].

Variations of TKA

In a typical TKA, the entire distal surface of the femoral condyles and proximal tibia condyles are resected and replaced with artificial components such that the two artificial surfaces articulate together to form the new tibiofemoral joint. In the early years, the designs were primarily to mimic the geometric anatomy of the natural knee, referred as anatomical approach. Anatomic models are designed to preserve and avoid the PCL and the ACL if it is retained [79]. Then, the designs were

developed with philosophy to simplify the knee biomechanics by removing both cruciate ligaments, referred as functional approach. Functional designs permitted "nonanatomical joint surface geometries intended to maximize surface area and reduce polyethylene stress" [79]. Both approaches resulted in some common features. However, as TKA advances, there are several different designs aspects; the most major variations are outlined below.

Materials

Low friction is the one of the most important factors in selecting TKA bearing. Polyethylene has been the primary bearing material due to its low friction property. Although modern hip arthroplasty are now migrating to more advanced materials, such as ceramic-on-ceramic (CoC), this is less appropriate for the knee. Unlike hip anatomy, which is spherical joint, knee has less conforming geometry as discussed in knee anatomy section. In addition, the brittle nature of ceramics and the inability of ceramic materials to withstand high-impact tensile forces is of concern for TKA applications. The femoral component is generally manufactured from cobalt-chromium (Co-Cr), providing high strength, good biocompatibility and excellent corrosion resistance. The tibial articulating insert is a medical grade ultra-high molecular weight polyethylene (UHMWPE), e.g. GUR-1020, GUR-1050 or GUR-4150; however experiences with early designs demonstrated that the lower stiffness of UHMWPE against cancellous bone could lead to failure [80], and it soon became standard for the tibial polyethylene insert to be mounted in a metal tray (often Co-Cr or titanium) for stiffer backing. However, it was previously found that polyethylene free radicals produced in the radiation process cause oxidative degradation which may threaten the long-term stability of these devices [81, 82]. Polyethylene properties can be modified by sterilization by radiation and by exposition to the oxidative environment; the effects are increase in density and elasticity of the materials itself. To counter these problems, a range of refinements have been made to the production processes for UHMWPE (e.g. gamma-ray vacuum sterilisation is used to encourage polymer cross-linking, which can further enhance the wear performance while providing oxidative stability [83].

Cruciate Retaining Vs Posterior Stabilizer

While the anterior cruciate ligament is usually resected in TKA for surgery access, the posterior cruciate ligament (PCL) may not be necessary resected as it helps stabilising the femur by preventing anterior translation during knee flexion. This is only true as long as its function is preserved by careful bone resection and adequately balancing the knee in flexion and extension. Prostheses designed for retaining the PCL are called cruciate retaining (CR). However, sometimes, the PCL may be incompetent due to injury or degeneration or surgeons may choose to sacrifice the PCL while performing TKA in cases where flexion is tight, to prevent excessive stresses and wear of the polyethylene insert. The prosthesis used for this scenario is called a posterior stabilizer (PS). This design substitutes the PCL functions by means of a central cam on the femoral implant, which is pushed back by the central post on the polyethylene insert (Figure 1.15). PS implants may provide better anteroposterior stability due to cam-to-post mechanism. However, one of the potential draw backs with this design is tightness (resulted in less ROM) in extension due to early contact between the cam and the post. Several studies have investigated the differences in outcomes between these two designs finding no clinically relevant differences between these two implants for clinical scores and gait [84-86]. Additionally, recent systematic review by Longo et al [87] compared clinical outcome scores, rate of complications and ROM of PS and CR knees. They found literature reported PS knees tend to achieve a higher post-operative ROM while CR and PS knees have similar clinica outcomes.

Figure 1.15. (a) Cruciate retaining implant. (b) Posterior stabilizer implant. The cam-to-post substitute the functions of PCL [79].

Variations of tibia bearing design

The use of metal backed insert is now widespread, and many designs now also introduce additional degree of freedom between the tray and the polyethylene insert. One design concept is to use a central peg, permitting only I-E rotation between the tray and insert; i.e. a rotating platform (Figure 1.16, centre). Another concept is a slotted peg permitting both rotation and translation; i.e. mobile bearings. These designs were introduced to prevent excessive stresses at articulating surfaces by providing more conforming contact during motion (increase surface contact area and hence decreasing contact stress) [88]. Nonetheless, fixed designs with no tibial bearing are still common. Although theoretically rotating and mobile bearings offer advantages, currently these benefits do not clearly translate to improved clinical results [89, 90].

Image removed due to copyright restriction.

Figure 1.16. Comparison of tibial bearing designs [73].

The Medial pivot design was introduced to address the issue of asymmetric tibiofemoral motion. Conformity on the medial side was intended to provide reduced AP motion; less constraint on the lateral side was intended to allow AP femoral translation. The asymmetry in the motion is provided by the tibial and femoral components shape, which is a conforming socket on the medial side and an arcuate surface around the centre point of the medial socket on the lateral side [91]. The design of this prosthesis was finalized in the mid-1990s, a time when wear of polyethylene was a major concern and low contact stresses on the tibial insert were critically important. The ball-and-socket conformity on the medial side resulted in large surface area and hence lower contact stresses. This attempt was accepted in the interest of limiting detrimental effects of wear debris [92].

Single radius Vs Multi radius femoral component

It is known that in vivo kinematics after TKA is influenced by the design of the implant. Single-radius femoral component design was introduced in an attempt to more accurately reproduce the kinematics of the natural knee. The design is based on the premise that there is only one knee functional-extension axis location [93, 94]. Unlike multi-radius design, the femoral component rotates against the tibial insert only in one radius in single-radius prosthesis. Until now, there have been few clinical reports about post-operative function of the single-radius design and they have been highly controversial [95, 96]. Ostermeir [97] reported single-radius design showed lower maximum extension forces and Wang et al [98] reported that the single-radius had better stability than the multi-radius one with respect to standing up from sitting position. On the contrary, two studies presented by

Stoddard et al [99] and Jenny et al [100] reported that improvement in using single-radius design could not be clinically demonstrated.

Image removed due to copyright restriction.

Figure 1.17. Single radius and dual radius femoral component [101].

Surgical Techniques

Patellar Resurfacing

The native patella may or may not be resurfaced in TKA. This is a continuous debate amongst orthopaedic surgeons. Advocates for either side of the debate raise a number of valid points to support their view on the matter. Orthopaedic surgeons who practice and support the notion to not resurface the patella support their decision based on the number of risks that are associated with resurfacing the patella. This includes patella component fracture, implant loosening and patella clunk syndrome. However, non-resurfacing of the patella is associated with a higher rate of anterior knee pain and re-operation [102-105].

Extensive literature have compared the outcomes between resurfaced and un-resurfaced patella in TKA [106]. A meta-analysis by Agrawal et al [107] reported that the existing literature shows that patellar resurfacing can reduce the risk of reoperation with no improvement in knee function or

patient satisfaction compared to patients without patellar resurfacing [107]. Despite of the controversy, the use of patellar resurfacing is continuously increasing, as shown in Figure 1.18.

Figure 1.18. Primary TKR by patella usage [1].

When the patella is resurfaced, the bone is resected with the aim to restore the patella's original thickness. In general, the patella component is all-polyethylene. The articular surface geometries of the patella component can be classified into five basic shapes: [108] convex or dome shaped; modified dome shaped; anatomically shaped; cylindrical or saddle shaped; mobile bearing.

Image removed due to copyright restriction.

Figure 1.19. Variations of patella button design available in the market [108].

Navigated TKA

It is well known that correct alignment of the components is one of the most important factors to a successful TKA; it is believed a well aligned TKA is likely to function well. Traditionally, intraoperative knee alignment has been achieved by instrumentation with intramedullary and extramedullary alignment rods and more recently using patient specific positioning guides which uses preoperative MRI or CT to design custom shape-fitting jigs [109]. Mechanical instrumentation can be fiddly which may lead to inconsistent or inaccuracy results. Recently, computer navigation systems have gained substantial popularity in TKA industry (as shown in AOANJR data in Figure 1.20). Their aim is to provide more accurate implantation by digital mapping based on standard anatomical landmarks and intra-operative assessments [110]. There are two different types of imaging systems, all of which need intraoperative registration of anatomical landmarks [111]. Image-based systems need the collection of morphological information by pre-operative computed tomography (CT) or intra-operative fluoroscopy. Imageless systems, which use a virtual model supplemented by registration data, have overcome concerns about exposure to radiation [112].

A number of studies [110, 113, 114] have suggested that there is improved alignment when navigation is used. In a meta-analysis, Mason et al [115] compared mechanical axis alignment between computer assisted and conventional knee replacements, and reported malalignment of greater than three degrees in 9% of computer assisted knee versus 31.8% of conventional TKAs. Despite this, contradictory evidence does exist with other recent meta-analyses arriving at markedly different conclusions. Bauwens et al [112] and Calliess et al [116] concluded that despite of few advantages that computer assisted TKA provides over conventional surgery on the basis of radiographic end points, its clinical benefits are unclear and remain to be defined on a larger scale. Barrett et al [117], in a multi-centre prospective randomized trial, reported a significant improvement in coronal tibial alignment following computer navigation, but this was associated with a significant increase in operative time.

Image removed due to copyright restriction.

Figure 1.20. Primary TKR by computer navigation[1].

Soft Tissue Balancing

In addition to correct limb alignment to achieve successful TKA, the knee need to be balanced the knee in both extension and flexion [118]. A balanced extension gap can be achieved by either aiming

for appropriate bone cuts or soft tissue release. Bone cuts will be attempted first. Only after these, if necessary, should a surgeon look at making soft tissue releases. Example of soft tissue release, lateral structures are released to balance a valgus preoperative deformity and medial structures are released to balance a varus knee. Femoral component rotation is essential in achieving symmetry flexion gap [119]. Improper femoral component rotation may result in asymmetric flexion gap which may lead to patellofemoral instability [120], anterior knee pain, arthrofibrosis, and patient discomfort due to instability on the knee [121-123].

There are two surgical approaches in achieving good components alignment and a balanced knee; measured resection and gap balancing. These approaches employ different techniques to determine femoral component rotation and ligament balancing.

1. Measured resection (MR): aims to resect an amount of bone equal in thickness to the prosthesis to be implanted. Distal femoral resection is angled in respect to the femoral shaft [124]. Femoral component rotation should be parallel to one these three bony landmarks; the epicondylar axis, posterior condylar axis, or the AP trochlear axis (Whiteside's line) [125-127]. The anteroposterior position, or size, of the femoral component can be determined with either anterior or posterior referencing [128, 129]. The tibial resection is done independently, perpendicular to the long axis of the tibia in the coronal plane. Ligament balancing is done once the trial components are in-situ.

2. Gap balancing (GB): distal femoral and proximal tibial resections are performed first. The femoral component rotation is positioned parallel to the resected proximal tibia with each collateral ligament equally tensioned to obtain a rectangular flexion and extension gap [119, 130, 131]

Few studies have reported that the determination of bony landmarks in MR technique varies and thus suggest GB may offer superior reliability compared to MR method [119, 123]. The variability of determining the bony landmarks may result in higher risk of femoral component malorientation [125].

Dennis et al [126] compared the stability of 40 MR TKAs and 20 GB TKAs and found that the incidence and magnitude of femoral condylar lift-off was much lower in GB than MR TKAs. Nevertheless, despite of the bony landmarks variability, MR showed better joint line preservation by avoiding excessive medial structures release [132].

On the other hand, a precise proximal tibial resection is critical when using a gap resection technique [119]. The tibial cut is utilized to create the flexion space at 90°. Consequently, any varus or valgus malalignment will result in increased internal rotation of the femoral component when the femoral component is placed parallel to the resected proximal tibia [131]. Additionally, it is critical in GB to accurately control the distraction forces while balancing in both extension and flexion.

Nagai et al [133] in their findings indicated that due to the lateral compartment stiffness being much lower than the medial compartment, the lateral compartment gap tends to be larger than the medial compartment gap as the joint gap distraction force increases. This suggests that if the surgeon only applies a low joint distraction force, the varus ligament balance is low and therefore the rotation of femoral posterior condyle resection is small. Another challenge in GB method is to achieve stability in mid-flexion. A recent study demonstrated that a significant proportion (36%) of TKAs showed midflexion laxity even when rectangular extension and 90° flexion gaps were achieved [134]. The flexion and extension gaps can be measured with ruler, lamina spreaders or tensioner. In addition, it is also critical to pay attention to patellofemoral joint while balancing the knee. Excessive femoral component rotation may alter patellar tilt angles [135] and kinematics [123, 136].

Failure of TKA – what are the causes?

Assuming the initial arthroplasty surgery is successful, there are still many risks of failure post-operatively. Interestingly in contemporary TKA, failure is no longer only categorized as the need for revision, but also a measure of patient satisfaction. For example, a patient may have limited functionality even though they do not require a revision surgery. This will be discussed further in the next section. Table 1.4 represents the causes of failure of large TKA revision reported in literature

[137, 138] and joint registry report [1, 139] . Sharkey et al., differentiated between early and late complications. Whereas infections are typical early complications, aseptic loosening and wear occur generally late after TKA implantation. Note that these factors are not independent or exclusive (e.g. wear-induced osteolysis may lead to loosening or increase the risk of direct mechanical failure of the component). Some of these factors are unrelated to mechanical environment and others depend strongly on joint mechanics (indicated in bold). In a recent follow up study by Sharkey et al., [140] infection was still the most common reason for early revision but polyethylene wear was no longer the primary reason for late revision. Aseptic loosening was the most common reason for late revision.

Table 1.4. Causes of TKA failure

causes of failure	**%[a]**	**%[b]**		**%[c]**	**%[d]**	**%[e]**	
		early	**late**			**early**	**late**
aseptic loosening	25	17	33	25.9	38.7	23	51.4
wear/osteolysis	15	11	44	3.7	9.6	5	10
instability	14	-	-	7.3	17.6	10	10
infection	11	25	10	22.5	5.8	37.6	21.9
mechanical failure	7	-	-	1.5	1.3	-	-
periprosthetic fracture	4.5	2	3	2.8	4.0	8	8
pain	2	-	-	8.6	16.9	-	-
dislocation	2	-	-	-	4.2	-	-
arthrofibrosis	-	18	20	3.5	5.9	10	5
malalignment	-	11	12	2.2	7.9	3	5
extensor mechanism deficiency/patellar complications	-	10	2	16	-	2	1
avascular necrosis patella	-	4	4	-	-	-	-
Incorrect sizing	-	-	-	1.2	-	-	-
other	-	-	-	4.9	21.1	-	-

[a] Gioe et al [137]
[b] Sharkey et al - 2002 [138]
[c] 2017 Australian Joint Registry [1]
[d] 2018 National Joint Registry for England, Wales, Northern Island and the Isle of Man Joint Registry [139]
[e] Sharkey et al – 2012 [140]

Outcomes of TKA

TKA is considered as one of the most successful operations when measured against longevity, the cumulative revision rate at 16 years is 8.0% or survivorship rate of 92.0% [1] (Figure 1.21). However, implant survival as an outcome (i.e. implant not removed from the patient's body) does not indicate patient is satisfied with the results from the surgery, as a patient may still be in pain or suffer from lack of function. This was highlighted in recent studies, where 15 to 20% of patient's were dissatisfied after surgery, including reports of persistent residual pain [141-147]. This discrepancy between successful survival outcomes and patient dissatisfaction supports the principle that a single discrete success/failure metric is not sufficient to define the outcome of TKA. At the core of the issue is a definitional difference between what constitutes a successful surgery, and the failure to fully align patient expectations with the reality of their likely surgical outcome.

In 2009, Bourne and colleagues carried out a study to determine the reasons of dissatisfaction after TKA. They found that when patients were most dissatisfied when their expectations were not met one year after surgery [143]. This notion is supported by the work of Mahomed et al., [148] who found that patients expectations could be low (i.e., expected to have no pain after recovery from surgery) and high (expected to have no functional limitations) [148].

Image removed due to copyright restriction.

Figure 1.21. Cumulative percent revision of primary TKR [1].

PROMS as outcome measurement

Revision rate is a common outcome measure in TKA [149-152] and even considered to be the gold standard for survival analyses of orthopaedic implants [153]. However, the reliability of using revision rate as an outcome measure has been questioned [150, 153].

In addition to revision rate, patient-reported outcome measures (PROMs), are subjective scores used as additional assessment to gauge the surgery's success from patient's perspective (clinical outcome) [154-157]. Oxford Knee Score (OKS) [156, 158-163], Knee injury and Osteoarthritis Outcome Score (KOOS) [158, 164-172], Western Ontario and McMaster Osteoarthritis index (WOMAC) [173, 174], Knee Society Score (KSS) [158, 175-178] are few most common PROMs questionaries. As PROMS are subjective scores, they tend to have high variability and may have low repeatability.

While there is a trend for PROMS to increase from pre-op to post-op, studies generally show that TKA patients still experience some pain and/or loss of function post-operatively. For example, Bourne et al [2] and others [141, 154, 179] have shown about 20% of patients are dissatisfied following TKA. This suggests that pain and function, rather than revision rate results in a much a higher failure rate, and probably provide a better outcome measure for success. There are also situations when revision rates mask poor outcomes, such as in poor functional outcomes which do not warrant revision, but may impede participation (i.e. restricted knee flexion range) [180].

Furthermore, pre-operative patient selection might mask the true effectiveness of the treatment. For example, patients who have higher expectations (e.g. younger patients) tend to show greater dissatisfaction [181-183]. One important conundrum of TKA outcomes is that patients with high pre-operative functional status are associated with worse subjective scores following TKA [182] and at the same time, patients with worse pre-operative functional status also exhibit the most dramatic improvement following TKA [181, 182]. This apparent contradiction highlights the fact that not only post-operative subjective scores values are important, but also the amount of improvement following TKA, as suggested by Losina et al [184]. In other words, an objective outcome for TKA requires to measure the improvement of pain and function considering the difference between a preoperative baseline and post-operative outcome measurements. Regardless of the increasing number of studies assessing outcomes of TKA [154, 185-191] , a consensus has yet to be reached on whether to define success based on the degree of improvement from pre-operative status (the journey), or based on the level of pain or functional status achieved at a specific point in time (the destination) [184].

Nevertheless, the literature has consistently shown about 20% of TKA patients are dissatisfied. In 2017 itself, there were an additional 52,836 TKAs performed in Australia from the previous year. Therefore, with the increasing number of TKA performed each year, it is critical to gain better understanding of the different approaches towards the procedure, how they are or are not addressing individual patient needs and engineer appropriate solutions to help towards improvement of patient's quality of life.

Component alignment as outcome measurement

It is of general acceptance that TKA procedures aim to have an overall lower limb alignment in coronal plane is 0° ± 3° [10, 112, 160, 192], so that the limb is aligned with the mechanical axis, which is believed to promote implant durability [193]. This target is described as mechanical alignment (MA). Misaligned implants may lead to wear and/or loosening of one or both components, or patella instability resulting in early failure and revision surgery [194-196]. Numerous studies have correlated the survivorship and post-operative function improvement with coronal plane limb alignment [157, 170, 177, 197-201] but the relationship is not well understood.

Recently, the philosophy of kinematic alignment (KA) or natural alignment has emerged as an alternative to restore normal knee motion and function [146, 175, 192, 196, 202]. Kinematic alignment is considered as restoration approach which aimed to align the angle and level of the distal joint line of the femoral component, posterior joint line of the femoral component, and joint line of the tibial component to those of the normal knee [144, 192, 202, 203]. This approach will achieve different component alignment for different patients, somewhat a step towards personalisation of component alignment [203] .

The clinical outcomes of kinematic alignment are still unclear although few studies have reported patients are doing well when short term functional outcomes (e.g. Oxford Knee Scores, WOMAC, ROM, Knee Society Score, KOOS) were measured at one year [170] and 2 years and with some studies showing improved outcomes using this approach compared with the traditional MA [204, 205]. Nevertheless, Despite the good intention of restoring the knee to the pre-disease state, there is on-going debate whether restoration (KA) or reconstruction (MA) will yield a better patient functional outcome [144, 196]. Concerns had been expressed in few studies that full restoration of the knee joint may result in extreme component alignment and may lead to early implant failure due to imbalance loading on the tibia insert compartments [202, 206-208]. However, studies have determined no difference in the risk of early failure between MA and KA [175] stating that the concern that kinematic

alignment compromises function and places the components at a high risk for catastrophic failure is unfounded [202]. Figure 1.22 below illustrates component alignment difference between MA and KA with respect to femur and tibia mechanical axis.

Other studies have recently looked at the restricted Kinematic Alignment (rKA) [146, 192], a more conservative approach. rKA is proposed when the native anatomy is considered to have an extreme deformity to the point when kinematic alignment is applied, it would impact function recovery with potential residual pain. This approach is a compromise between Mechanical and Kinematical alignment where the suggested alignment of the components will be placed within a value between the native anatomy and the mechanical alignment threshold.

Component alignment has been shown to impact postoperative PROMS. However, reported studies have not yet shown a consensus on which alignment philosophies yield better clinical outcomes. This would suggest that a single alignment philosophy may not be applicable as an optimal target for all patients.

Relationships between component alignment and joint dynamics behaviour have been previously shown to exist. Planckaert et al studied correlation of knee kinematics to dynamic behaviour of the knee and pain after TKA. [200]. Their findings showed dynamic knee flexion contractures, increased Q angle, patellar lateralization and internal rotation of the combined components, all of which are characteristics that tend to increase patellofemoral forces and could be the cause of anterior knee pain. Similarly, study by Barrack et al [209] indicated that patients with anterior knee pain had significant internal rotation at the tibial component and in the combined component of approximately 6 degrees and 4.7 degrees respectively.

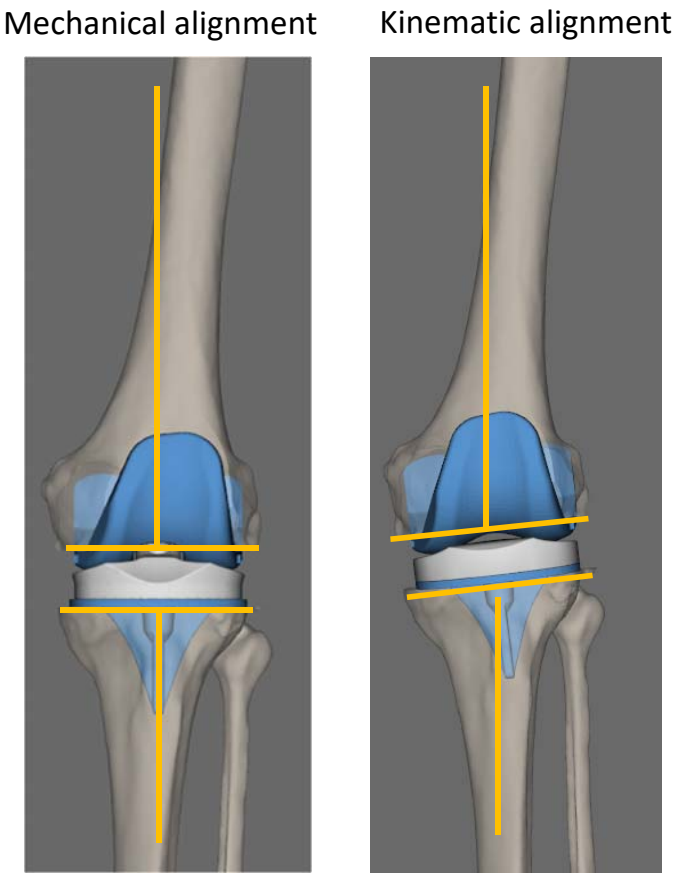

Figure 1.22. Illustration of mechanical and kinematic aligned components. Left is mechanical alignment where the components are aligned to bone mechanical axis. Right is kinematic alignment where components are aligned to bone's joint line.

Other examples include studies from University of Denver [210-213]. They have been studying the patellofemoral joint and the factors that affect its biomechanics. They investigated the resection thickness of patella on kinematics and quadriceps efficiency [210] and found that at lower flexion angles, there was a small increase in quadriceps force with thinner composite patellar thickness. In a different study, Keshmiri and colleagues [214] found that femur and tibia sagittal alignments had a significant influence on patellar kinematics but the rotational alignment did not have a significant effect.

Above examples show that joint dynamics may be more relevant to clinical outcomes than component placement alone. However, studies have not shown identifiable reproducible relationships with joint

dynamics clinical outcomes, indicating that clinical outcome of TKA is a product of complex interactions between surgical and patient factors. Surgical factors can be attributed to interactions between the component design, component alignment, and patient specific anatomic characteristics.

Joint dynamics can be measured with different techniques. Gait labs and video fluoroscopy techniques are a means of capturing patient's movement functionally. However, facilities for these techniques are not widely available, which may limit the scalability of its use in clinical setting. Mechanical simulator is an alternate technique but is limited in its capture of patient specific factors. Furthermore, mechanical simulator can only be done in cadaver specimen, which limits the applicability to study individual patients. Validated computational modelling is a more scalable alternative technique and allow to joint dynamics to be evaluated under various conditions and surgical factors. Computer simulations have been used to optimize implant designs [215, 216] and are increasingly used to study dynamic relationships [217, 218].

Computational Modelling

Computational models are used to describe, explain and predict real world events, such as weather, economy, social interactions, demographics, drug effects, and anatomical and physiological mechanisms in animals and humans. The complexity of the model will depend on the question researchers and scientists are attempting to answer, the assumptions made and the population under study. Simple models can be scalable and extrapolated to a wide population from few real data measurements and general parameters; more complex models the introduction of more parameters and more measurements as different sections of the population will present a considerable variation in parameters.

Computational modelling in biomechanics context can be categorised into two main groups based on the level of complexity, Rigid Body Modelling (RBM) and Finite Element Modelling (FEM). RBM simplifies the analysis with the assumption that the body segments under analysis are rigid, they do

not deform under the action of applied forces. These models are used to study the dynamics of human motion by calculating the displacements of each body segment with respect of each other and the overall motion on a global reference system. Unlike RBM, FEM allows for structures to be modelled as deformable bodies, by applying fundamental physical equations discretised across small spatial and/or temporal intervals. As these intervals become smaller, the approximation becomes better up to a certain limit, but computational effort also increases as the number of separate discretised equations increases. FEM models are often static or quasi-static due to the high computational effort. In other words, RBM is mainly used to study for overall kinematics ad kinetic analyses, whereas FEM is used for studies aimed to determine analysis of contact forces, stresses and deformation between segments.

Computational models of human motion can be separated further into two categories: inverse dynamics and forward dynamics. Both of these methods are currently used by those who simulate human motion [219], and both are able to provide estimations of muscle forces that are otherwise impossible to measure. The critical differences between these two models outlined in the following sections.

Inverse and forward dynamics

Inverse dynamic modelling is a computationally inexpensive technique, and can provide researchers with accurate and meaningful data, such as muscle forces and joint moments. When using inverse dynamics, the position, velocity, and acceleration of a segment are used to estimate muscle forces (Figure 1.23). These calculations rely on the measurement of segmental kinematics and kinetics calculated using 3D motion capture systems and force plates within an instrumented gait analysis laboratory. The inverse dynamics method requires calculation of moments about each joint from measured kinematics and ground reaction forces and muscle forces are estimated by solving a static optimization problem at each instant during the movement.

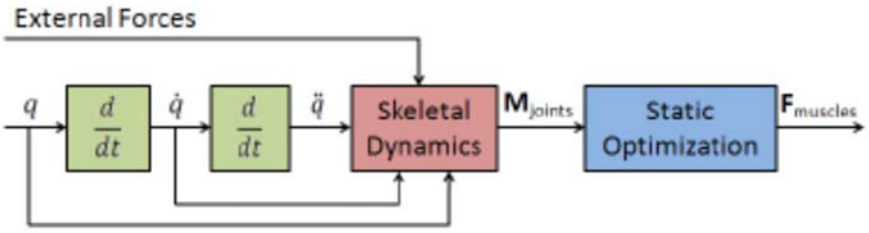

Figure 1.23. A block diagram of the inverse dynamics technique [220]. External forces, position, velocity and acceleration of a segment are used as inputs to solve for internal joint forces. Then the individual muscle and ligament forces are optimized based on the calculated internal joint forces.

On the other hand, forward dynamic modelling is more computationally expensive, as simulations are created by the numerical integration of differential equations describing the motion of body segments (Figure 1.24). Unlike inverse dynamics, which determines muscle forces from measured motions and external forces, forward simulations rely upon muscle forces as input to produce motions. Model parameters, such as muscular, ligamentous force, initial joint angels and velocity can be optimized at each time step in an effort to replicate the experimental kinematics as closely as possible.

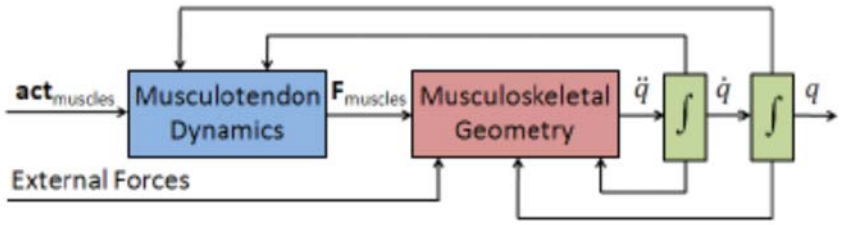

Figure 1.24. A block diagram of the forward dynamics technique [220]. Internal forces and external forces are used as inputs to produce motions of the model. Forward dynamics modelling is more computational expensive than inverse dynamics as the model needs to integrate numerous of differential equations to produce motions.

The application of computational models to knee joint

Computational models for the analysis of human movement have focused on analysing the knee complex, which is comprised of two joints, namely tibiofemoral and patellofemoral. The aim of these models has been to understand native movement, common injuries, the development and treatment

of osteoarthritis (OA) [216, 221-225]. These methods have been used to analyse contact behaviours, biomechanical properties of articular cartilage [226-228], ligament reconstruction [222, 229], meniscectomy [230, 231], and knee replacement [217, 218, 224, 232-236].

One of the earliest works in computational modelling of the knee was carried out by Blankevoort and colleagues in the early 1990s [237]. In this work, they analysed the kinematics of the knee joint during passive motion using a 3D mathematical model with ligament insertions and geometrical data obtained from experimental study. Their study is the first to compare the effect of rigid contact and deformable contact. They showed there was small difference between rigid and deformable contact kinematics for passive motion. In their model, ligaments were described with two or more spring elements representing ligament fiber bundles, which were assumed to be non-linear and the mechanical characteristics of the ligaments were derived from previous mechanical testing [238]. Also in 1990s, Abdel-Rahman et al [68] developed a 3D model to study the dynamic response of the knee joint. Their work focused on mathematical equations contact formulation. Similar to Blankevoort studies, they used 1D nonlinear spring elements to represent knee ligaments. There were other groups developed computational model to study the passive kinematics in 2D [239, 240]. During this period, most studies focused on algebraic equations describing the 3D dynamic behaviour of the joint [241] and as such no computational model that includes both tibio-femoral and patello-femoral joints has yet been developed [241].

In early 2000, Guess et al [242] developed a 3D computational model incorporating both tibio-femoral and patello-femoral joint to replicate the behaviour of a dynamic knee simulator. Their model was developed with a multibody dynamics solution software created by ADAMS (MSC Software Corporation; Santa Ana, CA). In this study, joint contact is modelled as a non-linear spring damper system. The goal was to develop and verify a 3D model of a knee simulator so that knee loads, and kinematics could be used as input to generate muscular force profiles for an identical experimental knee simulator.

A simplified rigid body model called KneeSim was created by LifeModeler, Inc, San Clemente, California in 2000s. This model also uses ADAMS as the underlying mathematical solver. The model consists of tibio-femoral and patella-femoral joints. The model replicates a deep knee bend simulator, Oxford Knee Rig [243]. The soft tissue were modelled as non-linear springs, subject specific [244] or scaled attachment sites [245, 246] can be used. This model has been used in literature by different research groups to analyse post-operative TKA kinematics or as pre-clinical tool to assess different implant system performance. Mihalko [247] studied how the kinematics vary with different combinations implant positioning in the transverse plane of both the femoral and tibial components. Mizu-uchi et al [244] compared the post-operative flexion range of TKA with clinical measurement and the simulation predict the flexion angles to be within 2°. Okamoto et al [248] studied the effect of tibia posterior slope on PS insert using the same model and Nakamura et al [249] investigated the effect of superior-inferior position of the patella component to anterior knee pain reported by patient.

Further historical use of computational model was discussed by Rullkoetter et al [216] and Walker et al [215]. They described how computational models had been used in pre-clinical environment as tool to study implant design features. They explained how this approach can be used to minimize the development cycle by reducing the time and expenditure in testing physical prototypes and allowing for the evaluation of multiple design concepts, thereby improving the clinical performance of implants [216]. In their publication, Rullkoetter exemplifies the use of computational models to improve the stability and mobility of knee implants by considering laxity assessment, compressive loads and muscle force requirements.

Soft tissue representation, particularly ligament in knee computational model is important. They have a large effect on knee joint kinematics and biomechanics. Galbusera et al [67] showed the wide range of element types and material models used in computer models. Similarly, in Beidokhti et al [66] investigated the effect of ligament modelling strategy on the predictive capability of computer models of the human knee joint. They reported that although 3D representation of ligament structures

resulted in a more accurate outcome variable comparison, however ligament represented with spring models provides a faster option with acceptable outcome when joint kinematics is the main interest.

Baldwin et al [217] developed and verified a knee model based on experiment data from Kansas Knee Simulator (KKS). In the study, each of the cadaver specimen was subjected to laxity-test and dynamic activities. Experimental laxity-test data were used to optimize the mechanical properties of tibiofemoral ligament structures on a specimen-specific basis. Each specimen is then subsequently analysed in a computational model that represent KKS dynamic activities. They reported they were able to achieve good agreement in trends and magnitudes between model predictions and experimental kinematics. Other researchers followed a similar approach to develop complex models to estimate patient specific soft tissue properties using data from testing laxity experimentally [250-253]. Although these models were able to derive subject specific ligament parameters, they required many hours of computational time to produce results, and hence limit the practicality to be used in clinical setting.

In contrast to using experimental data, some models rely on scaled parameters based on generic anatomy [254, 255], generic assumptions of soft and bony tissue morphological and physiological characteristics [245, 256, 257], or focused on isolated tibiofemoral joint [258-260]. Simplifications made in these models reduces computing power and can still show relevance in simulation outputs, particularly joint kinematics, as reported by [66]. An example of the use of a simplified model reported in literature. Ishikawa et al assessed patellofemoral and tibiofemoral kinematics behaviour of a mechanically and a kinematically aligned implants using rigid body modelling. Further, they studied the patellofemoral and tibiofemoral contact stresses using finite element analysis. Their model included assumptions on the characteristics of tibiofemoral and patellofemoral contact; tissue characteristics of LCL, MCL, PCL; elements of the knee capsule; and anatomical and physiological characteristics of the quadriceps muscle and tendon, patellar tendon, and hamstring muscles. In this approach, the LCL was modelled as a single fiber bundle; and the MCL as anterior and posterior

bundles; ligaments were modelled as nonlinear springs; and the PCL was defined as being composed of two bundles. Regardless of the assumed parameters, they were able to demonstrated that although kinematically aligned implants produced near normal knee motion, it increases contact stress after TKA when compared to mechanically aligned components [261].

Since the initial development phase in 1990s, there has been considerable improvement in the complexity, accuracy and functionality of the models. Geometries and mesh used in model have moved from idealised 2D to scaled anatomical based model and subject specific 3D model. The use of computational models has expanded from passive motions to dynamic motions. Efforts have been made to optimize subject specific ligament properties using experimental method. However, many of the developed computational model have not been validated. Furthermore, computational model used regularly as part of pre-operative surgical planning has yet been developed. The closest rigid body model that have been used by few researchers group is KneeSim developed by Lifemodeller. Even though subject specific geometry can be used, its application in pre-operative setting is not optimised. Outcome of TKA depends on both surgical and patient factors which can be studied using computational model. Therefore, there is a need to develop a validated low-cost computational model that is practical to be used regularly for TKA surgical planning.

Summary

Total knee replacement is a solution to end-stage osteoarthritis. Although TKA shows good survivorship, patient dissatisfaction is one of the major current concerns post-surgery. Improving patient quality of life is of paramount importance. Joint dynamics have shown to have relationship to clinical outcomes which affects patient satisfaction. Joint dynamics is a product of complex interactions between surgical and patient factors. Computational modelling is a scalable technique compared to other functional techniques and allow the study of both surgical and patient factors impact on joint dynamics following TKA. The computational model developed however need able to

be used practically in clinical setting, in other words low cost computational model in order to realise the use of such tool to optimise joint dynamics as part of TKA surgical planning.

Computational models can be highly complex depending on the research or clinical application for which they are developed. For instance, patient specific models tend to be highly complex and require measurements that would include, 3D motion analysis (kinematics and kinetics), electromyography. Nevertheless, acquiring such amount of information is time consuming, impractical and expensive as it would require several patient appointments, the use of extremely specialized equipment and the contribution of a multidisciplinary team for capturing, processing and interpreting all data.

On the other hand, a simple, generic model, scalable using crude anthropometric measurements and generalized anatomic relationships resulting in poor representation of an individual patient limiting the clinical significance of the model. Thus, a trade-off between complexity and clinical applicability must be sought. A model that is too complex require more specific inputs and longer time to simulate which in return require more data that potentially need to be collected clinically. On the other hand, model that is too simple, accuracy on clinical relevance will be reduced. The relationship between complexity and practicability of a computational model is represented graphically on Figure 1.25. Ideally, for clinical applications, a computational model is on the top right quadrant. However, with increasing complexity, computational and economical cost will increase.

Thus, a balance needs to be found in between the right quadrants. Another important aspect is the applicability of the developed computational model. All models have inherent inaccuracy within them, even with the most complex model. But a model would still be useful if it provides information that otherwise clinician won't have and can be related to clinical observations.

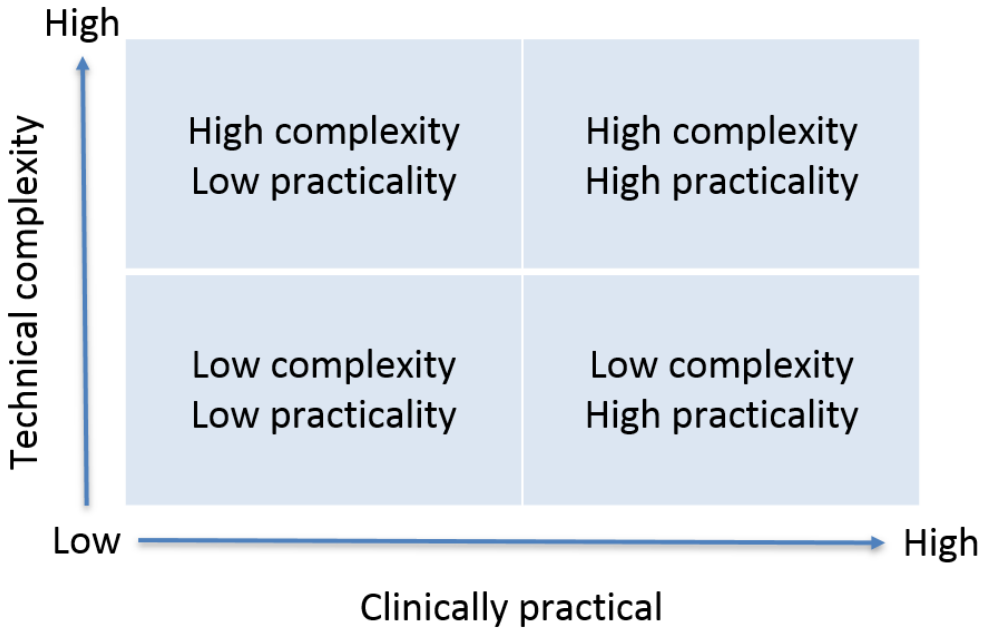

Figure 1.25. Complexity vs practicality matrix for computational model

Chapter 2

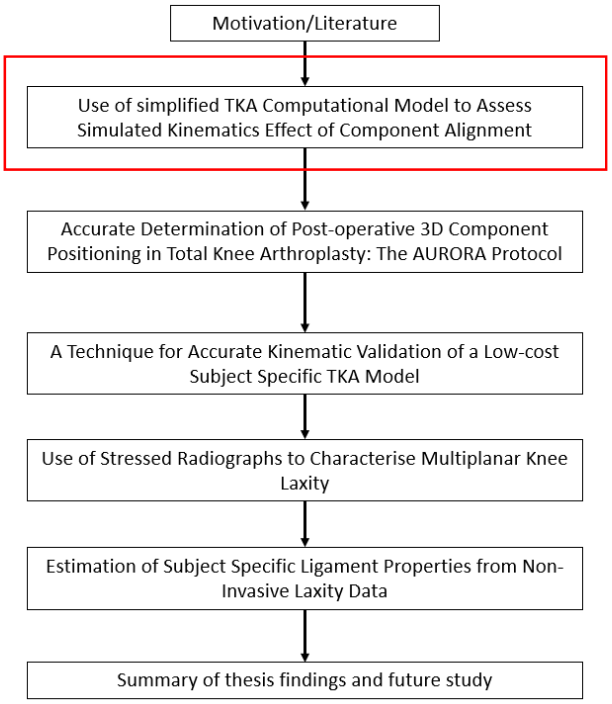

Variability in Static Alignment and Kinematics for Kinematically Aligned TKA

This chapter was published in The Knee Journal

Theodore W, Twiggs J, Kolos E, Roe J, Fritsch B, Dickison D, Liu D, Salmon L, Miles B, Howell S, "Variability in static alignment and kinematics for kinematically aligned TKA," (in eng), *Knee,* vol. 24, no. 4, pp. 733-744, Aug 2017.

This chapter presents the development of a simplified computational model of the knee replicating a mechanical simulator and its ability to differentiate simulated kinematics between mechanically and kinematically aligned components.

Introduction

Total knee arthroplasty (TKA) is an established procedure for improving pain and restoring a significant degree of function, especially for low-demand activities of daily living. However, an understanding of optimal alignment and patient specific kinematics are needed to restore knee motion closer to normal, allowing performance of physically demanding activities that more active patients consider important [262-264].

The philosophy of mechanical alignment of the implant after TKA has traditionally been done to preserve longevity of the implant and enhance post-operative knee function [177, 265, 266]. However, studies have shown that although a mechanically aligned TKA improves the patient's function, 20% to 25% of patients remain dissatisfied [2, 142]. In addition, recent data has challenged the importance of post-operative mechanical alignment in TKA. Paratte et al [267] in a study reviewing 398 TKAs, demonstrated no improvement in the fifteen year implant survival rate in patients within and outside of a post-operative mechanical alignment 0° ± 3°.

Recently, kinematic alignment has been proposed by Howell et al [263, 268, 269] as an alternative to restore normal knee motion and function. Kinematic alignment references the femoral transcylindrical axis, believed to be the flexion extension axis of the knee. The aim is to align the angle and level of the distal joint line of the femoral component, posterior joint line of the femoral component, and joint line of the tibial component to those of the normal knee [269].

Kinematically aligned TKA has been performed since 2006 however unanswered issues continue regarding patient outcomes, survivorship, surgical technique and use of specialised surgical guides [202, 205, 270, 271]. One factor could be that there is no literature reported on long term clinical outcome of kinematically aligned TKA yet. So far, studies up to 4 years are available and they reported similar findings. A randomized controlled study demonstrated kinematically aligned TKA resulted in better pain relief, post-operative function and range of motion than mechanically aligned TKA in 88

patients (88 knees) after 2 years [205]. Other studies emphasized higher function as assessed using the Oxford Knee Score and WOMAC^{TM} score on 198 patients (214 knees) after 4 years [202]; on 101 patients (101 knees) with kinematic alignment after 6 months [271]. However, one small series emphasized the potential for malalignment using the OtisKnee system, which places implants at higher risk of early failure [270].

The optimal targets for alignment in TKA remain unclear, and indeed a single philosophy may not be applicable to an optimal outcome in all patients. Computer simulations are powerful tools that can provide insight into how different alignments influence post-operative outcomes for TKA patients. It allows control of component alignment for the same subject in ways not possible with in-vivo studies. With imaging data, computer simulations are also able to include patient variations into the analysis [245, 247, 257, 272]. Previous studies with computational models have shown comparable kinematic and forces to those measured experimentally or with in-vivo fluoroscopy [217, 273-275].

Ishikawa et al [261] were able to analyse kinematic alignment for TKA using a computational knee simulation. Their study suggests kinematically aligned TKA produces near-normal knee kinematics and may provide better clinical results than mechanically aligned TKA. However, only a single model was used in the study and the kinematic alignment for that single model was defined with the clinical average and therefore its conclusions were limited.

The aim of our study was to compare the alignment and motion of kinematically and mechanically aligned TKAs with a computational knee simulation using pre-operative CT scans from a series of 20 patients undergoing TKA. Validated computer simulation of both kinematic and mechanical alignment was performed for each subject. Measures of tibio-femoral translation, tibio-femoral rotation, patellar tilt and patellar shift were taken and compared between kinematic and mechanically aligned knees.

Materials and Methods

Simulation Set-up

A validated musculoskeletal computational simulation was used to evaluate the kinematic behaviour of kinematically and mechanically aligned TKA in a series of 20 subjects selected from 'The Joint Dynamics Registry' which includes pre-operative CT scans of TKA patients (Bellberry Human Research Ethics Committee, approval number 2012-03-710). The simulation was developed using ADAMS MSC, California, a dynamic, quadriceps-driven, closed-kinetic-chain knee simulator based on the Oxford Knee Rig (OKR) [276]. Experimental validation results of the simulation model are provided in Appendix A - First Computational Model Experimental Validation.

Each model was assembled from CT scan segmentations of patient geometry using ScanIP segmentation software (Simpleware, Exeter, UK). CT scans were taken from degenerative joint diseased knees at a maximum of 6 weeks before scheduled TKA surgery. The population group had a mean age of 69.8 ± 7.3 years. Five of the patients were male and 15 were female. Of the simulated knees, 8 were left knees and 12 were right. CT scans were taken at 1.25mm slice thickness, with the other axial thicknesses varying but all less than 1.25mm.

Landmarks were defined in order to assemble a patient specific model of relevant axes, ligament and tendon attachment sites associated with the reconstructed 3D patient geometry as shown in Figure 2.1.

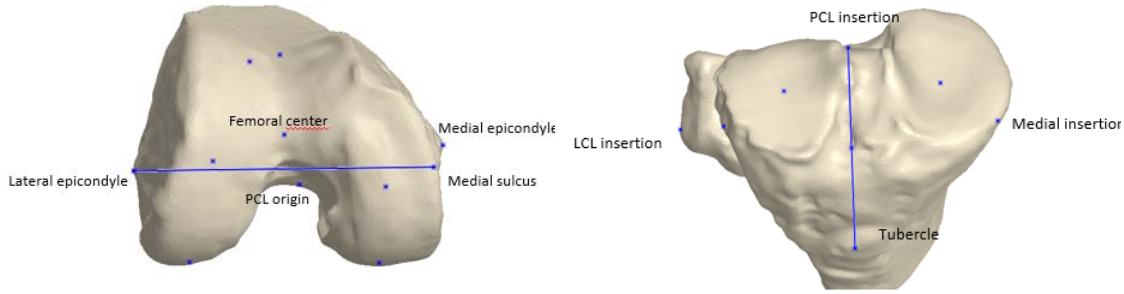

Figure 2.1. Schematic of landmarks and attachment points. Line connecting lateral epicondyle and medial sulcus define the surgical transepicondylar (TEA) axis of the femur. Line connecting PCL

insertion and tubercle define the tibia anterior-posterior (AP) axis which then projected onto a plane perpendicular to the mechanical axis to be used as AP rotational axis as defined by Insall [277].

The model includes the lateral collateral ligament (LCL), medial collateral ligament (MCL), posterior cruciate ligament (PCL), patella tendon, quadriceps tendon and posterior knee capsule. The LCL was considered to be a single fibre bundle and the MCL was considered to consist of anterior and posterior bundles. Likewise the PCL was modelled as an anterior and posterior bundle and was differentiated into anterior and posterior bundles by translation determined from experimental validation.

The femoral attachment points for the LCL and MCL were defined as the epicondylar prominences. The fibular LCL attachment was defined as attaching to the lateral-proximal centre of the fibular head. The tibial attachment points of the MCL bundles were modelled as attaching at the superior-inferior level of the peak medial prominence of the medial edge of the tibia distal to the plateau, with anterior-posterior position at the peak medial projection. The PCL's attachment on the femur was modelled as residing midway distally down the posterior intercondylar fossa when viewed from a posterior perspective, with the centre of attachment of the band placed one third of the width of the intercondylar fossa from the lateral edge of the medial condyle. Its tibial attachment was defined as the centre of the posterior intercondylar fossa.

The mechanical axis of the femur was defined as the line between the centre of the intercondylar notch to the centre of the femoral head, while the tibial mechanical axis was defined as the midpoint of the medial and lateral malleoli at the ankle to the midpoint of a line joining PCL insertion point and medial third of the tibial tubercle. The PCL insertion point and medial third of the tibial tubercle were then projected onto a plane perpendicular to the mechanical axis in order to define the tibial anterior-posterior (AP) rotational axis, as defined by Insall [277]. The surgical transepicondylar axis (the neutral femoral rotational axis) was defined by the lateral epicondylar point and the sulcus of the medial epicondyle.

Ligaments were modelled as point to point non-linear springs, shown in Equation 2.1 [257].

$$f = \frac{1}{4} k \frac{\varepsilon^2}{\varepsilon_l}, \qquad 0 \leq \varepsilon \leq 2\varepsilon_l$$
$$f = k(\varepsilon - \varepsilon_l), \qquad \varepsilon > 2\varepsilon_l$$
$$f = 0, \qquad \varepsilon < 0$$

Equation 2.1 Axial force sustain by ligament

Where f is the axial force sustained by the ligament, k is a stiffness parameter, ε is the strain and $2\varepsilon_l$ is the threshold strain which indicates the change from the toe to the linear regions. The threshold strain used is adapted from literature [68]. The stiffness coefficients of the PCL, LCL and MCL were initially adapted from previous studies [68, 237, 257, 278]. Ligament stiffness's were then adjusted based on experimental validation performed with a cadaver study. Initial pre-strain in each ligament in extension was assumed to match values reported previously in literature [68]. The patella tendon and quadriceps tendon were modelled as wrap-able segmented links with femoral component contact to allow for wrapping about the anterior femoral component in flexion.

The Simulation

The simulation model simulated a closed-kinetic-chain knee extension based on the OKR. All components were modelled as rigid bodies with kinematic and compliant constraints, using a penalty-based contact between components. The model initialised in extension and then the ankle joint was held rigid, which had three degrees of rotational freedom but was constrained in translation. The hip joint was positioned above the ankle joint and was allowed freedom in flexion-extension and varus-valgus, with the vertical motion guided by the axis drawn from the ankle-joint to the hip joint.

In the flexion cycle of the simulation, a negligible force was applied through the extensor mechanism to model soft tissue tension. Following the flexion cycle, the extensor mechanism was activated, using a force applied through the quadriceps tendon to drive the knee back into extension. A PID

(proportional-integral-derivative) controller was used to generate the reactive quadriceps force required to achieve extension [217, 279, 280], as seen in Figure 2.2. The simulation runs through the flexion and extension cycle over a 10 second period, simulated using a dynamic multibody solver. The hamstring force in the computational model is driven by the flexion angle and the constant vertical force applied onto the knee during the deep knee bend activity. This is the same as the OKR boundary condition where the hamstring is not actively loaded but driven based on the position of the leg.

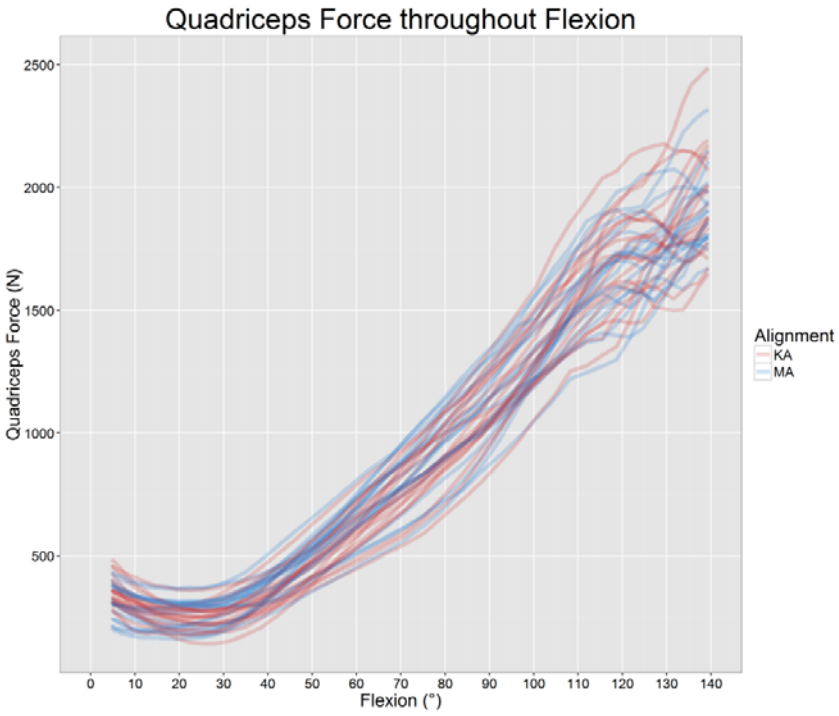

Figure 2.2. Quadriceps force throughout flexion for mechanical and kinematic alignment

Mechanical and Kinematic Component Placement

A fixed bearing, cruciate-retaining, symmetrical femoral and tibial condyle multi-radius implant design (Apex CR; OMNIlife science, East Taunton, MA, USA) was used to model both kinematic and mechanical TKAs for each of the 20 patients.

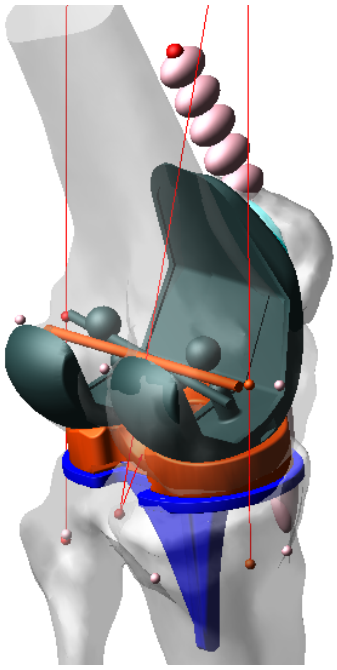

Figure 2.3. Simulation showing boundary conditions and ligaments present in the computational model (LCL, anterior MCL, posterior MCL, anterior PCL, posterior PCL). Ligaments were modelled as non-linear springs. Ligament forces were illustrated with the red lines.

The mechanically aligned femoral components were aligned in the coronal plane perpendicular to the mechanical axis of the femur and rotated to be parallel with the projection of the surgical transepicondylar axis. Translationally, the femoral components were placed such that the most distal condyle of the native femur was level with the most distal point on the condyle of the implant, and likewise for posterior placement [281].

Femoral component flexion and size were then set by incrementally flexing the component until the anterior flange was flush to the anterior surface of the femur. A maximum of 5° flexion was used as an upper limit before an upsized component was selected. Medial-lateral positioning was performed to result in equal amount of exposed bone on the medial and lateral sides.

The tibial component was placed perpendicular to the mechanical axis for all 20 mechanically aligned simulations and rotated to match tibial AP rotational axis defined above. The component was placed

proximally to match the resection level of the thinnest tibia insert and had its medial-lateral and antero-posterior position chosen to maximize coverage subject to those orientations. Posterior slope for all tibial components was set at 3° from a line perpendicular to tibia mechanical axis.

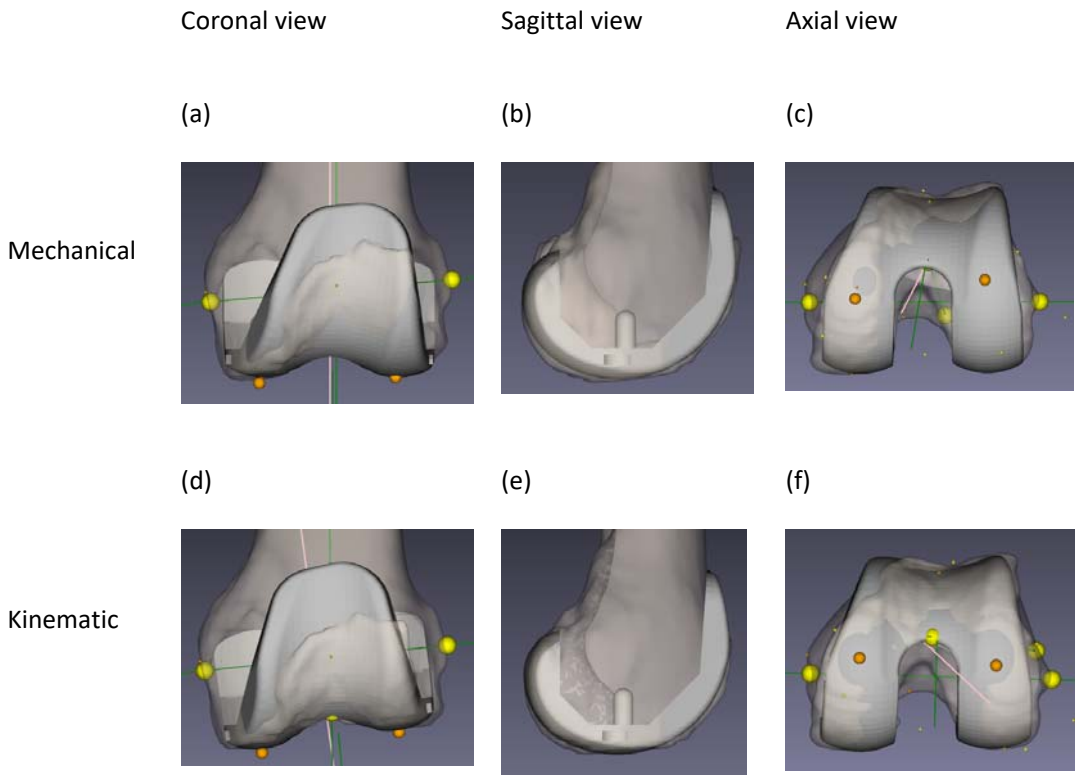

Figure 2.4. Mechanically aligned femoral component (a), (b) and (c); kinematically aligned femoral component (d), (e) and (f) in coronal, sagittal and axial views.

For the kinematically aligned knees, the femoral component was positioned such that the distal and posterior condyles of the femoral component match the joint line of the native femur. The component was then flexed and upsized as needed to avoid femoral component notching. For the tibial component, rotation was defined by a best fit ellipse drawn on the lateral plateau of the tibia in order to replicate the intra-operative technique described by Howell et al [269]. Posterior slope of the tibial component was set at 3° less than the posterior slope of the native medial condyle. Coronal plane alignment was set level to tibia joint line and proximalised to match the resection level of the thinnest

tibia insert. Medial lateral and antero-posterior placement of the component was performed to optimize coverage. No medial tibial bone wear was encountered for patient's included in this study.

For both the kinematic and mechanically aligned knees, patella implantation was modelled as an onlay patella matching the resected surface at its posterior apex with an 8mm thickness patella button. The largest patella button that could fit on the resected surface without overhang was implanted and centred on the resected plane. The resection plane was drawn parallel to the patella tendon-quadriceps tendon attachment point axis and the femoral transepicondylar axis projected from the CT scan. Components position of each subject was checked by experienced surgeons (JR, SH).

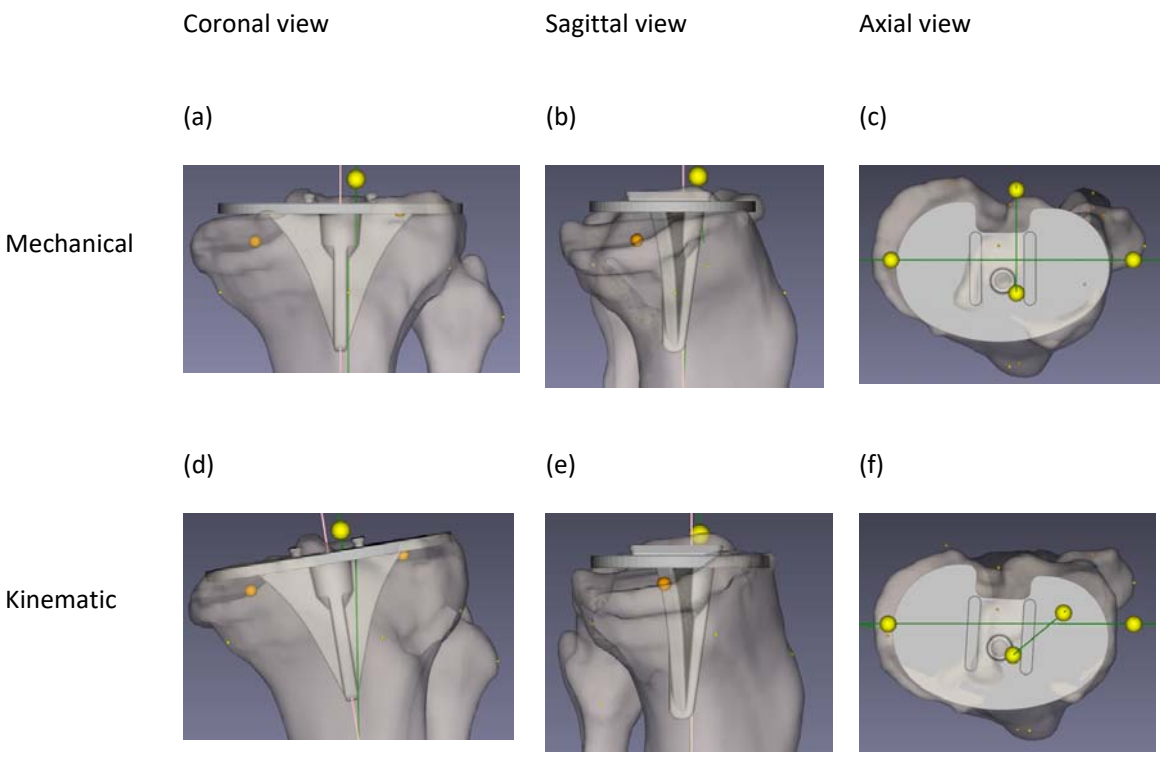

Figure 2.5. Mechanically aligned tibia component (a), (b) and (c); kinematically aligned tibia component (d), (e) and (f) in coronal, sagittal and axial views. Tibia height was positioned to the tibia center for visualisation purpose only. In computational model, the tibia height was positioned to fit 10mm poly thickness.

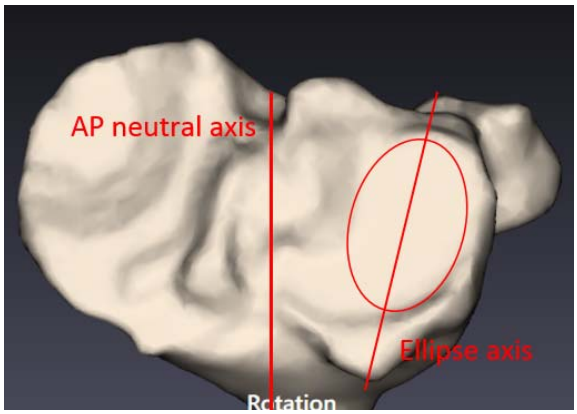

Figure 2.6. Ellipse used to define kinematic rotation angle and its angle relative to tibial AP rotational axis

Data Analysis

Kinematics was assessed using an implant to implant reference frame for both mechanical and kinematic alignment simulations and were based on the Grood-Suntay measurement system [27]. Reporting kinematics to bone based reference frames was trialled however the native mechanical axes results were dominated primarily by the static effects of component placement relative to the bone. Static placement of the implants in kinematic alignment was done independently.

Component placement for the kinematically aligned knees relative to the mechanical axes was then assessed. The simulated closed-kinetic-chain knee extension was performed, and measurements of position were extracted. The medial and lateral flexion facet centre (FFC) condyles were identified as the point equidistant from the most distal and posterior planes of the implant, as the multi radius implant design did not have a single flexion centre. These points were used as the reference points for measuring the movement of the femoral component relative to the tibia throughout the motion. The medial and lateral FFC measurements were taken from these reference points to the lowest dwell point on the tibial insert. Measurements were rescaled about the femoral AP measurement to account for implant size geometry.

Rollback was measured from the centre of these two FFC points to the tibial dwell point posterior translation of the transepicondylar line, hence is the average of the medial and lateral FFC translation measurements. The internal-external rotation measurement was the angle between the femoral and tibial components projected onto the tibial component plane. Patella lateral shift was defined as the translation from the centre of the patella button relative to the centre of the tibial insert, with positive in the lateral direction and negative in the medial direction. Patella external tilt was defined as external rotation of the patella relative to the transepicondylar axis of the femur projected onto the tibial plane.

Results

Simulation Component Alignment for Kinematically Aligned Knees

Native coronal alignment (hip-knee-ankle angle) for all knees as measured from CT scan had a mean of 3.1° ± 5.7° varus (range 8.7° valgus to 11.8° varus).

For mechanically aligned knees the femoral and tibial components were 0° to the mechanical axis. For kinematically aligned knees the mean tibial component coronal and axial alignment was 3.0° ± 2.4° (range -1.8° to 7.2°) varus to the mechanical axis and 7.2° ± 6.6° (range -9.4° to 15.4°) internal to tibial AP rotational axis respectively for kinematically aligned knees. Both component alignment parameter means were significantly different from mechanically aligned knees (0° varus and 0° rotation) ($p < 0.05$). Tibial slope in the kinematically aligned knees had a mean value of 4.6° ± 2.8° (range 0° to 11.2°). Kinematically aligned tibial slope mean was also statistically different to the mechanically aligned tibia slope (3° slope) ($p < 0.05$).

The mean femoral component coronal and axial alignment for kinematically aligned knees was 3.0° ± 2.3° (range -0.8° to 7.2°) valgus to the mechanical axis and 2.5° ± 1.6° (range -0.2° to 5.4°) internal to the surgical transepicondylar axis respectively. As with the tibial component placement, both component alignment parameter means were significantly different from mechanically aligned knees

($p < 0.05$). Femoral flexion in the kinematically aligned knees had a mean value of 2.4° ± 1.7° (range 0° to 5°, as per the planning process). Femoral flexion mean in the mechanically aligned dataset had a mean value of 3.3 ± 1.7° (range 0° to 5°) and was not statistically different to that of the kinematically aligned cases.

Figure 2.7 shows tibial and femoral component alignments for kinematically aligned knees. The horizontal and vertical lines represent 0° coronal and 0° axial alignment respectively. The cross section between the two lines is the mechanical alignment.

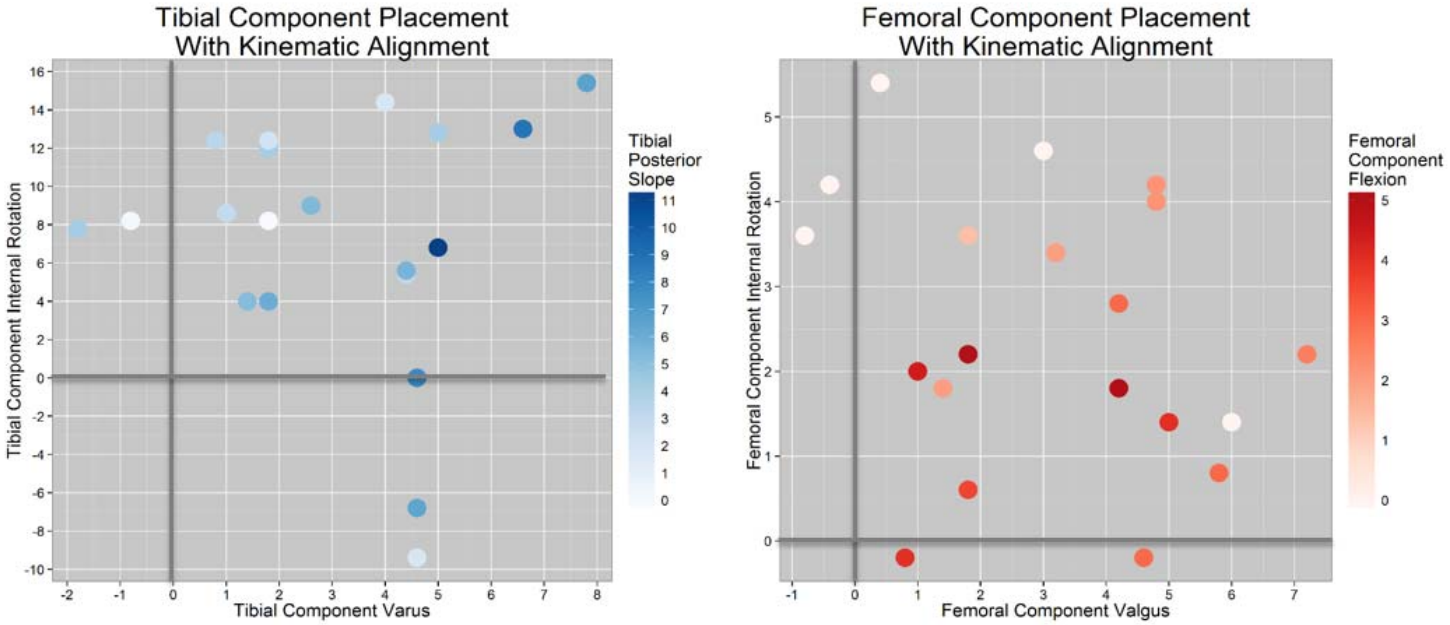

Figure 2.7. Coronal and axial component alignment for kinematically aligned knees. Left figure shows the tibia component alignment. Right figure shows the femur component alignment. The cross section of the 0° horizontal and vertical axis represents mechanical alignment.

Figure 2.8 shows kinematic femoral and tibial component coronal alignment shaded by the native coronal alignment angle. The reference lines represent a 3° varus (blue), neutral (black) and 3° valgus (red) as the final coronal alignment. There was variation in the level of joint line obliquity with a given tibio-femoral coronal alignment. However, a trend between the native and kinematic tibio-femoral

final alignment is present. Linear regression of final alignment as a function of native alignment yields an R^2 of 0.75.

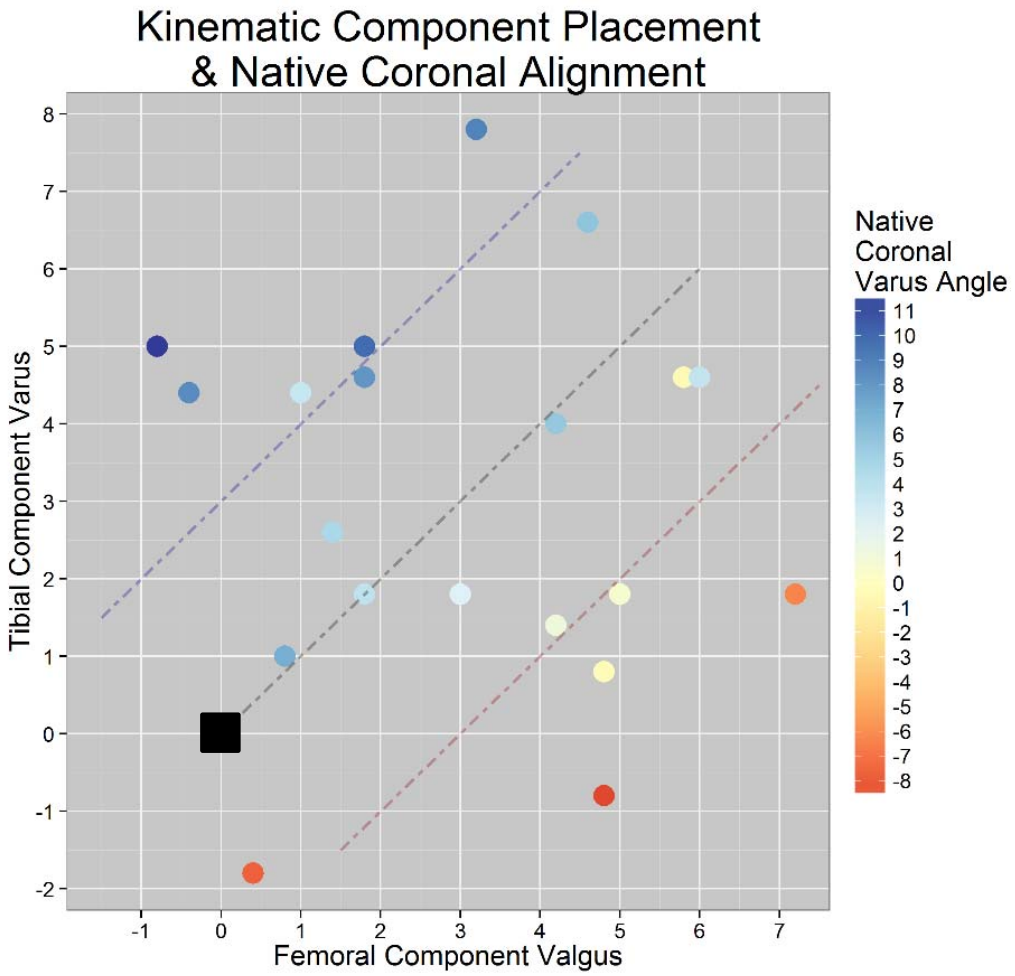

Figure 2.8. Kinematic alignment for femoral and tibial component valgus and varus angle shaded by the native coronal varus angle. The reference lines represent a 3° varus (blue), neutral (black) and 3° valgus (red) as the final coronal alignment. Mechanical alignment for femoral and tibial component is at zero (black square).

Simulated Tibio-Femoral Kinematics

Tibio-femoral kinematic results are shown in Figure 2.9. Statistically significant differences for paired t-tests at every time parameter were found ($p < 0.05$), with the exception of femoral AP translation

from 30° of flexion and lower. The difference between the mean results for medial FFC AP translation for the kinematic and mechanical simulations starts at 0.4 ± 0.9mm at 5° flexion, increasing steadily to 1.7 ± 1.4mm in deep flexion, kinematically aligned being anterior to mechanical. The lateral femoral FFC mean AP translation difference is 0.4 ± 0.6mm at 5°, increasing to 2.9 ± 1.9mm in deep flexion with mechanically aligned anterior. The change in medial and lateral femoral FFC throughout flexion also implicitly describes the tibio-femoral internal-external rotation; Kinematically aligned knees' lateral femoral FFC translates more posteriorly and medial femoral FFC translates more anteriorly than that of mechanically aligned knees', as flexion increases. Thus there is more external rotation of kinematically aligned knees. Also, there is relatively little difference in rollback behaviour, starting with no difference peaking at 0.8 ± 0.9mm at 96°, kinematically aligned posterior to mechanical.

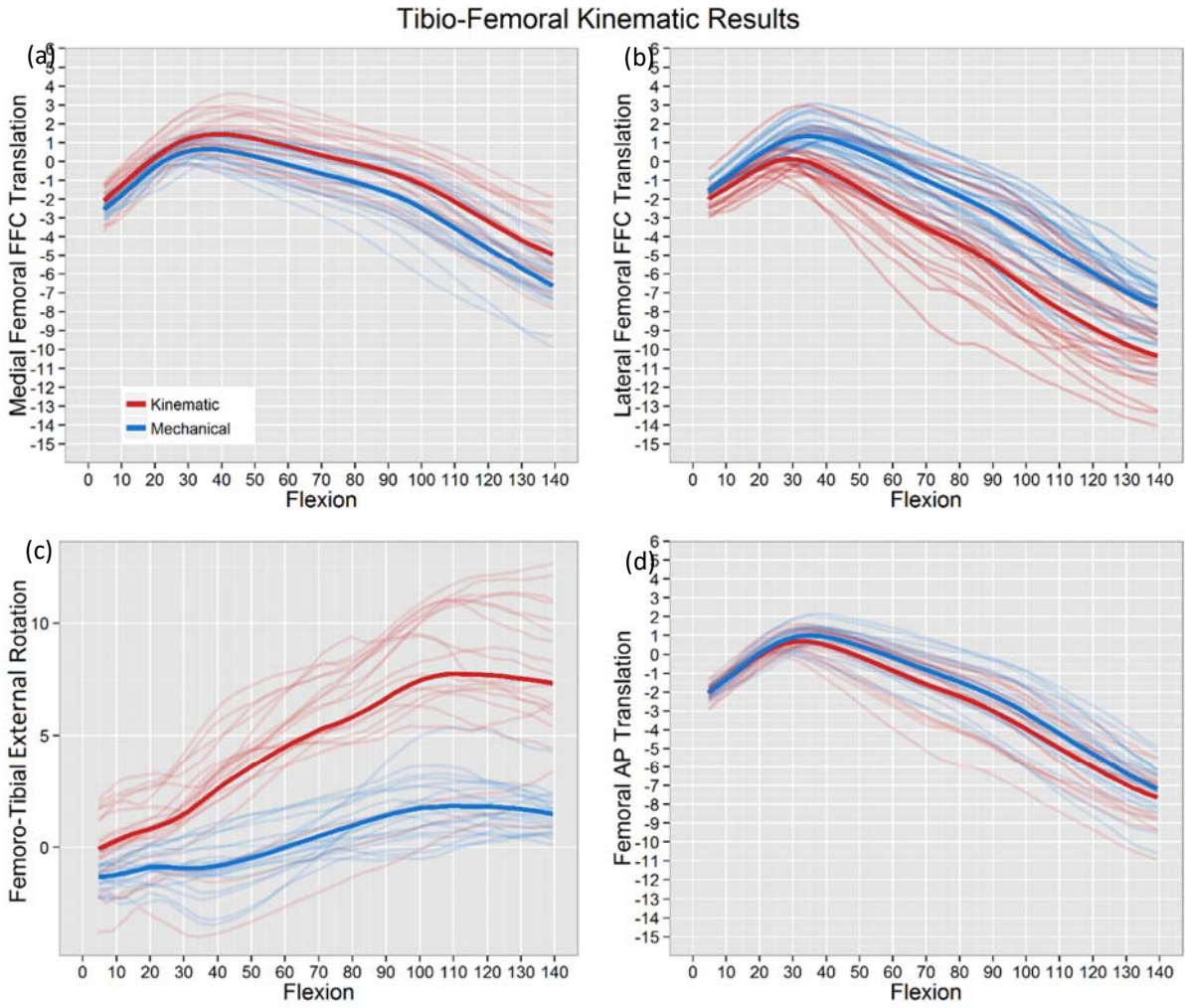

Figure 2.9. Tibio-femoral kinematic results for knee flexion. Red lines are kinematic alignment and blue lines are mechanical alignment. Solid lines are averages of each alignment. (a) and (b) medial and lateral flexion facet centre (FFC) antero-posterior drift from the lowest point of the tibial insert. Positive values indicate anterior translation. (c) Femoral-Tibial internal external rotation. Positive values indicate external rotation. (d) Femoral AP translation relative to the lowest point of the tibia insert.

Simulated Patello-Femoral Kinematics

The patello-femoral kinematic results are shown in Figure 2.10. Patella lateral shift exhibited statistically different parameter values for measurements of flexion between 10 and 40° and at angles

greater than 80°. Patella lateral shift for both alignment paradigms displayed a tendency towards medialising throughout the flexion cycle, though trend lines are different.

After starting in a common position, the kinematically aligned patellae tended towards shifting medially, peaking at 15° flexion where they were placed 1.8 ± 1.2mm more medial. The kinematically aligned patellae then tracked without further medial lateral shift while the mechanically aligned continue to drift medially, finishing in deep flexion 2.2 ± 1.6mm medial. Mean differences in patella lateral tilt under kinematic and mechanical alignment are significant up to 30° of flexion (p=0.05). Kinematic alignment begins the simulation at 2.7° ± 2.1° more internal tilt relative to the mechanically aligned at 5° flexion, with the kinematically aligned knees tilting internally by a mean 3.5° while the mechanically aligned knees are 0.8°. The means converge until about 60°, where they effectively show identical movement into 5° external tilt at 140° flexion.

Intra-patient differences for patella tracking are high, however, with the difference in tilt for a given patient with either alignment approach ranging from 6° more externally titled to 6.5° more internally tilted.

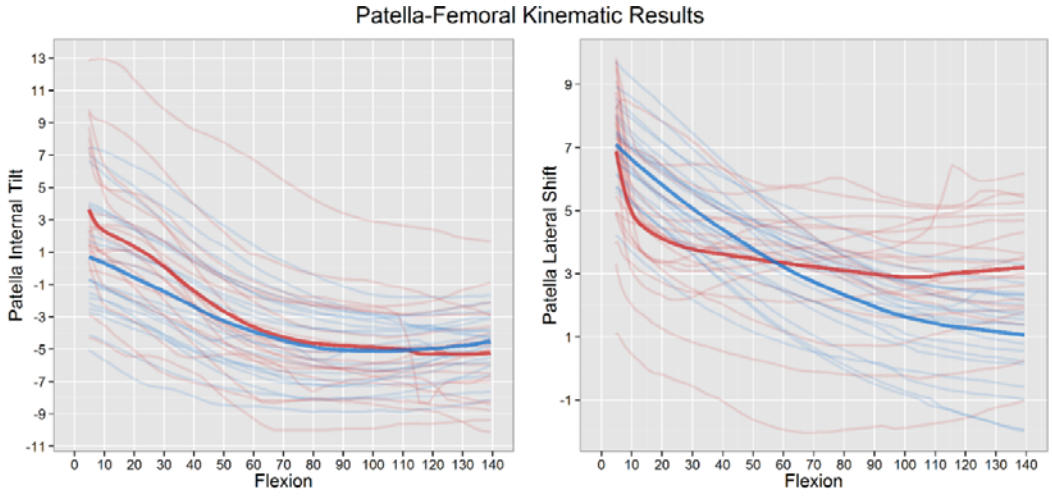

Figure 2.10. Patello-femoral kinematic results for patella external tilt (left) and patella lateral shift (right) for knee flexion. Red fine lines are kinematic alignment and blue fine lines are mechanical alignment. Solid lines are averages of each alignment.

Discussion

Recent data has challenged the importance of traditional mechanical alignment philosophy [267]. Recently, Bellemans et al [10] have introduced the concept of "constitutional varus", which hypothesizes that correction to a neutral mechanical alignment may not be "normal" for a significant proportion of the population. Their study showed 32% of asymptomatic men and 17% of asymptomatic women possess a natural mechanical alignment of 3° varus or more.

In conjunction with this principle, several surgeons have supported the restoration of kinematic, rather than mechanical, alignment in TKA [202, 205, 269] and Ji et al [282] reported that native and 'healthy' joint line were one and the same for Kinematically aligned knees. However, kinematically aligned knees shows lack of consistency regarding patient outcomes, survivorship, and surgical technique [170, 196, 202, 205, 269, 270]. Therefore, it remains unclear what are the optimal alignment targets for TKA despite of the emphasis on alignment philosophies for TKA.

Recently, Ishikawa et al [261] used computational model to analyse the kinematics of kinematically aligned knees. Their study suggests kinematically aligned knees produces near-normal knee kinematics. However, only a single model was used in the analysis and therefore the kinematics outcomes reported were limited.

In this study, pre-operative non-weight bearing CT scans of diseased joints in 20 patients were used to compare kinematic and mechanical alignment in a validated computational simulation. From patient CT scans, native coronal alignment was determined, and kinematic and mechanical alignment were planned (Figure 2.8). Ishikawa et al [261] used a clinically derived average kinematic alignment at 3° tibial component varus and 3° femoral component valgus which is equivalent to coordinates (3,3) on Figure 2.8. Our average alignment values were similar to reported alignment in clinical kinematic alignment studies [261, 282]. However instead of using an average kinematic alignment, our study accounts for significant variation of patient pre-operative anatomy.

Results for kinematic alignment (Figure 2.8) showed there was variation in the level of joint line obliquity with a set tibio-femoral coronal alignment. However, a trend between the native and kinematic tibio-femoral final alignment was observed. Any variation observed most likely occurred due to a condition of the pre-operative diseased joint and the wide range of adjustments necessary to attain kinematic alignment. When kinematically aligned, femoral components on average resulted in more valgus alignment to the mechanical axis and internally rotated to surgical transepicondylar axis whereas tibia component on average resulted in more varus alignment to the mechanical axis and internally rotated to the tibial AP rotational axis. This is consistent with other reports [205, 269].

In regards to tibio-femoral kinematics, both kinematic and mechanical alignment resulted in a broad trend towards anterior translation of the femoral component up to 30° flexion, followed by posterior translation as flexion increases (Figure 2.9). The kinematically aligned knees experience external rotation of the femoral component on the tibial component during flexion, with the angle increasing steadily from 1.2° ± 1.5° at 5° flexion to 5.9°± 3.3° at 140° flexion. This internal rotation of the femur relative to the tibia as the knee reaches full extension is comparable to screw home mechanism observed in native knee motion [15]. This effect is less so for mechanically aligned knees.

In regard to patello-femoral kinematics, for both kinematic and mechanical alignment there was high intra-patient differences for patella tracking (Figure 2.10). However, the difference in tilt for a given patient with either mechanical or kinematic alignment ranged from 6 degrees more externally titled to 6.5 degrees more internally tilted. There was less medial movement of the patella in deep flexion in kinematic aligned than mechanically aligned knees, though it arrived as its medial-lateral position earlier in the flexion. Differences in component alignment and potential impact on Q angle could explain some of the variation seen in patella-femoral kinematics for kinematically aligned knees.

Results for tibio-femoral kinematics for flexion and rotation as well as patello-femoral kinematics for tilt and shift were similar to that of previous computational biomechanical studies [217, 245, 261, 274, 275]. Variations existed primarily due to patient CT input, on which knee joint testing rig was

simulated, e.g. Oxford Knee Rig or Kansas Knee Simulator, or if the implant was cruciate retaining (CR) or substituting (PS), or the alignment strategy simulated.

Our results for tibio-femoral kinematics for flexion and rotation using both mechanical and kinematic alignment closely match results reported by Ishikawa et al [261]. All models exhibited anterior translation of the femoral component relative to the tibia during the early flexion phase and then posterior translation as flexion increased. The anterior translation from 0° to 30° of flexion was similar bilaterally in all models.

Patella lateral shift kinematics also replicated a similar pattern of mechanical alignment to that reported by Ishikawa et al [261]. However, patella lateral shift kinematics for kinematic alignment as well as patellar external tilt for both alignments varied markedly between our results and those reported by Ishikawa [261]. In the study reported by Ishikawa et al [261], in the kinematic alignment models the patella tilted more externally relative to the femoral component at 0° and 30° and after 60° increased in all models. It was similar in our study until 60-70° and then tilting plateaued. Plateauing after 60° flexion was also reported by Kobayashi et al [283] using healthy subjects in an in vivo study. Other explanations for this difference could be patient anatomy; Ishikawa study analysed 1 subject versus this study analysed 20 subjects, model assumptions, patellar button size or design of the intercondylar notch and anterior patella groove of the femoral component.

There were several limitations in this study. The study involved 20 subjects only and this may be insufficient given how variable knee alignment is across the population. Firstly, this study only assessed one implant design. The implants used in this study were multi-radius femoral component with a single design fixed bearing cruciate retaining TKA. Therefore, the results may not be applicable to other knee designs nor to mobile bearing or posterior stabilised knees. Also, the kinematics analysed were for closed-kinetic-chain knee extension and therefore functions such as walking or stair climbing may not be comparative. Furthermore, only kinematics was compared in this study. Ligament

forces and internal joint forces were not compared in this study as the computational model only validated for kinematic outputs.

The simulation model was subject to assumptions and variables common to many computational models: boundary conditions and muscle forces were assumed, only the lower extremity was modelled, there was limited soft tissue representation and cartilage was not accounted for. Such assumptions and variability are consistent with other computational modelling as well as in vitro modelling studies. However, computational modelling does offer the ability to simulate kinematics of different alignments on the same subject and thereby be potentially used as a predictive tool for pre-operative scenarios. Moreover, there are a number of studies that have shown that computational models could predict forces and kinematics that compared favourably to those found experimentally or in vivo fluoroscopy [217, 245, 274, 275].

Conclusions

In conclusion, kinematic alignment had more variation than mechanical alignment for all tibio-femoral and patella-femoral kinematics. This was particularly true for tilt and shift of the patella-femoral joint for kinematically aligned knees. Kinematic alignment corrects long leg alignment to a patient specific alignment which depends on the preoperative state of the knee. Also, when kinematically aligned, femoral components on average resulted in more valgus alignment to the mechanical axis and internally rotated to surgical transepicondylar axis whereas tibia component on average resulted in more varus alignment to the mechanical axis and internally rotated to the tibial AP rotational axis. The use of computational models has the potential to predict which alignment, kinematic or mechanical, could improve knee function patient specifically.

Chapter 3

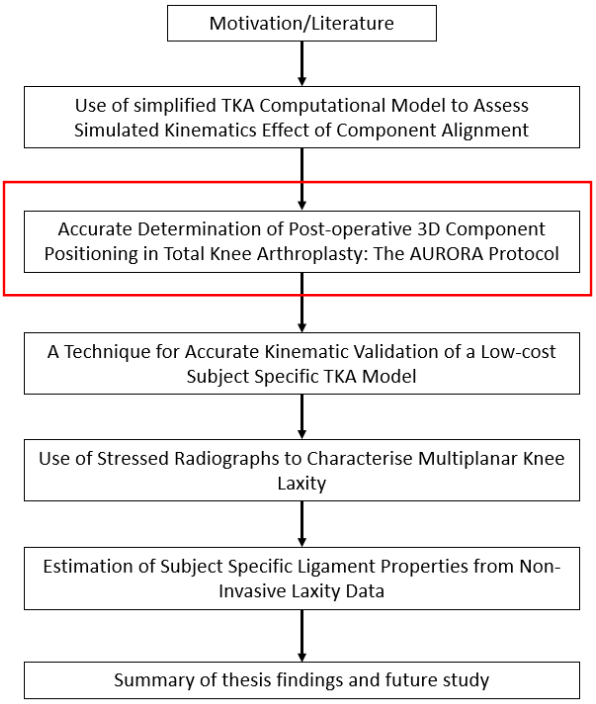

Accurate Determination of Post-operative 3D Component Positioning in Total Knee Arthroplasty: The AURORA Protocol

This chapter was published in Journal of Orthopaedic Surgery and Research

Wakelin EA, Tran L, Twiggs JG, Theodore W, Roe JP, Solomon MI, Fritsch BA, Miles BP., "Accurate determination of post-operative 3D component positioning in total knee arthroplasty: the AURORA protocol," (in eng), J Orthop Surg Res, vol. 13, no. 1, p. 275, Oct 30 2018.

In Chapter 2, we developed a knee computational model that replicates Oxford Knee Rig (OKR) deep knee bend and was able to demonstrate the model capability in demonstrating kinematic differences with different implant positions on the same subject. It was later realized that there was inconsistency in registration technique used to transform computational model and experimental reference frame in the first computational model validation. The computational models used for the first validation

were derived from post-op CT with implant CAD model registered against the scan. The anatomical landmarks were also derived from post-op CT which its determination affected by the metal flare in the post-op CT. Additionally, the experimental data was not registered accurately to the computational model reference frame resulting in inconsistent landmark definition used to compare the experimental kinematics and simulated kinematics.

This chapter describes a new technique to measure post-operative component position from Computed Tomography (CT). The technique developed involves registering both implant and preoperative bone 3D CT segmented models to a postoperative CT reference frame. Doing so allowed for a more accurate definition of component placement in all 3 planes, going beyond what 2D radiography can provide. The technique developed also eliminates the necessity to determine anatomical landmark from post-op CT, preventing inaccuracy of landmark determination due to metal flare.

This chapter was written as an independent published article, as such the content was targeted for more general readers. While not the primary author of this paper, my contribution to the publication includes the conception of the registration technique, development of the step-by-step instructions, designed and supervised the reproducibility study. In addition, I assisted in writing and reviewing the manuscript. I contributed 70% to the research design, 50% on data collection and 50% of manuscript preparation and review. Permission from the primary author has been provided.

Introduction

Dissatisfaction amongst total knee arthroplasty (TKA) is the result of a complex relationship between the patient anatomy, prosthesis design and position, and other patient specific factors. Prosthesis malalignment has been linked to poor patient outcomes in which coronal and axial malalignment have been most closely studied [204, 284]. To have confidence in the correlation between component alignment and outcome, the method used to determine component placement must be accurate and reliable.

Component alignment refers to the angular difference between the prosthetic components and patient derived antero-posterior (AP), medio-lateral (ML) and superior-inferior (SI) anatomic axes. This measurement has traditionally been the focus of post-operative analysis in TKA due to the ease of measurement [285-287]. Component placement refers to the translational movement of the prosthetic components along these patient specific axes. Due to difficulty in identifying the origin of these axes and accurately determining translation in space, component placement has been less well investigated. To understand the holistic effect of the TKA components on knee kinematics, both the alignment and placement must be taken in to account. Here we term the combination of component alignment and placement as 'component position'.

The pre-operative state of the patient is a critical source of missing data from most analyses which prevents accurate reporting of component position. Bony resections cannot be accurately determined from a post-op analysis alone and as a result there is very little data available on the outcome of TKA as a result of the modification of the anatomy [288, 289], highlighting the need for improved post-operative analysis techniques. Nevertheless, studies have investigated range of movement and maximum flexion as a function of the posterior condylar offset (PCO) [290-292]. In these publications a greater PCO resulted in higher maximum flexion due to reduced steric hinderance. Pre- and post-

operative measurements however were limited by the use of ML x-rays, indicating that the relationship must be strong to overcome such errors.

Alteration of the joint line and flexion/extension gaps are associated with a change in joint kinematics [293] and patient outcome [294]. In these studies, patients with less change to the coronal joint line reported improved WOMAC and Knee Society Clinical Rating Scores. Identification of such changes however can be difficult, as the joint line and joint gaps can be modified without affecting the appearance of the component alignment [287]. To better understand the effect of bone resections, joint line and gap modification, accurate pre-operative geometry data is required. Similarly, Bengs et al.[295] found that increasing patella button thickness without increasing the patella resection, decreased maximum passive flexion. Identification of appropriate patella resection for a given button thickness would not be possible with traditional post-operative analysis techniques.

Traditional methods of assessing TKA component alignment, including short leg x-rays [296-298], long leg x-rays [299], and post-operative 3D imaging only [300-304], have been shown to suffer inaccuracies from anatomic variability, projection errors, and difficulty in identifying patient specific landmarks from the post-operative imaging. To improve landmarking and component placement accuracy, a pre-operative CT is required. Fortunately, CT imaging is rapidly becoming a standard of care in pre-operative planning for TKA [305], and is available for a wide range of patients. Pre-operative CT imaging allows a volumetric registration of the pre-operative and post-operative bones and component geometries in 3D space eliminating any anatomic assumptions and projection errors. The models can then be used to determine bony resections and component placement. A method to compare the pre-operative state of the knee to the post-operative component position and bone resections, in which accuracy has not been affected by component flare has not yet been achieved.

Here we introduce a method of 3D reconstruction which utilises both a pre-operative and post-operative CT scan to determine the post-operative component position in TKA. The method may be extended to any joint replacement and is termed here the Australian Universal Resection, Orientation

and Rotation Analysis (AURORA) protocol. Landmarks and bone models unaffected by component flare obtained from the pre-operative scan are transformed into the post-operative frame of reference. Component position as defined by the landmarked patient specific axes and bony resections are reported. The reproducibility and reliability of this method are presented and compared to other post-operative analysis techniques. This registration method is considered accurate and suitable to be used when absolute difference in registration results is less than 1° and 1mm and repeatability intraclass correlation coefficient of at least 0.9.

Methods

CT Protocol

A series of patients received long leg pre-operative CT scans for routine pre-operative planning of TKA surgery [306] and to design patient specific instrumentation. Ethics approval for all data collection and accessing information from a joint registry for this study was approved by Bellberry Ethics (Sydney, Australia) (approval 2012-03-710). The same protocol is followed for post-operative CT imaging. This protocol requires the patient to be in supine at the isocentre of the gantry, with both legs fully extended and parallel to the horizontal plane. The legs are straightened and maintained in a relaxed position. Image acquisition involves a full leg pass CT scan taken through both limbs with all images taken in the same field of view, see Figure 3.1. This allows detection of any patient movement during the scanning process. Transverse slice thicknesses of 1.25 mm are taken, with less than 1 mm slices taken within the sagittal and coronal axis.

All patients investigated here had a TKA using OMNI APEX implants (Raynham, MA), from 4 different surgeons using 4 different techniques. Patients were randomly selected from a database of over 2000 TKA surgeries.

The CT dose is calculated by multiplying the dose-length-product (mGy.cm) provided as supporting information with the CT scan, by the length of the CT scan in which the patient is imaged. The dose

value is then converted to an effective dose based on anatomic conversion coefficients presented by Saltybaeva et al. [307] to allow comparison between different CT protocols. Movement in the scan can affect both individual bone and long leg measurements. Movement is detected by an engineer assessing the scan before processing. All patients were randomly selected from a database of patients scanned over a 3-month period previously confirmed to have not moved.

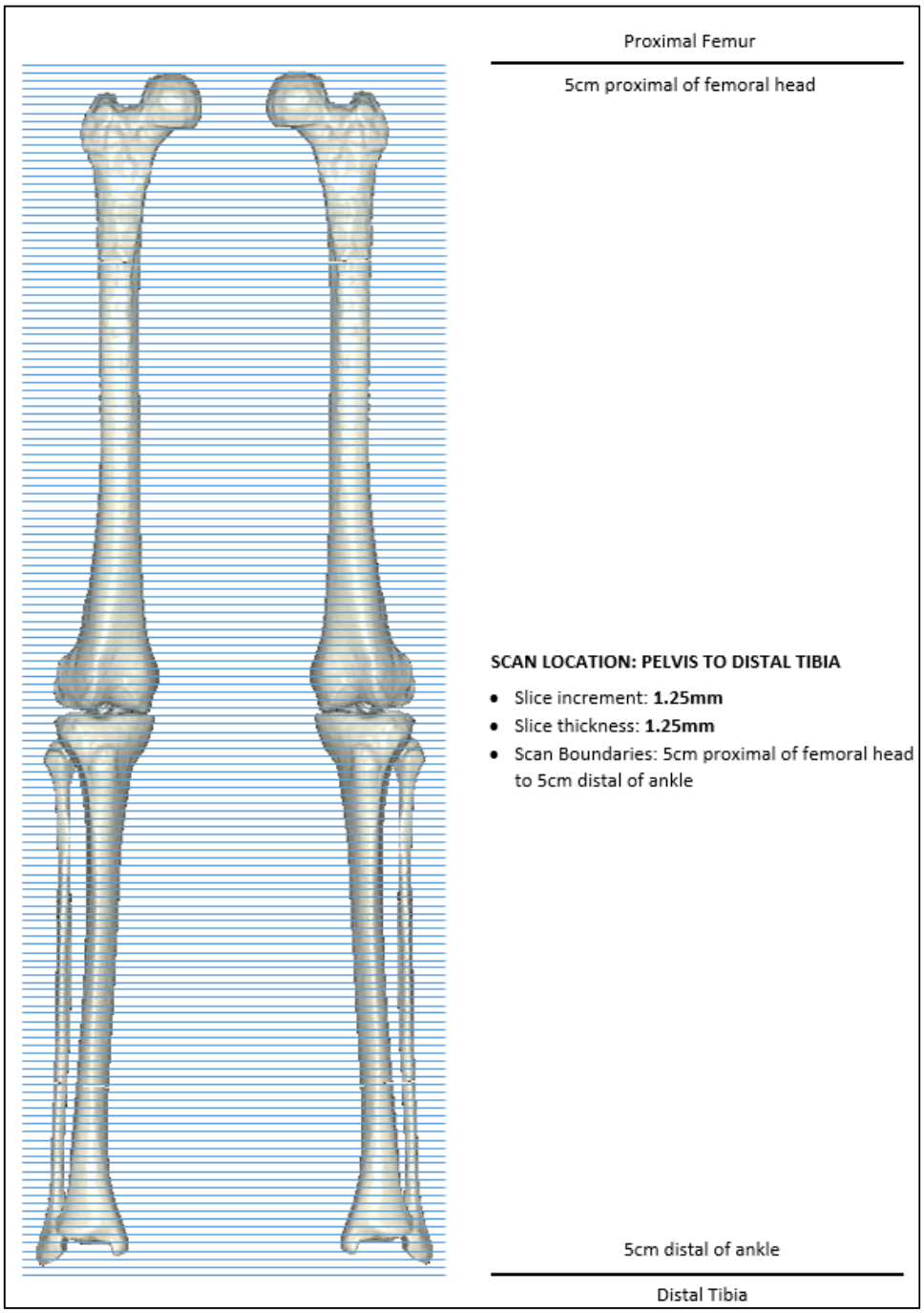

Figure 3.1. Single-pass CT scan through both limbs

Image processing and Volumetric Registration

3D reconstructed patient femur and tibia bones are generated within the pre-operative planning process through semi-automated segmentation, used to landmark and identify points of interest by biomedical engineers using the 3D imaging software, ScanIP (Simpleware, Exeter UK). The accuracy of

the landmarking process depends on the CT slice thickness. In this study, 1.25mm axial slice increment was used in CT protocol and therefore the landmarking accuracy is 1.25mm. The patient bones are converted to stereolithography (STL) files and manually landmarked twice by different engineers. The landmarking was done on the generated STLs with combination of reviewing them in the 2D CT slices. If any landmarks taken by first and second engineer differ by a threshold value (in this case 4 mm), the landmark was reviewed by a third trained engineer. Landmark references were used to define patient specific bone axes and soft tissue attachment sites, see Figure 3.2A. The femoral and hip centres are landmarked to define the mechanical axis of the femur. The tibial mechanical axis is defined from the midpoint of the lateral and medial malleoli to the midpoint of the medial 1/3 of the tubercle and PCL insertion. The tibial AP axis is defined along the medial 1/3 of the tubercle and PCL insertion, while the Transepicondylar Axis (TEA) is defined along the medial sulcus to the lateral epicondyle on the femur. These axes are used to define a frame of reference from which implant position may be calculated.

Using the post-operative full leg CT scan, 3D post-operative femur and tibia bone sections unaffected by the component flare are segmented, see Figure 3.2B. 3D registration is then performed, by registering the pre-operative femur and tibia models into the post-operative CT with reference to both the imaging and newly generated post-operative bone models, see Figure 3.2C. Point-to-point registration is performed on CAD models of the implanted prosthesis and segmented prosthesis models from the CT, see Figure 3.2C. All registration is refined using model outlines viewed in the full leg CT scan. A second engineer reviews both the registered femur and tibia bones, and the femoral and tibial implant components to further refine both bone and implant positions within the CT scan.

Euler transform matrices are obtained from the resulting registered pre-operative bones and used to transform the pre-operative bone landmarks into the post-operative CT reference frame. Using the transformed landmark references, component alignment and placement are determined within the local reference frames from the defined axes of landmarks identified pre-operatively.

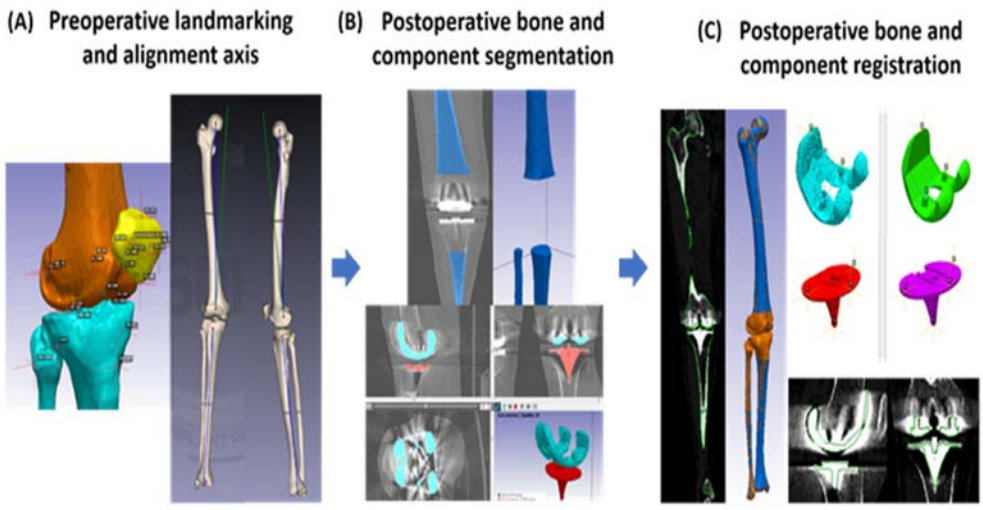

Figure 3.2. Post-operative process workflow showing a) pre-operative bone segmentation and landmarking, b) segmentation of post-operative bones and components, and c) registration of pre-operative to post-operative bones and components.

Accuracy testing

ScanIP software an FDA approved medical software specifically designed to process medical imaging and registration of 3D models. Therefore, the software measurements would have been validated before FDA approval. Further validation study was conducted internally to validate ScanIP measurement outputs (refer to Appendix C). Since ScanIP software outputs had been validated, the accuracy of the described registration method is dependent only on the operator who perform the tasks. Therefore, the accuracy is described using reproducibility and reliability analysis.

Reproducibility

Two primary TKR patients were processed post-operatively twice by 3 engineers in a 2-week period. Patient CT scans were segmented and registered by an engineer and then reviewed by a second. The same case was processed again by the initial engineer on another day at a different time of day and

then reviewed by a third engineer. This process was repeated across the 3 engineers for the 2 cases with alternating reviewers, and a total of 12 registrations was then analysed (see Figure 3.3).

Comparison of component alignment angles in flexion/extension (FE), varus/valgus (VV) and internal/external (IE) rotation, and component placement values by measuring the femoral medial and lateral, distal and posterior condyles, and the medial and lateral tibial plateau was recorded. Reproducibility was assessed from these angular and resection measurements by determining the maximum difference and standard deviation from the mean calculated for each patient, with the 95% confidence interval defined across both cases.

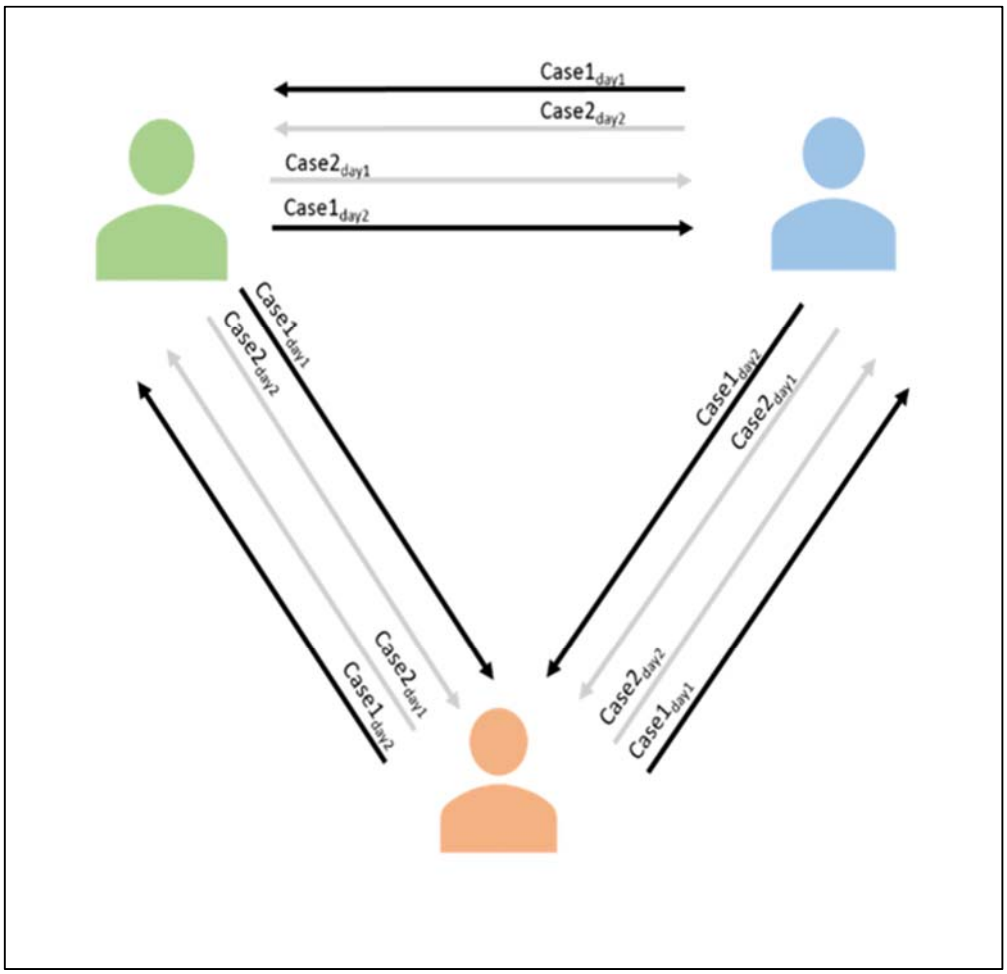

Figure 3.3. Flow diagram of reproducibility quality control.

Reliability

To describe the interobserver reliability, 11 TKR patients were processed post-operatively between 2 engineers. Each case was reviewed by a third and fourth engineer, with refinement of the bone and component registration made by the reviewing engineer if necessary. A set of 22 results were produced for comparison of the 3 rotation axes across two components and 6 resection measurements. The intraclass correlation coefficient (ICC) was calculated for each of the measurements. An ICC value of 1 shows perfect reliability, values greater than 0.9 indicates an excellent result, 0.81 to 0.9 is very good, 0.76 to 0.80 is good, 0.5 to 0.75 is moderate and <0.50 is considered to show poor reliability [308, 309].

Results

Radiation Dose

The average effective radiation dose received per CT scan using this protocol is 1.24 ± 0.96 mSv. This dose is compared to other CT and radiography protocols in Figure 3.4. The average received dose is lower than all protocols shown in the figure with the exception of the most recent Imperial Protocol [288] and a standard AP radiograph. The spread of values shown for the AURORA CT protocol used here reflect the large range of patient sizes scanned. Smaller patients receive a correspondingly lower dose of radiation and vice versa for larger patients.

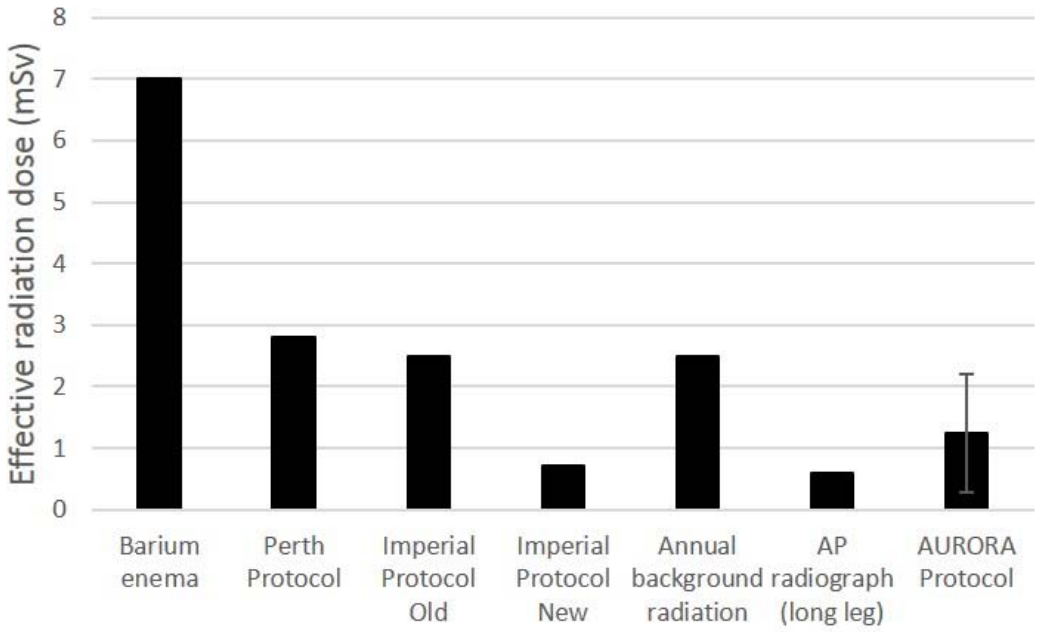

Figure 3.4. Comparison of the AURORA CT protocol with a barium enema and other relevant protocols for determining prosthesis positioning. AURORA protocol dose is calculated from CT reports, all other data taken from Henckel, et al [288].

Using the AURORA protocol, patient movement in the CT scan may be detected at any point along the length of the bone. In previous methods, such as the Perth CT and Imperial protocols, movement in the mid femur and mid tibia will not be detected, leaving any measurements to propagate through the protocol as an error. In a database of CT scans obtained for routine pre-operative planning of TKA, the rate of scans identified with movement over a 3-month period is 6.78% (total number of scans: 118). Of this fraction, all movement in the scans were detected in the mid femur and mid tibia regions.

Reproducibility

The alignment reproducibility results generated from three engineers processing two cases at two different time points which were then QC checked are shown in Table 3.1. The maximum difference from the mean angle is shown for each case. In both cases the maximum difference is reported for tibial component axial rotation, of 0.9^{o} for case 1 and 0.7^{o} for case 2. In all other angles, the maximum

difference in rotation is ≤ 0.5^{o}. The confidence intervals in all cases are less than 0.3^{o} with the exception of tibial tray IE rotation, which is 0.6^{o} for case 1, and 0.4^{o} for case 2.

The bony resection thicknesses are a proxy measure for the accuracy of measuring component placement and are shown in Table 3.2 for the distal medial and lateral condyles, posterior medial and lateral condyles, and tibial medial and lateral plateaus. The maximum difference from the mean resection is shown for each case. In both cases the maximum difference is reported for the medial tibial plateau, of 0.5 mm for case 1 and 0.3 mm for case 2. In all other resections, the maximum difference in resection is ≤ 0.3 mm. The confidence intervals in all cases are less than 0.3 mm.

Table 3.1 Reproducibility results showing the difference in calculated component angular alignment across two cases performed by three engineers at two different time points. The maximum average difference for each case and a 95% confidence interval is shown for all three axes of rotation for the femoral and tibial components.

Case	Operator	Run	Femoral Component Alignment			Tibial Component Alignment		
			F/E	V/V	IE	F/E	V/V	IE
Case 1	Sim Eng A	Run 1	1.1	-0.6	-0.8	7.1	0.6	5.9
Case 1	Sim Eng A	Run 2	1.0	-0.5	-1.2	7.0	0.4	6.2
Case 1	Sim Eng B	Run 1	1.0	-0.8	-1.5	7.0	0.5	4.5
Case 1	Sim Eng B	Run 2	0.8	-0.7	-0.8	7.4	0.4	4.7
Case 1	Sim Eng C	Run 1	1.1	-0.6	-1.8	6.9	0.8	5.5
Case 1	Sim Eng C	Run 2	1.1	-0.4	-1.0	7.2	0.6	5.9
Maximum Difference from Average (°) ± 95% CI			0.2 ± 0.1	0.2 ± 0.1	0.5 ± 0.3	0.3 ± 0.1	0.2 ± 0.1	0.9 ± 0.6
Case 2	Sim Eng A	Run 1	1.9	-0.9	0.1	8.2	1.5	3.0
Case 2	Sim Eng A	Run 2	2.3	-0.8	-0.1	7.7	1.8	2.7
Case 2	Sim Eng B	Run 1	2.3	-0.7	-0.2	7.9	1.7	1.7
Case 2	Sim Eng B	Run 2	2.1	-0.8	0.4	8.4	1.4	2.8
Case 2	Sim Eng C	Run 1	2.0	-0.7	-0.2	7.9	1.0	2.3
Case 2	Sim Eng C	Run 2	1.8	-0.8	0.0	8.4	1.5	2.8
Maximum Difference from Average (°) ± 95% CI			0.3 ± 0.2	0.1 ± 0.1	0.3 ± 0.2	0.3 ± 0.2	0.4 ± 0.2	0.7 ± 0.4

Table 3.2 Reproducibility results showing the difference in calculated bony resection thicknesses (giving a measure of the accuracy of component placement) for the distal medial and lateral condyles, posterior medial and lateral condyles, and tibial medial and lateral plateaus across two cases performed by three engineers at two different time points. The maximum average difference for each case and a 95% confidence interval is shown for all resections.

Case	Operator	Run	Femoral Resections				Tibial Resections	
			Lat. Condyle	Med. Condyle	Post. Lat. Condyle	Post. Med. Condyle	Lat. Plateau	Med. Plateau
Case 1	Sim Eng A	Run 1	6.5	6.0	10.0	10.3	11.2	10.0
Case 1	Sim Eng A	Run 2	6.2	5.7	10.0	10.7	10.3	9.0
Case 1	Sim Eng B	Run 1	6.1	5.4	10.2	11.1	10.5	9.3
Case 1	Sim Eng B	Run 2	6.8	6.1	10.2	10.6	11.1	9.8
Case 1	Sim Eng C	Run 1	6.2	5.7	9.5	10.7	10.7	9.6
Case 1	Sim Eng C	Run 2	6.4	6.0	9.9	10.3	11.1	9.9
Maximum Difference from Average (mm) ± 95% CI			0.3 ± 0.2	0.4 ± 0.2	0.4 ± 0.2	0.4 ± 0.2	0.4 ± 0.2	0.5 ± 0.3
Case 2	Sim Eng A	Run 1	6.0	7.4	10.9	10.3	11.0	6.7
Case 2	Sim Eng A	Run 2	6.2	7.8	10.8	10.3	11.1	7.0
Case 2	Sim Eng B	Run 1	6.1	7.7	10.6	10.2	10.9	6.7
Case 2	Sim Eng B	Run 2	6.1	7.6	10.8	9.9	11.2	6.9
Case 2	Sim Eng C	Run 1	5.9	7.5	11.0	10.6	11.0	6.3
Case 2	Sim Eng C	Run 2	6.0	7.4	10.9	10.4	10.9	6.6
Maximum Difference from Average (mm) ± 95% CI			0.2 ± 0.1	0.2 ± 0.1	0.2 ± 0.1	0.2 ± 0.1	0.2 ± 0.1	0.3 ± 0.2

Reliability

The rotational alignments and bony resections for the femur and tibial components reported for 11 cases performed twice (each time by a team of two different engineers) are shown in Figure 3.5 and Figure 3.6. The ICC value is given for each alignment and resection variable. The lowest reported ICC

variable is for femoral axial rotation, with an ICC of 0.93. These values are all above 0.9, indicating that across all rotations and resections in both the femur and tibia, the protocol reports excellent reliability.

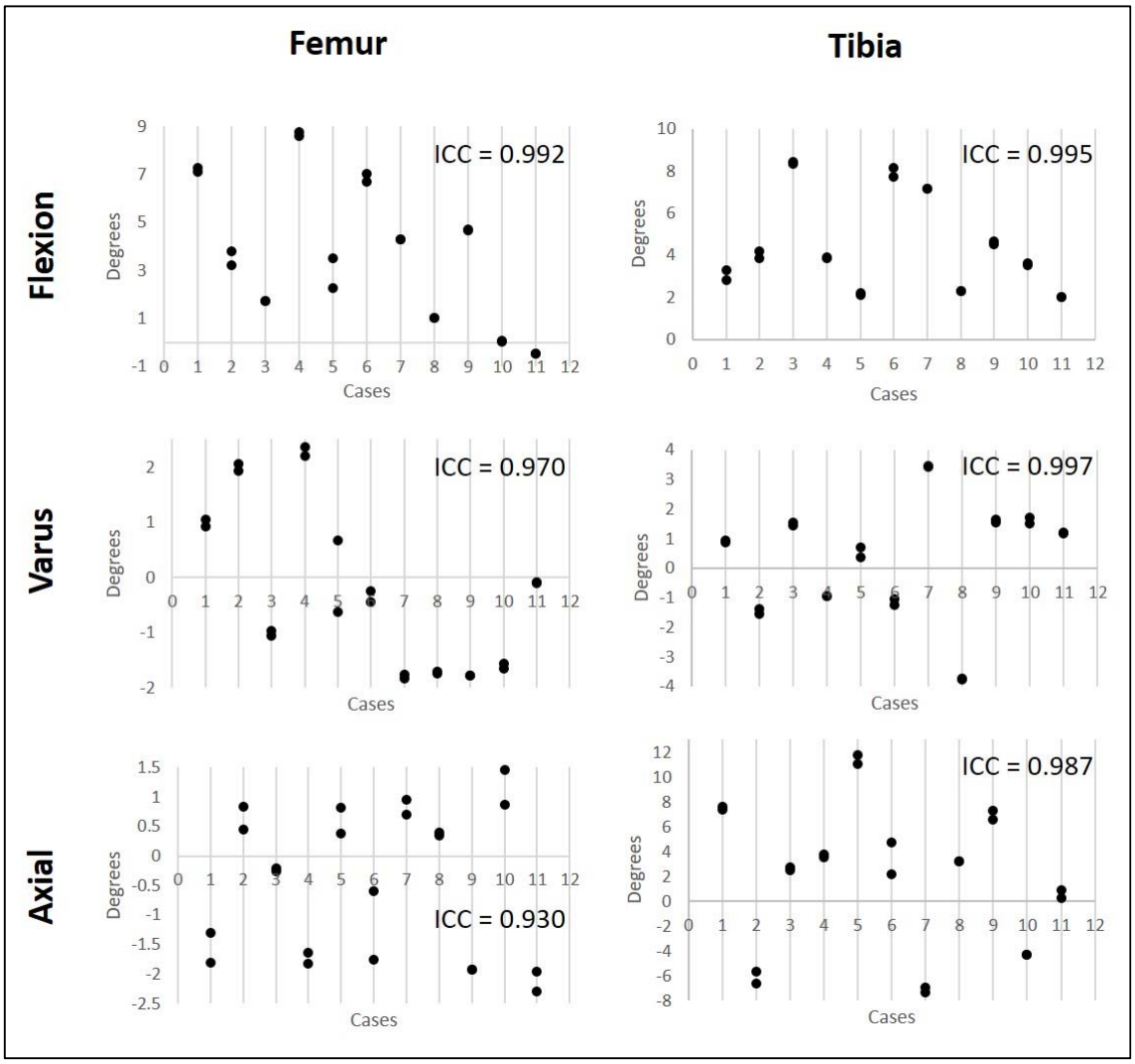

Figure 3.5. Reliability testing for femur and tibia placement showing the coronal, axial and sagittal rotation reported by the method across 11 cases performed by two engineers, followed by two additional engineers reviewing the placement. The ICC for each rotation in each component is reported. All values are greater than 0.9 indicating excellent reliability.

Discussion

The maximum component alignment differences from the mean within this study are low compared to previous literature and provide a confidence interval up to 10 fold narrower when compared to protocols in which individual CT slices were investigated [300, 301, 304, 310], or only post-operative CT scans were available [311, 312]. The maximum error of < 1^{o} is similar to protocols using more advanced techniques, such a computational edge detection, however these studies did not include ICC coefficients, so an assessment of the repeatability was not possible [313]. The highest deviation from the mean was the tibial IE rotation at 0.9^{o} and 0.7^{o} for the two cases, with a confidence interval of 0.6^{o} and 0.4^{o} respectively. These values represent an 8 fold improvement in accuracy compared to previous attempts to measure tibial rotation [314]. Previous attempts have reported difficulty in measuring tibial IE rotation due to the variability in the landmarks required to define a useful axis [315]. By combining the pre-op and post-op CT, the landmarks that define the AP axis can be identified more easily than using post-op CTs alone. Although there may still be some debate over which landmarks are the most appropriate, this method allows points to be defined that accurately reproduce an anatomic axis across multiple subjects. The origin of all axes may be redefined based on future literature if needed.

The resulting resection level measures of the femur and tibia also show high reproducibility, with the highest deviation seen for the medial tibial plateau resection at 0.5 mm and 0.3 mm between the two cases and confidence intervals of 0.6^{o} and 0.4^{o}, respectively. The magnitude of the error here, however, is only slightly above the other resections, indicating that there may not be a systematic reason for reduced accuracy when placing this component. Previous attempts have been made to investigate the effect on TKA outcome arising from resection levels. These studies have mainly focussed on the femur, particularly the posterior condylar offset [290, 316, 317]. These techniques however have primarily relied upon fluoroscopic images, and planar x-rays which were discussed previously to be inaccurate, limiting the reliability of such studies.

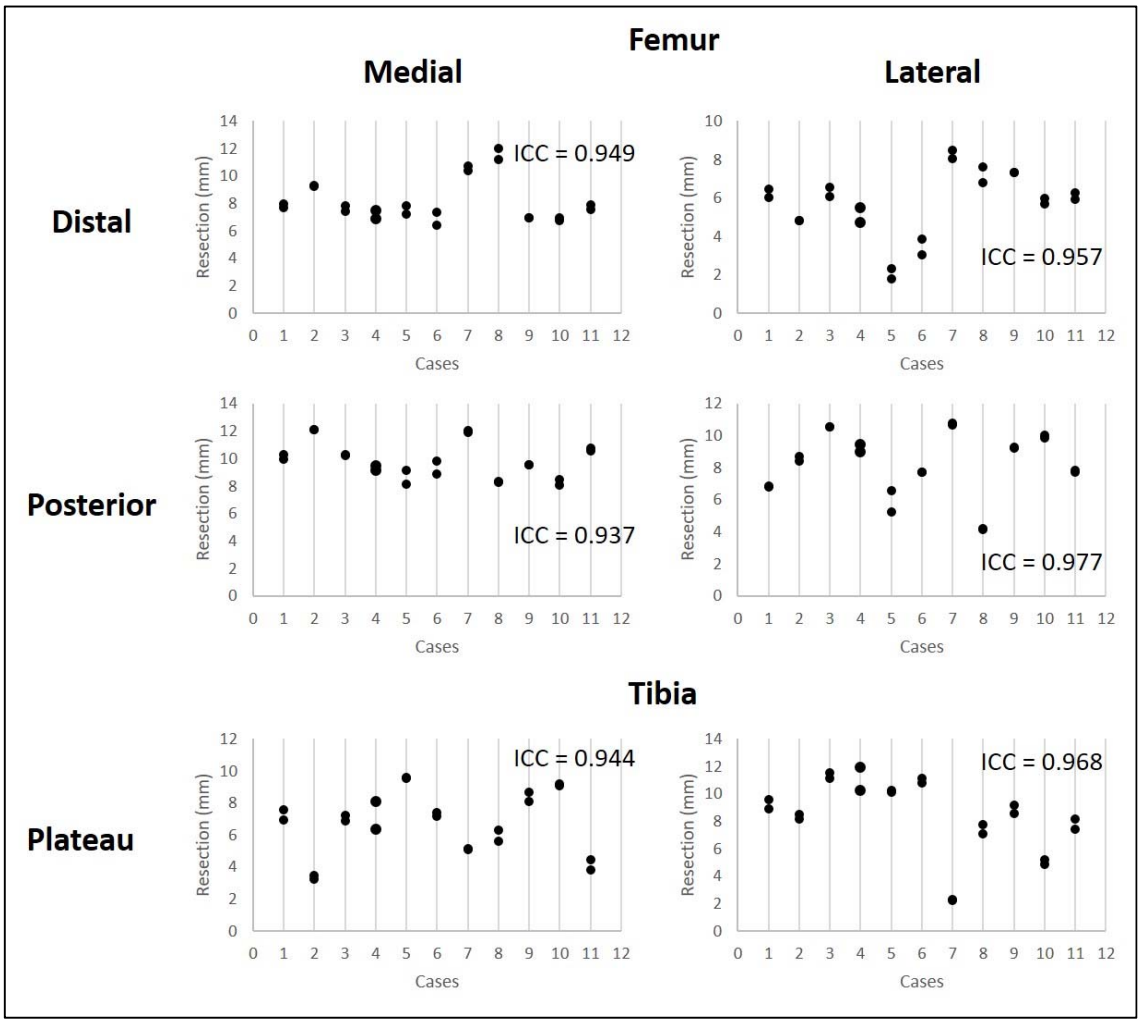

Figure 3.6. Reliability testing for femur and tibia bony resections reported by the method across 11 cases performed by two engineers, followed by two additional engineers reviewing the placement. The ICC for each rotation in each component is reported. are greater than 0.9 indicating excellent reliability.

Across both femoral and tibial component alignments and bony resections, this 3D pre-operative registration process shows excelled reliability, in which all ICC values report greater than 0.93. The lowest reported ICC value of 0.93, resulting from the femoral axial IE rotation measure, is primarily due to the difficulty of post-operative registration of the femur component. The posterior condyles, which dominate the axial rotation positioning, of the APEX implant used in this study are thicker than the distal condyles (11 mm vs 9 mm) and tibial tray (~3 mm). As such, the CT flare is greater in these regions, reducing the accuracy of the registration. The ICC values reported here are consistently similar

to or higher than other post-operative analysis techniques [289, 304, 318] indicating this method is not only accurate, but suitable for routine post-processing by multiple users.

The high reproducibility and reliability of calculating both component alignment and bony resections performed by surgeons, can lead to a better understanding of the influences of component alignment and component placement. Current literature has thoroughly reviewed the influence of component malalignment and poor patient outcomes [185, 319, 320]. Missing from all of these analyses however, is an understanding of the patient's preoperative anatomy, leading Hadi et al. [185] to conclude that there is a dubious link between component malalignment and patient outcomes. From this post-operative analysis, we can begin to determine how the bony resections and the combination of component placement and alignment influence outcome on a patient specific level in greater detail. For example, the use of reliable bone resection measures from pre-operative bones may provide insight into the change of a patient's soft tissue profile post-surgery. From the pre-operative CT scans, comparative ligament lengths and change in length resulting from component alignment and placement can be investigated from landmarked attachment sites. CT scans in this analysis however, are performed in a non-functional supine position, such that the distance between ligament attachment sites may not be representative of the functional length of the ligament. Functional imaging may be introduced to this workflow in future to this issue without a change in post-processing techniques.

The proposed 3D registration process for post-operative analysis involves additional pre-operative CT imaging compared to other processes [288, 300]. Though this increases x-ray exposure to the patient, pre-operative planning, generally requiring a CT scan, is becoming the standard of care for TKA [305], such that the pre-operative scans are not for post-operative analysis alone. The protocol used here is a low dose CT, with radiation exposure less than the typical yearly background radiation and similar to protocols currently in use [288]. All patient movement identified in pre-operative scans occurred in the mid femur and mid tibia regions, indicating that protocols which did not include the mid femur

and tibia sections would report inaccurate component placement. The resulting error in component position if these scans were used is the subject of further study.

Manual translation and rotation of the pre-operative bones and component geometries into the post-operative CT scan is reasonably labour intensive, requiring on average 60 minutes to complete, before the registration is quality control checked by a second engineer with additional experience. Further refinement of the proposed post-operative analysis process could include the use of an automated registration method. A preliminary automated registration process using the Iterative Closest Point method (ICP) [312] was performed on these cases. The registration time was observed to reduce to approximately 2 minutes, from which the results were then fine-tuned by one engineer and quality control checked by a second engineer, representing a 30-fold decrease in time. Further development of the ICP method to optimise parameters around fitting regions of interest, reliability, and time for analysis may allow accurate post-operative analysis to be part of routine care and is the subject of future studies.

Joint infection and component loosening are a cause of dissatisfaction and revision surgery. Joint infection can be identified by swelling of the joint and pathology reports, however these are not always conclusive. Combining component position as determined using the AURORA protocol with SPECT imaging could identify bone metabolism associated with infection or component movement [321]. Although current methods integrating SPECT imaging with CT do not improve the accuracy of determining component placement, such methods may be used to augment a pre-operative and post-operative CT 3D reconstruction to add metabolic activity.

The proposed post-operative 3D registration method described here has some limitations. The current time taken for this analysis as mentioned is approximately 60 minutes, this represents a high engineering burden, and must be reduced to improve use in routine analysis. Commercially, TKA component geometry varies between medical device manufacturers, forming a significant part of their IP portfolio, as such, the component geometries must be obtained from the implant companies, which

may be difficult – limiting the generalisability of this technique to engineering firms with a close relationship with implant companies. The reproducibility analysis performed here utilises 2 cases processed at multiple time points by multiple engineers of equal training. To better understand the reproducibility, particularly when processing outlier or severely pathological anatomy, a greater number of cases should be analysed. Furthermore, this method requires pre-op and post-op CT. Even though low dose CT is used for this method, there is still additional radiation and cost associated.

Other methods to assess component position such as bi-planar x-rays followed by 2D to 3D registration offer a number of advantages over a CT, such as providing long leg assessments in a functional state [322]. Such techniques however, may require fluoroscopic agents [323], may only capture the region around the knee, and are performed on apparatus less widely available than traditional x-ray or CT machines, limiting its use [313].

Conclusion

Component alignment has been of great interest in total knee arthroplasty, however the focus has previously been on achieved component alignment and identification of malalignment without regard for the component placement or pre-operative anatomy. The method presented here uses a low dose CT scan to analyse the position and rotation of all components in 3D space, with comparison to the pre-operative anatomy, allowing surgical changes to the joint to be determined. The method shows excellent reliability and reproducibility by removing sources of error that are typically associated with post-operative total knee arthroplasty analysis. Routine use of this analysis in TKA as well as other joint replacement procedures will allow surgeons and engineers to better understand the effect of component alignment as well as placement on outcome.

Chapter 4

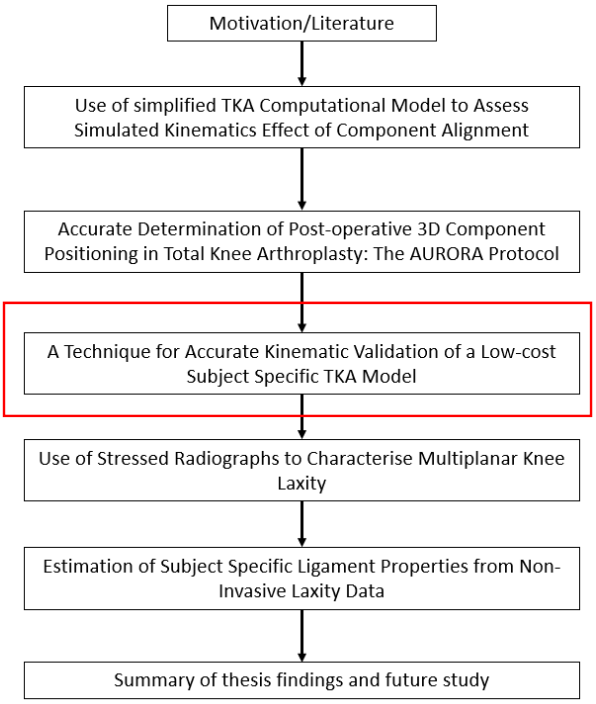

A Technique for Kinematic Validation of a Low-cost Subject Specific TKR Model Derived from CT Scan

This chapter was submitted to journal Recent Advances in Arthroplasty

Willy Theodore; Joseph Little; Edgar A Wakelin; Justin Roe; Darryl D'lima; Mark Taylor; Brad Miles

Introduction

Total Knee Arthroplasty (TKA) is a highly successful surgical intervention that relieves pain and improves the quality of life for osteoarthritis sufferers. Despite low revision rates, as many as 20% of recipients remain dissatisfied with long term pain after surgery [141, 324, 325]. Component alignment [326-328] as well as patient specific anatomical variation [306, 329, 330] has been shown to alter the kinematics and performance of the knee. Knee kinematics post-TKA therefore, are a product of complex interactions between the component design, component alignment, and patient specific anatomic characteristics [140, 331, 332]. Understanding these complex interactions pre- and intra-operatively can help surgeons better plan surgery to achieve optimal outcomes.

Techniques such as ex-vivo force-controlled mechanical simulators [333-336], video fluoroscopy [337] and gait labs [338] have been used to study knee kinematics under simulated and real dynamic activities. This process however is expensive and inefficient to iterate experiments over a wide variety of variables (i.e. alignment and position of each component, variable anatomy etc.). Furthermore, ex-vivo testing is limited to cadaver specimens and therefore has limited applicability to be used as a tool to study complex interactions pre-operatively. Computational modelling however, is a scalable alternative [339] that allows the study of both patient and surgical factors and their interactions on knee kinematics.

In Chapter 2, we developed a knee computational model that replicates Oxford Knee Rig (OKR) deep knee bend and was able to demonstrate the model capability in demonstrating kinematic differences with different implant positions on the same subject. It was later realized that there was inconsistency in registration technique used to transform computational model and experimental reference frame in the first computational model validation. In previous chapter, we demonstrated a registration technique to obtain accurate 3D implant position using pre-operative and post-operative CT. The technique developed will be utilized in this chapter. It was also realized in the first model validation

that inconsistent landmark definition was used to compare the experimental kinematics and simulated kinematics.

Previous model development that replicates OKR deep knee bend validation studies have compared simulated kinematics against kinematics recorded in an experiment knee simulator with definition described in the Grood and Suntay coordinate system [244, 246, 261, 340]. However, the landmarks used to create the experimental kinematics were not identical to the landmarks used to create the simulated kinematics. For example, Colwell et al [246] digitized bony attachments during the experiment to calculate the experimental coordinate system but the simulated kinematics coordinate system was created using scaled bony attachment sites. This resulted in fundamental difference in kinematics definition. Furthermore, a previous study by Victor et al [305] reported that there is high variability in anatomical feature localisation or landmarking, particularly from post-operative CT where metal flares present. Therefore, if only post-op CT is used to define the cadaver computational model, there is a high chance the anatomical axes digitized may not represent the true axes.

More recent studies have reported improved kinematics comparison technique however it is still unclear whether the landmarks used in creating both coordinate system were identical [250-252]. Kansas research group in their computational model studies [217, 341] dissected the knee specimen after experiment and register the experimental digitized landmark points to the CT model using rigid body fixtures. This method has a risk of unwanted movement of the fixtures during experiment particularly after cutting and dissecting the bones which may introduce different relative landmark position at different stages of experiment. Kia et al [342] and Vanheule et al [343] used different workflow in their technique. They attached rigid markers onto the specimen bone before radiographic imaging, allowing the rigid markers identifiable during image segmentation. The rigid markers were also digitized in experiment to allow registration between the two reference frames. Registration between experiment and computational model was done on identified features of the rigid markers.

In this study, we present a series of registration technique that transform experimental outputs from a mechanical simulator to computational model reference frame in which the only digitization points are from the implanted components. This ensures identical landmark definitions are used when comparing model-predicted and experiment kinematics, eliminating a source of error identified in previous validation procedures. Further objective of this work was to use the described method to validate a CT-based subject-specific computational model that incorporates literature-based soft tissue properties. The model was developed to have sufficient complexity to achieve accuracy in kinematics when compared against experimental data while limiting invasive data capture to improve clinical utility.

Method

Cadaveric Testing

Ten fresh-frozen human cadaver knees underwent pre-operative CT scans. TKA was then performed on each of the cadaver knees with fixed-bearing, ultracongruent (with PCL sacrificed), TKA components (GMK, Medacta, Switzerland), after which a post-operative CT was obtained.

A surgical navigation system (Stryker Navigation 4.0 Research Version, Kalamazoo, Michigan, USA) was used to record kinematics throughout a deep knee bend. The accuracy of the Stryker navigation system is 1° and 2mm [344]. Navigation arrays were attached to the femur, tibia and patella. The implant geometry surface (IGS) of each component were then digitized, allowing the position of the implants and bone to be mapped relative to the navigation arrays respectively. Figure *4.1* shows the overview of experiment steps in a flow chart.

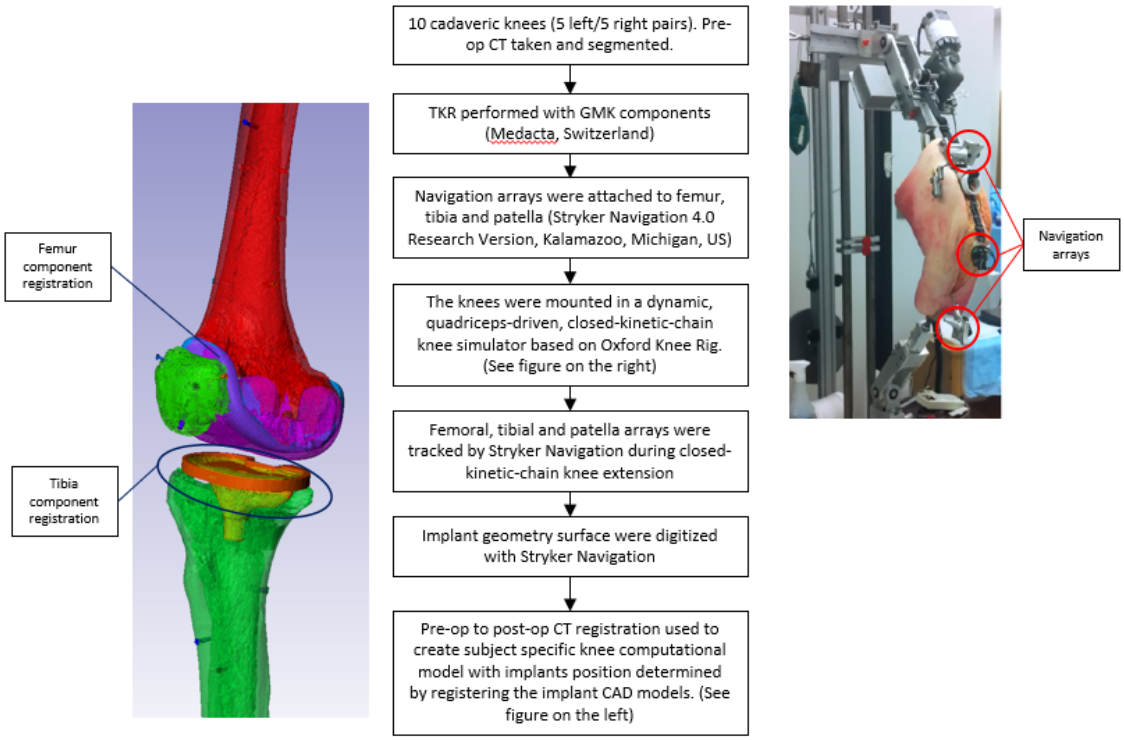

Figure 4.1. Overview of experiment procedure.

Each cadaver was mounted in a dynamic, quadriceps-driven, closed-kinetic-chain knee simulator based on the OKR design, as previously described [276]. Steel rods were cemented into the femoral and tibial medullary canals, fixing the bones to the testing apparatus. The femoral rod was attached with a lateral offset of 5° from the hip joint to reproduce the average anatomic valgus in the femoral shaft [276]. The ankle joint was fixed rigidly to prevent translation, but the rotational degrees of freedom were left unconstrained. The hip joint was positioned directly vertical to the ankle joint and allowed to translate vertically, as well as rotate in flexion-extension and varus-valgus. A vertical load was applied through the hip joint to generate a peak knee-flexion moment of approximately 40 Nm, similar to that reported for stair climbing after TKA [246]. The attached navigation arrays were tracked using the navigation unit during the second half of the deep knee bend cycle, i.e during extension.

Computational model

A knee computational model (KCM), with subject specific inputs derived from a CT scan only and designed to replicate the experimental mechanical simulator, was developed in rigid body modelling software, ADAMS (MSC, California, US), as described in [345]. Image processing and segmentation was performed on both pre-op and post-op CT's taken for each cadaver using ScanIP (Simpleware, Exeter, UK). The native geometry of the femur, tibia and patella were generated and anatomic landmarks were recorded from the pre-op CT on all bones to define local and global axes, as well as soft tissue attachments, similar to those defined by Theodore et al [345], in which anatomic morphology and CT pixel intensity were used to inform landmark positions. The pre-operative bones and implanted TKA CAD geometries were then registered to the post-operative CT to obtain the relative position of the prostheses to the bones using +CAD (Simpleware, Exeter, UK). This method was described in Chapter 3. The transformation matrix for each registered pre-operative bone was then used to re-position the pre-operative landmarks in the post-operative reference frame, allowing accurate post-operative landmarking unaffected by metal component flare in the CT. Transformed pre-operative bone geometries, transformed landmarks and registered components were exported from +CAD into the KCM to generate a patient specific computational model, an example of which is shown in *Figure 4.2*.

The computational model assumes contact for the femoral component, tibia component, patella button and resected patella bone. Although the femur and tibia segmented bone are technically not used in the model, they are needed to define the anatomical landmarks and registration between post-op and pre-op CT. Furthermore, having the patient specific bones in the model can help visualise the bony axes relative to other axes.

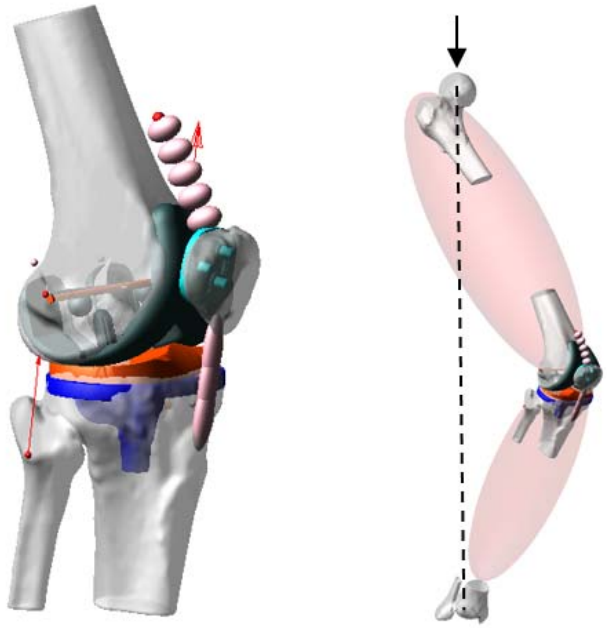

Figure 4.2. (Left) The patient specific anatomy and implant position were determined from CT imaging. (Right) A schematic of KCM undergoing a deep knee bend. A vertical load was applied to the hip joint and the hip joint was positioned directly vertical to the ankle joint. The ankle joint was fixed rigidly in translation but has 3 degrees of rotational freedom.

The model includes the lateral collateral ligament (LCL), medial collateral ligament (MCL), patella tendon, quadriceps tendon and posterior knee capsule. The LCL was modeled with a single fibre bundle and the MCL was modeled with anterior and posterior bundles. The posterior capsule and quadriceps tendon were generated with origin and insertion points dictated by relevant landmark positions. The posterior cruciate ligament (PCL) was not included in the model because the tibia insert implanted required resection of the PCL.

All ligaments were modelled as non-linear springs according to the equations shown in *Equation 4.*, where f is the axial force sustained by the ligament, k is the stiffness parameter, ε is the instantaneous ligament strain and $2\varepsilon_l$ is the threshold strain which dictates the change from the non-linear to linear regions [67]. The unstrained ligament lengths (free length) were calculated using a reference strain

method by defining the ligament strain when the knee is at full extension according to *Equation 4.2*, where ε_r is the ligament strain at full extension, l_r is the length of the ligament at full extension and l_0 is the ligament free length. The free length is then used to calculate ε in *Equation 4.2*. The reference strain and ligament stiffness values were obtained from previous studies [68, 257, 278] and are shown in *Table 4.1*.

The quadriceps tendon inserts in the midline of the superior patella and originates from the greater trochanter. The patellar tendon originates at the inferior apex of the patella and inserts at the medial third of the tibial tubercle. The patellar and quadriceps tendons force-length relationships were based on literature [346]. Contact was modelled between the: tibial insert and femoral component; femoral and patellar component; quadriceps tendon and femoral component; and between patellar tendon and tibial insert. All components were modelled as rigid bodies with kinematic and compliant constraints, using a penalty-based contact between components.

Equation 4.1. Mathematical description of ligament behaviour. Where f is the ligament force, ε is ligament strain, εl the threshold strain at which the stress/strain behaviour of the ligament changes, and k is the spring constant.

$$f = \frac{1}{4} k \frac{\varepsilon^2}{\varepsilon_l}, \qquad 0 \leq \varepsilon \leq 2\varepsilon_l$$
$$f = k(\varepsilon - \varepsilon_l), \qquad \varepsilon > 2\varepsilon_l$$
$$f = 0, \qquad \varepsilon < 0$$

Equation 4.2. Method of calculating reference ligament strain

$$\varepsilon_r = \frac{l_r - l_0}{l_0}$$

Table 4.1. Details of ligament properties used in simulation. [68, 257, 278]

Ligament/tendon	Stiffness (N)	Reference strain at full extension
Anterior MCL	2750	-0.06
Posterior MCL	2750	0.03
LCL	2000	0.05

The model was initialized in extension with a vertical load applied at the hip centre equal to that applied experimentally. During initialization of the model, all components were allowed to settle into contact, and ligaments were pre-strained. A deep knee bend was then simulated in which the rotational and translational boundary conditions matched those of the OKR. A proportional–integral–derivative (PID) controller was used to generate the reactive quadriceps force required to achieve extension. The kinematics were recorded during a deep knee bend between full extension and 90° flexion. All component and bone positions are described using a three-dimensional cylindrical description of motion, as described by Grood and Suntay [347].

Kinematics comparison and validation protocol

Figure 4.3 describes the steps taken to compare experimental and model-predicted kinematics. TKA CAD geometries were registered to best match the experimentally digitized IGS, allowing the digitized implant surface to be modelled as a whole component. The CAD geometries were registered to the implanted component position as observed in the post-operative CT during KCM generation. Experimental data were then transformed to the post-op CT frame of reference maintaining the relative position of the experimental femur and patella CAD geometry to the tibia CAD geometry by normalizing the position of the tibia tray to that observed in the post-op CT.

Previously transformed pre-op CT anatomical landmarks were then duplicated and re-transformed accordingly to the respective positions of the experimental components. This gives 2 sets of registered

components and landmarks for each specimen. The first set forms the subject specific model with anatomical landmarks from the pre-op CT and component positions as measured from the post-op CT. The second set is the virtualized experimental data extracted from the navigation system transformed to the post-op CT reference frame. Therefore, a single set of anatomical landmarks, first generated from the pre-op CT only, define identical axes in the same relative position against all components in both the model and experimental data.

The positional data recorded by the navigation system during testing describes the relative kinematics of the tibia and patella against the femur. This data was applied to the digitized landmarks and components to recreate the motion recorded experimentally. The kinematics were then computed using the transformed anatomical landmarks using the Grood and Suntay definition, thus generating a set of Virtualised Experimental Kinematics (VEK) with identical definitions to the KCM.

To compare the overall difference between the VEK and KCM predicted kinematics, the root-mean-square (RMS) difference of each specimen was calculated between flexion angles of full extension and

90°. The average absolute difference at 10° intervals was also calculated, giving a measure of variability throughout regions of the flexion cycle.

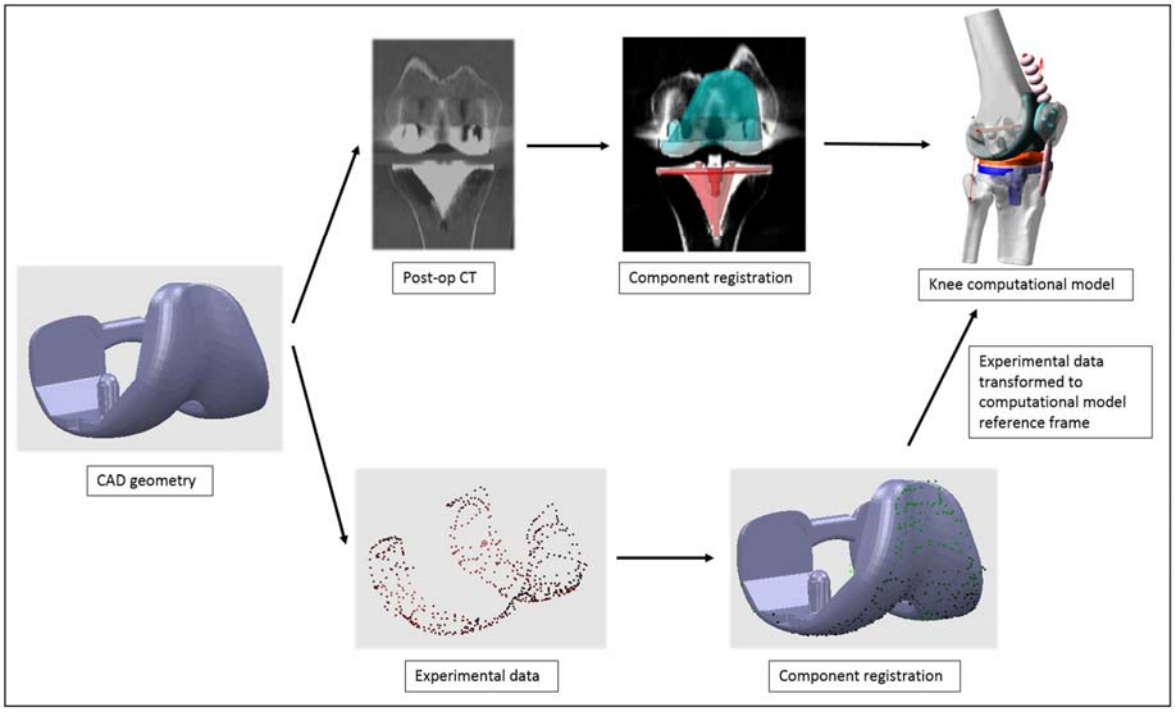

Figure 4.3. Generation of VEK and computational model kinematics comparison. Implanted TKA CAD geometries registered to both post-op CT and implant geometry surface (IGS) reference frame. Experimental data were transformed to the computational model reference frame using the transformation matrix sequence of the registered CAD geometries. Experimental data were firstly transformed to the CAD geometry reference frame using the inverse of the component registration transformation, then transformed to knee computational model using the transformation matrix from CAD geometry to post-op CT reference frame. Transformed experimental tibia CAD geometry was then normalized against the post-op CT tibia tray. Relative positional experimental data were then applied to femur and patella against the normalized tibia.

Results

Experimental data from specimen 1 and 5 were not captured correctly and excluded from analysis. All deep knee bend simulations required less than 3 minutes computational time to complete on a standard performance workstation (i7- 4.00 GHz, 32GB RAM). Comparison of the model predicted subject specific tibiofemoral and patellofemoral kinematics with the VEK for a representative specimen (specimen 6) is shown in Figure 4.4. In general, the KCM was able to capture the trend and magnitude of translation and rotation across all measures.

The tibiofemoral and patellofemoral RMS differences between the KCM and VEK for each specimen between full extension and 90° flexion are presented in *Table 4.2* and *Table 4.3* respectively. RMS differences for all tibiofemoral kinematic measures show the KCM has good agreement with VEK, with a maximum RMS difference reported for tibiofemoral internal-external (IE) rotation of 2.11°. Tibiofemoral varus-valgus (VV) rotational kinematics show the lowest difference with an average RMS of 0.50°, followed by IE rotation with an average RMS of 1.44°. Component translational RMS differences show superior-inferior (SI) shift is reported most accurately with an RMS of 0.53 mm, followed by medial-lateral (ML) and anterior-posterior (AP) shift with an RMS of 1.22 mm and 1.74 mm respectively. The average tibiofemoral RMS difference in flexion-extension (FE) is 7.50°, which can be attributed to the large magnitude of the flexion values and gives similar results to the other axes when considered as a relative difference. Patellofemoral ML translation RMS was the lowest with a value of 0.87°, followed by AP shift with an RMS of 1.73 mm. IE rotation reports an RMS difference of 3.41°. Patellofemoral FE and SI RMS were similar to tibiofemoral flexion RMS with a difference of 6.62° and 5.59 mm respectively.

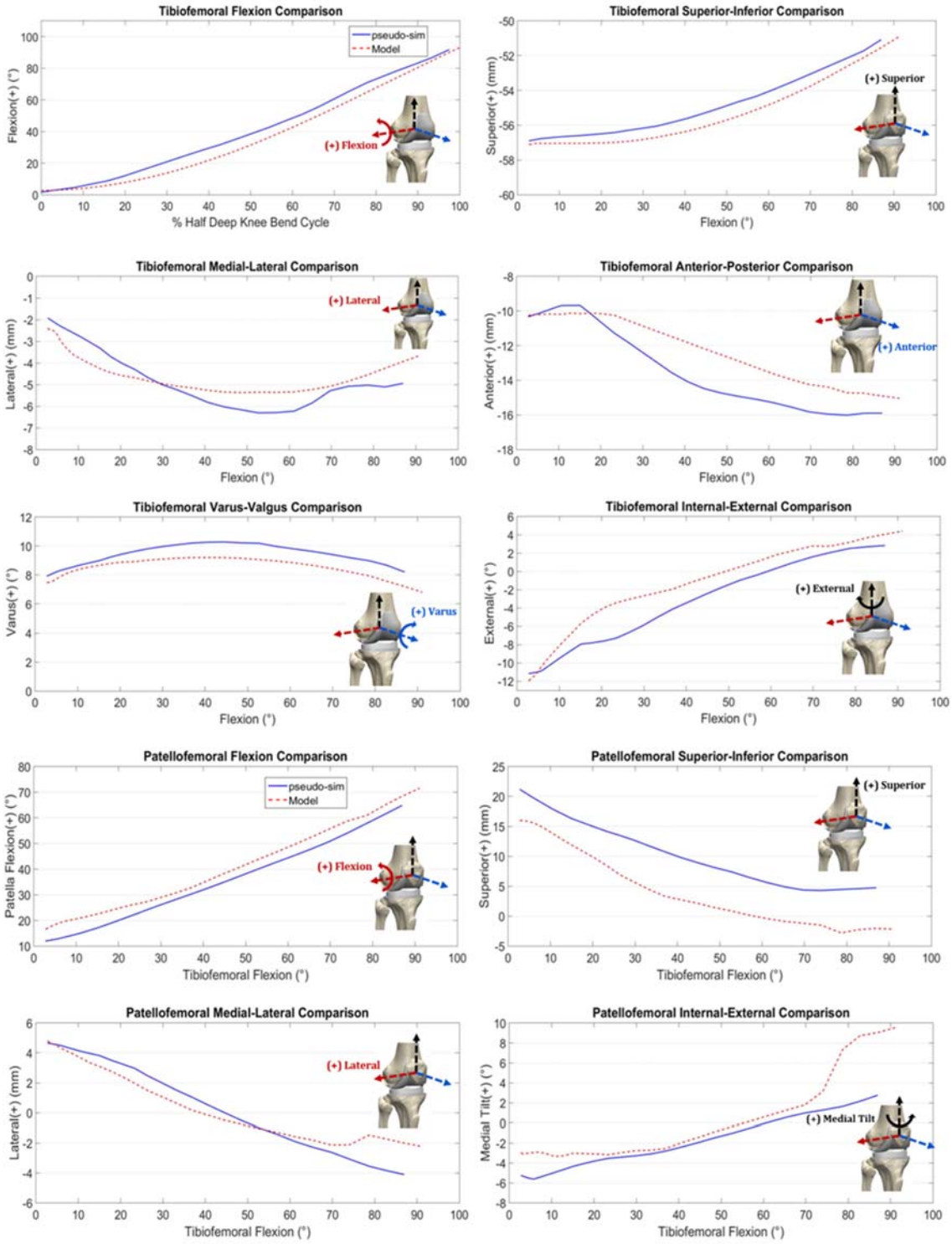

Figure 4.4. Comparison of tibiofemoral VEK and model-predicted kinematics for single representative specimen (specimen 6).

Table 4.2. Tibiofemoral (TF) KCM kinematics RMS difference compared to the VEK.

Specimen	Tibiofemoral kinematics RMS				
	TF_VV (°)	TF_IE (°)	TF_ML (mm)	TF_AP (mm)	TF_SI (mm)
2	0.47	1.13	1.10	1.95	0.58
3	0.72	0.61	1.52	1.84	0.19
4	0.46	1.97	1.38	1.98	0.70
6	0.62	1.18	0.60	1.07	0.46
7	0.24	1.32	1.44	2.43	1.00
8	0.38	1.88	1.10	1.35	0.31
9	0.43	1.36	1.02	2.17	0.50
10	0.69	2.11	1.61	1.14	0.52
Average	**0.50**	**1.44**	**1.22**	**1.74**	**0.53**
Standard deviation	**0.17**	**0.51**	**0.33**	**0.50**	**0.25**
Max RMS	**0.72**	**2.11**	**1.61**	**2.43**	**1.00**

Table 4.3. Patellofemoral (PF) KCM kinematics RMS difference compared to the VEK.

Specimen	Patellofemoral Kinematics RMS				
	PF_FE (°)	PF_IE (°)	PF_ML (mm)	PF_AP (mm)	PF_SI (mm)
2	12.82	6.24	0.23	4.48	4.91
3	4.48	4.53	1.60	1.74	7.26
4	7.66	5.04	1.06	2.34	8.50
6	4.30	1.11	1.00	0.61	2.11
7	2.04	1.85	0.80	0.81	5.22
8	8.12	2.24	0.30	1.46	3.08
9	4.93	2.09	1.29	0.59	4.31
10	8.58	4.17	0.70	1.82	9.33
Average	**6.62**	**3.41**	**0.87**	**1.73**	**5.59**
Standard deviation	**3.37**	**1.83**	**0.47**	**1.28**	**2.56**
Max RMS	**12.82**	**6.24**	**1.60**	**4.48**	**9.33**

The average absolute difference between the KCM results and VEK between 0° - 90° flexion for tibiofemoral kinematics are less than 2 mm or 2° for all clinically relevant kinematic measures, shown as the bold lines in Figure 4.5A. Tibial VV are the most accurately predicted kinematics with an average absolute difference of less than 1°. IE rotation and AP shift have greater differences, reaching 1.33° and 1.97 mm respectively. The patellofemoral average absolute difference in kinematics from 0° - 90° flexion is shown in

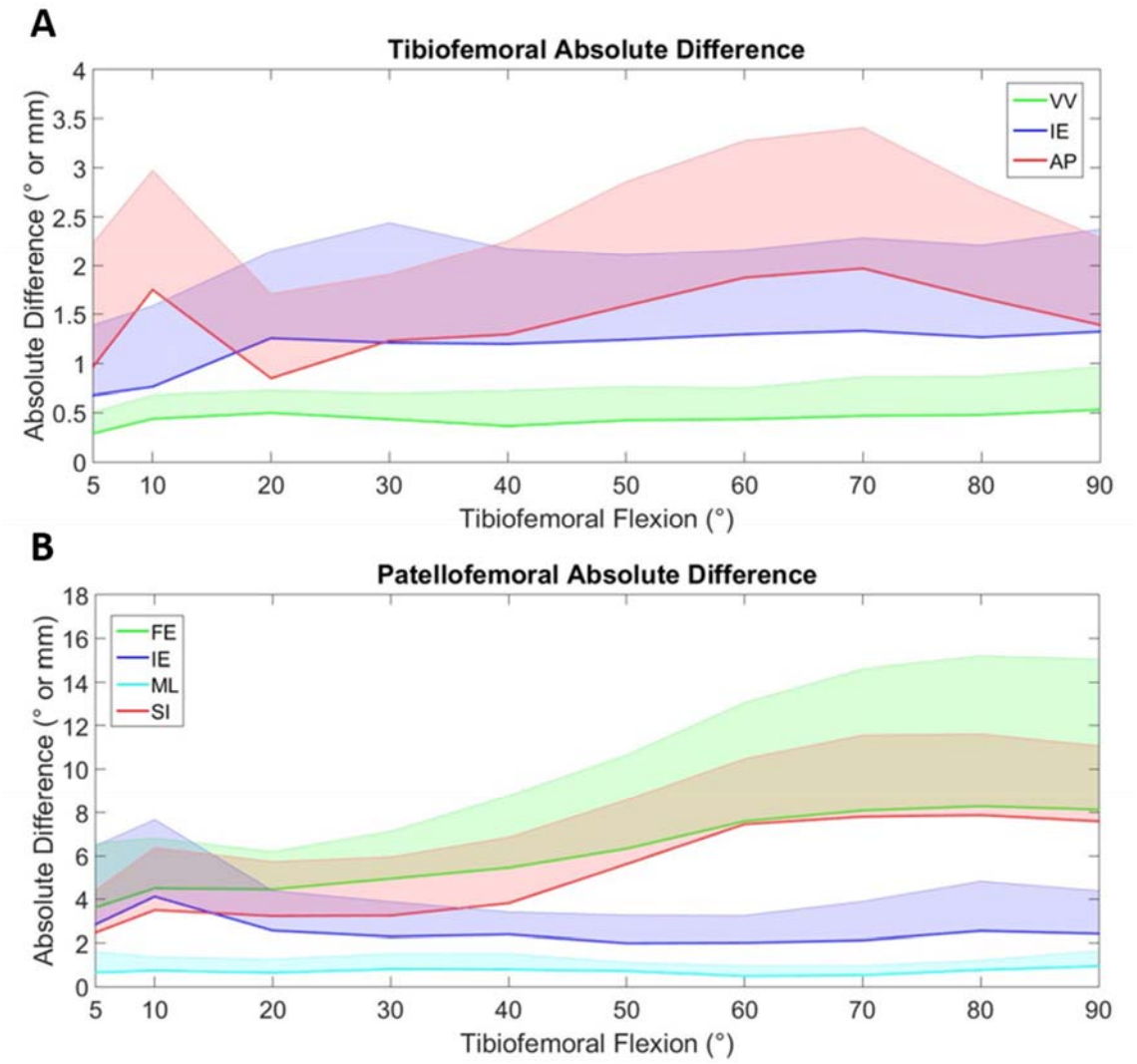

Figure 4.5B. ML shift and IE rotation are best modelled by the KCM with an average absolute difference of less than 1 mm and 4° respectively at all flexion angles. FE rotation and SI shift exhibit low absolute differences at low flexion angles (of 3.61° and 2.46 mm respectively). Differences in these measures increase from 50° flexion to a maximum of 8.34° and 7.87 mm respectively.

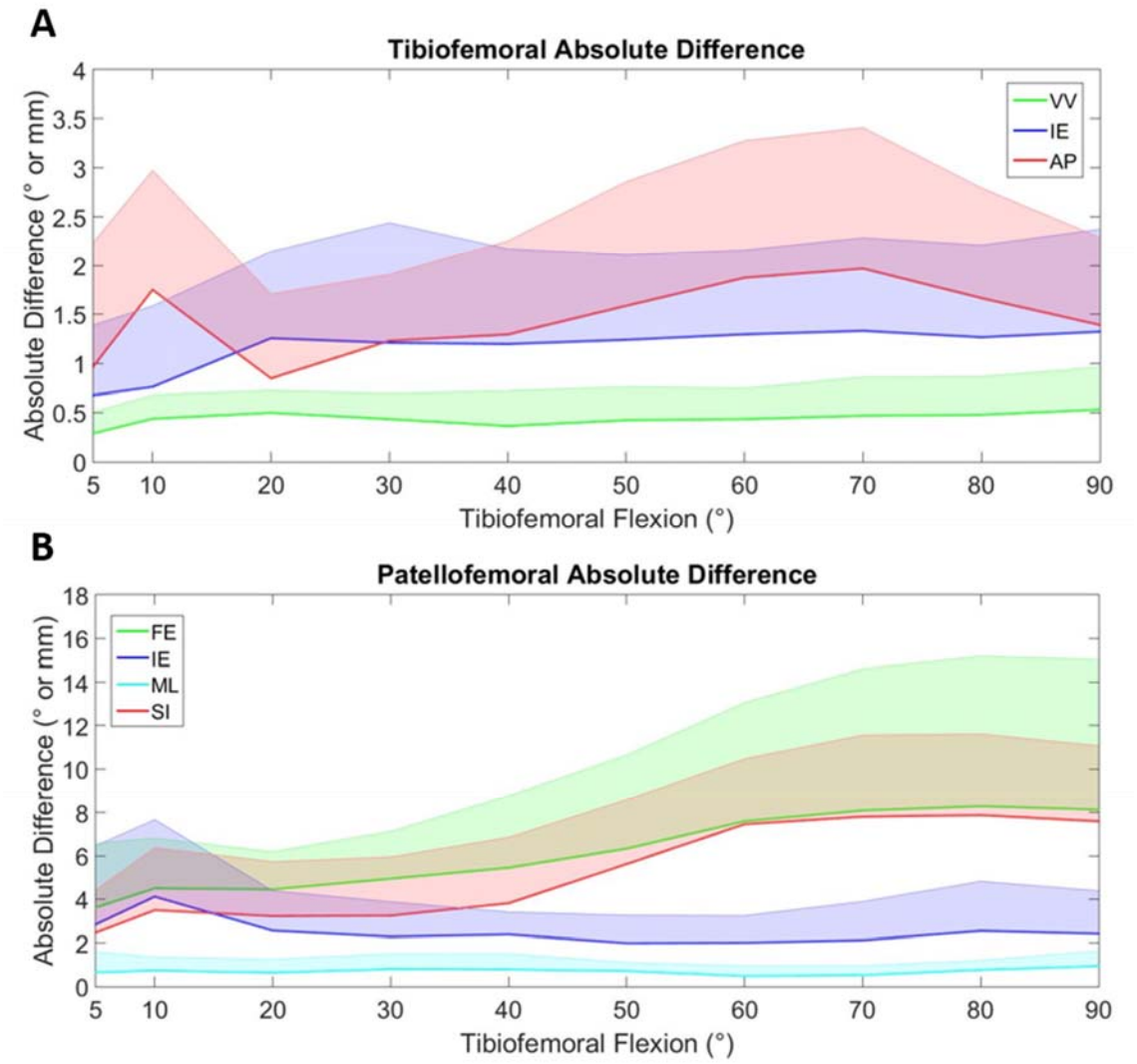

Figure 4.5. Bold lines show the average absolute difference between the KCM kinematics and VEK from 0 and 90° flexion. Shaded region represents 1 standard deviation. Varus-valgus = green, Internal-external rotation = blue, Anterior-posterior shift = red.

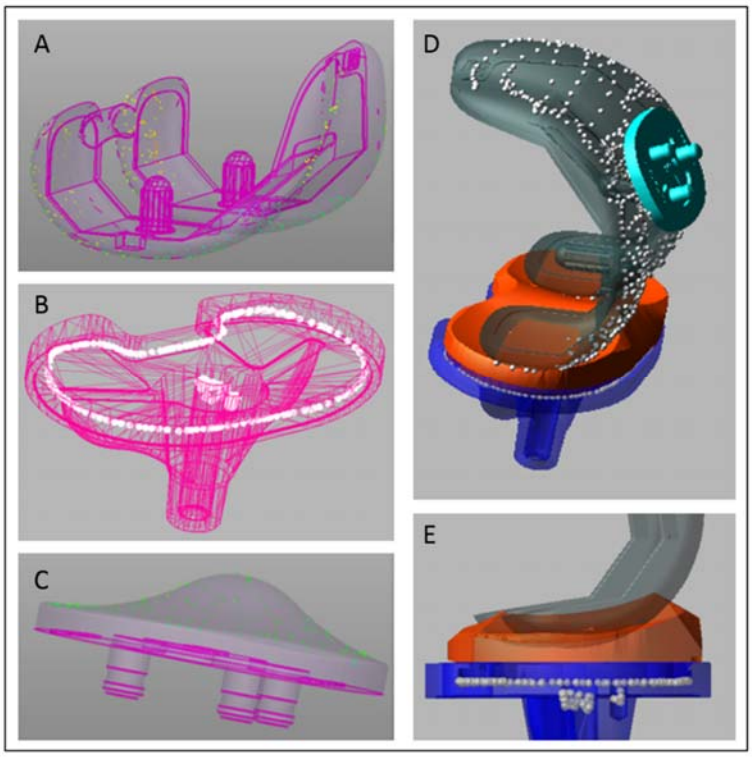

Figure 4.6 Example images of IGS data (dots) with registered component geometries to the Femur (A), tibia tray (B), patella button (C) and whole knee (D). (D) and (E) showed an example of where the femur penetrates the tibia insert in the motion generated by VEK. This could indicate registration inaccuracy or data capture error that caused the components are not articulating on the respective surfaces in VEK.

Accuracy in registering CAD geometries against the experimental data was investigated by calculating the error between the nearest point of the component geometries and the IGS points. A typical example of the registered implants can be seen in Figure 4.6. The average error between the femur, tibia and patella prostheses are 0.39 standard deviation (SD) 0.41 mm, 0.15 SD 0.16 mm and 0.17 SD 0.17 mm respectively. Figure 4.6E shows penetration of the femur and tibia tray during flexion of 1.7 mm.

Discussion

This study describes a model validation technique that allow experimental and model-predicted kinematics to be compared using a single reference frame originating from a pre-operative CT scan. The consistent RMS differences between specimen indicate that the technique used to generate this model captures sufficient patient specificity to replicate individualized kinematics. Previous reported studies have compared experimental kinematics that were computed with anatomical landmarks probed during testing against model-predicted kinematics that were defined with anatomical landmarks identified from 3D imaging [217, 244, 246, 250-252, 261, 340-343]. These studies however, as discussed in the introduction, may suffer from inconsistencies of landmark placement leading to inconsistency of kinematic definition as source of error.

The method developed involved a series of registration points, from pre-op CT to post-op CT, CAD to post-op CT and CAD to digitized Implant Geometry Surface (IGS). Using sequence of transformation matrix, experimental recorded positional data was aligned to computational model reference frame. This created a secondary model to view the digitized IGS with overlaid CAD file in its relative position from one to another as recorded experimentally. When recorded positional data applied to the model, visualization of the components movement during experiment can be reviewed and its kinematics can be computed, termed Virtualised Experimental Kinematics (VEK). Other than the ability to compare experimental and model-predicted kinematics in a consistent kinematics definition, VEK can also be used to visually inspect whether the experimental kinematics behaved as expected. This can help with troubleshooting if there were mistake in post-processing the data. For example, penetration between components seen during the playback of VEK could indicate registration inaccuracy or data capture error. This allows earlier source of error detection before experimental kinematics even compared with computational model results for validation. This example was experienced in this study and shown in Figure 4.6. Individual component registration results showed less than 0.5mm difference. However, during VEK playback, 1.7mm amount of penetration was observed between posterior

condyles and tibia insert in flexion, suggesting there is other source of error other than registration. In summary, VEK can be used to perform initial validation of a computational model against experimental setup before cadaver specimen is used. This would eliminate the source of error to the model development or transform math itself. This will be useful before real validation is performed using cadaver specimen where other source of error may arise

Apart from modelling and kinematic definition errors, validation results may also be affected by experimental data capture error. The infrared cameras used in the navigation system have intrinsic measurement error. The navigation arrays were assumed to be rigidly fixed to the bone but could have unintentionally moved during the experiment. Human error in digitizing, such as probes capturing points when not contacting the articular surface, combined with movement of the navigation arrays can affect the registration of the implant CAD geometries. Each of these sources of error will propagate throughout each calculation when generating the VEK. All mechanical simulators have limitations [216], and when coupled with experimental procedure setup, the cumulative probability of unintentional errors increase.

Knee kinematics post-TKA are a product of complex interactions between the component design, component alignment, and patient specific anatomic characteristics [140, 331, 332]. Computational modelling is a scalable technology to study the complex interactions of these factors and can help surgeons better plan surgery to achieve optimal outcomes. However, such models need to balance clinical practicality with the complexity required to distinguish individual subjects. Further objective of this study was to use described technique to validate a CT-based subject-specific computational model that incorporates literature-based soft tissue properties. Based on previous literature, 3° is an acceptable threshold of component alignment accuracy for longevity and function [198, 348]. Assuming linear effect, that would translate as tolerance of 3° and 3mm in kinematics. Therefore, 3° or 3mm would be considered a good threshold value when comparing the simulated kinematics

against the experimental data based on clinical impact for tibio-femoral kinematics. Patella-femoral kinematics are more difficult to quantify as the patellofemoral kinematics is less quantifiable clinically.

The Knee Computational Model (KCM) in this study was derived from subject-specific CT scans only, and literature-based values were used for the soft tissue representation. Good agreement was found in trend and magnitude between model-predicted and experimental kinematics in all 8 specimens using the method described. The kinematic differences observed in this study were comparable to previous studies [217, 222, 274, 343], particularly for tibiofemoral (TF) kinematics (within 3° and 3mm). Patellofemoral (PF) kinematics RMS difference was slightly higher in our model than previously reported by Baldwin et al, [217] which could be attributed to the simplification of the extensor mechanism in the model. The extensor mechanism was modelled with single point insertions of the quadriceps tendon and patella tendon, without retinaculum tissue or other medial and lateral structures. These simplifications appear to not affect predictions in ML shift and IE rotation (given the relatively lower RMS differences) but may explain some of the differences in PF flexion. The simplification, however, was justified for computational efficiency, given that TF and PF ML shift and IE rotation are clinically more relevant. The KCM in this study completed a single deep knee bend within a few minutes, an efficiency that was not seen in more complex models [217, 250, 251, 341, 342, 349].

There are a number of limitations to this study. Firstly, there could have been unintentional errors during cadaveric testing. Data used for the method described was based on previously collected experimental data. The model-predicted kinematics could have been compared to experimental data with sequential data collection and registration errors due to availability of data. Error propagation such as this prevents differences between the KCM and VEK from being solely attributed to modelling errors. A more controlled experimental set-up that focuses on accurate digitization and controlled data collection specific for registration method described will help differentiate modelling error from experimental error and will be the subject of future work.

The KCM utilised a simplified model to represent soft tissue properties. Previously published validated computational knee models have conducted experimental studies to calibrate subject specific ligament properties. Baldwin et al.[217, 341], Ewing et al.[251], and Mootanah et al. [250] performed passive laxity testing on cadaver specimens to determine characteristic VV and IE resistance. Inclusion of subject specific ligament characteristics may improve model accuracy, however, capturing patient specific ligament data is invasive and cannot be obtained in a clinical setting – preventing any such model from clinical use.

Model accuracy obtained from these studies, therefore, will not necessarily translate to subjects in which invasive soft tissue data is not available. A recent study by Beidokhti et al suggested that although subject specific modelled ligaments improved contact accuracy, when joint kinematics are of most interest, multi spring elements like those modelled here are the most efficient in terms of combining modelling accuracy with computational efficiency [66]. Similar findings were also reported by Pianigiani et al [350]. They studied effect of material properties on native knee where menisci still present. They reported effects of material properties on kinematics are much less significant compared to contact stresses, which is expected when soft tissue cartilage and menisci are present. Our study simulates post-op model where the articular surface is replaced with implant components.

KCM in the present study was able to distinguish individual specimen kinematic characteristics well in early and mid-flexion but not so well in deep flexion, when the soft tissue envelope is more active. Future development of the model is needed to include non-invasive techniques to obtain patient specific ligament properties. Recent studies have proposed of utilising stress X-rays to quantify ligament characteristics [351, 352]. Investigation is needed to assess the feasibility and clinical applicability to use functional X-rays as a surrogate to derive soft tissue properties in a computational model.

Other limitations to this study relate to the implant components investigated. Ultra-congruent PCL sacrificing prostheses were used. The increased congruency of these implants compared to, for

example, cruciate retaining (CR) implants, reduces the relative role of the ligaments in generating patient specific kinematics. A greater range of patient specific kinematics would be expected from a deep knee bend using CR implants. An experiment comparing CR implants with this simulation may lead to greater simulation errors due to the use of literature values for the soft tissue profile.

Other limitation was that the initial position of the leg in the model was not normalised to the same loaded initial position as the cadaveric testing. Baldwin et al. highlighted a similar source of error in their study [217]. Difficulty in tuning the initial loaded position was attributed to the experiment data capture technique. Differences in starting position can introduce an absolute offset of the kinematics between the two data sets which may have been reflected in patellofemoral flexion and superior-inferior translation. Despite these challenges, the model demonstrated good agreement with both tibiofemoral and patellofemoral VEK in all eight cadaver specimens under the conditions tested here.

Conclusions

In this study, a validation technique that allow experimental and model-predicted kinematics to be compared with identical landmark and kinematic definitions was presented. Due to experimental error propagation, model validation studies need to place careful consideration on experimental procedure to prevent compound errors from masking the accuracy of computational models. Using the method described, a relatively simplified knee computational model was able to achieve good kinematic agreement while maintaining computational efficiency. Further developments of this model and evaluation against supporting clinical data may lead to utilisation of computational modelling as part of computer assisted surgical planning for TKA.

Chapter 5

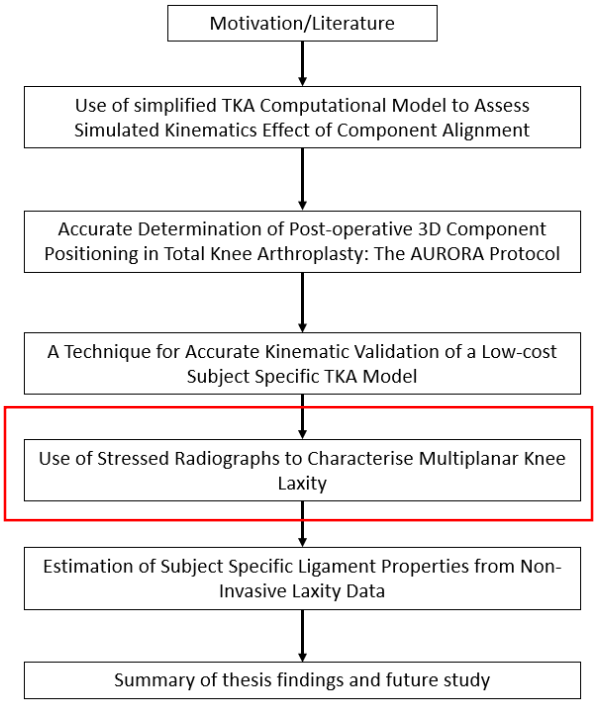

Use of Stressed Radiographs to Characterise Multiplanar Knee Laxity

A version of this chapter has been submitted to multiple conferences

Australian Orthopaedic Association, Cairns, October 2016 - **Non-functional Radiology is Unable to Predict Deformity Correctability in Total Knee Arthroplasty** (Podium Presentation)

International Society of Arthroscopy, Shanghai, June 2017 - **Patient Specific Planning Incorporating Ligament Laxity** (Poster)

European Knee Society, London, April 2017 - **Functional Radiography As A Means Of Integrating Joint Correctability Into Pre-Planning Workflows** (Special E Poster)

Introduction

Computational modelling can be used to evaluate various surgical and anatomical parameters and its effect to TKA biomechanical behaviour prior to the surgery [215, 216]. The accuracy of subject-specific computational models is dependent on anatomical geometry, material properties, and boundary conditions [353]. In previous chapter, we presented a validation method that allow same anatomical geometry and boundary conditions to be compared between a computational model and experimental data. However, ligament parameters in the developed computational model have not been corroborated against subject-specific ligament characteristics. Literature reported ligament properties were used instead. Ligament properties can have strong effect on simulated kinematics [278, 354, 355].

Determination of subject-specific ligament properties remains a challenge. Various researchers have attempted to evaluate subject-specific ligament properties. These studies include inverse dynamics modelling of gait lab with instrumented implants [356] or experimental methods using a load sensor to collect soft tissue laxity envelope and tracker to collect displacement/kinematic data [217, 250, 251, 357]. The kinematic data needs to be synchronised with the load data and specimen-specific ligament properties were estimated by optimizing to the force-displacement response of the knee [217, 250, 251]. This technique is usually performed on cadaver specimen with load sensor and trackers to record movement of the knee. These methods require a lot of resources to collect and invasive when trackers are used. This technique can be suitable for developing a computational model when a single validated subject model is used for its context of use, however its scalability potential limits the practicality needed for computational model used as part of surgical planning on subject specific level. This chapter is going to investigate the use of stress radiographs to quantify subject's knee laxity as a surrogate for displacement and applied load data for subject's ligament properties determination study in the next chapter.

Numerous studies have attempted to quantify knee laxity using instrumented in vivo assessments, such as arthrometry. These assessments typically divided into 2 types, clinical arthrometry and stress radiography. Clinical arthrometry is usually performed by applying load to the joint in combination with mechanical displacement measurements whereas stress radiograph uses combination of a mechanically imposed load with simultaneous radiograph imaging. Laxity is measured as the angle or displacement change within the constraints of the soft tissues when an external force is applied to the joint [358-360]. Laxity depends on the shape of the involved bony surfaces, the mechanical behaviour of the joint's soft tissue structures and contributions from other supporting structures [361].

Stress radiography is a widely used clinical tool to evaluate the knee ligament laxity [362]. Previous studies have used stress radiography to evaluate anterior-posterior knee laxity [363, 364]. Okazaki et al [365] studied the medial and lateral knee laxity profile in extension and flexion on healthy knees. Ishii [366] examined the correlation of non-weight bearing tibiofemoral angle to varus valgus laxity on 120 knees undergoing Total Knee Arthroplasty (TKA). And Tsukeoka et al [360] used stress radiograph to evaluate knee laxity after TKA surgery.

In these studies, stress radiographs were taken with the knee at specific flexion with load applied in the direction of laxity assessment. There are several techniques to evaluate the stress radiographs but typically the radiographs were evaluated by identifying bony landmarks on the planar radiographs. Skeletal displacement were determined by the distance between identified bony landmarks or line drawn across bony landmarks. James et al [362] conducted a systematic review on stress radiograph and reported excellent reliability was reported by most studies. Jackman et al [364] reported intraobserver interclass correlation coefficient (ICC) of 0.973 and interobserver ICC of 0.955 when using 2D stress radiograph measurements to evaluate posterior knee laxity. Schulz et al [367] also reported similar ICC, 0.95 for intraobserver and 0.91 for interobserver. Although stress radiography provides great reliability, its accuracy can be influenced by several important components [364], particularly precise x-ray beam direction, rotation of the limb or coupled rotation. 2D measurements

done on the planar radiograph is prone to error when the x-ray beam is not perpendicular to the radiograph plate and the error can be compounded with rotation of the limb. Moreover, 2D stress radiograph measurement technique only allows assessing single plane laxity. Knee laxity must be assessed in multiple Degree of Freedom (DOF) in order to fully capture the complexity of the joint structures and the interplay between ligaments [368].

In recent years, 3D-2D image registration has become one of the enabling technologies for image-guided interventions [369]. The goal of the registration technique is to quantify the geometric transformation which spatially aligns the 2D projection of a 3D volume and a 2D image [370]. 3D volume is typically obtained using computed tomography (CT) or magnetic resonance imaging, while the 2D image obtained from single X-ray or a frame of in-vivo fluoroscopy. This technique has been applied to quantify joint kinematics in native [371-373] and replaced knees [374, 375] and pathological knees with anterior cruciate ligament deficiency [376]. To our knowledge, there have been no studies of using this technique to quantify multiplanar 3D knee laxity measured with stress radiograph.

The ability to quantify pre-operative knee laxity using clinically ready tool can help further research in determining subject's ligament properties. Therefore, the main objective of this study was to quantify multiplanar knee laxity from stress radiograph using 3D-2D technique. Secondary objective was to compare knee laxity assessed from stress radiograph to intra-operative laxity data assessed by orthopaedic surgeon using computer navigation system.

Method

Patient selection

Fifty-five TKA candidates were selected consecutively for this study, providing data on 58 knees (3 bilaterals). In all patients, the preoperative diagnosis was osteoarthritis. Twenty-four males (43%) and 31 females (56%) with a mean age of 68 (range 49-84) were included. Each patient received supine

long leg CT scans, standing radiographs and a series of stress radiographs preoperatively. All TKA's were performed by a single surgeon at single centre.

Stress radiograph acquisition

Stress radiographs were acquired using a mechanical Telos stress device (Metax, Hungen-Obbornhofen, Germany) to assess anterior-posterior laxity and abduction-adduction (varus-valgus) laxity. The Telos device is equipped with a screw threaded shaft that permits a force to be applied gradually while the load is displayed on a digital readout. Telos stress device has accuracy measurement of ±1daN. In the anterior-posterior (AP) laxity test, the force was applied to the anterior proximal tibia at the level of tibial tubercle when the patient was in lateral decubitus position with the knee in 20° and 90° flexion. These flexion angles were selected to quantify the laxity data in extension and flexion. Four stress X-rays will be collected at each flexion angle. In varus-valgus (VV) laxity test, the force was applied at the level of the tibial tubercle with the patient lying supine with the knee in 20° and 90° flexion, see Figure 5.1. In both laxity tests, the force applied was increased in incrementally to a maximum of 150 N or until the patient indicated that they were uncomfortable with the stress and lateral X-ray was captured while the knee was held in the stressed position. The flexion was measured by radiographer using goniometer. Assessment at 20° flexion is considered as extension and 90° flexion as flexion. Due to miscommunication with imaging centre in the early study, a group of patients received varus-valgus stress radiograph at 45° flexion instead of 90°. These two are grouped into flexion assessment group.

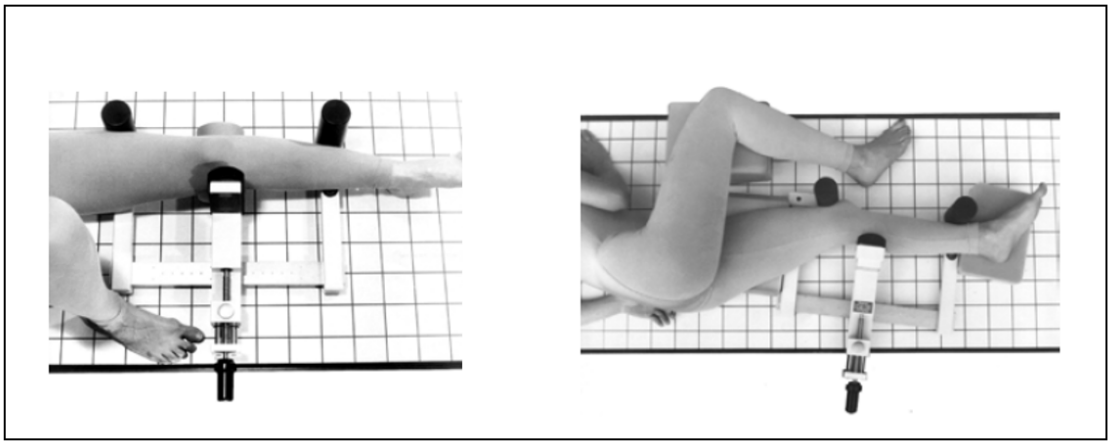

Figure 5.1. example of stress radiograph position for varus stress and anterior draw test (taken from TELOS instructions for use).

Registration technique

Acquired CT scan was segmented to generate 3D models of the patient's lower limb and bony landmarks were identified to create anatomical reference frames using ScanIP (Simpleware). Figure 5.2 shows the bony landmarks used to define femur and tibia reference frame. 3D-2D registration was performed using Mimics (Materialize, Leuven, Belgium) to transform the generated 3D bone models from CT reference frame to the bone position evident in the stress radiograph. The distance of the tube-to-cassette assumed to be 1.5m for all X-rays for consistency. As the 3D model being manipulated, the projected 2D silhouette was overlaid to the X-ray. This process was iterated manually until the projected 3D silhouette matches with the silhouette of the X-ray. The femur and tibia were registered independently but their respective position in space was checked by other qualified engineer for quality assurance and interference before finalising the registration. The in and out-plane position of femur and tibia relative to each other was also reviewed to ensure the femur condyles are sitting on top of tibia plateau in a sensible medial-lateral position. At the time of processing, no quantifiable accuracy measure was available in Mimics when comparing the silhouette. Therefore, a reviewer is needed to check the first registration

After passing quality check, the bone models were exported for each registered stress radiograph. The femur and tibia 3D model were combined into a single 3D model for each registered position. The

femur bones from each position were then normalised to the femur position in CT reference frame while maintaining the tibia-to-femur relative registered position. Figure 5.3 shows schematic of the registration steps taken. The normalisation of the femur allowed for quality check for registered position and 3D visual comparison of stress radiographs knee alignment.

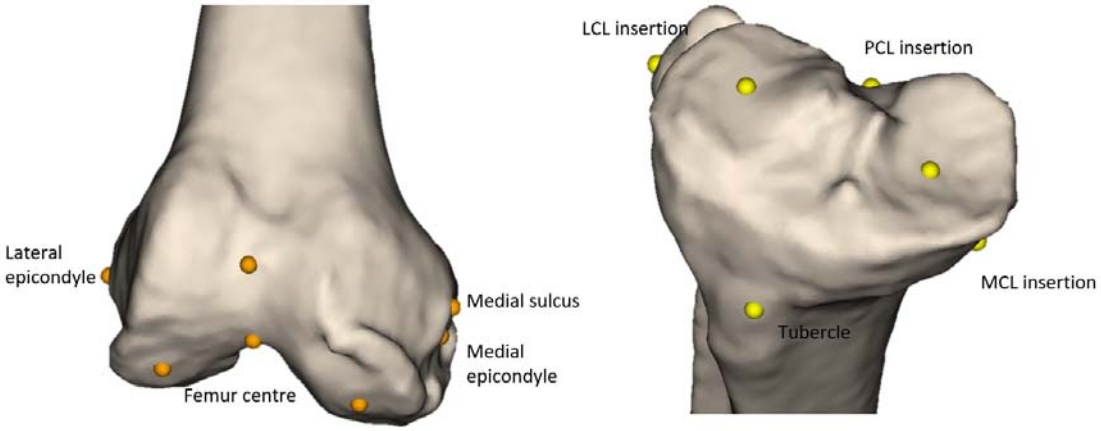

Figure 5.2.bony landmarks used to define femur and tibia reference frame. Femoral head centre and ankle centre are not shown here.

CT scan tibia bone model was then aligned to each tibia registered position using Iterative Closest Point (ICP) alignment method in Powershape (Autodesk, California, United States). Since the tibia 3D models are identical but in different position, the alignment should result with no deviation between the models. The output of the alignment was transformation matrix of tibia bone model in CT reference frame to the registered stress radiograph position. This transformation matrix was applied to the tibia landmarks coordinates defined from CT scan so that knee alignment at each registered radiograph can be quantified. Grood and Suntay [377] convention was used to describe the knee alignment, giving 3D position of tibia relative to femur.

Mechanical axis of femur was defined by a line drawn from femur centre to hip centre whereas ankle centre and mid-point between PCL-insertion and tubercle landmark (tibia centre) defined the

mechanical axis of tibia. The line connecting the epicondyles (transepicondylar axis) defined the ML axis of femur and femur anterior-posterior (AP) axis is perpendicular to mechanical axis and ML axis. The AP axis of tibia was defined by PCL insertion to tubercle line and ML axis is perpendicular to mechanical axis and AP axis. Varus/valgus knee alignment was defined as the angle between femur mechanical and tibia mechanical axis projected to femur coronal plane and internal/external (IE) rotation was defined as the angle between femur transepicondylar axis and tibia AP axis projected to tibia axial plane. AP position was defined as the distance between mid-point of transepicondylar axis and tibia centre projected to tibia sagittal plane. These measurements were measured for each stress radiograph. A verification study of described method can be found in Appendix B.

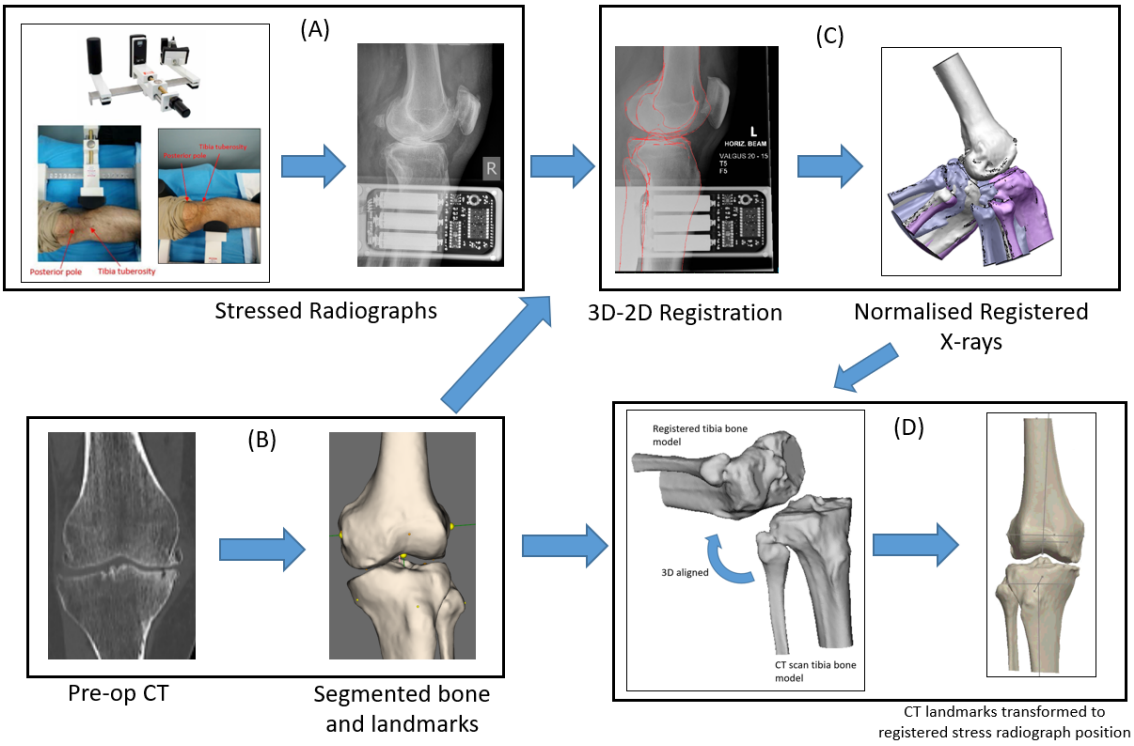

Figure 5.3. Flowchart of registration steps. (A) Stressed radiographs were taken. (B) CT scan was segmented and landmarked. (C) Segmented bone models exported and 3D-2D registered against stress radiographs in Mimics (Materialize, Leuven, Belgium). Registered femur bone models were normalised to CT reference frame while maintaining tibia-femur relationship from registered position. (D) CT scan tibia bone model was then aligned to each tibia registered position using Iterative Closest Point (ICP)

alignment method in Powershape (Autodesk, California, United States), giving transformation matrix that applied to tibia landmarks in CT scan reference frame. This gives a set of femur and tibia landmarks that describe knee alignment in each stress radiograph.

To describe the interobserver reliability, the registration technique was conducted on 6 stress radiographs by 2 qualified engineers. Each case was reviewed by a third engineer, with refinement of bones registration made by the reviewing engineer if necessary. The intraclass correlation coefficient (ICC) was calculated for registered bone position (flexion, varus/valgus, internal/external, anterior/posterior). An ICC value of 1 shows perfect reliability, values greater than 0.9 indicates an excellent result, 0.81 to 0.9 is very good, 0.76 to 0.80 is good, 0.5 to 0.75 is moderate and <0.50 is considered to show poor reliability [308, 309].

Intra-operative laxity data

Each patient received TKA by one surgeon performed with Navigation System (OMNIlife Science, Raynham, USA) with nominal accuracy up to 1mm and 1° [378]. The knee was exposed, and infrared trackers were attached on femur and tibia. The centres of the femur, knee, and ankle were registered to create mechanical axes by joining these centres. Subsequently, other anatomical landmarks are registered to create anatomical reference frames of the femur and tibia. The navigation system provides real time information about the 3D bone position and orientation of the femur and tibia by corresponding pinned infrared trackers, allowing joint kinematics to be tracked and stored. At the beginning of the surgery, laxity assessment was performed throughout flexion arc prior to osteophyte removal. The surgeon then removed osteophytes and laxity was assessed again as another data capture. This procedure was part of surgeon's routine surgical workflow. Sufficient force was applied by surgeon onto the knee to recruit the appropriate ligaments during assessment. The flexion and varus-valgus angles were recorded as the laxity assessment was performed. Navigation system used in this study did not record internal-external alignment during laxity assessment. At the end of the surgery, the navigation report was saved and transcribed for use.

Results

Of 55 patients enrolled, 48 knees have complete stress radiographs (extension and flexion), 10 knees have partial complete stress radiographs (extension only) due to radiographer's confusion with the imaging protocol. 25 of flexion VV laxity test was completed at 45° flexion. 52 intra-operative Navigation data was recorded. None of the patients had evidence of trauma, infection, tumour or any congenital disorder.

The mean coronal (varus-valgus) leg alignment in CT and standing radiographs were 5.0° varus (SD 3.9°, ranging from 7.7° valgus to 11.6° varus) and 6.0° varus (SD 4.9°, ranging from 12.8° valgus to 13.1° varus) respectively. The CT coronal alignment is strongly correlated with standing radiographs ($r = 0.96$ and $p<0.05$). There were 46 (79.3%) varus, 3 (5.2%) valgus and 9 (15.5%) neutral knees when $\pm 3°$ is used as the varus-valgus alignment threshold.

Accuracy and Reliability

The accuracy of this method was 0.6mm for in-plane translation, 1.8mm for out-of-plane translation and 0.7° for rotations. Similar accuracy was reported by Matsuki et al [371] (0.5mm for in-plane rotation, 1.6mm for out-plane, and 0.5° for rotations). Table 5.1 shows the ICC value for each measurement. The lowest reported ICC variable is for IE rotation, with an ICC of 0.92. All ICC values are above 0.9, indicating excellent reliability.

Table 5.1. Reliability testing for 3D-2D registration. All ICC values are greater than 0.9 indicating excellent reliability.

	Flexion	**VV**	**IE**	**AP**
ICC	0.99	0.95	0.92	0.98

Registered Stress Radiograph

The load applied during VV laxity test was converted to a measurement of torque in coronal plane using the moment arm distance of the TELOS stress device. Table 5.2 shows the average load applied on each laxity test. The overall average load applied for VV laxity test was 10.2Nm ±3.5Nm with the load applied at flexion is slightly lower than at extension. AP laxity applied load overall averaged at 126.7N ± 39.2N with similar average in both extension and flexion. Posterior laxity test showed lower average than anterior laxity test.

Figure 5.4 shows examples of registered CT bone model to stress radiograph. Table 5.3 shows the average knee alignment and translation position from each laxity test. The mean knee alignment of varus test in extension and flexion were 6.7° and 6.6° respectively, which was approximately 1.6° more than the knee alignment in CT scan. The mean knee alignment of valgus test in both extension and flexion showed a positive varus alignment, suggesting medial tightness was present that prevents the knee to be corrected to or over mechanical alignment (0°) under valgus load. The valgus test knee alignment is approximately 1.9° less than the knee alignment in CT scan. Both anterior and posterior test average AP position is larger in extension than flexion, indicating the femur sits more anteriorly relative to the tibia during AP loading in extension. AP laxity test in flexion showed the most interpatient variation with standard deviation of 5mm.

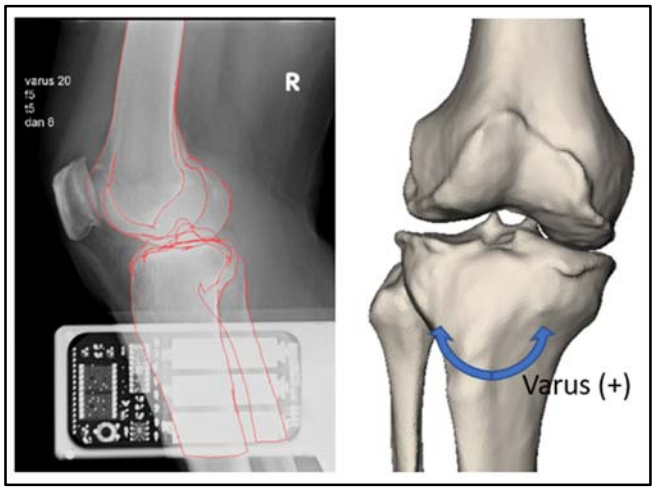

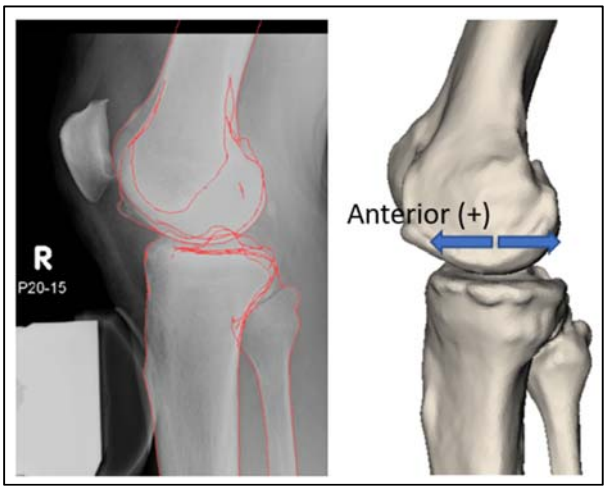

Figure 5.4. A representative of registered CT bone model to varus test and posterior test stress radiograph. Varus alignment is positive and AP position is positive when mid-point of transepicondylar axis sits anterior to the tibia centre projected to tibia sagittal plane.

Table 5.2. Magnitude of loads applied to each laxity test.

Load applied	Extension (Nm)		Flexion (Nm)		Extension (N)		Flexion (N)	
	Varus	Valgus	Varus	Valgus	Anterior	Posterior	Anterior	Posterior
AVERAGE	10.2	11.0	9.7	10.1	130.2	119.3	132.4	124.9
STD.DEV	3.4	2.9	4.0	3.5	38.6	43.1	33.2	41.8
MIN	2.0	2.0	1.0	3.0	20.0	20.0	20.0	10
MAX	13.0	13.0	13.0	13.0	150.0	150.0	150.0	150

Table 5.3. Knee alignment and translation position measured from 3D-2D registered stress radiographs.

	Coronal alignment on CT (°)	Extension (°)		Flexion (°)		Extension (mm)		Flexion (mm)	
		Varus	Valgus	Varus	Valgus	Anterior	Posterior	Anterior	Posterior
AVERAGE	5.0	6.7	2.7	6.6	3.6	6.4	12.1	3.5	1.5
STD.DEV	3.9	3.7	4.3	3.7	4.4	4.5	4.7	5.1	5.4
MIN	-7.7	-5.1	-10.7	-3.7	-11.0	-5.7	1.0	-8.7	-8.9
MAX	11.6	13.5	10.6	12.1	11.9	14.6	21.1	14.7	15.3

Primary Laxity

Primary laxity is defined as laxity in the same plane as the load applied in. VV laxity is the range measurement from varus to valgus stress radiograph and AP laxity is the range measurement from anterior to posterior stress radiograph. Extension and flexion VV laxity resulted in average of 4.0° (SD 2.4°, ranging from 0.2° to 10.1°) and 3.0° (SD, 2.4°, ranging from 0.1° to 8.8°) respectively. Extension and flexion AP laxity resulted in average of 6.1mm (SD 3.9mm, ranging from 0.2 to 16.2mm) and 6.0mm (SD 4.4mm, ranging from 0.3 to 21.1mm). Histograms and density plot of the laxity are shown in Figure 5.5**Error! Reference source not found.**. The density plot shows the laxity distribution and the VV laxity in extension concentrated at around 5° while VV laxity in flexion concentrated at 2°. The VV laxity in flexion has shorter tail, indicating not many high laxity values. AP laxity showed similar average

value in both extension and flexion; The density plot shows the AP laxity concentrated at 5mm in extension and 6mm in flexion.

Intra-operative Laxity VS Stress Radiograph Laxity

The Navigation VV laxity data at 20° and 90° flexion were compared to laxity data from stress radiograph using Bland Altman plots, shown in Figure 5.6**Error! Reference source not found.**. The plots show the mean difference and limit of agreements (LoA), which defined as the mean difference ± 1.96 SD of differences. The plots show there is a bias between the two methods to measure VV laxity, with stress radiograph laxity tends to be tighter than intra-operative assessment. This trend was observed on both before and after osteophyte removal laxity. The mean difference for laxity in extension was 4.6° (LoA were between -0.3° and 9.5°) prior to osteophyte removal and 5.2° (LoA were between 0.42° and 10.7°) for after. Similarly, the mean difference of stress radiograph with prior osteophyte removal laxity in flexion was 2.6° (LoA were between -4.1° and 9.3°) and for after was 2.8° (LoA were between -3.0° and 8.6°).

This difference could be due to patient's tolerance to pain during loading of stress radiograph. Figure 5.7 shows a boxplot of laxity range and categorisation of average applied load magnitude. A statistically significant correlation between magnitude of load applied and VV laxity range was found for extension (0.33, p = 0.01) but not for flexion (0.13, P = 0.38). This indicates that low load may not be the only factor that contribute to the tighter laxity measured from stress radiograph.

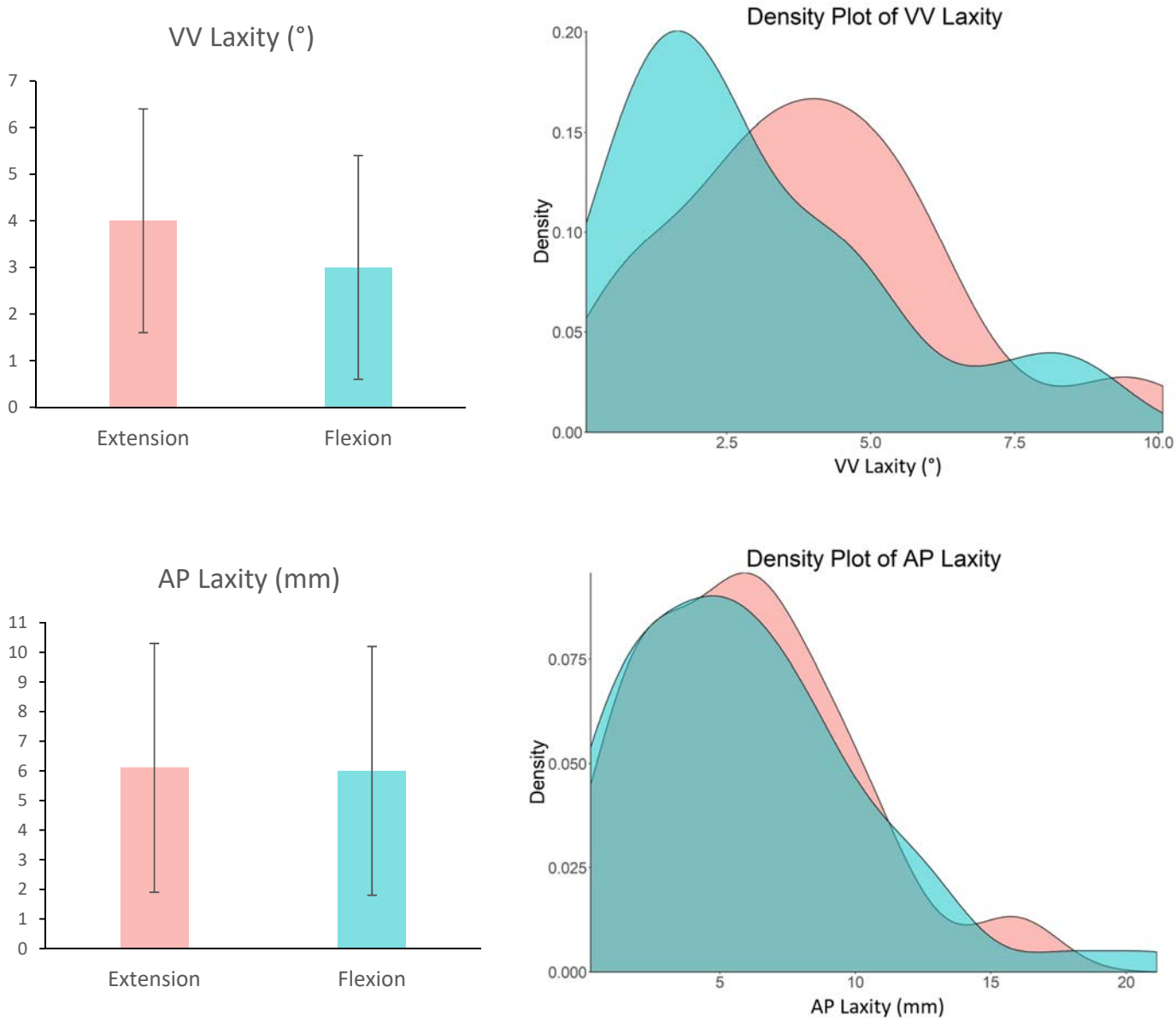

Figure 5.5. VV and AP laxity measured from 3D-2D registered stress radiographs.

Secondary Laxity

Secondary laxity is defined as laxity in any other plane than the load is applied in. Secondary laxity could be the other factor contributing to the Navigation-stress radiograph laxity difference. Unfortunately, the Navigation system used in this study only report the VV alignment during laxity assessment so secondary laxity from the two methods cannot be compared. A graphical

representation of the relationship between VV primary laxity and internal-external (IE) secondary laxity from stress radiograph is presented in Figure 5.8. There are 24 and 29 datapoints where the IE laxity is larger than the VV laxity in extension and flexion respectively. As shown in the plots, the Navigation-stress radiograph laxity difference tends to get larger when the secondary laxity is larger than the primary laxity.

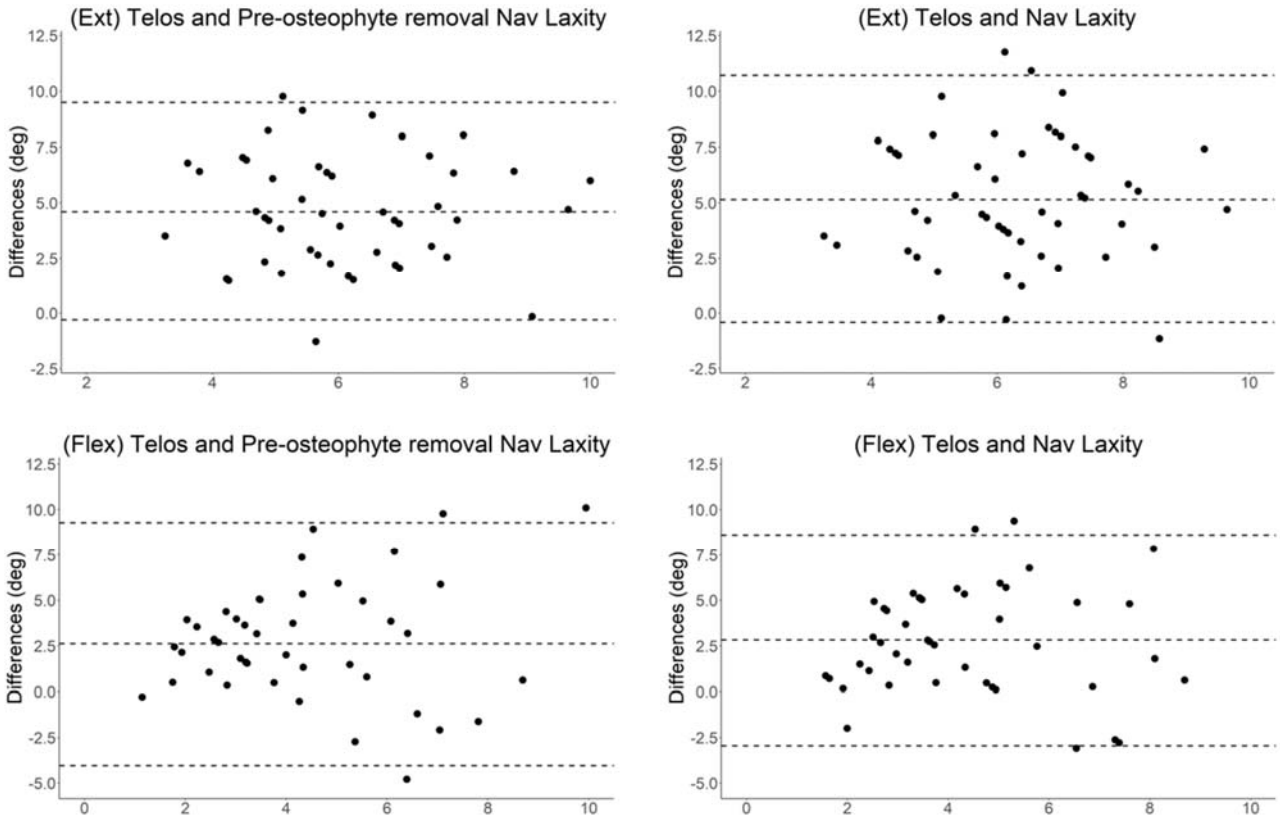

Figure 5.6. Bland Altman plots of VV laxity measured by Navigation system and stress radiographs.

Discussion

This study demonstrated a technique to measure multiplanar knee laxity using 3D-2D registration against stress radiograph. This technique showed distinct interpatient laxity profiles under varus-valgus and anterior-posterior laxity test. The accuracy of 3D-2D registration method was similar to

previous study [371]. Excellent reliability was observed and is comparable to other stress radiography studies [364, 367].

Freisinger et al [379] attempted to systematically review the available literature to assess VV laxity and osteoarthritis patients but concluded that meta-analysis was not possible due to heterogeneity of the subject populations and differences in laxity measurement devices, applied loading, and laxity definitions. Even though direct comparison of laxity measured in this study couldn't be made, there were few relevant studies found. Ishii et al [366] performed stress radiograph to assess VV laxity in extension on 120 TKA candidate knees. They reported a mean varus test knee alignment of 8° and mean valgus test knee alignment of 0°. The alignment was measured as the angle between line drawn on femur distal condyle and line drawn on tibia plateau on captured coronal Xray. In the present study, knee alignment of varus and valgus test in extension were 6.7° and 2.7° respectively. Even though, stress radiograph was used to assess the laxity, different measurement techniques and definitions were used between the two studies. Similar technique to Ishii was used by Okazaki et al [365]. They reported knee alignment of 4.9° for varus and 2.4° for valgus test in extension, and 4.8° for varus and 1.7° for valgus test in flexion. Creaby et al [380] in separate study reported VV laxity of 17.7° (knee alignment is 8.5° varus for varus test and 9.2° valgus for valgus test). They assessed the laxity using custom dynamometer (modified Kin-Com) with VV angulation measured directly from the device. Sharma et al [381] compared AP and VV laxity between healthy and osteoarthritis patients. They found osteoarthritis patients had AP laxity of 6mm and VV laxity of 4.5°. In the present study, the AP laxity and VV laxity were 6.1mm and 4.0° respectively in extension. Therefore, the laxity values measured in this study are within the bounds of previously reported in the literature.

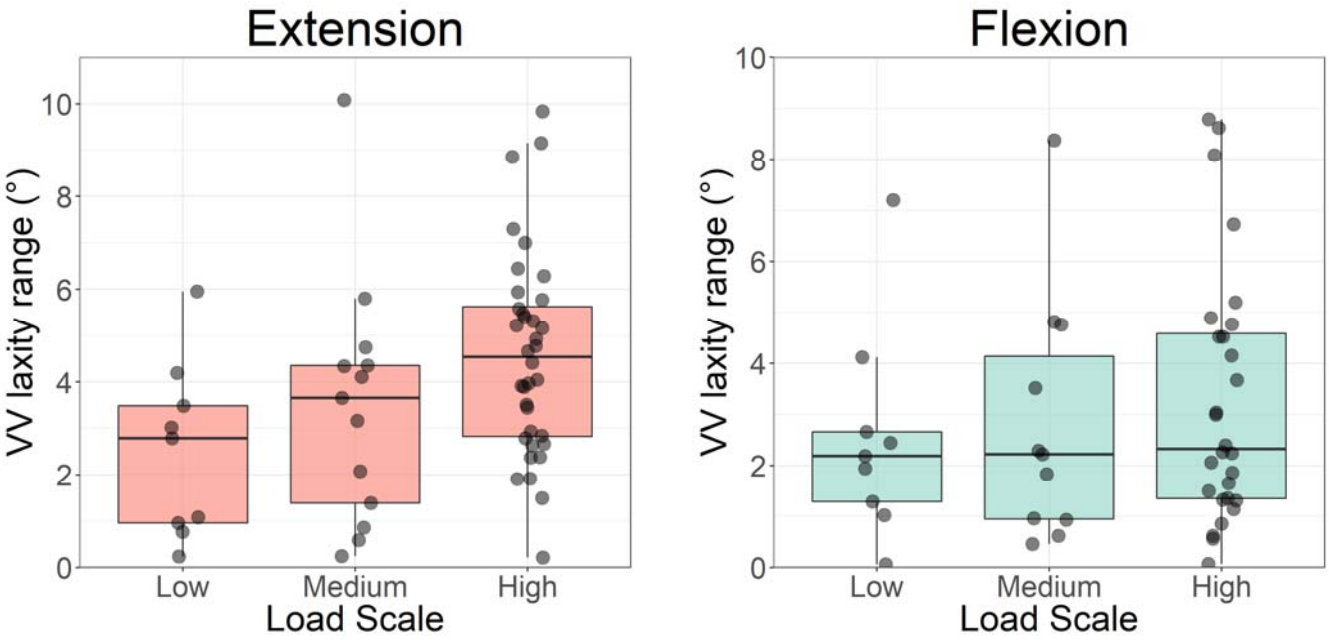

Figure 5.7. Box plots with scatter points of laxity range across categorisation of average applied load magnitude in extension and flexion (high >10Nm, medium is between 7Nm and 10Nm, and low is <7Nm).

The secondary objective of this study was to compare the stress radiograph laxity to intra-operative laxity assessment measured by Navigation system. Figure 5.6 shows that there is a bias between the two methods to measure VV laxity, with stress radiograph laxity tends to be tighter than intra-operative assessment. This can be attributed to different reference frame definition used in Navigation system to calculate knee alignment, and the patient's pain tolerance during stress radiograph assessment leading to low load applied that resulted in incomplete true laxity assessment. This was shown in Figure 5.7 where high load seems to lead to higher laxity, particularly in extension. The imaging protocol instructed radiographer to gradually increase the load to maximum of 150N or until the patient indicated that they were uncomfortable with the stress. However, it was observed in few occasions that older patients were afraid of the pain feeling which led the radiographer limit the load applied early. This might have some effects on the laxity observed. The high load in flexion not

translated to higher VV laxity could be due to bigger coupled motion in response to applied load in flexion.

Other factors include muscle activity in resisting the motion, secondary laxity and un-controlled applied stress by surgeon during intra-operative assessment. Tsukeoka et al [360] evaluated knee laxity without and under anaesthesia and reported laxity significantly increased under anaesthesia with 23% of patients' laxity changed by more than 3°. Other studies by Zhang et al [382, 383] showed that passive resistance moments increased linearly with increasing knee valgus and varus angles. Mean difference for laxity was 4.6° in extension and 2.6° in flexion. Some of the patients in this study could have unconsciously resisted the motion as the load being applied during stress radiograph assessment. On the other hand, surgeons applied load for laxity assessment could also contributed to the mean difference. No load reading was used intra-operatively and the maximum load applied was subjective.

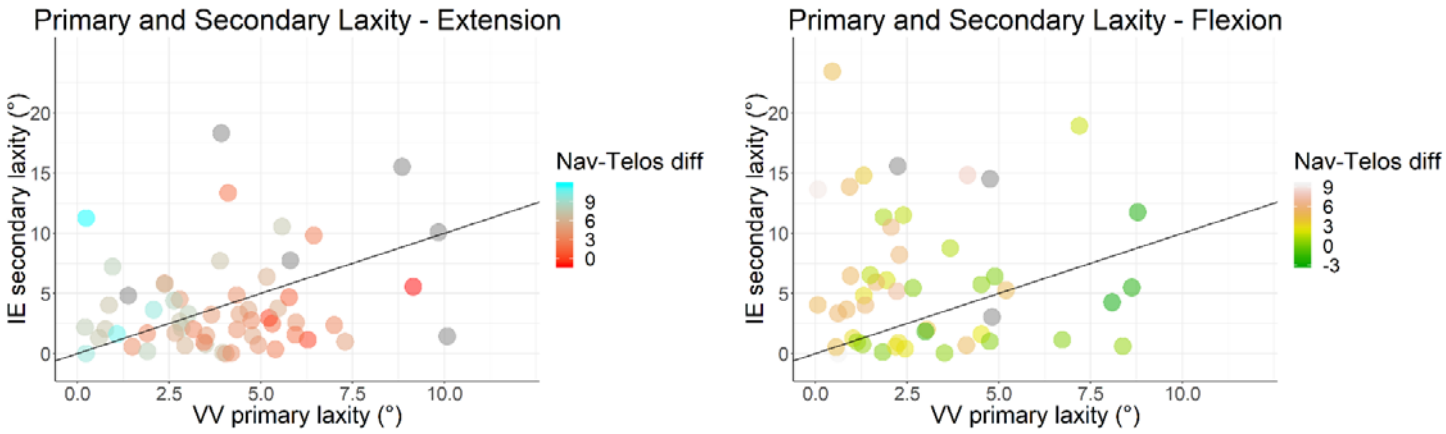

Figure 5.8. Relationship of VV primary laxity and IE secondary laxity in extension and flexion shaded by the Navigation-stress radiograph laxity difference. The black line represents y=x line as a reference line to indicate which patient has larger IE laxity than VV laxity.

Secondary laxity or coupled motions could be the other factor contributing to the Navigation-stress radiograph laxity difference. Figure 5.8**Error! Reference source not found.** shows that knees which had larger secondary IE laxity than VV laxity had an increased Navigation-stress radiograph laxity

difference to those that had lower IE laxity. The plots also show the secondary laxity increased from extension to flexion. The average IE laxity for the knees above the reference line is 3.6° ± 3.6° in extension and 6.6° ± 5.3° in flexion. This observation was similar to Gladnick et al [384] findings, the coupled motion of IE increases towards flexion in response to applied varus and valgus load. The increased secondary IE laxity in flexion could be related to screw home mechanism of the knee, where the popliteal muscle contracts as the knee flexes, causing the femur to rotate externally [13, 14].The ability to identify and measure coupled motions in the knee is one of the advantages of the presented method. Only IE coupled motion was discussed in this study as it was the most relevance when comparing VV laxity.

There were several limitations in this study. Firstly, the flexion angle of the knee was not accurately controlled during stress radiograph. Radiographer visually flexed the knee to the desired angle and briefly checked with goniometer. However, the measurement depends on where the arms of the goniometer were placed, and it could be difficult to determine for patients with high BMI. Secondly, the knee was not constrained during VV loading in flexion which could lead to femur rotation. This could have contributed to the larger IE coupled motion in flexion. Kobayashi et al [385] used a rubber band to fix the femur to prevent the rotation of a femur.

Other limitation in this study relate to the 3D bone model was manually registered to the Xray. Although verification and reliability study were performed, this technique relies on the operator to be trained and careful in registering the 3D model. Other studies used a version of automated matching algorithm to optimize the 3D-2D registration [371, 386]. In this study, the registered Xray was checked by other qualified engineer for quality assurance before finalising the registration. Navigation system used only record VV angulation. This limits the comparison of coupled motion of laxity assessment. Finally, intra-operative digitized bony landmarks could be different to the landmarks identified from CT scan, resulting in inconsistency knee alignment measurement definition.

Stress radiograph in combination with 3D-2D registration technique showed to be a suitable method to evaluate multiplanar knee laxity non-invasively. The method described preserves the bony landmarks definition to be used to calculate knee alignment in different position. Measured laxity from stress radiograph shown to be different from laxity measured intra-operatively. Patient consciousness during assessment, pain tolerance and coupled motions in response to the applied load seem to affect the laxity measured. Stress radiograph and pain level perhaps could be a good indicator of what the post-operative laxity target should be for individual patient.

The ability to quantify patient's knee laxity in 6 DOF non-invasively enables next development phase of knee computational modelling. Quantified 3D knee position with applied load can be used as a surrogate to corroborate displacement and load relationship of the knee in computational modelling to determine subject specific ligament characteristics.

Chapter 6

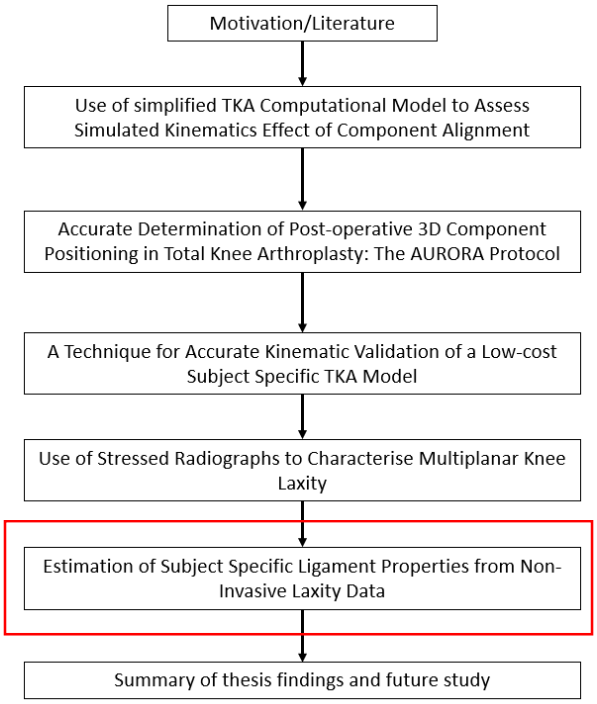

Estimation of Subject Specific Ligament Properties from Non-Invasive Laxity Data

This chapter was published as extended abstract at CAOS 2017, 17th Annual Meeting of the International Society for Computer Assisted Orthopaedic Surgery

Theodore W, Little J, Liu D, Bare J, Dickison D, Taylor M, Miles B, "A novel method for defining ligament characteristics in subject specific dynamic surgical planning"

Introduction

Computational modelling is a scalable technique that allows the study of both patient and surgical factors and their interactions on knee dynamics. Development of knee computational model is a continual challenge. Often, the details in published models varied considerably, including the number and complexity of included structures, material behaviour, or the use of generic versus subject-specific representations of bone and ligament parameters [387]. Regardless of the complexity, subject specific information has been identified as important inputs to knee models [66, 387, 388]. At the same time, a low-cost computational model is needed in order to realise the use of such tool to optimise joint dynamics as part of TKA surgical planning. In previous chapter, we presented a non-invasive 3D-2D registration technique used to characterise knee laxity in 3D captured from stress radiograph. This method preserves the bony landmarks definition used to calculate knee alignment in different position. This chapter presents a technique to corroborate the quantified 3D knee laxity position and load relationship to determine subject specific ligament characteristics.

Previous computational studies have attempted subject specific ligament characteristics evaluation by optimizing load-displacement response of the knee. Baldwin et al [217] subjected cadaver knees to passive laxity assessment using an instrumented prosthetic foot. Tibiofemoral ligament properties were optimized to fit the experimental data. Similarly, Ewing et al [251] measured knee load-displacement relationship using a custom navigation system and stability device. Mootanah et al [250] in their study used robot actuator to move the cadaver specimen from extension to flexion. The ligament properties were adjusted iteratively until the model kinematics closely matched those in-vitro.

Three cadaver specimens were assessed, and ligament stiffness and reference strain were optimized in Baldwin et al [217] study. Optimized ligament reference strain varied from -4% to 4% and RMS error less than 1.8mm and 2.2° were achieved when the optimized computational model kinematics

compared to in-vitro kinematics. Meanwhile, Ewing et al [251] evaluated seven cadaveric specimens and reported a wide variability of reference strain, up to 40% reference strain between specimens. Their study showed RMS error of 3.5° when optimized ligament properties were used. Mootanah et al [250] validated their model by measuring intra-articular force and pressure measurements. They used different ligament properties for different knee flexion and achieved up to 6% error compared to in-vitro recorded compartmental loads.

Even though these studies showed good model validation with optimized ligament properties, the assessments process were invasive. These methods can be suitable for developing a computational model that only use single or few subjects as its representative. However, these methods are not scalable for computational model used on subject specific level in clinical setting. Additionally, these studies have only measured in-vitro ligament properties. In-vivo properties may be different with the ligaments becoming stiffer after death [389].

Kang et al [351] introduced a method to evaluate in-vivo ligament properties using a probabilistic approach accompanied with laxity test under Computed Tomography (CT) scan. CT and stress device, TELOS, were used to record the Anterior-Posterior (AP) drawer laxity test in extension and flexion. The ligament stiffness and reference strain were optimized to minimize the difference between the movement of the knee in the model and stress radiographs. In their follow up study, Kang et al [352] compared the model kinematics to those observed from laxity test under CT and reported differences up to 2mm. However, only use 1 healthy knee subject was used in the study and multiple CT were used to capture the laxity test which increased amount of radiation exposure to the subject.

The main objective of this study was to present a novel method that use clinically attained knee laxity data as surrogate for load-displacement relationship to determine subject specific ligament free length. Knee laxity data was obtained from stressed radiograph and virtualised using 3D-2D registration. Reference strain from optimized ligaments free length were compared to previous reported studies. Secondary objective was to compare the computational model outputs of ligaments

generic reference strain and optimized reference strain using knee computational model developed in chapter 4.

Method

Knee Laxity Data

In this study, the knee laxity data of nine randomly selected TKA candidates from chapter 5 were obtained. Each subject received supine long leg CT scans, standing radiographs and a series of pre-operative stress radiographs (varus, valgus, anterior, posterior test). Nine subjects were chosen as a proof of concept of the technique described. In this study, only varus and valgus stress radiographs were used to optimize Lateral Collateral Ligament (LCL) and Medial Collateral Ligament (MCL) properties.

The pre-operative CT scans and stressed radiographs were processed using the method detailed in Chapter 5. In brief, the CT scans were segmented using ScanIP software (Simpleware) and bony anatomical points, including ligament attachment sites were landmarked. 3D-2D registrations were performed in Mimics (Materialize, Leuven, Belgium) using the segmented femur and tibia against the radiographs to determine knee alignment for each stress radiograph. Registered femur bone models were normalised to CT reference frame while maintaining tibia-femur relationship from registered position. The tibia in CT reference frame is registered to each of the registered tibia is calculated. The transformation matrix is used to transform the anatomical landmarks taken in the CT reference frame to the registered positions to determine the knee alignment for each stress radiograph. Femur and tibia mechanical axis were determined from anatomical landmarks and were used to calculate the knee alignment. Refer to **Error! Reference source not found.**3 in Chapter 5 for detailed description.

Tibio-femoral Knee Laxity Model

Subject specific rigid body models were created in multibody dynamics simulation software, ADAMS (MSc) for pre-operative native tibio-femoral joint. The model includes patient reconstructed bony geometries, anatomical landmarks and ligaments (LCL and MCL). The LCL was considered to be a single fibre bundle and the MCL was considered to consist of anterior and posterior bundles. The bony axes and ligament attachment points were determined as described in Chapter 4. Each ligament was modelled as 1D non-linear spring elements, shown in Equation (1) Where k is the stiffness parameter obtained from the literature [257] (2000N and 2750N for LCL and MCL respectively), $lfree$ is the free length of the ligament, and ε_l is the spring parameter assumed to be 0.03 [61].

$$f = \frac{1}{4}\, k \frac{\varepsilon^2}{\varepsilon_l}, \qquad 0 \leq \varepsilon \leq 2\varepsilon_l$$
$$f = k\,(\varepsilon - \varepsilon_l), \qquad \varepsilon > 2\varepsilon_l \qquad \textit{Equation (1)}$$
$$f = 0, \qquad \varepsilon < 0$$

$$\varepsilon = \frac{l - l_{free}}{l_{free}} \qquad \textit{Equation (2)}$$

$$\varepsilon = \frac{l - l_{free}}{l_{free}} + (flexion * ff) \qquad \textit{Equation (3)}$$

The free length is defined as the length of the ligament when it first becomes taut. Reference strain was defined as the strain in the ligament when the leg is in a neutral position, which in this study is defined with the leg in full extension in CT scan. Thus, reference length is the ligament length when the leg is in full extension in CT scan.

Most previous studies used the reference strain to determine ligament free length. This will be referred as reference strain method in this study. In this method, the free length is calculated using Equation (2) in which the reference strain is adopted from literature or derived from other sources. Galbusera et al [67] published a review on ligament models and properties used previous computational modelling studies. The study showed most previous computational studies referenced at least some form of literature values for ligament parameters, often from Blankevoort et al [62], Rahman et al [68], or Wisman et al [61]. The reference strain from these studies are shown in Table 6.1.

This study does not use reference strain method, rather the ligament free length is derived from known ligament forces at known positions. Although the subject specific ligament attachment sites were identified from CT, the ligament length was modelled as 3D distance between the insertion and origin attachments. We introduced another factor, flexion factor (ff) in the strain calculation formula, Equation (3), to account for the effect of bone wrapping of the ligament. The parameter is used to lengthen or shorten the strain based on the knee flexion angle. Equation (3) is also used to calculate the reference strain once the ligament free length is derived. The ligament length is calculated as 3D distance between attachment points.

All components were modelled as rigid bodies using a penalty-based contact between components. The pre-operative native model was virtually positioned to the stress radiograph positions to simulate the boundary conditions when the knee is stressed. The model was allowed to translate superior-inferiorly while maintaining the knee alignment during simulation to induce contact between distal femur and proximal tibia. See Figure 6.1 (A) and (B).

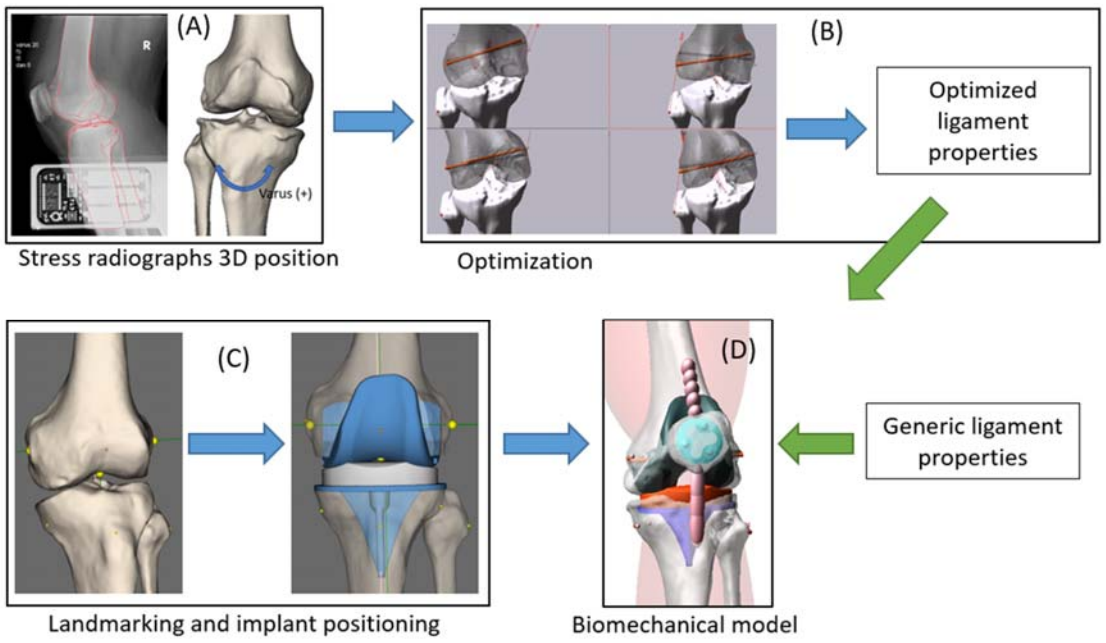

Figure 6.1. Flowchart of steps. (A) 3D position of native femur and tibia obtained from 3D-2D registration against stress radiographs. (B) Subject specific pre-operative native tibio-femoral knee model created. The model replicates the knee positions measured in stress radiographs. Measured laxity load applied, and ligament free lengths were optimized. (C) Implant components were positioned in mechanical alignment on segmented bones. (D) Subject specific post-operative knee computational model created to simulate deep knee bend. Simulation was run with generic and optimized ligament properties.

Ligament Parameters Optimization

Initially, a nominal load of 100N is applied on each ligament and then perturbed by 5N sequentially, giving a set of ligament force-joint load sensitivities. A surrogate model at each stressed position is created by combining these sensitivities with the 3D insertion-origin ligament length at that particular stressed position and the known force-strain-displacement relationships from Equation (1). This surrogate model is to calculate joint loads for a given ligament parameters during optimization.

The objective function, Equation (4), of the optimization was to minimise the resultant internal joint load discrepancy on the knee measured in stress radiographs and the simulated internal joint load. Equation (5) calculated the difference between the resultant internal joint load on the knee measured in stress radiographs and the simulated internal joint load for each stress radiograph position. Parameter optimisation was performed using gradient descent method in Python. $lfree$ and ff were the optimization parameters. The initial values for $lfree$ were determined using the reference strains method taken from literature [68] (expressed as percent strain). The values are shown in Table 6.1. Initial value of 0 was used for ff. By design, ff is a function of flexion and therefore it is more dominant for resolving load discrepancy in flexion.

$$J_{total} = J_{var\_ext} + J_{val\_ext} + J_{var\_flx} + J_{val\_flx} \qquad Equation\ (4)$$

$$J = \sqrt{(M_{telos} - M_{model})^2} \qquad Equation\ (5)$$

Valgus stress radiograph in extension and flexion was used for Anterior MCL (antMCL) and Posterior MCL (postMCL) and varus stress radiograph in extension and flexion were used for LCL. A post-operative TKA knee model was constructed for each subject as described in next sub-section. Subject specific reference strains were then calculated using Equation (3) at 0° flexion with the optimised ligament parameters and compared to reported reference strains from previous studies.

Knee Computational Model

This study used the low-cost knee computational model developed in Chapter 4. Refer to that chapter for detailed description of the model development. After the subject's CT was segmented and landmarked, Total Knee Arthroplasty (TKA) implant components were positioned relative to subject's bone to create a subject specific post-operative TKA knee model. A fixed bearing, cruciate-retaining, symmetrical femoral and tibial condyle multi-radius implant design (Apex CR; OMNIlife science, East Taunton, MA, USA) was used. The implants were aligned to the respective bone mechanical axis.

The knee computational model was setup to simulate deep knee bend to replicate experimental mechanical simulator, Oxford Knee Rig. Two simulations were run for each subject. The first simulation group was run with LCL and MCL $lfree$ derived using reference strain method and generic literature values [68]. Equation (2) was used to calculate the strain for first simulation. Second simulation group was run with optimized LCL and MCL $lfree$ and ff. Equation (3) was used to the calculate the strain. Two posterior Cruciate Ligament (PCL) bundles were included in both simulations. Their stiffness and reference strain were adopted from literature [68, 257], anterior bundle stiffness 9000N and reference strain 0.4%, posterior bundle stiffness 9000N and reference strain 8%. The kinematics outputs of ligaments generic reference strain and optimized reference strain model was compared. Paired T-test and F-test was used to compare the mean and variance between the 2 groups.

Results

Optimized Reference Strains

The mean coronal alignment in CT was 3.9° varus, ranging from 7.7° valgus to 8.8° varus. Each subject had a varus valgus laxity calculated from the stress radiographs taken. The mean varus valgus laxity range in extension and flexion were 4.7° (SD, 2.9°) and 3.9° (SD, 3.0°) respectively.

Subject specific reference strains determined from optimized ligament parameters are summarised in Table 6.1. There was a wide variation in the optimized reference strain values between subjects and ligaments. The LCL ligament showed the greatest variation in reference strain, with a range of 39% strain between subjects. Then followed by antMCL with a range of 37% strain and the least variation, postMCL, with a range of 19% strain between subjects. Standard deviations of optimized reference strains were similar to Ewing et al [251] findings. Table 6.2 shows the Pearson's correlation of optimized reference strain against coronal alignment and laxity measured. LCL and postMCL showed strong and statistically significant correlation against coronal alignment but only postMCL showed strong and statistically significant correlation against laxity measured.

Table 6.3 shows the $lfree$ calculated using the 2 methods, reference strain method with adopted literature value [68] and optimized lengths. LCL showed the highest $lfree$ variation in both generic and optimized groups while both antMCL and postMCL showed similar variation. $lfree$ average difference between generic and optimized group for antMCL and postMCL were 4.0 $\pm$ 4.7mm (t-test significance, μ <0.05) and -3.1 $\pm$ 2.9 mm (μ <0.05) respectively; meanwhile LCL difference was -4.2 $\pm$ 6.2mm (μ = 0.08) and not significant between the two groups.

Table 6.1. Optimized reference strains (as % strain); reference strains reported in previous studies; Coronal alignment in CT scan and varus valgus laxity in extension and flexion (Varus angle is positive).

	LCL (%)	antMCL (%)	postMCL (%)	Coronal alignment in CT (°)	Varus valgus laxity range	
					extension (°)	flexion (°)
Wismans et al., 1980 [61]	5	-3	5			
Blankevoort et al., 1991 [62]	-5	4	3			
Rahman et al., 1998 [68]	5	-6	3			
Average from Ewing et al (7 specimens)	-2 ± 15	-11 ± 14	-8 ± 8			
Average from Baldwin et al (3 specimens)	-1 ± 4	0 ± 3	1 ± 4			
Subject 1	-3	26	-4	4.7	5.2	8.8
Subject 2	-1	8	-4	8.8	1.1	1.1
Subject 3	-5	10	2	8.5	1.9	1.1
Subject 4	-8	-4	-3	3.8	5.7	2.8
Subject 5	-5	3	3	5.3	0.8	1.0
Subject 6	-5	-6	-7	5.2	6.9	4.0
Subject 7	-13	0	1	7.0	9.3	3.8
Subject 8	9	0	-1	-0.2	6.0	4.0
Subject 9	26	-11	-16	-7.7	5.6	8.6
Average ± std	**-1 ± 12**	**3 ± 11**	**-3 ± 6**	**3.9 ± 5.1**	**4.7 ± 2.9**	**3.9 ± 3.0**

Table 6.2 Pearson's correlation for optimized reference strain against knee coronal alignment and laxity. [a] Denotes significant correlation from 0 to P <.05

Optimized reference strain	Alignment in CT (°)	Laxity extension (°)	Laxity flexion (°)
LCL	-0.88[a]	-0.03	0.54
antMCL	0.51	-0.33	0.08
postMCL	0.74[a]	-0.25	-0.69[a]

Table 6.3. $lfree$ *measured with* reference strain method with adopted literature values [68] and optimized $lfree$. Units is in mm.

Subject	Generic			Optimized		
	LCL	**antMCL**	**postMCL**	**LCL**	**antMCL**	**postMCL**
1	59.7	55.8	57.2	64.5	41.8	61.1
2	58.6	43.2	44.9	62.4	37.3	48.0
3	64.2	49.9	51.6	71.3	42.5	51.9
4	62.4	52.1	53.7	71.7	51.1	56.8
5	51.9	44.2	46.1	57.8	40.2	46.0
6	69.7	52.1	53.6	76.9	52.2	59.3
7	52.9	40.8	43.1	63.8	38.4	44.0
8	69.7	49.5	51.1	66.9	46.4	52.9
9	50.8	40.3	42.9	42.1	42.1	52.1
Average	60.0	47.6	49.4	64.2	43.6	52.5
Std	7.2	5.6	5.2	10.1	5.3	5.9

Kinematics Outputs

Strain of each ligament was measured throughout flexion of the knee computational model. Figure 6.2 shows box plots of strain of the 2 simulation groups at 0°, 30°, 60°, 90° flexion. PostMCL showed statistically significant mean difference and variation throughout flexion whereas MCL showed significant mean difference in extension only but significant variation difference throughout flexion. On the other hand, LCL showed no significance in mean difference but significant variation difference in almost all flexion increment between the 2 groups. PostMCL of optimized ligament properties had

opposite trend to the generic ligament properties group, ligament measured distance shorten as flexion increases.

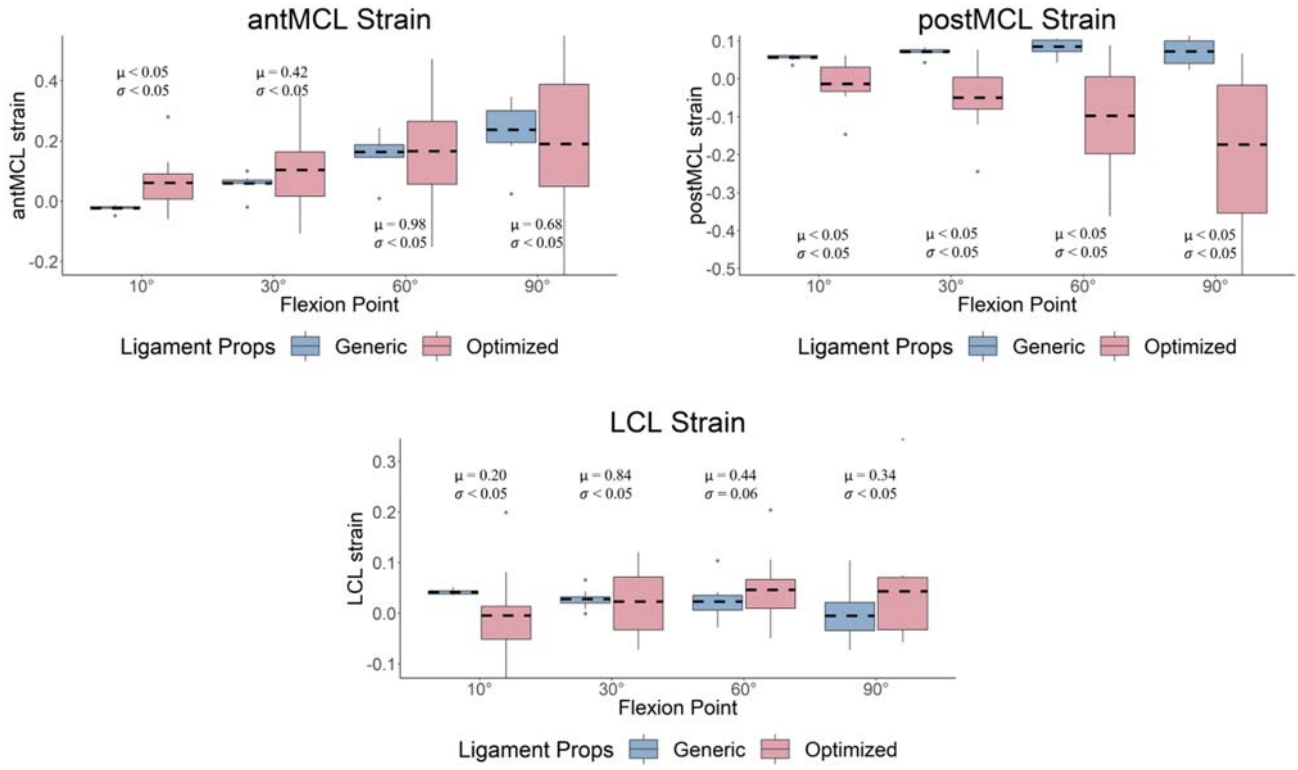

Figure 6.2. Box plots of strain at 4 flexion increments. Dashed line represents mean of the strain at that flexion. Scatter points represent outliers. μ = significance of T-test, σ = significance of F-test.

Figure 6.3 shows the kinematics outputs for each subject and **Error! Reference source not found.** shows the box plots of the kinematics with mean difference and variation difference significance. There was no significant difference in mean for internal-external (IE) rotation and patella tilt kinematics. However, IE rotation of group 2 showed significantly higher variation in early flexion. Femoral rollback showed significant mean difference at 30° flexion but then the 2 groups converged towards flexion. No significant difference for both mean and variation for varus valgus between the 2 groups. But there were few outliers on group 2 where the knee is in high varus in early flexion. These were subjects 1, 2 and 7 where the optimized antMCL free length is significantly shorter than LCL or in other words when the antMCL has significantly higher reference strain than LCL. The high varus in

early flexion characteristics of these subjects were due to the LCL ligament force was not high enough to balance the antMCL ligament force.

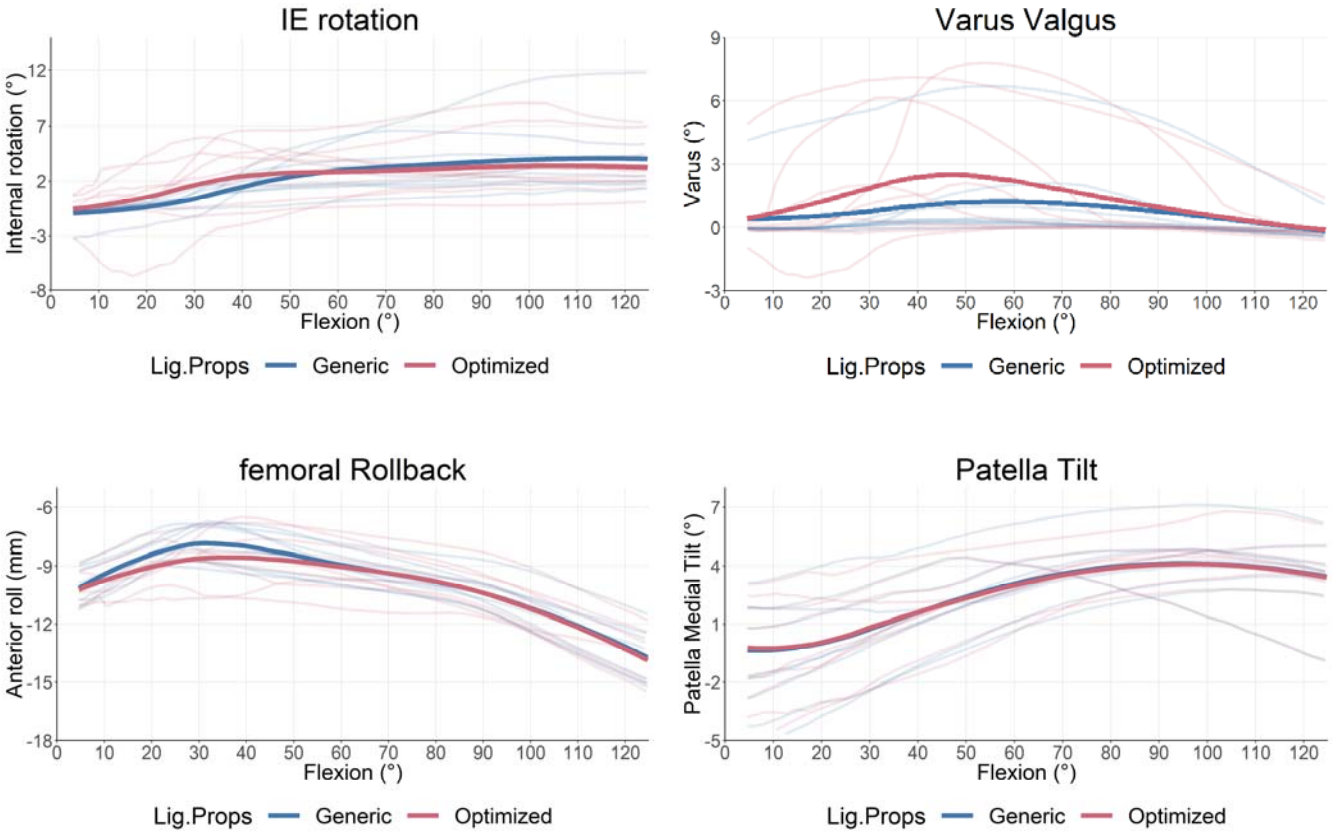

Figure 6.3. Line plots of simulated kinematics. Transparent lines represent each subject kinematics and dark solid line represents mean of the simulated group kinematics. Internal-rotation is measured in femur reference frame. Positive internal rotation represent tibia is internally rotated relative to femur.

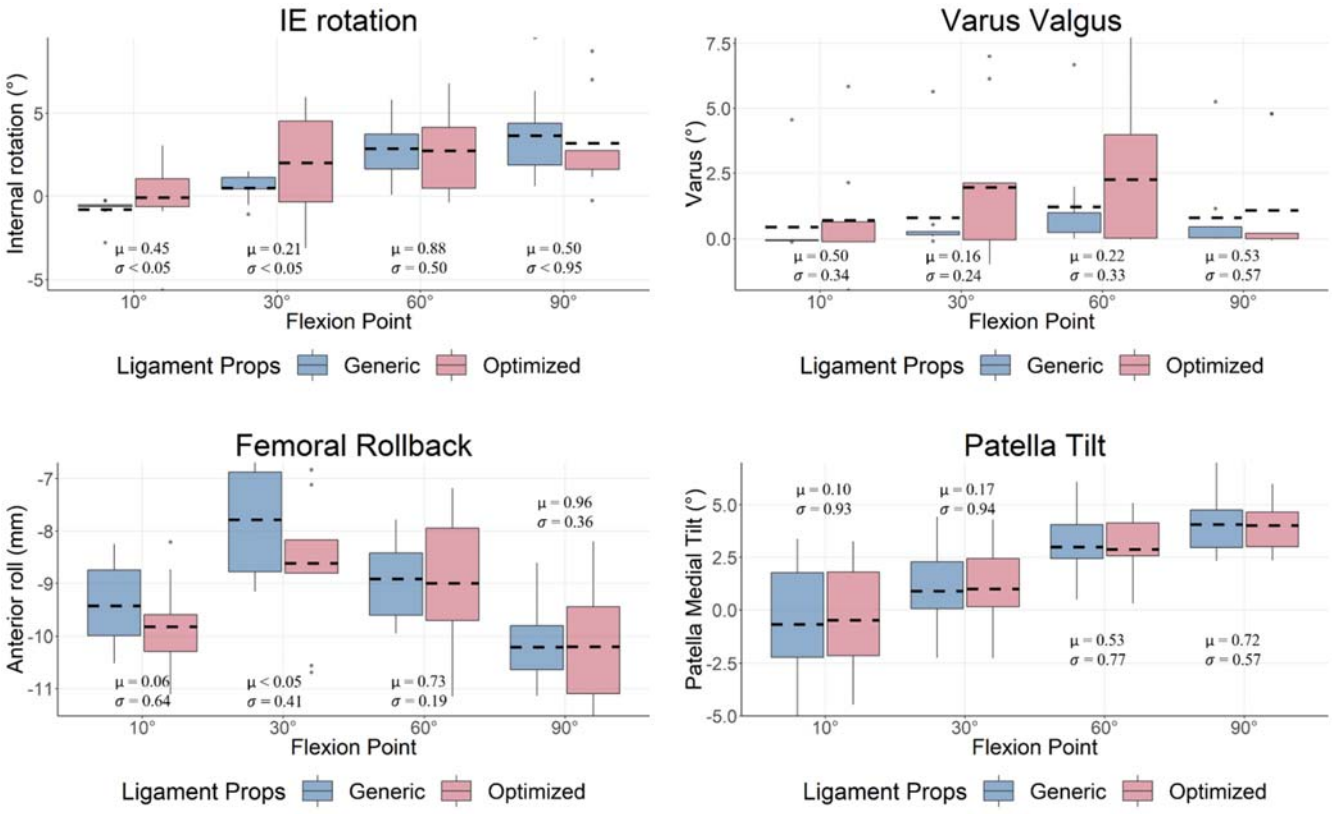

Figure 6.4. Box plots of kinematics at 4 flexion increments. Dashed line represents mean of the strain at that flexion. Scatter points represent outliers. μ = significance of T-test, σ = significance of F-test. Only femoral rollback in early flexion showed significant mean difference between the 2 simulation groups while only Internal-External (IE) rotation showed significant variation difference in early flexion.

Discussion

Computational modelling can be used to evaluate various surgical and anatomical parameters and its effect to TKA biomechanical behaviour prior to the surgery [215, 216]. Knee extension is usually considered as the reference state from which different motions can be simulated. In this state, the ligaments are strained and therefore already sustaining a load [66, 67]. Previous computational studies often use this as reference state to measure the ligament free length, known as reference strain method [278]. Although there are studies which have performed experimental test to determine ligament properties, most studies are still referencing old studies for ligament spring model

properties. This could be due to the complexity of experimental protocols and variability between different subjects, particularly the age of donor and/or pathologies that might have affected ligament mechanical behaviour [67]. However, several computational model studies have attempted subject specific ligament characteristics evaluation by optimizing load-displacement response of the knee [217, 250, 251, 351].

The objectives of this study were to: 1) present a method to determine subject specific ligament free length using non-invasive attainable clinical data, 2) determine reference strain from optimized free lengths and compare to previous studies, 3) compare the computational model outputs of optimized free lengths to the free lengths obtained using reference strain method.

In summary, this study demonstrated a technique to characterise in-vivo subject specific ligament properties using non-invasive attainable clinical data, knee laxity from stress radiographs, as surrogate of the load-displacement response of the knee. Statistically significant difference was found between optimized and generic free lengths for antMCL and postMCL but not LCL. Our findings show that generic reference strain values reported in literature [61, 62, 68] differ significantly from numerically obtained reference strain. Furthermore, there was a wide variation in reference strains between subjects and ligaments, with variations ranging from 19% to 39% strain. However, from computational model outputs comparison, subject specific ligament properties did not show statistically significant difference in the observed measures.

Standard deviations or variations of optimized referenced strains in this study show similar characteristics to Ewing et al study [251]. However, compared to Baldwin et al [217] findings, our optimized reference strain has larger variations. Differences were seen in the average reference strain values found, particularly for MCL ligaments. This could perhaps due to subjects used in the study. Baldwin et al [217] and Ewing et al [251] used cadaver specimens which introduced possibility of the ligaments becoming stiffer after death [389]. Additionally, it was not described if the specimens used in their study had osteoarthritis. Subjects in this study were TKA candidates who had end-stage

osteoarthritis. Therefore, knees assessed in this study have severe bony deformity and osteophytes present. The severe bony deformity can cause instability of the knee which may result in slack ligament [366, 381]. However, the presence of abundant osteophytes in addition to severe bony deformity may cause joint contracture on the deformed side which may result in tighter ligament on one side [390-392]. This was observed in this study, with the antMCL ligament on average has higher reference strain than the LCL, particularly for high varus knee. Moreover, the 3D model used in Ewing et al study was developed by scaling of reference values from previous studies without using 3D reconstruction method based on the medical image. The individual subject's ligament attachment points may not agree with scaled points. The attachment points in this study were taken from subject's CT scan.

Calculated reference strain for each specimen in this study fall within a physiologically possible range but do exhibit a larger standard deviation than some previous experimental studies that directly measured ligament properties [60, 393]. This large deviation could be due to the variability of subjects' anatomy and measured joint laxity. Large variation in knee joint laxity was seen between subjects and from Table 6.2, it appears that there is no strong relationship between subject's laxity, coronal alignment and ligaments reference strain. This suggest the ligaments characteristics vary widely between subjects and non-functional imaging is insufficient to determine their characteristics.

Figure 6.2 shows strain comparison of the ligaments throughout deep knee flexion. Both antMCL and LCL strain calculated using optimized ligament parameters showed similar characteristics to the strains calculated using reference strain method. However, strain of optimized postMCL parameters showed opposite trend to the generic ligament model; it decreases as flexion increases. This means the 3D ligament insertion-origin distance of the postMCL ligament gets shorten relative to the free length in flexion. This could be due to the coupled motion in response to applied varus and valgus load as observed from Chapter 5. It was shown in Chapter 5 that coupled motion of Internal-external (IE) laxity increases towards flexion. In this study, the femur is on average 10° externally rotated relative to the tibia in flexion stress radiograph. The postMCL insertion-origin length increases when the femur is in

high external position, which led the postMCL free length to increase during optimization to satisfy the load boundary condition. However, as seen in Figure 6.3, the IE rotation during deep knee bend simulation was not as high as the stressed position and therefore the postMCL insertion-origin length calculated is shorter than the optimized free length and resulted in negative strain value. Moreover, the femur rolls back towards flexion which helps shorten the postMCL insertion-origin distance.

Even though the mean and variance of ligaments strains were shown to be different in most flexion increments, there was no statistically significant difference in mean and variance of kinematics between the 2 simulation groups. One possible explanation is that the implant geometry used in this study has relatively higher congruency between the femur component and tibia insert compared to other contemporary knee implant designs [394]. Other explanation is that deep knee bend simulated in this study does not differentiate enough to pick up the sensitivity of the change in ligament parameters. The computational model replicated Oxford Knee Rig (OKR) mechanical simulator which prescribed the deep knee bend motion that constraint the hip joint to translate vertically with respect to the ankle [246, 276, 395].

However, kinematics range reported in this study are comparable to previous computational studies simulating OKR deep knee bend [261, 336, 396]. Ishikawa et al [261] IE rotation and rollback range from extension to flexion was approximately 6° and 10mm respectively. D'lima et al [396] showed IE rotation and varus-valgus angulation range of approximately 8° and 3° respectively. It was the intention of TKA procedure to improve stability of the knee after surgery and therefore the implant geometry has high contribution to the resultant kinematics [98-100]. As demonstrated in Patil et al [276, 336] and D'lima et al [396] studies, implanted knees kinematics progression, particularly IE rotation, were more linear from extension to flexion compared to native knees.

On the other hand, there were few varus kinematics outliers when optimised ligament properties were used. This was observed in subjects 1, 2 and 7 where the optimized antMCL free length is significantly shorter than LCL. The ligament parameters were optimized using native tibio-femoral

knee model but the deep knee bend kinematics was simulated with post-operative knee model where the implant components positioned at mechanical alignment. Mechanical alignment is achieved by aligning the femur and tibia components against the respective mechanical axis in coronal plane and resecting bone to match implant thickness. Often, the components in this position may not align with the native joint line. This resulted in the bone resection of one side will be less than the component thickness, more significantly so when the native joint line is in high varus or valgus. In other words, the components thickness replaces more than what was resected, adding more material on the knee, which will stretch the ligament when the femur is in contact with the tibia. The high varus kinematics of subjects 1, 2 and 7 could be explained by this phenomenon. A combination of short antMCL free length, high pre-operative varus knee deformity, and mechanically aligned planned components stretched the antMCL ligaments such that the high ligament force was not balanced by the LCL ligament force.

The results of the current study need to be seen within the light of the following limitations. Firstly, no meniscus was modelled in the native tibio-femoral knee model used for ligament optimization. This may affect the contact force calculated in the simulation during optimization as one of meniscus's functions is to distribute the loads experienced by the knee. Kang et al [397] developed a method to probabilistically determine meniscal horn attachment properties using combination of MRI scan at different flexion angles. The current model is developed with CT scan as inputs and meniscus is not visible in CT. Part of future work is to adapt the model for magnetic resonance imaging (MRI) and include meniscus in the model.

Secondly, the optimisation was performed only on 2 parameters. Ligaments of the knee are among the most complicated structures to simulate. Most computational models simplified the ligament attachment areas as a single point to minimise computing cost and therefore limits the effective line of action movement of the ligament force in the model. Practicality is a critical factor for a computational model to be used as surgical planning tool and thus the justification of the

simplification. In this study, a variable was introduced to consider the wrapping behaviour of the ligament and it is varied based on flexion angle. Several studies have reported the sensitivity of ligament attachment sites and its effects to simulated kinematics [350, 354, 398]. Further work is to improve the mechanical role of the 1D non-linear spring by implementing the ability to simulate the movement of the force line of action, particularly in the anterior-posterior direction. With further development, this movement could be characterized with 1-2 additional parameters and solved for in a similar manner as for free length and flexion factor.

Thirdly, only collateral ligaments were investigated in this study. Further work will incorporate the Anterior-Posterior stress radiograph laxity data to determine the cruciate ligament parameters. Multiple bundle ligaments should also be investigated. Other limitation in this study relate to the laxity assessment performed when subject is conscious. This could have affected the true laxity measurement. However, data used in this study reflects actual clinical measurements from TKA candidate. To our knowledge, previous studies used either cadaveric specimen or healthy volunteer data to determine subject specific ligament characteristics. Despite that, if multiple laxity measurements are conducted, the total radiation exposure may become problematic. Therefore, an effort to establish which laxity measurements provide the most useful information should be made to reduce the number of measurements. Another limitation is that only one implant design was evaluated in this study. Other less conforming implant system may have larger impact on simulated kinematics.

Computational model holds great potential to help understand the complex interactions between implant component design, component alignment, and subject specific anatomic characteristics. We demonstrated a proof-of-concept technique to incorporate subject specific ligament properties obtained from non-invasive clinical data to a low-cost computational model. Our findings showed that the estimated ligament characteristics for each subject were distinctly different from one another and from the generic reported values. There were no strong relationships between the subject's long leg

alignment, laxity and soft tissue characteristics. Further study should evaluate other implant designs and the combination effect of subject specific ligament properties, implant component design and component alignments.

Chapter 7

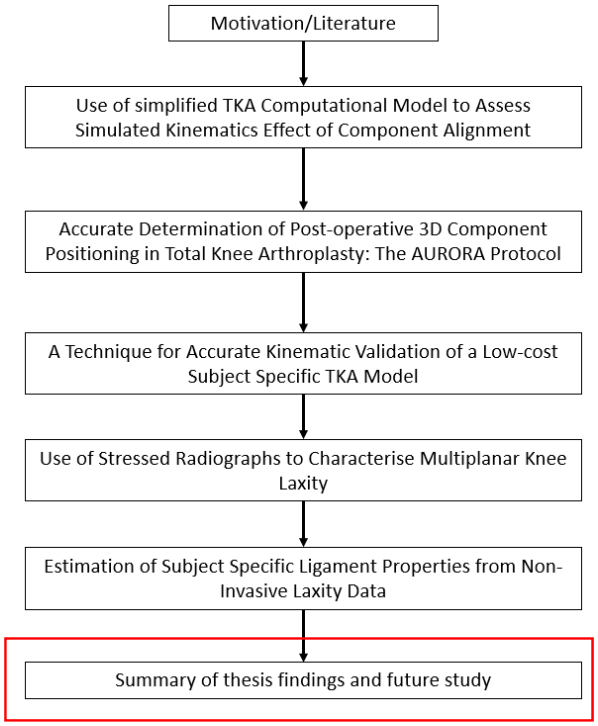

Discussion

The knee is one of the most complex joints in the body, it has the important function of providing support and mobility during standing and gait. It has a role in almost all daily activities and hence, susceptible to failure particularly degenerative joint diseases like osteoarthritis.

Total Knee Arthroplasty (TKA) is considered to be the last solution for end stage osteoarthritis. TKA is a successful surgery when longevity is used as surgery outcome metrics. However, in contemporary TKA, implant survivorship is no longer the only outcome metrics as it does not indicate whether patient is satisfied with the results from the surgery. Multiple studies have shown about 15-20% of TKA recipients are dissatisfied [141, 143, 154, 179]. Patient satisfaction is known to be a complex multifactorial issue [142, 143, 183, 399]. Patient expectation [143, 400, 401], functional [402, 403], pain relief [142, 404], experience of healthcare delivery [405] is only few of the factors. Many studies have attempted to correlate or predicts patient's satisfaction, but no consensus has been reached yet [186, 406-409]. It could be due to the lack of standardisation and validity of adequate outcome measures that makes it difficult to determine which elements before, during and after surgery; and throughout the rehabilitation process that affect the outcomes of TKA.

On the other hand, healthcare cost nowadays is expensive and is increasing as reported by many institutions and government bodies [410-413]. An episode of TKA involves multiple healthcare providers and each one of them have associated cost. For example, TKA episode of care starts with patient visits general practitioner (GP) about their discomfort or pain. Then GP will refer patient to specialist if they deem patient is an appropriate TKA candidate. An Orthopaedic specialist will then consult the patient and booked for surgery or refer to other specialists if they are not a suitable candidate. Patient may be referred to pre-habilitation physiotherapy before surgery. In surgery, there are options of implant system and delivery system technology (e.g. Navigation system) for Orthopaedic surgeon to choose from and their cost varies according to the setup between hospitals and implant providers. After surgery, the patient often will be referred to rehabilitation program either within the hospital or in a physiotherapy clinic. Above is a high-level summary of a typical

patient journey in TKA. There are other intricacies in the journey that were not mentioned. However, the above example illustrates there are many options in how to treat patients while there is no concrete evidence that each patient will be satisfied if they are prescribed with the same pathway. This suggests the cost of a TKA episode can be reduced with appropriate selection for each patient. Therefore, different solutions need to be explored to help clinicians triage patients, helping them to make decision on what resources need to be spent on a patient.

Surgical planning is one key aspect that can help clinicians better choose options for surgery. With the evolution of patient centred care, technological advances in hardware and software, there is an opportunity to combine clinical and biomechanical data collected prior, during and after surgery with computational modelling to improve patient management from surgical planning to rehabilitation programs and, as a consequence, the overall clinical outcome for each individual patient. Currently, most of knee surgical planning has done by assessing the pre-operative long leg alignment or joint line angle and component placement. Surgical delivery using patient specific instrument (PSI) involves planning of intended implant system to fit with patient's bone in terms of placement and size. This planning helps surgeon to be aware of extreme or unusual anatomical deformity pre-operatively and helps them prepare the surgery accordingly. Even though this kind of planning is valuable, static alignment may not differentiate enough as previous studies showed no consensus on the clinical outcomes of different alignment philosophies. As discussed in Chapter 1, joint dynamics may be more relevant to clinical outcomes than component placement alone. However, studies have not shown identifiable, reproducible relationships between joint dynamics clinical outcomes, indicating that clinical outcome of TKA is a product of complex interactions between surgical and patient factors. Surgical factors can be attributed to interactions between the component design, component alignment, and patient specific anatomic characteristics.

Computational modelling is a scalable technique compared to other functional techniques and allows the study of both surgical and patient factors impact on joint dynamics following TKA. Previously,

computational models have extensively been used as pre-clinical evaluation for implant design performance [215, 216]. For use in clinical setting, the application of computational modelling needs to consider following considerations:

- Practicality in clinical setting. i.e. computational model needs to be low-cost (minimal patient specific data input and computing power needed to obtain simulation results within few minutes).

  The model needs to be able to provide information in matter of minutes not hours.
- Inputs to the model are clinically attainable.

  The application of computational modelling cannot be scaled if the process of attaining the model inputs is complicated or requires information not routinely collected as the standard of care.
- Have the relevant complexity to represent the intended reality.

  Generate a model to truly represent entire system would be too complex and for which there would be insufficient data to be formulated in a useful way. A model should be able to predict the behaviour of its intention, at least in a comparative or relative way, even if not absolutely.

This is summarised in Figure 7.1. A balance needs to be found between the right quadrants for a computational model to be used in clinical setting. This thesis aimed to provide a series of studies towards the development of a low-cost knee computational model that intended to be used as part of surgical planning tool to help clinicians triage patient treatments.

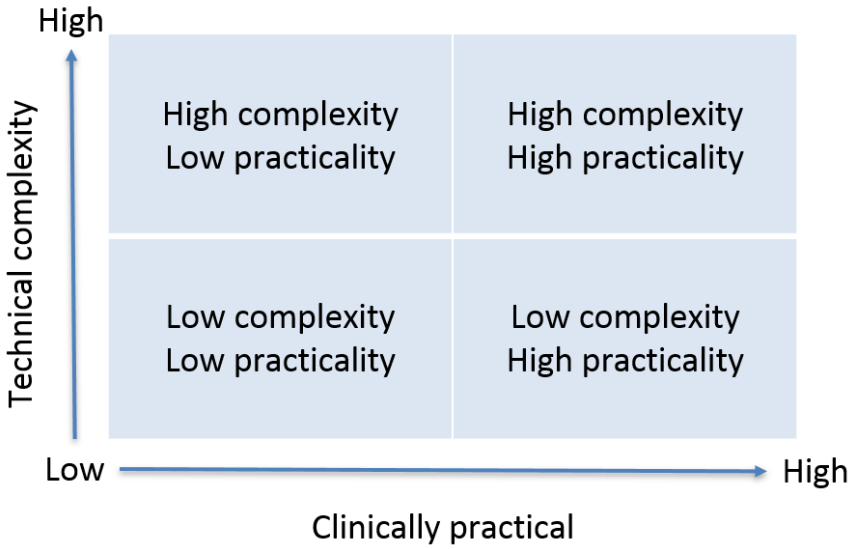

Figure 7.1. Complexity vs practicality matrix for computational model. (Replicated from Chapter 1)

Summary of Key Results

Chapter 2 presented the development of a low-cost computational model of the knee replicating a mechanical simulator and its ability to differentiate simulated kinematics between mechanically and kinematically aligned components on the same subject. The model only used CT scan as inputs. Patient specific bone geometry and soft tissue attachments were obtained from CT scan. Ligament parameters were initially obtained from literature review and adjusted based on experimental validation performed with a cadaver study. Twenty TKA candidate's pre-op CT were processed and Cruciate Retaining (CR) components were positioned to mechanical alignment and kinematic alignment for each patient. Kinematic alignment group showed more kinematic variation than mechanical alignment group. Our findings were comparable to previous reported simulation studies and the simulated kinematics for kinematic alignment group shared some similar characteristics with in-vivo study.

The knee computational model developed was validated by comparing kinematics obtained from in-vitro cadaver study. After re-reviewing the validation steps taken, it was realised there was inconsistency in registration technique used to transform the experimental outputs to the computational model reference frame. It was also realized in the first model validation that inconsistent landmark definition was used to compare the experimental kinematics and simulated kinematics. Upon reviewing previous validation studies, it is unclear whether the earlier computational model works had fully considered this aspect. This might affect the validated ligament parameters derived and simulated kinematics results. Therefore, Chapter 3 and 4 focused on technique to perform accurate registration between reference frames at different steps of the validation process. Chapter 2 was intended to show that a simplified low-cost model could show clinically relevant differences on kinematics for different component alignment. This chapter sets the basis of the theory for technically complex and clinically practical computational model.

Chapter 3 described a new technique to measure post-operative component position from CT by registering segmented pre-operative CT bones and implant geometries to post-operative CT reference frame. The technique showed excellent reliability and reproducibility with the maximum component alignment differences from the mean within this study are low compared to previous literature. Our results also showed a confidence interval up to 10-fold narrower when compared to previous protocols used to quantify component position. This technique allows us to analyse the position and rotation of all components in 3D space with comparison to pre-operative anatomy, allowing us to maintain accurate attachment ligament landmarks obtained from pre-operative CT. If only post-operative CT is used, the landmarking could be inaccurate due to the metal flare visible on the CT, particularly surrounding the implants. The method developed in this chapter can also be used to quantify post-operative 3D component position for clinical use, with comparison to the pre-operative anatomy, allowing surgical changes to the joint to be determined.

Subsequently, using similar technique, Chapter 4 described a series of registration technique that transform cadaver experimental outputs from a mechanical simulator to computational model reference frame which allows identical landmark definition to be used for kinematics comparison. Implant geometries were registered to best match the experimentally digitized implant articular surface. Recorded experimental data was sequentially transformed to the computational model reference frame using the implant geometries default reference frame as the common reference frame. This process allows us to recreate the motion recorded experimentally using the same bony landmarks definition, generating a set of Virtualised Experimental Kinematics (VEK). At the same time, this enable us to overlay the VEK onto the computational model to visually inspect whether the experimental kinematics behaved as expected. This is useful to help identify whether the differences seen between model and experimental come from following sources:

- registration process,
- experimental data capture error or
- modelling of the computational model

Chapter 4 also demonstrated that a low-cost knee computational model with sufficient complexity was able to achieve accuracy in kinematics when compared against experimental data. This has high potential for clinical use. The model used CT imaging data only as its input and ligaments were modelled using literature-based values. This fulfils the factor “Inputs to the model is clinically attainable” in realising the application of computational modelling in clinical setting. The model completed a deep knee bend cycle within few minutes, which fulfils the “practicality in clinical setting” factor. Good agreement was found in trend and magnitude between model-predicted and experimental kinematics in all 8 specimens. The kinematic differences observed in this study were comparable to previous studies, particularly for tibiofemoral (TF) kinematics. This demonstrates the model fulfils the factor “have the relevant complexity to represent the intended reality” which in this context the intended reality is deep knee bend from mechanical simulator. However, even though the

computational model in this study was able to distinguish individual specimen kinematic characteristics well in early and mid-flexion, the kinematics comparison in flexion was not that good. This could be due the simplification of the model and generic ligament parameters used.

Therefore, it was realised there is a need to include subject specific ligament properties into the developed model. However, the method to collect data needed to consider the practicality and attainability factor to maintain the efficiency needed for clinical use. Chapter 5 investigated the use of stress radiograph to attain load-displacement relationship of the knee non-invasively. The chapter focused on 3D-2D registration technique to quantify subject's knee laxity and compared the laxity to what was measured intra-operatively. The results showed there was distinct interpatient laxity profiles under varus-valgus and anterior-posterior laxity test. The described technique showed excellent reliability and was comparable to other stress radiography studies. Other advantages of the technique were the ability to quantify coupled motion and minimise the projection error as compared to laxity quantified from 2D measurement on the planar radiograph. Additionally, this method preserves the bony landmarks definition that were used to calculate knee alignment in different stress radiograph position.

However, the measured laxity from stress radiograph was shown to be different from laxity measured intra-operatively. Patient consciousness during assessment, pain tolerance and coupled motions in response to the applied load seem to affect the laxity measured. This difference does not mean the stress radiograph is not clinically relevant. In fact, this could be a useful combination data of in-vivo laxity and patient's pain tolerance level as part of surgical planning. Despite of this difference, Chapter 5 demonstrated the ability to quantify patient's knee laxity in 6 DOF non-invasively to enable the next development phase of knee computational modelling.

Subsequently, Chapter 6 presents a technique to corroborate the quantified 3D knee laxity position and load relationship to determine subject specific ligament characteristics while maintaining the efficiency of the computational model. Ligament free lengths and flexion factor, a factor introduced

to include the wrapping behaviour of the ligament, were optimized for the displacement-load relationship observed from stress radiographs. Statistically significant difference was found between optimized and generic free lengths for antMCL and postMCL but not LCL. Furthermore, with optimized ligament parameters, there was a wide variation in reference strains between subjects and ligaments, with variations ranging from 19% to 39% strain. This highlights that the estimated ligament characteristics for each subject were distinctly different from one another and from the generic reported values. There were no strong direct relationships between the subject's long leg alignment, laxity and soft tissue characteristics.

However, from TKA computational model outputs comparison, subject specific ligament properties did not show statistically significant difference in the observed kinematics measures. There were distinct differences in early flexion Internal-External (IE) motion but these were not statistically significant. This could be due to the implant system used in this study; It has relatively higher congruency between the femur component and tibia insert compared to other contemporary knee implant designs. The higher congruency suggests that this implant geometry has higher contribution in the resultant knee kinematics than the soft tissue, especially when the soft tissues are under normal tension. Another possible explanation is that the simulated deep knee bend is not sensitive to perturbations in the ligament parameters. However, the simulated kinematics characteristics were similar to previous computational studies simulating deep knee bend motion.

This thesis so far has presented a series of studies towards the development of a knee computational model that aimed to be used as part of surgical planning tool to help clinicians triage patient treatments. After Chapter 6, it was concluded that further study is needed to evaluate other implant designs and the overall combination effect of subject specific ligament properties, implant component design and component alignments to the developed model.

On a separate note, kinetics also affects kinematics [414]. The computational model developed in this thesis simulates closed-kinetic-chain boundary conditions with the hip and ankle joint constrained in

the vertical motion. The external forces applied on each subject's computational model is the same as per the boundary condition described for Oxford Knee Rig. This normalisation is one of the benefits in the simplified model such that less patient specific inputs are needed for the simulation. Kinetics output quadriceps force is included but others are not emphasized. It also needs to be acknowledged that no instruments were available at the time of cadaver lab testing to measure internal joint forces and therefore validation against internal forces could not be performed. Despite that, the computational model developed in this thesis has demonstrated the balance between complexity and practicality for clinical use when assessing kinematics.

The validated computational model is intended to be used as comparative tool between subjects and therefore it was justified to focus on comparing relative kinematics outputs between subjects so that relative kinematic differences attributed to implant component design, position and anatomic characteristics can be compared. The computational model outputs are also intended to be used in conjunction with other clinical data, like Patient Reported Outcomes and surgeon clinical assessment. In this final chapter, examples of applications of the current model will be discussed.

Development of TKR computational model with balanced technical complexity and clinical practicality

This section of the thesis aims to discuss the experience and knowledge learnt from developing a low-cost computational model. As shown in Figure 7.2Figure 7., a computational model needs to have the balance in the right quadrants to be able to be used in clinical setting. Firstly, to achieve this, there were compromises that needed to be made. One of the compromises was the standardisation of the model loading and boundary conditions, i.e. deep knee bend motion as per Oxford Knee Rig (OKR) mechanical simulator. Each patient specific knee model is simulated with same external forces to recreate the deep knee bend motion. There are about 50,000 TKA procedures performed in Australia in 2017 alone. If gait lab or a special lab is needed to obtain model inputs, the adoption of such

application will be hindered by the scalability of the process. Secondly, currently only CT scan is used as the model input. Even though CT scan imaging is readily available in most areas, some countries, like US, charge extra fee to patients. MRI scans can be used but, from my experience, it took much longer to process MRI compared to CT.

Regardless of the complexity of the model developed, all models still need to be validated to ensure its outputs agree with the its intended use. The main lesson learnt in this thesis study is that reference frame definition is very important for computational model validation. This was realised at the end of Chapter 2 and consequently Chapter 3 and 4 attempted to address the reference frame inconsistency. With further thought, the reference frame is a 3-way problem, shown in Figure 7.2.

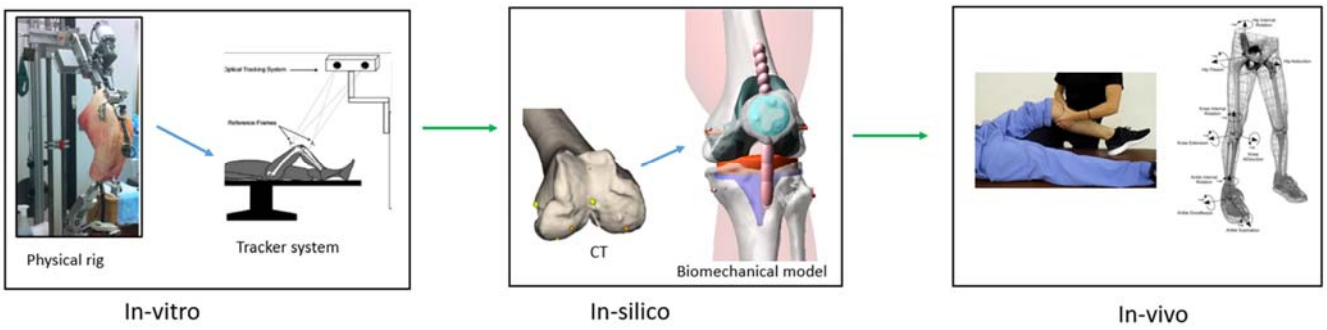

Figure 7.2. Illustration of reference frame used for each environment. In in-vitro environment, the physical rig position is recorded by a tracker (motion capture) system. Movement of the components were measured relatively to each other using rigid body markers attached. In in-silico environment, CT or imaging inputs are transformed to the biomechanical model reference frame. The kinematics measurement definition in-silico need to be relevant and interpretable by clinicians in-vivo. The blue arrow depicts the transformation that happen in the same environment and green allow depicts the transformation between environment. Development of computational modelling need to pay attention to the definition of the reference frames used in each environment and ensure the data transformed in each environment is still relevant to one another.

Reference frame transformation from in-vitro to in-silico is often overlooked. In Chapter 4, we highlighted this challenge and attempted to address it by generating VEK to ensure identical reference frame definition is used when comparing in-silico to in-vitro data. In Chapter 3, a technique was

developed to perform transformation of bony landmarks from pre-operative CT to post-operative CT to ensure identical and accurate landmarks definition are used to generate the knee computational model within the in-silico environment.

During this thesis, a collaboration with Cleveland Clinic and Scripps Biomechanics lab were established for the validation studies. During the collaboration, it became apparent that the Biomechanics lab experts also encounter same challenges and consistency of reference frame definition was often overlooked in their previous in-silico to in-vitro comparison. I consider this is one of the most difficult challenge in validating computational model, especially if experts from different domains are not involved with the work from other domain experts. For example, biomechanics lab operator won't necessarily know reference axes and kinematics definition developed in the computational model and vice versa. Recently, an abstract was accepted to Orthopaedic Research Society conference 2019 [415] with collaboration with Cleveland Clinic Biomechanics lab in utilising our registration method developed in Chapter 4 to identify the differences between recorded kinematics reported by testing rig positional sensor and motion capture system.

Even though we attempted to create identical reference frame for in-silico and in-vitro comparison in Chapter 4, there were still limitations. One in particular was the initial starting position of the knee components experimentally were not recreated in the computational model. This was due to the cadaver study was done prior to the development of the registration method. For future studies, following are suggestions from things we learnt in conducting cadaver experiment for computational model comparison.

- Plan and document lab protocol thoroughly. This will help in making sure data collected during the lab aligns with what needed.
- Digitize implant articular surface with respect to rigid body marker.

- Have the processed pre-operative CT data ready. Register the digitized articular surface to the pre-operative CT reference frame using same technique described in Chapter 4 to ensure good registration can be made from the data collected. If not, recollect the data.
- After mechanical simulator is run, register the recorded data again to generate VEK. Review the VEK and ensure that the virtualised experimental data behaves as expected, e.g. no penetration is seen between components. If there is penetration, identify the potential sources of error. Doing this early will help filter the sources of differences when comparing the computational model outputs to experimental outputs as any differences between the two after experimental study is due to the modelling technique.
- Lastly, ensure starting position of the mechanical simulator is captured. To achieve the best representation of the position, a 3D reverse engineering scanner can be used. The scanner can capture the physical rig in 3D format and then respective computational model components can be registered (using surface-to-surface) to best match the captured 3D data. This allows recreation of the physical rig starting position in in-silico reference frame.

On the other hand, transformation of in-silico to in-vivo reference frame is also important. Many clinicians may not follow the technical description of kinematics used in-silico. Grood and Suntay kinematics description is the most widely adopted definition in knee computational modelling. Even though the description sounds logical from technical and mathematical perspective, it may still not fully translate to in-vivo description, particularly for patello-femoral kinematics. Future studies should consider this factor when the outputs of computational model is used in clinical setting.

The use patient specific ligament properties when developing a model should also be considered. However, the method used to capture patient ligament characteristics during development have to be reproducible clinically. The potential of using stress radiograph as surrogate of the load-displacement response of the knee has been demonstrated. Future study should include validation of Chapter 5 and 6 technique in cadaver study.

Implant geometry also plays an important role in the simulated kinematics results. Contemporary knee implant designs have different level of constraints, such as cruciate retaining (CR), posterior-stabilising (PS) or medial pivot knees. Morra et al [394] in their study compared the constraint level of knee implant models from various implant manufacturers and they showed great variations among designs.

This thesis showed it is possible to develop a knee computational model that have balance complexity and practicality for clinical use. There were compromises need to be made in the model, but the model can still be useful as long as the outputs are reproducible and represent the context of use. A model should be able to predict the behaviour of its intention, at least in a comparative or relative way, even if not absolutely.

Clinical application of current model

The validated model developed in this thesis has been used in post-operative and pre-operative context to evaluate the relative difference of joint dynamics between patients. The application of this thesis has been used in 360KneeSystems*, whose vision is to improve the clinical outcomes of TKA patients using holistic approach towards patient centered care pathway. One aspect is surgical planning. Instead of static surgical planning, they provide dynamic surgical plans that utilize the model developed in this thesis. **Author is an employee of 360KneeSystems.*

Femoral Component:	Omni Apex Right CR Femur Size 2
Tibial Component:	Omni Apex Tibial Tray Size 1
Tibial Insert:	Omni Apex Ultra Insert Size 2 14mm
Patellar Button:	Omni Apex Patella Button Size 29 8mm

Component Placement Information

Femoral Comp. Flexion:	4.5°
Femoral Comp. Valgus:	2.6°
Femoral Comp. Internal:	2.2°
Tibial Comp. Flexion:	3.6°
Tibial Comp. Varus:	1.9°
Tibial Comp. Internal:	11.6°

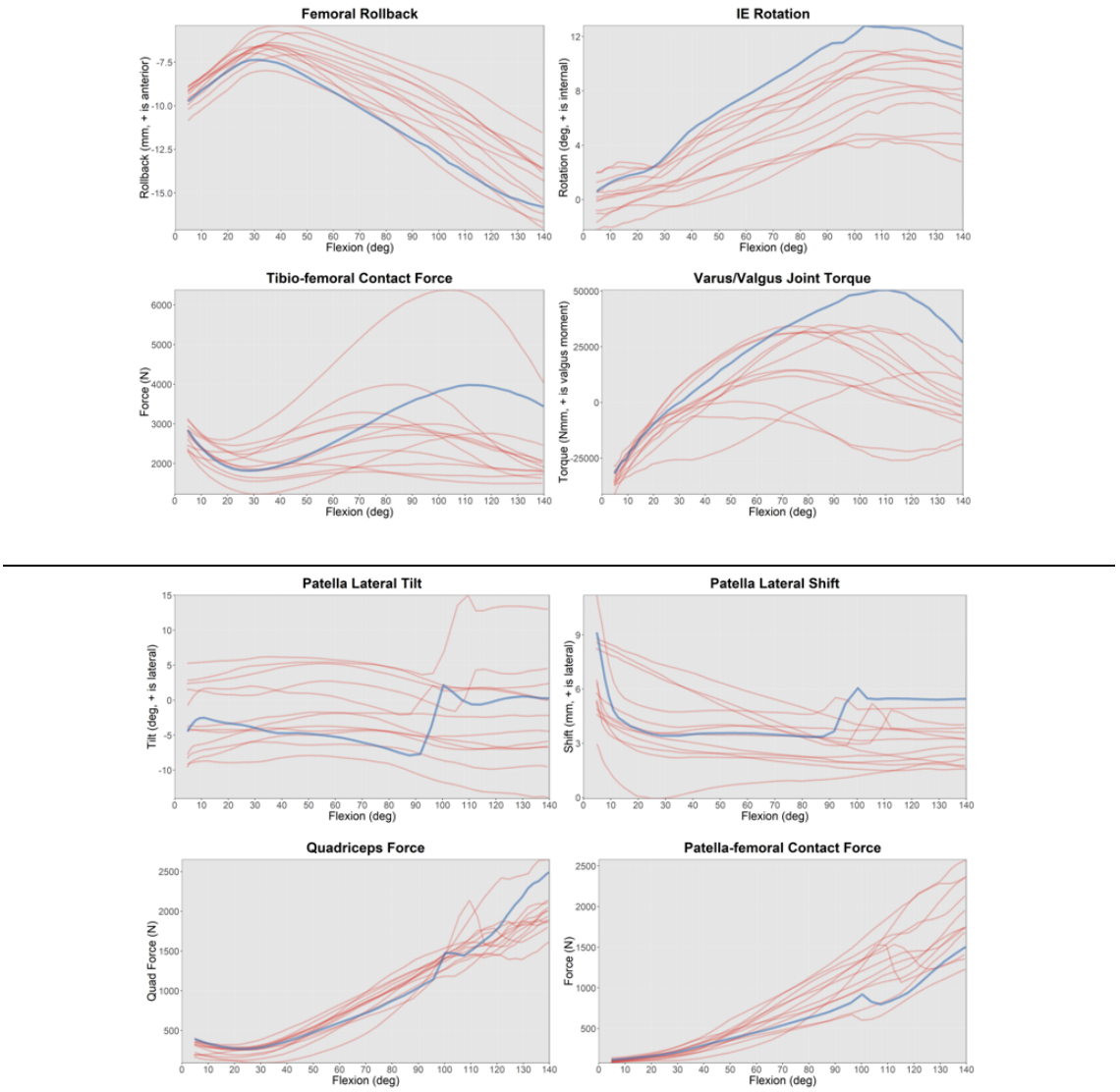

Figure 7.3. Example of post-operative joint dynamics analysis of patient showing tightness in flexion symptoms. Blue lines represent the simulated target patient and red lines represent previously simulated patients.

Initially, the model was used as post-operative analysis tool. When clinicians are faced with dissatisfied patients, often they don't know the root cause of the dissatisfaction or the bad functional outcomes. The computational model can produce joint dynamics in an efficient way that otherwise would be very difficult to obtain to help identify the root cause. The model outputs can be used in a comparative way (against other simulated dynamics) or correlation to recorded PROMs or clinical assessment.

Figure 7.3 shows an example of a post-operative dynamics analysis. From clinical assessment, patient presented with tightness in flexion. The surgeon was uncertain what caused the tightness and requested a dynamics analysis. From post-operative CT, the implanted components were measured as shown in the top picture. Both femur and tibia components were measured to be internally rotated, but the coronal angle is within 3° relative to mechanical alignment. The computational model predicted the tibia to be continuously internally rotated relative to the femur as flexion increases resulting in higher tibio-femoral IE mismatch. Consequently, higher varus-valgus joint torque difference is seen in flexion. The predicted dynamics also showed relatively higher tibio-femoral contact force compared to previously simulated patients, which is a surrogate measure of tightness in the joint (resultant high reaction force between tibia and femur indicating joint is tight). This was in accordance with the observed clinical assessment. Another observation was that the model showed a sudden jump of patella tilt in deep flexion, indicating patella fell in the femoral groove which could be due to the small size implants implanted. However, this observation was not seen clinically. Surgeon used the simulated dynamics information as adjunct to what they observed clinically and finally decided not to revise the patient as the potential gain vs effort of revising was not worthwhile. Instead, they referred the patient to physiotherapy to improve the balance in flexion. If the surgeon was to revise the knee, the model could also be used to model different tibia component alignment and compare the resultant dynamics. In this analysis, only patient CT scan was used as inputs. Image segmentation and landmarking was performed so that the computational model can be generated. The surgeon's clinical assessment was then compared to predicted dynamics outputs. This process took approximately 3 hours (from CT segmentation to produce simulation results).

With sufficient number of post-operative simulated dynamics and corresponding PROMs, correlation between the dynamics characteristics that led to good outcomes as measured by PROMs could be made. The correlation work is outside of this thesis main body. However, Twiggs et al [169], colleagues at 360KneeSystems recently published a study where they found a few predicted dynamics

characteristics were significantly correlated to post-operative PROMs. This work extends the application of the current developed model further to pre-operative context.

Figure 7.4 illustrates how computational modelling can be used pre-operatively as part of surgical planning. If we know which dynamics characteristics led to good clinical outcomes, the factors affecting to the dynamics outcomes can be predicted. We know the patient specific anatomy from imaging data, implant geometry from implant manufacturer and component alignment can be virtually planned at different positions.

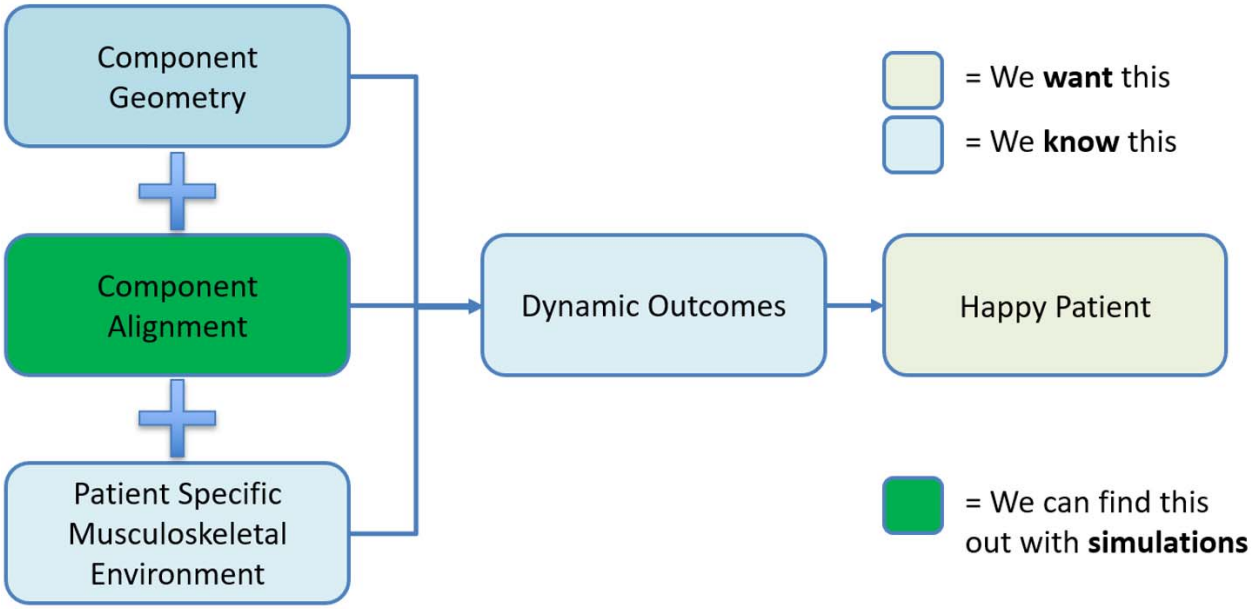

Figure 7.4. Illustration of application of computational model in surgical planning. If correlation of dynamics outcome to clinical outcomes is known, i.e. what dynamics characteristics correlate to happy patients, we can find the best component alignment to achieve the desired dynamics with computational modelling given the known component geometry and patient specific anatomy factors.

One example of the application of the correlation found is to present the predicted dynamics characteristics associated with post-operative PROMs with a score using penalty function. This summarises the predicted dynamics results in an easy interpretable format for clinicians. The score represents whether the predicted dynamics is associated with good or bad post-operative PROMS based on the correlation analysis. Figure 7.5 shows an example of the application in pre-operative

surgical planning. In this example, the tibia Internal-External (IE) rotation and slope are iterated in the computational model. Each corner of the plot represents a predicted dynamics result with specified component position and geometry. The higher percentage score means the predicted dynamics is associated with good post-operative PROMs score and low score associated with bad post-operative PROMs. The score is highlighted with colour status (green associates with high percentage score while red associates with low percentage score) so it is easily interpretable which component position and geometry predicted dynamics result is associated with good and bad post-operative PROMs. Additionally, this analysis provides comparison of relative sensitivity of patient specific predicted dynamics to component position and geometry. The right plots of Figure 7.5 shows the predicted dynamics in each corner is associated with good post-operative PROMs regardless of tibia component position range and geometry selected. This implied the predicted dynamics of the specific patient is not sensitive to tibia component position and geometry. Whereas, left plots of Figure 7.5 shows good and bad post-operative PROMs association. The plots show the predicted dynamics is associated with good outcomes when the congruent tibial insert geometry is used and placed at high tibia slope. These analyses are not intended to directly predict the patient's post-operative clinical outcome but as adjunct information to surgeons so that they are better informed before the surgery and can make appropriate assessment during surgery.

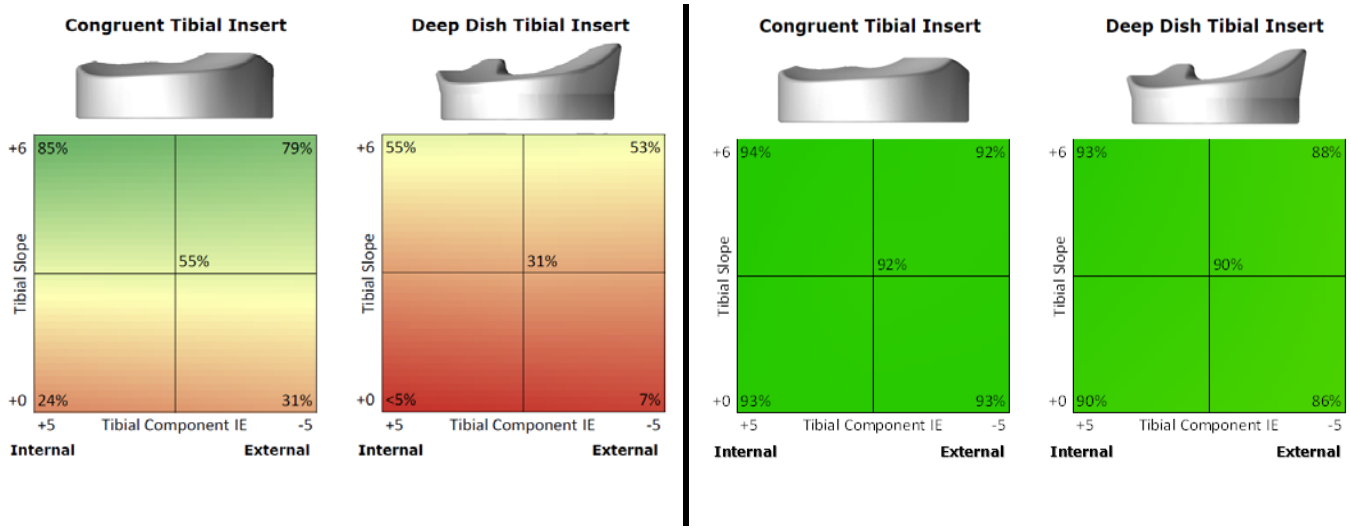

Figure 7.5. Predicted dynamics is presented as a score associated with post-operative PROMs based on the correlation analysis. The score is highlighted with colour status (green associates with high percentage score while red associates with low percentage score). Left side plots show the predicted dynamics is associated with good post-operative PROMs when congruent tibia insert is used and placed at high slope. Whereas the right-side plots show the predicted dynamics in all selected tibia geometry and position are associated with good post-operative PROMs. These analyses are used as adjunct information for surgeons to help them better plan the surgery and plan appropriate assessments for implant selection.

Above example shows the variation of tibia component placement only. Occasionally, there are cases where the predicted dynamics of all selected tibia component geometries and positions are associated with bad post-operative PROMs, i.e. red colour plots in all corners. In that instance, variations of the femur component can be made to study which combination of femur, tibia and patella component placement will result in good PROMs association. Surgeons are then better informed and can plan appropriate assessments to make decision thoroughly intra-operatively. There were examples where the computational model results suggested to anteriorise the femur components by few millimetres to reduce the tibio-femoral tightness in flexion, which matched with surgeon findings intra-operatively.

Another application of studies conducted in this thesis was the attempt to predict the optimal femur cuts to achieve joint gaps balance for gap balancing surgical technique. Quantification of 3D knee laxity using technique described in Chapter 5 can provide more information to clinician pre-operatively of

whether the knee is correctable to mechanical alignment. If the knee does not cross the neutral mechanical alignment during varus-valgus stress assessment, it is considered the knee is not correctable and may need component alignment other than mechanical alignment to achieve balance. Additionally, using the ligament parameters optimization technique described in Chapter 6, we can measure the joint gaps of the knee under specific tension for gap balancing surgical technique. Gap balancing require resecting the tibia bone first. Then, a tensioner is inserted to the joint to assess the gaps in extension and flexion. The aim of the technique is to achieve equal gap in extension and flexion. With the known ligament parameters to simulate the soft tissue tightness, the model can simulate what femur cuts needed to achieve the joint gaps balance in extension and flexion. An example of the concept report is shown in Figure 7.6.

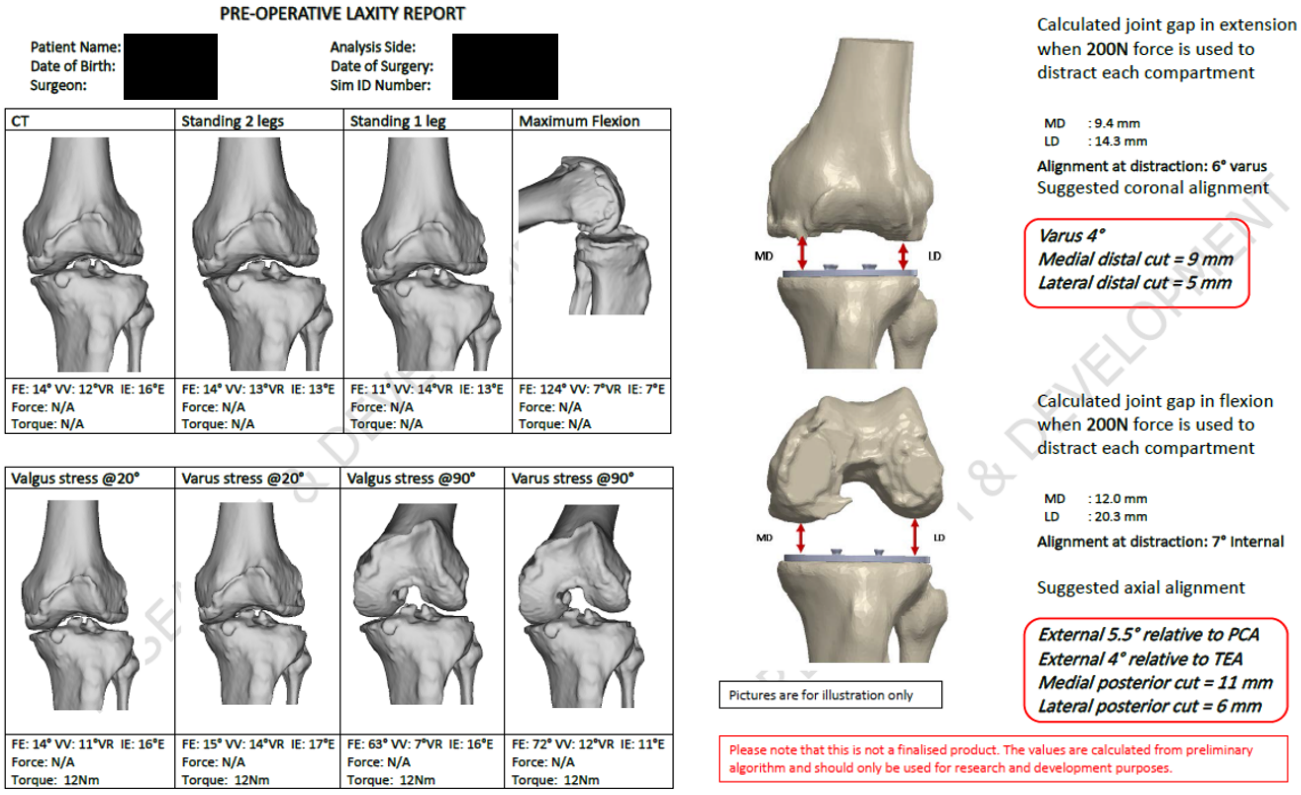

Figure 7.6. A concept of ligament laxity report that utilises stress radiograph data to predict the joint gaps for gap balancing surgical technique. The ligament parameters were optimized as per Chapter 6,

then used in a separate computational model to predict the optimal femur cuts to achieve a joint gap balance in extension and flexion.

The knee computational model developed in this thesis has been used to analyse approximately 1,800 post-operative CT's. Meanwhile, the dynamic surgical planning has been provided for over 3,000 TKA. This highlights the high utility of the model developed, with the capacity to simulate a large volume cases in clinical setting. Undoubtably, not every single analysis had shown direct correlations to the intra-operative observation, but this is on-going work. Part of the development work is data collection. Patients are being followed up at 12 months for PROMs and post-operative CT. This provides a complete loop of data that bridges the pre-operative, intra-operative and post-operative environments. The data collected is a combination of physics, clinical and knowledge data; simulated dynamics and PROMS or other clinical assessments. Overtime, this data may be the key to show a reproducible relationship between joint dynamics and clinical outcomes.

Further application to help managing patient clinical outcomes

The continual collection of physics, clinical and knowledge data have large potential to develop a successful patient centred care pathway. One extension from this study is to use Machine Learning to further explore the correlations of joint dynamics and PROMs. Machine Learning techniques such as supervised learning or un-supervised learning can be used to study and learn the complex relationships between soft tissue laxity, anatomical morphology, disease stage, joint dynamics and PROMs. This will further enhance the current dynamics surgical planning.

Patient expectation is one of the key factors to the un-met satisfaction [401]. Using similar concept, Machine Learning can be used to predict patient satisfaction score based on their current pre-operative state and expectations. Further extension of physics and knowledge data is perhaps to derive patient's optimal dynamics characteristics based on their expectations (e.g. what activity they would like to be able to do after TKA), and then plan the component position accordingly to achieve

the targeted dynamics. Then the desired dynamics is communicated to physiotherapist so that they can tailor the rehabilitation program to support the patient's needs.

Intra-operative delivery technology also plays an important role in patient centred care pathway. The surgeons need to be able to achieve the planned surgical plan. Use of Navigation system is increasing in TKA procedures and is becoming more accessible to most hospitals. Ideally, surgical planning is integrated with intra-operative delivery technology so that if surgeon deviates from the initial plan, the surgical planning tool can update the information and re-calculate what component position adjustments need to be made to still achieve the targeted joint dynamics, i.e. re-run simulation in intra-operative setting. Current simulation takes few minutes to complete and one of the next development pathways is to enable the model to complete a simulation under a minute. Further application is to use Navigation system to collect the knee laxity data intra-operatively and if the model is efficient enough, ligament parameters optimization can be done at that time. Hence, it is important to keep a balance of the model complexity so that it can be efficiently integrated to clinical setting. This thesis started the focus in surgical planning in the patient centred care pathway and hopefully can expand its application to other areas.

Use of Computational model as medical device

There are many developed knee computational models published in literature but not many of them are used as medical device. This could be due to lack of guidance from regulatory bodies in how they would assess software as a medical device, particularly software that provides in-silico analysis. Additionally, there are variations on regulatory requirements from different regulatory bodies, for example Australia Therapeutic Goods Administration (TGA) accepts a medical device that has CE marking while United States Food and Drug Administration (FDA) and Japan Pharmaceuticals and Medical Devices Agency (PMDA) do not. Even though each regulatory body purpose is to control, supervise and regulate medical devices, they have different specifics on their requirements. However,

regulatory bodies in the past few years have been aligning their requirements and moving towards Medical Device Single Audit Program (MDSAP) which will allow medical device manufactures to be audited once for compliance with the standard and regulatory requirements of up to five different medical device markets: Australia, Brazil, Canada, Japan and the United States [416].

The other reason for lack of guidance is that medical devices traditionally have been mainly hardware medical devices and regulatory safety and efficacy assessment is different from software devices. There is software approved as medical devices but not many that are specific to computational modelling technology. They are mainly used either in manufacturing or maintenance of a medical device or software that resides in a medical device, e.g. Navigation system or Electromyograph equipment. Hence, the assessment process for in-silico software is vague. However recently, FDA in collaboration with medical device developers, regulatory agencies and research institutions have published new guidance to provide a framework to communicate computational modelling verification and validation efforts. This guidance is published as "V&V 40 Verification and Validation in Computational Modelling of Medical Devices" [417]. This guidance outlines recommendations on key aspects of verification and validations steps so that the consistency and predictability of the medical device review of computational modelling studies by FDA reviewers can be improved. The guidance highlighted the first important factor is the "Context of Use" of the computational model. The Context of Use sets the expectation on how the computational model is going to be used as well as provide an overview for risks associated with the use. The level of credibility of the computational model during verification and validation phase is then determined by the Context of Use and risks identified. Overall, this is a good step from regulatory bodies to standardise the review process for in-silico software as medical device and this will enable the adoption of computational modelling as medical device.

Realising TKA computational model for clinical use

The knee model developed and validated in Chapter 4 has obtained CE marking and TGA approval as medical device. A brief summary on the process taken to achieve the regulatory approval will be described. First, a medical device company need to have a Quality Management System (QMS) to manufacture and distribute a medical device. Depending on the classification of the medical device, there are different level of compliance on QMS needed. Typically, the QMS needs to comply with ISO 13485 standard, for CE marking and TGA, or 21 CFR Part 820 for FDA. In this case, 360 Knee systems comply with ISO 13485. Then, the safety classification of the intended medical device was determined. Based on the classification, level of documentation and testing is determined. For CE marking, a checklist is used to scope the requirements needed to fulfil the regulatory bodies. The checklist is called "Essential principal checklist". The checklist outlines the areas the reviewer will assess, such as verification, validation, requirements of the medical device, traceability between requirements and testing, risk assessment and labelling. CE marking also require clinical evaluation to be performed to ensure there is sufficient clinical evidence to confirm compliance with relevant essential requirements for safety and performance of the device [418].

Within 360 Knee Systems, my role includes the computational model development and medical device registration. I played a significant role in producing the documentation and evidence for the medical device certification of the knee computational model. The software requirements and software design specifications of the knee computational model was documented. Verification of the computational model was conducted through cadaver lab experiment, as described in chapter 2, 3 and 4. Clinical evaluation included surgeons' expert feedback on the relevance of the predicted joint dynamics to intra-operative observation. Post-operative data collection was also part of the clinical evaluation to monitor the performance and relevance of the medical device. In summary, the main body of this thesis was aimed at development of knee computational model as medical device as oppose to pure research tool. Even though there are simplifications and limitations in the current model, the model developed have been successfully gained approval and used as medical device and has the required balance to be used as part of surgical planning.

As a thought exercise, what would be required to make changes to the current approved knee computational model? For example, include a new implant system or simulate other activity or update methodology used in creating the knee model. These changes can be categorised as minor and major change.

For minor change, where no new risk introduced or context of use remains the same, technical documents of the medical device, such as software requirements or software specifications need to be updated for traceability purposes and testing need to be performed. Since it is minor change, testing can be against benchmark cases to ensure the updated model produce same predicted dynamics to the validated version. Benchmark cases can be the cadaver data used for validation. New version release needs to be documented as part of QMS requirements. Re-submission for regulatory approval is not needed as no change in intended use and no new risk introduced.

For major change, where new significant risks are introduced or context of use is updated, the version change involves more steps. Firstly, the new risks or updated context of use need to be identified and assessed. These need to be assessed against the essential requirement checklist and any gaps need to be determined introduced by the change request. Determine and document the new requirements needed for the change. Testing coverage need to be assessed for the new requirements. If cadaver testing is required because the current testing coverage is insufficient to cover the new functions or features, define the scope of the new verification testing and reporting structure against V&V40 guidelines.

Re-establish the verification and validation goals based on the updated context of use and risks. For effective outcomes, ensure the testing is planned sufficiently. There are different levels of testing that need to be performed. On the low level, software testing needs to be performed to ensure that new features or functions introduced works as intended. Then, experimental testing such as cadaver testing can be used to verify the computational model outputs. The cadaver testing needs to be planned with suggestions described earlier. Finally, the updated model needs to be validated to ensure

outputs of the updated model are clinically relevant for its context of use. Clinical evaluation protocol needs to be updated and ensure the reporting structure meets the regulatory requirements.

Once required testing for the proposed changes have been completed, documentation needs to be updated for regulatory submission. Major change on registered medical device needs to be reported to regulatory bodies in jurisdiction where the changes are going to be released on. For example, regulatory body for CE mark will have to review the updated documentation and clinical evaluation. For FDA, the reviewers will go through the change rationale to determine whether the medical device is suitable for special 510k or require a new 510k application. Special 510k is a type of 510k application that do not go through all review process as standard 510k process.

Concluding remarks

This thesis presented a series of studies towards the development of a low-cost computational model that aimed to be used as part of surgical planning tool to help clinicians triage patient treatments. Consistent definitions of reference frames when validating a computational model need to be emphasized to ensure no accuracy loss in data translation. Limitations were highlighted on the validation steps but had outlined suggestions for future studies to avoid the mistakes that occurred. Patient specific ligament characteristics were also shown to be important. Further work needs to scope the validation of the optimization technique described and explore the combination effects of patient specific ligament characteristics, implant geometry and component placements in the model. The current model has been used as part of a medical device to compare the relative difference of joint dynamics between patients. Regulatory bodies are catching up in this field and has recently worked on standardizing verification and validation framework. Future work in realising computational model as medical device need to align the development strategy against the guidance to ensure successful regulatory application.

There are still a proportion of TKA patients who are dissatisfied. With increasing healthcare cost, advances in patient centred care is important to help clinicians choose the best and most efficient treatment plans for individual patient. This thesis started that journey with surgical planning that utilises computational modelling technology to enhance patient outcomes.

Appendices

Appendix A - First Computational Model Experimental Validation

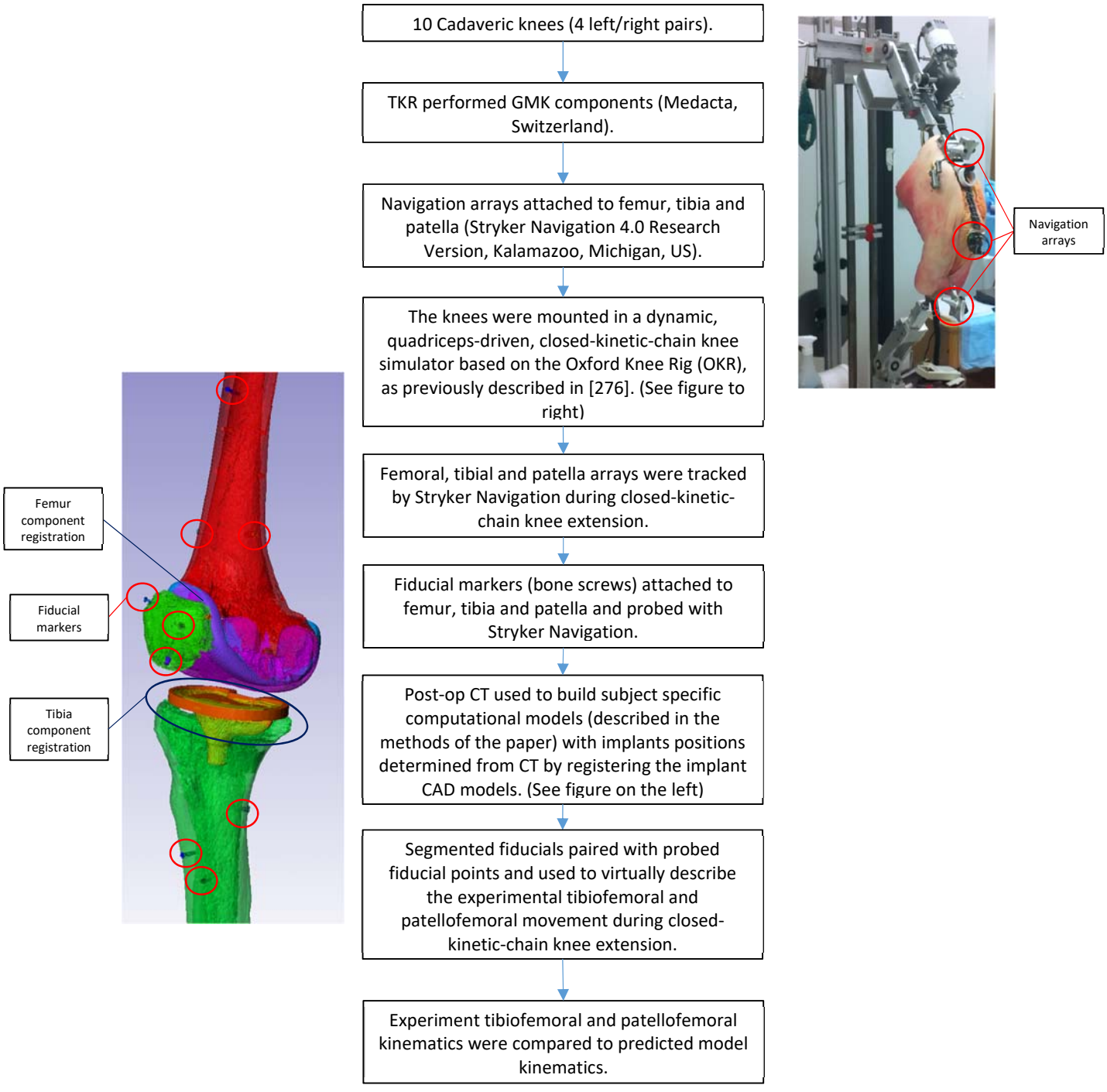

Figure 2.7. Validation process of the developed computational model

Determination of Ligament stiffness

The stiffness coefficients of the PCL, LCL and MCL were initially adapted from previous studies [276]. They were then fined tuned so that the parameters can be used to achieve good correlations between the experimental and predicted model kinematics for each cadaver subject. Tuned stiffness for anterior MCL was 1.7×10^4 N, posterior MCL was 3.7×10^4 N, LCL was 6.4×10^4N, anterior PCL was 1.2×10^4 N and posterior PCL was 1.1×10^4 N.

Comparison of experimental and predicted model kinematics

For tibiofemoral kinematics, observations were made for tibiofemoral varus/valgus (Varus), tibiofemoral axial rotation (IE Rotation), posterior translation of the mid-point of the transepicondylar line (Rollback), and medial and lateral flexion facet centre (FFC) where anterior position was relative to the centre of the tibia plateau (Medial FFC AP & Lateral FFC AP). Correlations between the experimental validation (test) and the simulation (model) for tibiofemoral kinematics are shown in Figure *2.8* and the mean for each specimen, standard deviation and Pearson correlation coefficient (r) are shown in *Table 2.*

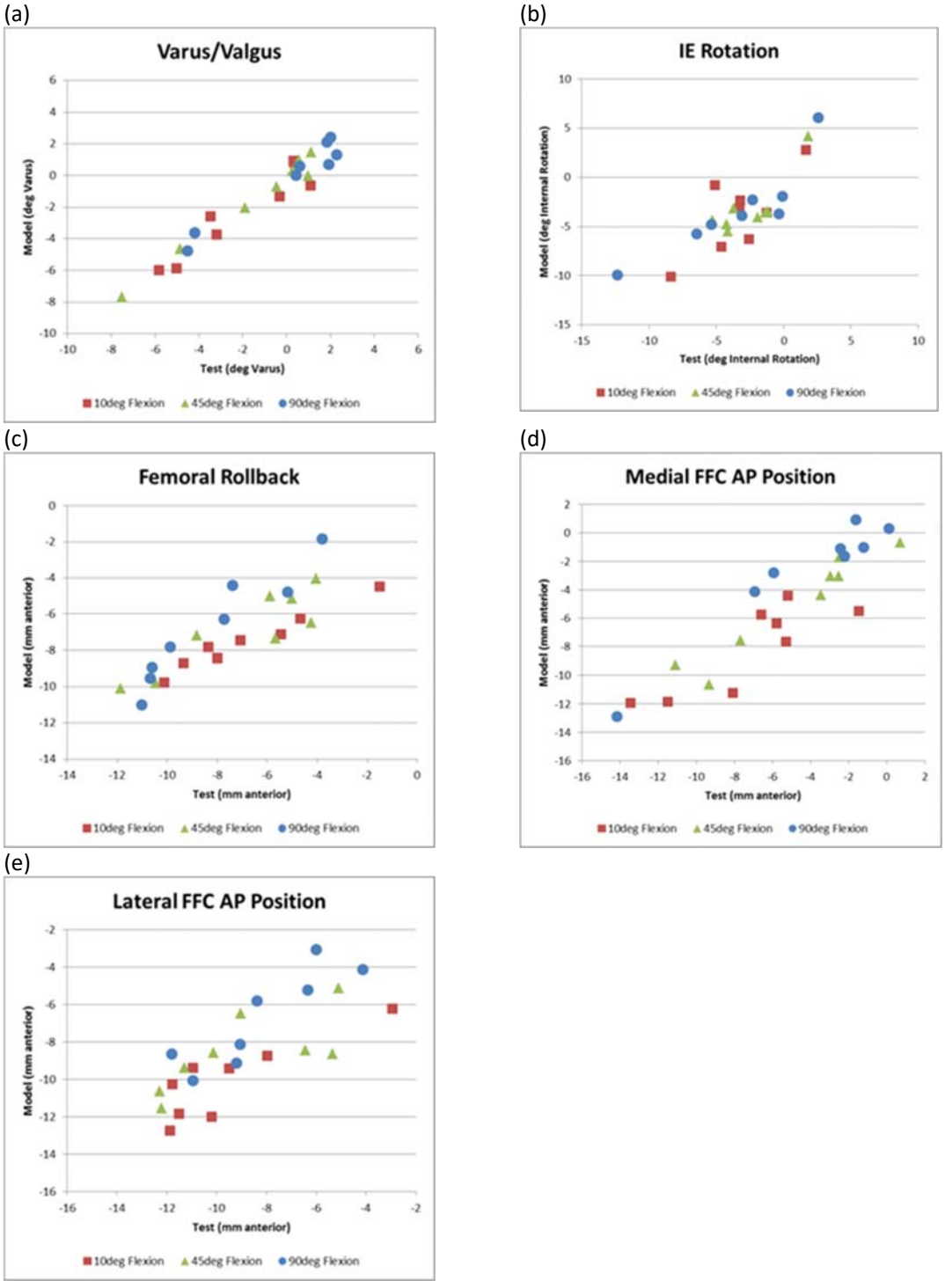

Figure 2.8 Correlations for tibiofemoral kinematics (a) varus-valgus; (b) IE rotation; (c) femoral rollback; (d) medial FFC AP position; and (e) lateral FFC AP position

Table 2.1 Experimental validation and test mean (± standard deviation) and Pearson linear correlation coefficient (r) for tibiofemoral kinematics

	10°			45°			90°		
	Test	**Model**	**r**	**Test**	**Model**	**r**	**Test**	**Model**	**r**
Varus	-2.01 ± 2.51	-2.30 ± 2.56	0.94	-1.47 ± 2.93	-1.55 ± 2.95	0.99	0.05 ± 2.62	-0.15 ± 2.46	0.97
IE Rotation	-3.35 ± 2.73	-3.81 ± 3.74	0.76	-2.49 ± 2.15	-3.11 ± 2.84	0.82	-3.42 ± 4.34	-3.27 ± 4.24	0.88
Rollback	-6.82 ± 2.64	-7.51 ± 1.52	0.98	-7.00 ± 2.79	-6.89 ± 2.05	0.88	-8.29 ± 2.55	-6.82 ± 2.86	0.95
Medial FFC AP	-7.17 ± 3.56	-8.10 ± 2.90	0.85	-4.85 ± 3.78	-5.05 ± 3.43	0.96	-4.31 ± 4.34	-2.80 ± 4.10	0.97
Lateral FFC AP	-9.59 ± 2.80	-10.07 ± 1.98	0.85	-8.98 ± 2.80	-8.62 ± 1.95	0.73	-8.23 ± 2.44	-6.77 ± 2.40	0.88

For patellofemoral kinematics, observations were made for lateral translation of the patella (lateral shift) and IE rotation about the patella centreline (patella tilt). Both measures were relative to a coordinate system embedded in the femur. There were some linear trends for 10° and 45° however less so for 90° particularly for patella tilt. Correlations between the experimental validation (test) and the simulation (model) for patellofemoral kinematics are shown in Figure 2.9 and the mean for each specimen, standard deviation and Pearson correlation coefficient (r) are shown in Table 2.2.

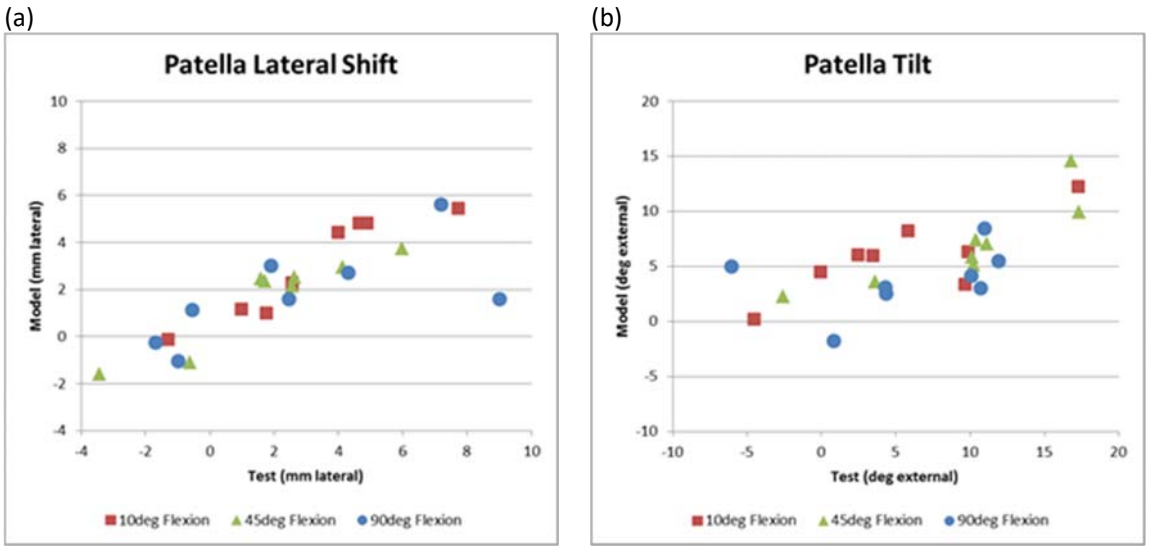

Figure 2.9 Correlations for patellofemoral kinematics (a) patella lateral shift and (b) patella tilt

Table 2.2. Experimental validation and test mean (± standard deviation) and Pearson linear correlation coefficient (r) for patellofemoral kinematics

	10°			45°			90°		
	Test	**Model**	**r**	**Test**	**Model**	**r**	**Test**	**Model**	**r**
Patella lateral shift	3.16 ± 2.59	2.99 ± 2.01	0.95	1.82 ± 2.68	1.68 ± 1.82	0.93	2.71 ± 3.65	1.80 ± 1.93	0.67
Patella tilt	5.49 ± 6.33	5.87 ± 3.29	0.79	9.63 ± 6.13	6.97 ± 3.64	0.87	5.89 ± 5.87	3.73 ± 2.74	0.38

Appendix B - Verification of 3D-2D Registration technique using Sawbone Model

In order to determine the accuracy of described 3D-2D registration and the methods used to calculate knee alignment, a sawbone model was constructed to allow manipulation to specific flexion angle. The model contains full length of the femur, tibia and fibula, interconnected by 4 stretchable ligaments representing the anterior & posterior cruciate ligaments and the medial & lateral collateral ligaments. The sawbone was taken for CT scan and segmentation and landmarking was performed on the scan. The sawbone chosen for the purpose of this study is made up on two types of material – a dense foam shell to represent the cortical bone and a highly porous interconnected structure to represent the cancellous bone. While the density of these materials is significantly lower than that of human bone, the density of the sawbone model is sufficient to visible under x-ray.

A mechanical frame was constructed to hold the sawbone model at specific flexion angle. 6mm holes were drilled into the dense, cortical and porous, cancellous bones, a steel nut is inserted through to lock the 6 degrees of freedom, see Figure 5.9. Mechanical frame constructed to hold the sawbone at different flexion angles**Error! Reference source not found.**. Holes are drilled into both the fixation rig and the sawbone model in order to achieve the following positions:

- Extension
- Midflexion
- Flexion (90°)

Figure 5.9. Mechanical frame constructed to hold the sawbone at different flexion angles

The sawbone was then taken for lateral and anterior-posterior (AP) X-ray for each of the flexion position. Figure 5.10. Example of AP and lateral X-ray taken for sawbone model at 90° flexion. shows example of when the sawbone's X-ray was taken.

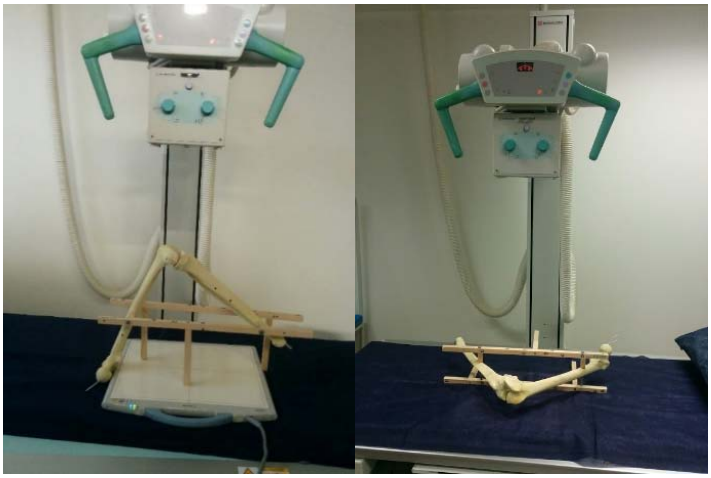

Figure 5.10. Example of AP and lateral X-ray taken for sawbone model at 90° flexion.

3D-2D registration technique described in Method section was performed to determine the knee alignment of the sawbone position. Figure 5.11 shows the 3D-2D registration screenshots.

A handheld 3D scanner, HandyScan (Creaform Inc, Quebec, Canada) was used to capture the surface geometry of the sawbone at each specified flexion angle. Output of this scan was 3D model of the

femur and tibia in space. A resolution of 0.6mm is used in the scanning process. With the sawbone in place, the anterior and posterior surfaces of the bones cannot be captured in a single scan. Thus, multiple scans are taken so that the anterior and posterior surfaces can be stitched to form a 3D model using processing software part of the handheld device, VX elements (Creaform Inc, Quebec, Canada). Figure 5.12 shows an example of the scanning and stitching process of the handheld device.

Segmented CT scan 3D model was aligned to the generated 3D surface model of the sawbone at each specified flexion position using Iterative Closest Point (ICP) alignment method in Powershape (Autodesk, California, United States). The knee alignment of this registration is considered to be the benchmark because surface-to-surface registration is more deterministic than 3D-2D registration method, especially when the surface compared are identical. Following similar steps described in Method section, once the CT bone models were registered to scanned position, the landmarks determined from CT were transformed using the bone models' transformation matrix. The knee alignment is then described using Grood and Suntay convention.

Knee alignment derived using 3D-2D registration technique was compared to the knee alignment derived using surface-to-surface registration.

ExtensionAP	Mid-FlexionAP	FlexionAP
		
Extension Lateral	Mid-Flexion Lateral	Flexion Lateral
		

Figure 5.11. screenshots of 3D-2D registration of the sawbone at each flexion angle for AP and lateral X-ray.

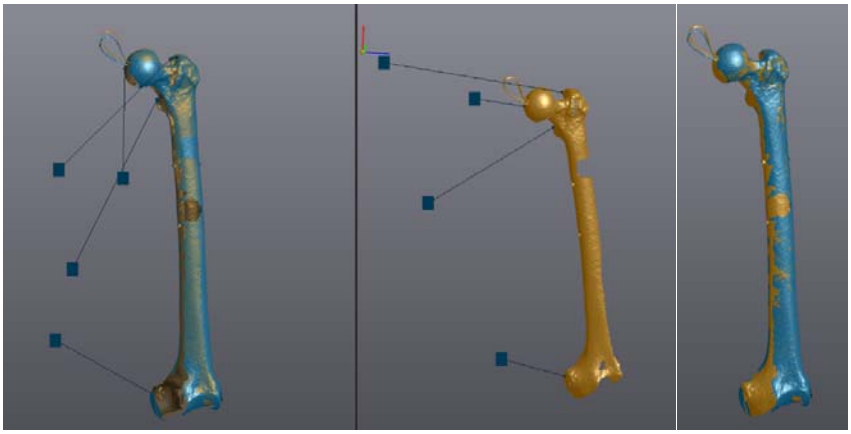

Figure 5.12. HandyScan captured surface geometry of femur. Left and centre: Align tool in VX Elements to stich two meshes together. Right: merged mesh showing missing features and surfaces filled.

Results

Verification of 3D-2D registration techniques was conducted by comparing data obtained from 3D scans with alignment calculations from geometry registered using 3D-2D x-ray registration.

Table 5.4: Alignment information calculated from 3D scan in fixed positions.

Position	FE	VV	IE	ML	AP	SI
Extension	2.4	6.7	0.8	5.5	12.3	-43.1
Flexion	101.6	4.3	-3.1	7.4	14.5	-43.0
Mid-Flexion	67.9	7.9	-7.3	1.6	13.9	-43.8

Table 5.5: Alignment information calculated from X-ray registration of both anterior posterior (AP) and lateral x-rays.

Position	Direction of X-ray	FE	VV	IE	ML	AP	SI
Extension	AP	4.2	7.1	2.0	6.9	18.4	-42.7
	Lateral	2.8	6.6	1.9	5.8	12.6	-43.3
Flexion	AP	104.9	4.2	-2.0	7.6	12.0	-44.8
	Lateral	101.6	4.6	-2.5	5.0	13.5	-43.8
Mid-Flexion	AP	64.4	7.2	-6.7	1.4	12.8	-43.8
	Lateral	67.7	7.3	-7.0	4.3	14.4	-43.6

Table 5.6: Comparison of the 6 degrees of freedom in terms of alignment between the 3D scan method and the x-ray registration method.

Differences	FE	VV	IE	ML	AP	SI
Extension_AP	1.8	0.4	1.2	1.4	6.1	0.5
Extension_L	0.4	0.1	1.1	0.3	0.2	0.2
Flexion_AP	3.4	0.2	1.1	0.2	2.5	1.8
Flexion_L	0.1	0.3	0.6	2.4	1.0	0.8
MidFlexion_AP	3.5	0.7	0.6	0.2	1.1	0.0
MidFlexion_L	0.2	0.6	0.4	2.7	0.5	0.2
Average	**1.6**	**0.4**	**0.8**	**1.2**	**1.9**	**0.6**
Average exclude AP Xrays	**0.2**	**0.3**	**0.7**	**1.8**	**0.6**	**0.4**

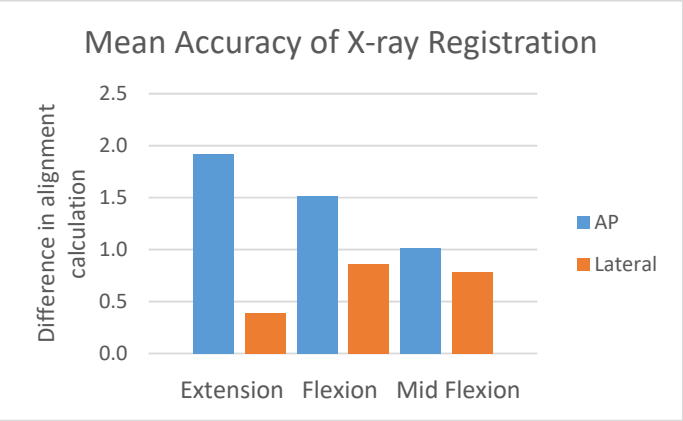

Figure 5.13. Verification of the 3D-2D Registration and post-processing

From Table 5.6Table 5. and Figure 5.1, it can be seen that the greatest variation in all x-rays is the anterior and posterior position in the Extension AP X-ray. AP X-rays showed the greatest deviation in the anterior-posterior direction and lateral x-rays showed the greatest deviation in the medial lateral direction.

It was anticipated that the greatest degree of variation will be the translational degree of freedom that is perpendicular to the x-ray plate (in and out-plane). i.e. for AP x-rays, translation in the AP direction will be the most difficult to define. The difference in translation about this axis is subjective given that the effects of magnification do not clearly show even when the geometry is translated by several millimetres towards or away from the x-ray. Largest difference in registered AP X-ray was 6.4mm for AP position and for lateral X-ray was 2.7mm for ML position.

This study showed that the overall accuracy for method described (both types of x-rays). AP Xrays were found to be less accurate for flexion angle and AP measurements due to the out-of-plane motion. Only lateral AP Xrays were used in this study and when AP Xrays were excluded, the accuracy of this method was 0.6mm for in-plane translation, 1.8mm for out-of-plane translation and 0.7° for rotations. The relative registered position between femur and tibia need to be reviewed closely for absurdity to minimise in-plane translational distance error.

Appendix C – Validation of ScanIP Software Measurements

As described in Chapter 3, ScanIP is an FDA approved medical software specifically designed to process medical imaging and registration of 3D models. It is important to ensure the software outputs are correct in order to interpret the analysis accurately. The test protocol and report described below is part of 360KneeSystems technical file for their surgical planning medical device. Permissions have been granted by 360KneeSystems to only describe the protocol and report as summary.

Test Protocol

A CT calibration phantom with known geometry was used in the test. The calibration phantom contains radiopaque screws at specified location with known measurements. Figure 13.7 below shows the calibration phantom engineering drawings with known measurements. The physical calibration phantom was sent to 3 different radiology centres to be CT scanned. The CT scan of the calibration phantom from each centre was segmented and landmarked using ScanIP. Figure 3.8 shows an example of the segmented and landmarked calibration phantom screws. The landmarked measurements were then compared to the engineering drawings for comparison. The acceptance criteria of the ScanIP outputs is to be within 1mm and 0.7° from the reference measurements.

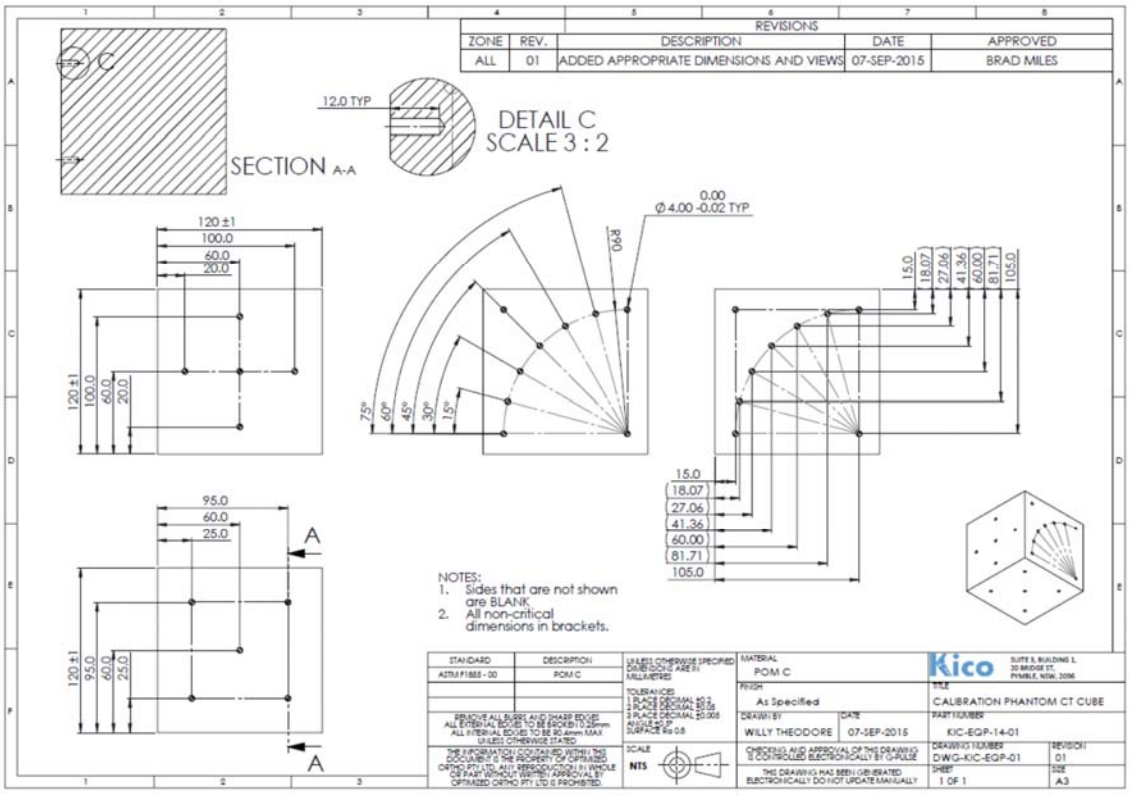

Figure 13.7. Engineering drawing of CT calibration phantom used to validate ScanIP software measurements.

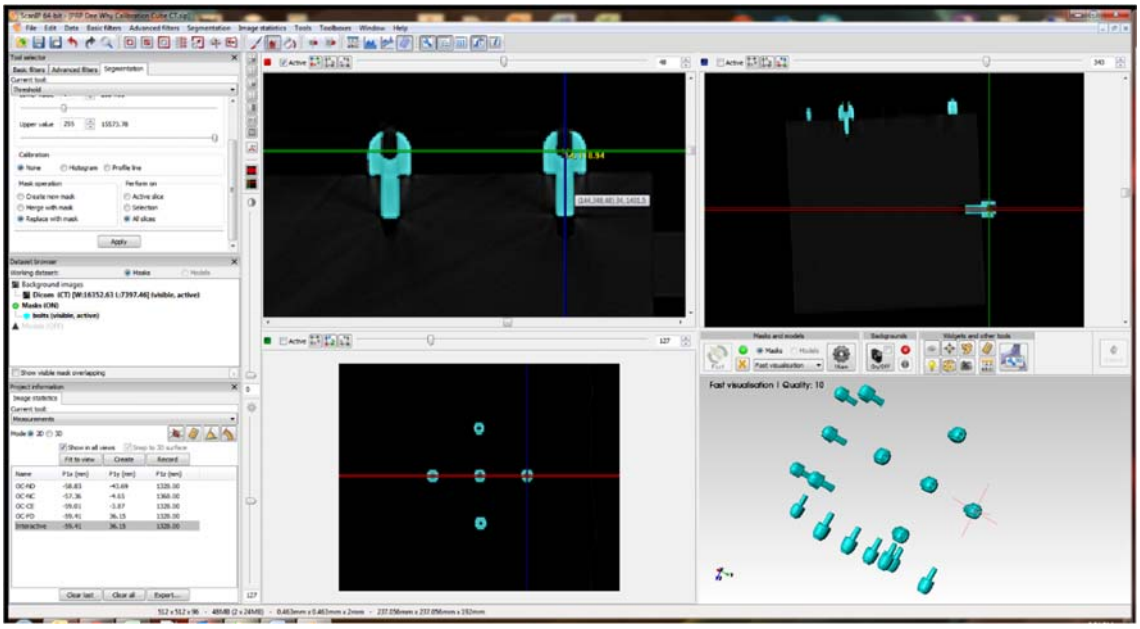

Figure 3.814. Example of the segmented and landmarked calibration phantom

Results

Measurement deviations of processed CT calibration phantom scanned at each radiology centre were shown in Figure 3.9 and Figure 3.10. As can be seen from the graphs, all measurements from ScanIP were under the set maximum acceptance level and therefore we can be confident that ScanIP measurement outputs are reliable.

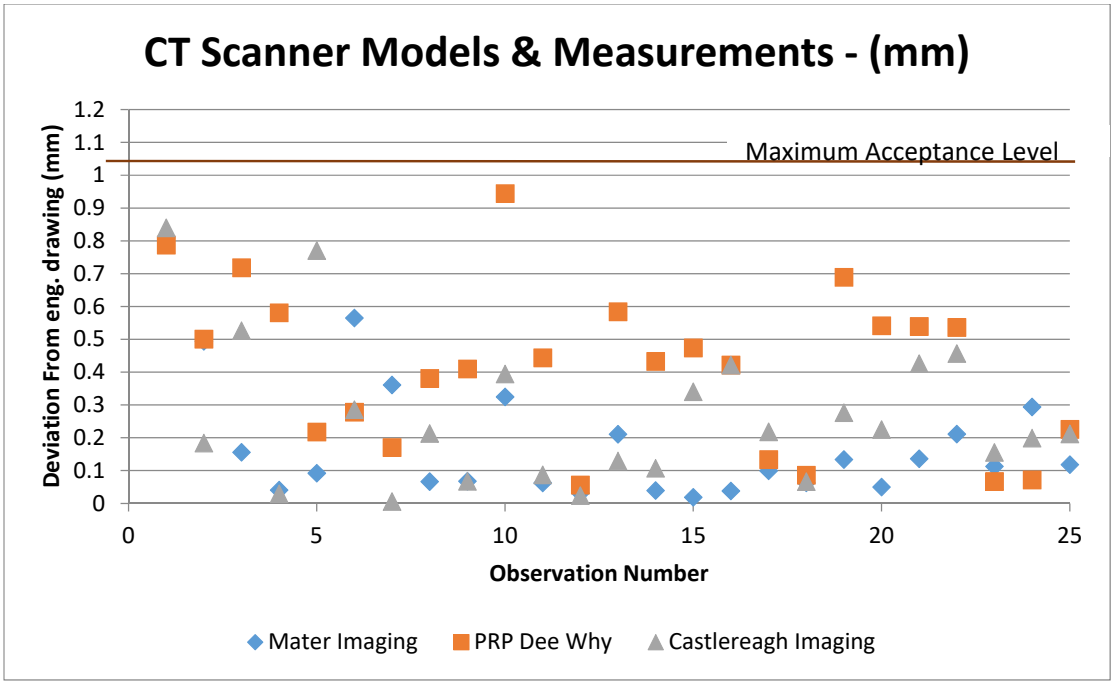

Figure 3.9. Distance measurements deviation between processed CT calibration phantom against engineering drawing. All measurements are within acceptance criteria (1mm).

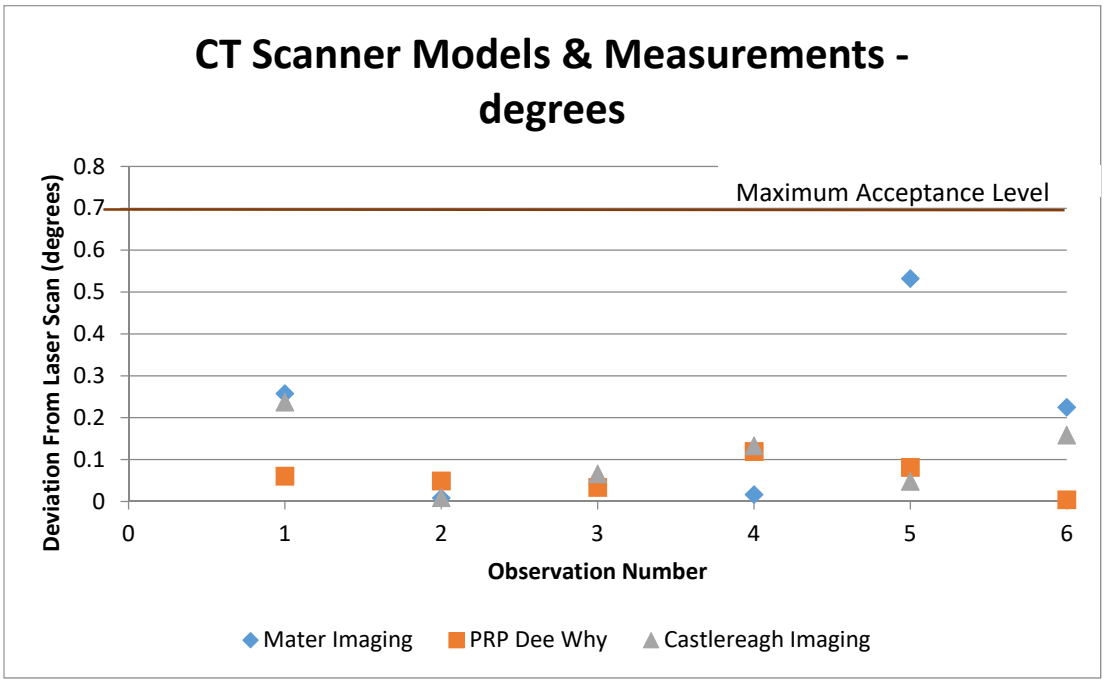

Figure 3.1015. Angular measurements deviation between processed CT calibration phantom against engineering drawing. All measurements are within acceptance criteria (0.7°).

References

[1] "National Joint Replacement Registry Annual Report," Australian Orthopaedic Association, Adelaide2017.

[2] R. B. Bourne, B. M. Chesworth, A. M. Davis, N. N. Mahomed, and K. D. J. Charron, "Patient satisfaction after total knee arthroplasty: Who is satisfied and who is not?," *Clinical Orthopaedics and Related Research,* 2010.

[3] W. Muller, *The Knee - Form, Function, and Ligament Reconstruction*. Springer, 1982.

[4] G. R. T. Scuderi, A. J., *The Knee*. SG: World Scientific, 2010.

[5] H. Gray, *Anatomy of the Human body 20th edition*. Philadelphia: Lea & Febiger, 1918.

[6] A. M. Amendola, S.; Menetrey, J.; Bellemans, J., *The Knee Joint: Surgical Techniques and Strategies*. Springer, 2012.

[7] E. Thienpont, *Improving Accuracy in Knee Arthroplasty*. New Delhi: Jaypee, 2012.

[8] E. Y. Chao, E. V. Neluheni, R. W. Hsu, and D. Paley, "Biomechanics of malalignment," *Orthop Clin North Am,* vol. 25, no. 3, pp. 379-386, 1994.

[9] D. Paley, J. E. Herzenberg, K. Tetsworth, J. McKie, and A. Bhave, "Deformity planning for frontal and sagittal plane corrective osteotomies," *Orthop Clin North Am,* vol. 25, no. 3, pp. 425-465, 1994.

[10] J. Bellemans, W. Colyn, H. Vandenneucker, and J. Victor, "The Chitranjan Ranawat award: is neutral mechanical alignment normal for all patients? The concept of constitutional varus," *Clinical orthopaedics and related research,* vol. 470, no. 1, pp. 45-53, 2012.

[11] A. Escalante, M. J. Lichtenstein, R. Dhanda, J. E. Cornell, and H. P. Hazuda, "Determinants of hip and knee flexion range: results from the San Antonio Longitudinal Study of Aging," (in eng), *Arthritis Care Res,* vol. 12, no. 1, pp. 8-18, 1999.

[12] K. E. Roach and T. P. Miles, "Normal hip and knee active range of motion: the relationship to age," (in eng), *Physical Therapy,* vol. 71, no. 9, pp. 656-665, 1991.

[13] M. A. Strickland, M. Browne, and M. Taylor, "Could passive knee laxity be related to active gait mechanics? An exploratory computational biomechanical study using probabilistic methods," *Computer Methods in Biomechanics and Biomedical Engineering,* vol. 12, no. 6, pp. 709-720, 2009.

[14] L. G. Hallen and O. Lindahl, "The "screw-home" movement in the knee-joint," (in eng), *Acta Orthop Scand,* vol. 37, no. 1, pp. 97-106, 1966.

[15] V. Pinskerova *et al.*, "Does the femur roll-back with flexion?," *J Bone Joint Surg Br,* vol. 86, no. 6, pp. 925-931, 2004.

[16] S. A. Banks, G. D. Markovich, and W. A. Hodge, "In vivo kinematics of cruciate-retaining and -substituting knee arthroplasties," (in eng), *J Arthroplasty,* vol. 12, no. 3, pp. 297-304, 1997.

[17] J. B. Stiehl, D. A. Dennis, R. D. Komistek, and H. S. Crane, "In vivo determination of condylar lift-off and screw-home in a mobile-bearing total knee arthroplasty," (in eng), *J Arthroplasty,* vol. 14, no. 3, pp. 293-299, 1999.

[18] D. A. Dennis, R. D. Komistek, J. B. Stiehl, S. A. Walker, and K. N. Dennis, "Range of motion after total knee arthroplasty. The effect of implant design and weight-bearing conditions," *Journal of Arthroplasty,* vol. 13, pp. 748-752, 1998.

[19] C. W. Clary, C. K. Fitzpatrick, L. P. Maletsky, and P. J. Rullkoetter, "The influence of total knee arthroplasty geometry on mid-flexion stability: an experimental and finite element study," (in eng), *J Biomech,* vol. 46, no. 7, pp. 1351-7, Apr 26 2013.

[20] G. Yildirim, P. S. Walker, and J. Boyer, "Total knees designed for normal kinematics evaluated in an up-and-down crouching machine," (in eng), *J Orthop Res,* vol. 27, no. 8, pp. 1022-7, Aug 2009.

[21] R. Shenoy, P. S. Pastides, and D. Nathwani, "(iii) Biomechanics of the knee and TKR," *Orthopaedics and Trauma,* vol. 27, no. 6, pp. 364-371, 2013.

[22] M. A. R. Freeman and V. Pinskerova, "The movement of the normal tibio-femoral joint," (in eng), *Journal of Biomechanics,* vol. 38, no. 2, pp. 197-208, 2005.
[23] J. Victor, L. Labey, P. Wong, B. Innocenti, and J. Bellemans, "The influence of muscle load on tibiofemoral knee kinematics," (in eng), *J Orthop Res,* vol. 28, no. 4, pp. 419-28, Apr 2010.
[24] H. Iwaki, V. Pinskerova, and M. A. Freeman, "Tibiofemoral movement 1: the shapes and relative movements of the femur and tibia in the unloaded cadaver knee," (in eng), *J Bone Joint Surg Br,* vol. 82, no. 8, pp. 1189-95, Nov 2000.
[25] J. S. Li, A. Hosseini, L. Cancre, N. Ryan, H. E. Rubash, and G. Li, "Kinematic characteristics of the tibiofemoral joint during a step-up activity," (in eng), *Gait Posture,* vol. 38, no. 4, pp. 712-6, Sep 2013.
[26] E. Most, J. Axe, H. Rubash, and G. Li, "Sensitivity of the knee joint kinematics calculation to selection of flexion axes," (in eng), *J Biomech,* vol. 37, no. 11, pp. 1743-8, Nov 2004.
[27] E. S. Grood and W. J. Suntay, "A joint coordinate system for the clinical description of three-dimensional motions: application to the knee," *J Biomech Eng,* vol. 105, no. 2, pp. 136-144, 1983.
[28] B. J. Fregly, W. G. Sawyer, M. K. Harman, and S. A. Banks, "Computational wear prediction of a total knee replacement from in vivo kinematics," *J Biomech,* vol. 38, no. 2, pp. 305-314, 2005.
[29] J. Morrison, "The mechanics of the knee joint in relation to normal walking," *Journal of Biomechanics,* vol. 3, pp. 51-61, 1970.
[30] T. P. Andriacchi, G. B. Andersson, R. W. Fermier, D. Stern, and J. O. Galante, "A study of lower-limb mechanics during stair-climbing," (in eng), *Journal of Bone and Joint Surgery [Am],* vol. 62, no. 5, pp. 749-757, 1980.
[31] G. Bergmann, F. Graichen, and A. Rohlmann, "Hip joint loading during walking and running, measured in two patients," (in eng), *J Biomech,* vol. 26, no. 8, pp. 969-990, 1993.
[32] S. J. G. Taylor, J. S. Perry, J. M. Meswania, N. Donaldson, P. S. Walker, and S. R. Cannon, "Telemetry of forces from proximal femoral replacements and relevance to fixation," *Journal of Biomechanics,* vol. 30, pp. 225-234, 1997.
[33] S. J. Taylor and P. S. Walker, "Forces and moments telemetered from two distal femoral replacements during various activities," *J Biomech,* vol. 34, no. 7, pp. 839-848, 2001.
[34] K. R. Kaufman, N. Kovacevic, S. E. Irby, and C. W. Colwell, "Instrumented implant for measuring tibiofemoral forces," *J Biomech,* vol. 29, no. 5, pp. 667-671, 1996.
[35] I. Kutzner *et al.*, "Loading of the knee joint during activities of daily living measured in vivo in five subjects," *Journal of Biomechanics,* vol. 43, no. 11, pp. 2164-2173, 2010.
[36] D. D. D'Lima, S. Patil, N. Steklov, S. Chien, and Colwell C.W, Jr., "In vivo knee moments and shear after total knee arthroplasty," *Journal of Biomechanics,* vol. 40, pp. S11-S17, 2007.
[37] D. D. D'Lima, S. Patil, N. Steklov, J. E. Slamin, and C. W. Colwell Jr, "Tibial forces measured in vivo after total knee arthroplasty," *J Arthroplasty,* vol. 21, no. 2, pp. 255-262, 2006.
[38] D. T. Reilly and M. Martens, "Experimental Analysis of the Quadriceps Muscle Force and Patello-Femoral Joint Reaction Force for Various Activities," *Acta Orthopaedica Scandinavica,* vol. 43, no. 2, pp. 126-137, 1972/01/01 1972.
[39] K. B. Shelburne, M. R. Torry, and M. G. Pandy, "Muscle, ligament, and joint-contact forces at the knee during walking," (in eng), *Med Sci Sports Exerc,* vol. 37, no. 11, pp. 1948-56, Nov 2005.
[40] D. E. Toutoungi, T. W. Lu, A. Leardini, F. Catani, and J. J. O'Connor, "Cruciate ligament forces in the human knee during rehabilitation exercises," (in eng), *Clin Biomech (Bristol, Avon),* vol. 15, no. 3, pp. 176-87, Mar 2000.
[41] J. M. B. Jacquelin Perry, "Gait Analysis: Normal and Pathological Function," *Journal of Sports Science & Medicine,* vol. 9, no. 2, pp. 353-353, 2010.
[42] "Kinematics of the knee during gait."
[43] W. R. Taylor, M. O. Heller, G. Bergmann, and G. N. Duda, "Tibio-femoral loading during human gait and stair climbing," *J Orthop Res,* vol. 22, no. 3, pp. 625-632, 2004.

[44] P. A. Costigan, K. J. Deluzio, and U. P. Wyss, "Knee and hip kinetics during normal stair climbing," *Gait & Posture,* vol. 16, no. 1, pp. 31-37, 2002.
[45] V. Pinskerova, K. M. Samuelson, J. Stammers, K. Maruthainar, A. Sosna, and M. A. Freeman, "The knee in full flexion: an anatomical study," *J Bone Joint Surg Br,* vol. 91, no. 6, pp. 830-834, 2009.
[46] M. A. R. Freeman and V. Pinskerova, "The movement of the knee studied by magnetic resonance imaging," (in eng), *Clinical Orthopaedics and Related Research,* no. 410, pp. 35-43, 2003.
[47] K. M. Varadarajan, R. E. Harry, T. Johnson, and G. Li, "Can in vitro systems capture the characteristic differences between the flexion-extension kinematics of the healthy and TKA knee?," *Med Eng Phys,* vol. 31, no. 8, pp. 899-906, 2009.
[48] G. Li, T. W. Rudy, M. Sakane, A. Kanamori, C. B. Ma, and S. L. Woo, "The importance of quadriceps and hamstring muscle loading on knee kinematics and in-situ forces in the ACL," (in eng), *J Biomech,* vol. 32, no. 4, pp. 395-400, Apr 1999.
[49] M. L. Zimny, M. Schutte, and E. Dabezies, "Mechanoreceptors in the human anterior cruciate ligament," (in eng), *Anat Rec,* vol. 214, no. 2, pp. 204-9, Feb 1986.
[50] R. A. Schultz, D. C. Miller, C. S. Kerr, and L. Micheli, "Mechanoreceptors in human cruciate ligaments. A histological study," (in eng), *J Bone Joint Surg Am,* vol. 66, no. 7, pp. 1072-6, Sep 1984.
[51] M. J. Schutte, E. J. Dabezies, M. L. Zimny, and L. T. Happel, "Neural anatomy of the human anterior cruciate ligament," (in eng), *J Bone Joint Surg Am,* vol. 69, no. 2, pp. 243-7, Feb 1987.
[52] Z. Halata, C. Wagner, and K. I. Baumann, "Sensory nerve endings in the anterior cruciate ligament (Lig. cruciatum anterius) of sheep," (in eng), *Anat Rec,* vol. 254, no. 1, pp. 13-21, Jan 1999.
[53] B. Fromm and W. Kummer, "Nerve supply of anterior cruciate ligaments and of cryopreserved anterior cruciate ligament allografts: a new method for the differentiation of the nervous tissues," (in eng), *Knee Surg Sports Traumatol Arthrosc,* vol. 2, no. 2, pp. 118-22, 1994.
[54] G. Limbert, "Finite element modelling of biological connective soft tissues: Applications to the ligaments of the human knee," University of Southampton, 2001.
[55] A. Viidik, "A rheological model for uncalcified parallel-fibred collagenous tissue," (in eng), *J Biomech,* vol. 1, no. 1, pp. 3-11, 1968.
[56] M. Abrahams, "Mechanical behavior of tendon in vitro," *Medical & Biological Engineering,* vol. 5, no. 433, 1967.
[57] E. S. Butler Grood and F. R. D. L. Noyes, "Biomechanics of ligaments and tendons," *Exercise and Sport Sciences Reviews,* vol. 6: 125, 1978.
[58] T. J. Momersteeg, L. Blankevoort, R. Huiskes, J. G. Kooloos, J. M. Kauer, and J. C. Hendriks, "The effect of variable relative insertion orientation of human knee bone-ligament-bone complexes on the tensile stiffness," (in eng), *Journal of Biomechanics,* vol. 28, no. 6, pp. 745-752, 1995.
[59] T. J. Mommersteeg, L. Blankevoort, R. Huiskes, J. G. Kooloos, and J. M. Kauer, "Characterization of the mechanical behavior of human knee ligaments: a numerical-experimental approach," *J Biomech,* vol. 29, no. 2, pp. 151-160, 1996.
[60] P. S. Trent, P. S. Walker, and B. Wolf, "Ligament length patterns, strength, and rotational axes of the knee joint," (in eng), *Clin Orthop Relat Res,* no. 117, pp. 263-70, Jun 1976.
[61] J. Wismans, F. Veldpaus, J. Janssen, A. Huson, and P. Struben, "A three-dimensional mathematical model of the knee-joint," *Journal of Biomechanics,* vol. 13, pp. 9-9.
[62] L. Blankevoort and R. Huiskes, "Ligament-bone interaction in a three-dimensional model of the knee," *J Biomech Eng,* vol. 113, no. 3, pp. 263-269, 1991.
[63] D. L. Butler, E. S. Grood, F. R. Noyes, R. F. Zernicke, and K. Brackett, "Effects of structure and strain measurement technique on the material properties of young human tendons and fascia," (in eng), *J Biomech,* vol. 17, no. 8, pp. 579-96, 1984.

[64] A. Race and A. A. Amis, "The mechanical properties of the two bundles of the human posterior cruciate ligament," *J Biomech,* vol. 27, no. 1, pp. 13-24, 1994.
[65] M. Freutel, H. Schmidt, L. Durselen, A. Ignatius, and F. Galbusera, "Finite element modeling of soft tissues: material models, tissue interaction and challenges," (in eng), *Clin Biomech (Bristol, Avon),* vol. 29, no. 4, pp. 363-72, Apr 2014.
[66] H. Naghibi Beidokhti, D. Janssen, S. van de Groes, J. Hazrati, T. Van den Boogaard, and N. Verdonschot, "The influence of ligament modelling strategies on the predictive capability of finite element models of the human knee joint," *J Biomech,* vol. 65, pp. 1-11, Dec 8 2017.
[67] F. Galbusera *et al.*, "Material models and properties in the finite element analysis of knee ligaments: a literature review," *Front Bioeng Biotechnol,* vol. 2, p. 54, 2014.
[68] E. M. Abdel-Rahman and M. S. Hefzy, "Three-dimensional dynamic behaviour of the human knee joint under impact loading," *Medical Engineering & Physics,* vol. 20, no. 4, pp. 276-290, 1998.
[69] V. K. Srikanth, J. L. Fryer, G. Zhai, T. M. Winzenberg, D. Hosmer, and G. Jones, "A meta-analysis of sex differences prevalence, incidence and severity of osteoarthritis," (in eng), *Osteoarthritis Cartilage,* vol. 13, no. 9, pp. 769-81, Sep 2005.
[70] V. Silverwood, M. Blagojevic-Bucknall, C. Jinks, J. L. Jordan, J. Protheroe, and K. P. Jordan, "Current evidence on risk factors for knee osteoarthritis in older adults: a systematic review and meta-analysis," (in eng), *Osteoarthritis Cartilage,* vol. 23, no. 4, pp. 507-15, Apr 2015.
[71] J. A. C. van Tunen *et al.*, "Association of osteoarthritis risk factors with knee and hip pain in a population-based sample of 29-59 year olds in Denmark: a cross-sectional analysis," (in eng), *BMC Musculoskelet Disord,* vol. 19, no. 1, p. 300, Aug 21 2018.
[72] P. Suri, D. C. Morgenroth, and D. J. Hunter, "Epidemiology of osteoarthritis and associated comorbidities," (in eng), *Pm r,* vol. 4, no. 5 Suppl, pp. S10-9, 2012.
[73] J. R. Bellemans, Michael D; Victor, Jan M.K., *Total Knee Arthroplasty*, 1 ed. (A Guide to Get Better Performance). Springer-Verlag Berlin Heidelberg, 2005.
[74] "Swedish Knee Arthoplasty Register: Annual Report 2008," Department of Orthopaedics, University Hospital in Lund, Sweden2008, Available: http://internal-pdf//Swedish knee arthroplasty report 2008Engl_1.1-2509343488/Swedish knee arthroplasty report 2008Engl_1.1.pdf.
[75] M. J. Walton, A. E. Weale, and J. H. Newman, "The progression of arthritis following lateral unicompartmental knee replacement," *The Knee,* vol. 13, no. 5, pp. 374-377, 2006.
[76] P. V. Papas, F. D. Cushner, and G. R. Scuderi, "The History of Total Knee Arthroplasty," *Techniques in Orthopaedics,* vol. 33, no. 1, pp. 2-6, 2018.
[77] U. N. J. Registry, "National Joint Registry for England, Wales, Northern Ireland and the Isle of Man," 2018.
[78] L. University, "Swedish Knee Arthroplasty Registry," 2018.
[79] B. C. Carr and T. Goswami, "Knee implants - Review of models and biomechanics," *Materials & Design,* vol. 30, no. 2, pp. 398-413, 2009.
[80] P. Ducheyne, A. Kagan 2nd, and J. A. Lacey, "Failure of total knee arthroplasty due to loosening and deformation of the tibial component," (in eng), *J Bone Joint Surg Am,* vol. 60, no. 3, pp. 384-391, 1978.
[81] S. M. Kurtz, H. A. Gawel, and J. D. Patel, "History and systematic review of wear and osteolysis outcomes for first-generation highly crosslinked polyethylene," (in eng), *Clin Orthop Relat Res,* vol. 469, no. 8, pp. 2262-2277, 2011.
[82] D. D. D. T. L. Amendola M. Fosco, "History of Condylar Total Knee Arthroplasty," *Interchopen,* 2012.
[83] S. D. Reinitz, B. H. Currier, D. W. Van Citters, R. A. Levine, and J. P. Collier, "Oxidation and other property changes of retrieved sequentially annealed UHMWPE acetabular and tibial bearings," *J Biomed Mater Res B Appl Biomater,* 2014.

[84] S. Joglekar, T. J. Gioe, P. Yoon, and M. H. Schwartz, "Gait analysis comparison of cruciate retaining and substituting TKA following PCL sacrifice," (in eng), *Knee,* vol. 19, no. 4, pp. 279-85, Aug 2012.

[85] B. S. Parsley, M. A. Conditt, R. Bertolusso, and P. C. Noble, "Posterior cruciate ligament substitution is not essential for excellent postoperative outcomes in total knee arthroplasty," (in eng), *J Arthroplasty,* vol. 21, no. 6 Suppl 2, pp. 127-31, Sep 2006.

[86] C. L. Peters, P. Mulkey, J. Erickson, M. B. Anderson, and C. E. Pelt, "Comparison of total knee arthroplasty with highly congruent anterior-stabilized bearings versus a cruciate-retaining design," (in eng), *Clin Orthop Relat Res,* vol. 472, no. 1, pp. 175-80, Jan 2014.

[87] U. G. Longo *et al.*, "Outcomes of Posterior-Stabilized Compared with Cruciate-Retaining Total Knee Arthroplasty," (in eng), *J Knee Surg,* vol. 31, no. 4, pp. 321-340, Apr 2018.

[88] M. S. Kuster and G. W. Stachowiak, "Factors affecting polyethylene wear in total knee arthroplasty," (in eng), *Orthopedics,* vol. 25, no. 2 Suppl, pp. s235-42, 2002.

[89] Y. H. Kim, S. H. Yoon, and J. S. Kim, "The long-term results of simultaneous fixed-bearing and mobile-bearing total knee replacements performed in the same patient," (in eng), *J Bone Joint Surg Br,* vol. 89, no. 10, pp. 1317-1323, 2007.

[90] M. W. Pagnano and R. M. Menghini, "Rotating platform knees: an emerging clinical standard: in opposition," (in eng), *J Arthroplasty,* vol. 21, no. 4 Suppl 1, pp. 37-39, 2006.

[91] C. L. Barnes, J. D. Blaha, D. DeBoer, P. Stemniski, R. Obert, and M. Carroll, "Assessment of a medial pivot total knee arthroplasty design in a cadaveric knee extension test model," *J Arthroplasty,* vol. 27, no. 8, pp. 1460-1468 e1, 2012.

[92] J. D. Blaha, "A medial pivot geometry," (in eng), *Orthopedics,* vol. 25, no. 9, pp. 963-964, 2002.

[93] A. M. Hollister, S. Jatana, A. K. Singh, W. W. Sullivan, and A. G. Lupichuk, "The axes of rotation of the knee," (in eng), *Clin Orthop Relat Res,* no. 290, pp. 259-268, 1993.

[94] N. Shimizu, T. Tomita, T. Yamazaki, H. Yoshikawa, and K. Sugamoto, "In Vivo Movement of Femoral Flexion Axis of a Single-Radius Total Knee Arthroplasty," *J Arthroplasty,* 2013.

[95] A. R. Jo, E. K. Song, K. B. Lee, H. Y. Seo, S. K. Kim, and J. K. Seon, "A Comparison of Stability and Clinical Outcomes in Single-Radius Versus Multi-Radius Femoral Design for Total Knee Arthroplasty," *J Arthroplasty,* 2014.

[96] J. Palmer, K. Sloan, and G. Clark, "Functional outcomes comparing Triathlon versus Duracon total knee arthroplasty: does the Triathlon outperform its predecessor?," *Int Orthop,* vol. 38, no. 7, pp. 1375-1378, 2014.

[97] S. Ostermeier and C. Stukenborg-Colsman, "Quadriceps force after TKA with femoral single radius," (in eng), *Acta Orthop,* vol. 82, no. 3, pp. 339-343, 2011.

[98] H. Wang, K. J. Simpson, M. S. Ferrara, S. Chamnongkich, T. Kinsey, and O. M. Mahoney, "Biomechanical differences exhibited during sit-to-stand between total knee arthroplasty designs of varying radii," (in eng), *J Arthroplasty,* vol. 21, no. 8, pp. 1193-1199, 2006.

[99] J. E. Stoddard, D. J. Deehan, A. M. Bull, A. W. McCaskie, and A. A. Amis, "The kinematics and stability of single-radius versus multi-radius femoral components related to mid-range instability after TKA," *J Orthop Res,* vol. 31, no. 1, pp. 53-58, 2013.

[100] J. Y. Jenny *et al.*, "Single-radius, multidirectional total knee replacement," *Knee Surg Sports Traumatol Arthrosc,* vol. 21, no. 12, pp. 2764-2769, 2013.

[101] O. Kessler, L. Durselen, S. Banks, H. Mannel, and F. Marin, "Sagittal curvature of total knee replacements predicts in vivo kinematics," *Clin Biomech (Bristol, Avon),* vol. 22, no. 1, pp. 52-58, 2007.

[102] E. E. Pakos, E. E. Ntzani, and T. A. Trikalinos, "Patellar resurfacing in total knee arthroplasty. A meta-analysis," *J Bone Joint Surg Am,* vol. 87, no. 7, pp. 1438-1445, 2005.

[103] R. S. Nizard *et al.*, "A meta-analysis of patellar replacement in total knee arthroplasty," *Clin Orthop Relat Res,* no. 432, pp. 196-203, 2005.

[104] M. C. Forster, "Patellar resurfacing in total knee arthroplasty for osteoarthritis: a systematic review," *Knee,* vol. 11, no. 6, pp. 427-430, 2004.

[105] S. Li, Y. Chen, W. Su, J. Zhao, S. He, and X. Luo, "Systematic review of patellar resurfacing in total knee arthroplasty," *Int Orthop,* vol. 35, no. 3, pp. 305-316, 2011.
[106] V. Metsna, S. Vorobjov, and A. Märtson, "Prevalence of anterior knee pain among patients following total knee arthroplasty with nonreplaced patella: A retrospective study of 1778 knees," *Medicina,* no. 0.
[107] M. Agrawal, V. Jain, V. P. Yadav, and V. Bhardwaj, "Patellar resurfacing in total knee arthroplasty," *Journal of Clinical Orthopaedics and Trauma,* vol. 2, no. 2, pp. 77-81, 2011.
[108] O. S. Schindler, "Basic kinematics and biomechanics of the patellofemoral joint part 2: the patella in total knee arthroplasty," (in eng), *Acta Orthop Belg,* vol. 78, no. 1, pp. 11-29, 2012.
[109] V. Y. Ng, J. H. DeClaire, K. R. Berend, B. C. Gulick, and A. V. Lombardi, Jr., "Improved accuracy of alignment with patient-specific positioning guides compared with manual instrumentation in TKA," (in eng), *Clin Orthop Relat Res,* vol. 470, no. 1, pp. 99-107, Jan 2012.
[110] S. K. Chauhan, R. G. Scott, W. Breidahl, and R. J. Beaver, "Computer-assisted knee arthroplasty versus a conventional jig-based technique. A randomised, prospective trial," *J Bone Joint Surg Br,* vol. 86, no. 3, pp. 372-377, 2004.
[111] J. M. Sikorski and S. Chauhan, "Computer-assisted orthopaedic surgery: do we need CAOS?," *J Bone Joint Surg Br,* vol. 85, no. 3, pp. 319-323, 2003.
[112] K. Bauwens *et al.*, "Navigated total knee replacement. A meta-analysis," *J Bone Joint Surg Am,* vol. 89, no. 2, pp. 261-269, 2007.
[113] J. Cip, M. Widemschek, M. Luegmair, M. B. Sheinkop, T. Benesch, and A. Martin, "Conventional Versus Computer-Assisted Technique for Total Knee Arthroplasty: A Minimum of 5-Year Follow-up of 200 Patients in a Prospective Randomized Comparative Trial," *J Arthroplasty,* 2014.
[114] G. R. Scuderi, M. Fallaha, V. Masse, P. Lavigne, L. P. Amiot, and M. J. Berthiaume, "Total knee arthroplasty with a novel navigation system within the surgical field," (in eng), *Orthop Clin North Am,* vol. 45, no. 2, pp. 167-173, 2014.
[115] J. B. Mason, T. K. Fehring, R. Estok, D. Banel, and K. Fahrbach, "Meta-analysis of alignment outcomes in computer-assisted total knee arthroplasty surgery," *J Arthroplasty,* vol. 22, no. 8, pp. 1097-1106, 2007.
[116] T. Calliess, M. Ettinger, and H. Windhagen, "[Computer-assisted systems in total knee arthroplasty. Useful aid or only additional costs]," (in ger), *Orthopade,* vol. 43, no. 6, pp. 529-533, 2014.
[117] W. P. Barrett, J. B. Mason, J. T. Moskal, D. F. Dalury, A. Oliashirazi, and D. A. Fisher, "Comparison of radiographic alignment of imageless computer-assisted surgery vs conventional instrumentation in primary total knee arthroplasty," *J Arthroplasty,* vol. 26, no. 8, pp. 1273-1284 e1, 2011.
[118] C. P. Christensen, A. H. Stewart, and C. A. Jacobs, "Soft tissue releases affect the femoral component rotation necessary to create a balanced flexion gap during total knee arthroplasty," *J Arthroplasty,* vol. 28, no. 9, pp. 1528-1532, 2013.
[119] B. D. Springer, S. Parratte, and M. P. Abdel, "Measured resection versus gap balancing for total knee arthroplasty," (in eng), *Clin Orthop Relat Res,* vol. 472, no. 7, pp. 2016-2022, 2014.
[120] R. A. Berger, L. S. Crossett, J. J. Jacobs, and H. E. Rubash, "Malrotation causing patellofemoral complications after total knee arthroplasty," *Clin Orthop Relat Res,* no. 356, pp. 144-153, 1998.
[121] J. G. Boldt, J. B. Stiehl, J. Hodler, M. Zanetti, and U. Munzinger, "Femoral component rotation and arthrofibrosis following mobile-bearing total knee arthroplasty," *Int Orthop,* vol. 30, no. 5, pp. 420-425, 2006.
[122] J. Romero, T. Stahelin, C. Binkert, C. Pfirrmann, J. Hodler, and O. Kessler, "The clinical consequences of flexion gap asymmetry in total knee arthroplasty," *J Arthroplasty,* vol. 22, no. 2, pp. 235-240, 2007.

[123] A. M. Merican, K. M. Ghosh, F. Iranpour, D. J. Deehan, and A. A. Amis, "The effect of femoral component rotation on the kinematics of the tibiofemoral and patellofemoral joints after total knee arthroplasty," *Knee Surg Sports Traumatol Arthrosc,* vol. 19, no. 9, pp. 1479-1487, 2011.

[124] D. Tigani, G. Sabbioni, R. Ben Ayad, M. Filanti, N. Rani, and N. Del Piccolo, "Comparison between two computer-assisted total knee arthroplasty: gap-balancing versus measured resection technique," (in eng), *Knee Surg Sports Traumatol Arthrosc,* vol. 18, no. 10, pp. 1304-1310, 2010.

[125] R. A. Berger, H. E. Rubash, M. J. Seel, W. H. Thompson, and L. S. Crossett, "Determining the rotational alignment of the femoral component in total knee arthroplasty using the epicondylar axis," *Clinical orthopaedics and related research,* vol. 286, no. 286, pp. 40-47, 1993.

[126] D. A. Dennis, R. D. Komistek, R. H. Kim, and A. Sharma, "Gap balancing versus measured resection technique for total knee arthroplasty," (in eng), *Clin Orthop Relat Res,* vol. 468, no. 1, pp. 102-107, 2010.

[127] L. A. Whiteside and J. Arima, "The anteroposterior axis for femoral rotational alignment in valgus total knee arthroplasty," *Clin Orthop Relat Res,* no. 321, pp. 168-172, 1995.

[128] P. L. Poilvache, J. N. Insall, G. R. Scuderi, and D. E. Font-Rodriguez, "Rotational landmarks and sizing of the distal femur in total knee arthroplasty," *Clinical orthopaedics and related research,* no. 331, pp. 35-46, 1996.

[129] R. S. Laskin, "Flexion space configuration in total knee arthroplasty," *J Arthroplasty,* vol. 10, no. 5, pp. 657-660, 1995.

[130] J. B. Stiehl and D. A. Heck, "How Precise Is Computer-navigated Gap Assessment in TKA?," (in Eng), *Clin Orthop Relat Res,* 2014.

[131] B. K. Daines and D. A. Dennis, "Gap balancing vs. measured resection technique in total knee arthroplasty," (in eng), *Clin Orthop Surg,* vol. 6, no. 1, pp. 1-8, 2014.

[132] T. Matsumoto, H. Muratsu, S. Kubo, T. Matsushita, M. Kurosaka, and R. Kuroda, "Soft tissue tension in cruciate-retaining and posterior-stabilized total knee arthroplasty," *J Arthroplasty,* vol. 26, no. 5, pp. 788-795, 2011.

[133] K. Nagai, H. Muratsu, T. Matsumoto, H. Miya, R. Kuroda, and M. Kurosaka, "Soft tissue balance changes depending on joint distraction force in total knee arthroplasty," *J Arthroplasty,* vol. 29, no. 3, pp. 520-524, 2014.

[134] J. R. Yoon, H. I. Jeong, K. J. Oh, and J. H. Yang, "In vivo gap analysis in various knee flexion angles during navigation-assisted total knee arthroplasty," (in eng), *J Arthroplasty,* vol. 28, no. 10, pp. 1796-1800, 2013.

[135] T. Classen, A. Wegner, R. D. Muller, and M. Von Knoch, "Femoral component rotation and Laurin angle after total knee arthroplasty," *Acta Orthop Belg,* vol. 76, no. 1, pp. 69-73, 2010.

[136] Y. S. Anouchi, L. A. Whiteside, A. D. Kaiser, and M. T. Milliano, "The effects of axial rotational alignment of the femoral component on knee stability and patellar tracking in total knee arthroplasty demonstrated on autopsy specimens," *Clin Orthop Relat Res,* no. 287, pp. 170-177, 1993.

[137] T. J. Gioe, K. K. Killeen, K. Grimm, S. Mehle, and K. Scheltema, "Why are total knee replacements revised?: analysis of early revision in a community knee implant registry," *Clin Orthop Relat Res,* no. 428, pp. 100-106, 2004.

[138] P. F. Sharkey, W. J. Hozack, R. H. Rothman, S. Shastri, and S. M. Jacoby, "Insall Award paper. Why are total knee arthroplasties failing today?," *Clin Orthop Relat Res,* no. 404, pp. 7-13, 2002.

[139] "National Joint Registry for England, Wales, Northern Island and the Isle of Man Joint Registry," United Kingdom2018.

[140] P. F. Sharkey, P. M. Lichstein, C. Shen, A. T. Tokarski, and J. Parvizi, "Why are total knee arthroplasties failing today—has anything changed after 10 years?," *The Journal of arthroplasty,* vol. 29, no. 9, pp. 1774-1778, 2014.

[141] A. D. Beswick, V. Wylde, R. Gooberman-Hill, A. Blom, and P. Dieppe, "What proportion of patients report long-term pain after total hip or knee replacement for osteoarthritis? A systematic review of Prospective studies in unselected patients," *BMJ Open,* vol. 2, no. 1, 2012.

[142] P. Baker, J. Van der Meulen, J. Lewsey, and P. Gregg, "The role of pain and function in determining patient satisfaction after total knee replacement," *Bone & Joint Journal,* vol. 89, no. 7, pp. 893-900, 2007.

[143] R. B. Bourne, B. M. Chesworth, A. M. Davis, N. N. Mahomed, and K. D. J. Charron, "Patient satisfaction after total knee arthroplasty: who is satisfied and who is not?," 2009.

[144] J. Hutt, V. Massé, M. Lavigne, and P. A. Vendittoli, "Functional joint line obliquity after kinematic total knee arthroplasty," *International Orthopaedics,* 2016.

[145] C. Rivière *et al.*, "Mechanical alignment technique for TKA: Are there intrinsic technical limitations?," *Orthopaedics and Traumatology: Surgery and Research,* vol. 103, no. 7, pp. 1057-1067, 2017.

[146] C. Rivière *et al.*, "Alignment options for total knee arthroplasty: A systematic review," *Orthopaedics and Traumatology: Surgery and Research,* vol. 103, no. 7, pp. 1047-1056, 2017.

[147] A. Rothwell, A. Henwood, and T. Hobbs, *New Zealand Orthopaedic Association the New Zealand Joint Registry Twelve Year Report January 1999 To December 2010*. 2010.

[148] N. N. Mahomed *et al.*, "The importance of patient expectations in predicting functional outcomes after total joint arthroplasty," (in eng), *J Rheumatol,* vol. 29, no. 6, pp. 1273-9, Jun 2002.

[149] D. C. Albrecht and A. Ottersbach, "Retrospective 5-Year Analysis of Revision Rate and Functional Outcome of TKA With and Without Patella Implant," *Orthopedics,* vol. 39, no. 3, pp. S31-S35, 2016.

[150] J. W. Goodfellow, J. J. O'Connor, and D. W. Murray, "A critique of revision rate as an outcome measure: RE-INTERPRETATION OF KNEE JOINT REGISTRY DATA," *Journal of Bone and Joint Surgery - British Volume,* vol. 92-B, no. 12, pp. 1628-1631, 2010.

[151] C. Pabinger, D. Benjamin Lumenta, D. Cupak, A. Berghold, and G. Labek, "Quality of outcome data in knee arthroplasty Comparison of registry data and worldwide non-registry studies from 4 decades," *Acta Orthopaedica,* vol. 86, no. 1, pp. 58-62, 2015.

[152] S. W. Young, J. Mutu-Grigg, C. M. Frampton, and J. Cullen, "Does Speed Matter? Revision Rates and Functional Outcomes in TKA in Relation to Duration of Surgery," *Journal of Arthroplasty,* vol. 29, pp. 1473-1477.e1, 2014.

[153] A. J. Price *et al.*, "Are pain and function better measures of outcome than revision rates after TKR in the younger patient?," (in English), *Knee,* vol. 17, no. 3, pp. 196-199, 2010.

[154] Y. J. Choi and H. J. Ra, "Patient Satisfaction after Total Knee Arthroplasty," (in eng), *Knee Surg Relat Res,* vol. 28, no. 1, pp. 1-15, Mar 2016.

[155] K. Gromov, M. Korchi, M. G. Thomsen, H. Husted, and A. Troelsen, "What is the optimal alignment of the tibial and femoral com- ponents in knee arthroplasty? An overview of the literature," *Acta Orthopaedica,* vol. 85, no. 5, pp. 480-487, 2014.

[156] H. J. T. A. M. Huijbregts, R. J. K. Khan, E. Sorensen, D. P. Fick, and S. Haebich, "Patient-specific instrumentation does not improve radiographic alignment or clinical outcomes after total knee arthroplasty: A meta-analysis," *Acta Orthopaedica,* vol. 87, no. 4, pp. 386-394, 2016.

[157] Y. Niki, S. Kobayashi, T. Nagura, K. Udagawa, and K. Harato, "Joint Line Modification in Kinematically Aligned Total Knee Arthroplasty Improves Functional Activity but Not Patient Satisfaction," in *Journal of Arthroplasty* vol. 33, ed, 2018, pp. 2125-2130.

[158] M. P. Abdel *et al.*, "No benefit of patient-specific instrumentation in TKA on functional and gait outcomes: a randomized clinical trial," *Clin Orthop Relat Res,* vol. 472, no. 8, pp. 2468-76, Aug 2014.

[159] N. D. Clement, A. D. Duckworth, S. P. MacKenzie, Y. X. Nie, and C. H. Tiemessen, "Medium-term results of Oxford phase-3 medial unicompartmental knee arthroplasty," *Journal of orthopaedic surgery (Hong Kong),* vol. 20, pp. 157-61, 2012.

[160] T. Lording, S. Lustig, and P. Neyret, "Coronal alignment after total knee arthroplasty," *Knee EFORT open reviews,* vol. 1, no. 1, pp. 12-17, 2016.

[161] A. J. Nedopil, A. K. Singh, S. M. Howell, and M. L. Hull, "Primary Arthroplasty Does Calipered Kinematically Aligned TKA Restore Native Left to Right Symmetry of the Lower Limb and Improve Function?," 2018.

[162] S. O'Brien, D. Bennett, E. Doran, and D. E. Beverland, "Comparison of hip and knee arthroplasty outcomes at early and intermediate follow-up," *Orthopedics,* vol. 32, no. 3, pp. 168-168, 2009.

[163] A. V. Wiik, A. Aqil, S. Tankard, A. A. Amis, and J. P. Cobb, "Downhill walking gait pattern discriminates between types of knee arthroplasty: improved physiological knee functionality in UKA versus TKA," *Knee Surgery, Sports Traumatology, Arthroscopy,* vol. 23, no. 6, pp. 1748-1755, 2015.

[164] M. Christen, E. Aghayev, and B. Christen, "Short-term functional versus patient-reported outcome of the bicruciate stabilized total knee arthroplasty: prospective consecutive case series," *BMC musculoskeletal disorders,* vol. 15, pp. 435-435, 2014.

[165] J. R. B. Hutt, M. A. LeBlanc, V. Massé, M. Lavigne, and P. A. Vendittoli, "Kinematic TKA using navigation: Surgical technique and initial results," *Orthopaedics and Traumatology: Surgery and Research,* vol. 102, no. 1, pp. 99-104, 2016.

[166] R. C. Mather *et al.*, "Cost-Effectiveness Analysis of Early Reconstruction Versus Rehabilitation and Delayed Reconstruction for Anterior Cruciate Ligament Tears," *The American journal of sports medicine,* vol. 42, no. 7, pp. 1583-1591, 2014.

[167] M. Moutzouri, P. Tsoumpos, E. Billis, A. Papoutsidakis, and J. Gliatis, "Cross-cultural translation and validation of the Greek version of the Knee Injury and Osteoarthritis Outcome Score (KOOS) in patients with total knee replacement," *Disability and rehabilitation,* pp. 1-7, 2014.

[168] D. L. Riddle and W. A. Jiranek, "Knee osteoarthritis radiographic progression and associations with pain and function prior to knee arthroplasty: a multicenter comparative cohort study," *Osteoarthritis and cartilage / OARS, Osteoarthritis Research Society,* 2014.

[169] J. G. Twiggs *et al.*, "Patient-Specific Simulated Dynamics After Total Knee Arthroplasty Correlate With Patient-Reported Outcomes," *The Journal of Arthroplasty,* 2018.

[170] H. B. Waterson, N. D. Clement, K. S. Eyres, V. I. Mandalia, and A. D. Toms, "The early outcome of kinematic versus mechanical alignment in total knee arthroplasty: A PROSPECTIVE RANDOMISED CONTROL TRIAL," *Bone and Joint Journal,* vol. 98-B, no. 10, pp. 1360-1368, 2016.

[171] P. Ornetti, J. F. F. Maillefert, D. Laroche, C. Morisset, M. Dougados, and L. Gossec, "Gait analysis as a quantifiable outcome measure in hip or knee osteoarthritis: A systematic review," *Joint Bone Spine,* vol. 77, pp. 421-425, 2010.

[172] G. Varadi *et al.*, "Randomized clinical trial evaluating transdermal Ibuprofen for moderate to severe knee osteoarthritis," *Pain physician,* vol. 16, no. 6, pp. E749-62.

[173] U. Lindemann *et al.*, "Gait analysis and WOMAC are complementary in assessing functional outcome in total hip replacement," *Clin Rehabil,* vol. 20, pp. 413-420, 2006.

[174] S. S. Mahmood, S. S. Mukka, S. Crnalic, and A. S. Sayed-Noor, "The Influence of Leg Length Discrepancy after Total Hip Arthroplasty on Function and Quality of Life: A Prospective Cohort Study," *The Journal of Arthroplasty,* vol. 30, no. 9, pp. 1638-1642, 2015.

[175] H. G. Dossett, G. J. Swartz, N. A. Estrada, G. W. LeFevre, and B. G. Kwasman, "Kinematically Versus Mechanically Aligned Total Knee Arthroplasty," *Orthopedics,* vol. 35, no. 2, pp. e160-9, 2012.

[176] T. K. Fehring, S. Odum, W. L. Griffin, and J. B. Mason, "Outcome comparison of partial and full component revision TKA," *Clinical orthopaedics and related research,* vol. 440, pp. 131-134, 2005.
[177] L. M. Longstaff, K. Sloan, N. Stamp, M. Scaddan, and R. Beaver, "Good Alignment After Total Knee Arthroplasty Leads to Faster Rehabilitation and Better Function," *Journal of Arthroplasty,* vol. 24, no. 4, pp. 570-578, 2009.
[178] L. Vanlommel, J. Vanlommel, S. Claes, and J. Bellemans, "Slight undercorrection following total knee arthroplasty results in superior clinical outcomes in varus knees," *Knee surgery, sports traumatology, arthroscopy : official journal of the ESSKA,* vol. 21, no. 10, pp. 2325-30, 2013.
[179] O. Robertsson, M. Dunbar, T. Pehrsson, K. Knutson, and L. Lidgren, "Patient satisfaction after knee arthroplasty: a report on 27,372 knees operated on between 1981 and 1995 in Sweden," (in eng), *Acta Orthop Scand,* vol. 71, no. 3, pp. 262-267, 2000.
[180] J. Kim, C. L. Nelson, and P. A. Lotke, "Stiffness after total knee arthroplasty. Prevalence of the complication and outcomes of revision," *J Bone Joint Surg Am,* vol. 86-A, no. 7, pp. 1479-1484, 2004.
[181] P. N. Baker *et al.*, "The effect of surgical factors on early patient-reported outcome measures (PROMS) following total knee replacement," *J Bone Joint Surg Br,* vol. 94, no. 8, pp. 1058-1066, 2012.
[182] A. Judge *et al.*, "Predictors of outcomes of total knee replacement surgery," *Rheumatology (Oxford),* vol. 51, no. 10, pp. 1804-1813, 2012.
[183] C. E. H. Scott, W. M. Oliver, D. MacDonald, F. A. Wade, M. Moran, and S. J. Breusch, "Predicting dissatisfaction following total knee arthroplasty in patients under 55 years of age," *The Bone & Joint Journal,* vol. 98-B, no. 12, pp. 1625-1634, 2016.
[184] E. Losina and J. N. Katz, "Total knee replacement: pursuit of the paramount result," (in eng), *Rheumatology (Oxford),* vol. 51, no. 10, pp. 1735-1736, 2012.
[185] M. Hadi, T. Barlow, I. Ahmed, M. Dunbar, P. McCulloch, and D. Griffin, "Does malalignment affect patient reported outcomes following total knee arthroplasty: a systematic review of the literature," (in eng), *Springerplus,* vol. 5, no. 1, p. 1201, 2016.
[186] D. P. Williams *et al.*, "Early postoperative predictors of satisfaction following total knee arthroplasty," (in eng), *Knee,* vol. 20, no. 6, pp. 442-6, Dec 2013.
[187] D. F. Hamilton *et al.*, "Making the Oxford Hip and Knee Scores meaningful at the patient level through normative scoring and registry data," (in eng), *Bone Joint Res,* vol. 4, no. 8, pp. 137-44, Aug 2015.
[188] P. N. Ramkumar, J. D. Harris, and P. C. Noble, "Patient-reported outcome measures after total knee arthroplasty: a systematic review," (in eng), *Bone Joint Res,* vol. 4, no. 7, pp. 120-7, Jul 2015.
[189] S. A. Bolink, B. Grimm, and I. C. Heyligers, "Patient-reported outcome measures versus inertial performance-based outcome measures: A prospective study in patients undergoing primary total knee arthroplasty," (in eng), *Knee,* vol. 22, no. 6, pp. 618-23, Dec 2015.
[190] P. Baker, P. Cowling, S. Kurtz, S. Jameson, P. Gregg, and D. Deehan, "Reason for revision influences early patient outcomes after aseptic knee revision," (in eng), *Clin Orthop Relat Res,* vol. 470, no. 8, pp. 2244-52, Aug 2012.
[191] S. Lyman, Y. Y. Lee, P. D. Franklin, W. Li, M. B. Cross, and D. E. Padgett, "Validation of the KOOS, JR: A Short-form Knee Arthroplasty Outcomes Survey," (in eng), *Clin Orthop Relat Res,* vol. 474, no. 6, pp. 1461-71, Jun 2016.
[192] A. M. Almaawi, J. R. B. Hutt, V. Masse, M. Lavigne, and P. A. Vendittoli, "The Impact of Mechanical and Restricted Kinematic Alignment on Knee Anatomy in Total Knee Arthroplasty," *Journal of Arthroplasty,* vol. 32, no. 7, pp. 2133-2140, 2017.
[193] R. S. Jeffery, R. W. Morris, and R. A. Denham, "Coronal alignment after total knee replacement," *J Bone Joint Surg Br,* vol. 73, no. 5, pp. 709-714, 1991.

[194] M. A. Ritter, M. E. Berend, J. B. Meding, E. M. Keating, P. M. Faris, and B. M. Crites, "Long-term followup of anatomic graduated components posterior cruciate-retaining total knee replacement," *Clin Orthop Relat Res,* no. 388, pp. 51-57, 2001.

[195] F. W. Werner, D. C. Ayers, L. P. Maletsky, and P. J. Rullkoetter, "The effect of valgus/varus malalignment on load distribution in total knee replacements," *J Biomech,* vol. 38, no. 2, pp. 349-355, 2005.

[196] S. W. Young, M. L. Walker, A. Bayan, T. Briant-Evans, P. Pavlou, and B. Farrington, "The Chitranjan S. Ranawat Award: No Difference in 2-year Functional Outcomes Using Kinematic versus Mechanical Alignment in TKA: A Randomized Controlled Clinical Trial," *Clinical Orthopaedics and Related Research,* vol. 475, no. 1, pp. 9-20, 2017.

[197] A. Bonnefoy-Mazure, S. Armand, Y. Sagawa, D. Suvà, H. Miozzari, and K. Turcot, "Knee Kinematic and Clinical Outcomes Evolution Before, 3 Months, and 1 Year After Total Knee Arthroplasty," *Journal of Arthroplasty,* vol. 32, no. 3, pp. 793-800, 2017.

[198] P. F. Choong, M. M. Dowsey, and J. D. Stoney, "Does accurate anatomical alignment result in better function and quality of life? Comparing conventional and computer-assisted total knee arthroplasty," *J Arthroplasty,* vol. 24, no. 4, pp. 560-569, 2009.

[199] R. A. Magnussen, F. Weppe, G. Demey, E. Servien, and S. Lustig, "Residual varus alignment does not compromise results of TKAs in patients with preoperative varus," *Clinical Orthopaedics and Related Research,* vol. 469, no. 12, pp. 3443-3450, 2011.

[200] C. Planckaert, G. Larose, P. Ranger, M. Lacelle, A. Fuentes, and N. Hagemeister, "Total knee arthroplasty with unexplained pain: new insights from kinematics," *Archives of Orthopaedic and Trauma Surgery,* vol. 138, no. 4, pp. 553-561, 2018.

[201] L. Sosdian *et al.*, "Longitudinal changes in knee kinematics and moments following knee arthroplasty: A systematic review," *Knee,* vol. 21, no. 6, pp. 994-1008, 2014.

[202] S. M. Howell, S. J. Howell, K. T. Kuznik, J. Cohen, and M. L. Hull, "Does a kinematically aligned total knee arthroplasty restore function without failure regardless of alignment category? Knee," *Clinical Orthopaedics and Related Research,* vol. 471, no. 3, pp. 1000-1007, 2013.

[203] C. Riviere, S. Lazic, L. Villet, Y. Wiart, S. M. Allwood, and J. Cobb, "Kinematic alignment technique for total hip and knee arthroplasty: The personalized implant positioning surgery," *EFORT Open Rev,* vol. 3, no. 3, pp. 98-105, 2018.

[204] T. Takahashi, J. Ansari, and H. Pandit, "Kinematically Aligned Total Knee Arthroplasty or Mechanically Aligned Total Knee Arthroplasty," *The Journal of Knee Surgery,* 2018.

[205] H. G. Dossett, N. A. Estrada, G. J. Swartz, G. W. LeFevre, and B. G. Kwasman, "A randomised controlled trial of kinematically and mechanically aligned total knee replacements: two-year clinical results," (in eng), *Bone Joint J,* vol. 96-b, no. 7, pp. 907-13, Jul 2014.

[206] M. E. Berend *et al.*, "Tibial component failure mechanisms in total knee arthroplasty," *Clinical Orthopaedics and Related Research,* no. 428, pp. 26-34, 2004.

[207] N. M. Brown *et al.*, "Total knee arthroplasty has higher postoperative morbidity than unicompartmental knee arthroplasty: A multicenter analysis," *Journal of Arthroplasty,* vol. 27, pp. 86-90, 2012.

[208] J. J. Cherian, B. H. Kapadia, S. Banerjee, J. J. Jauregui, K. Issa, and M. A. Mont, "Mechanical, anatomical, and kinematic axis in TKA: Concepts and practical applications," vol. 7, pp. 89-95.

[209] R. L. Barrack, T. Schrader, A. J. Bertot, M. W. Wolfe, and L. Myers, "Component rotation and anterior knee pain after total knee arthroplasty," (in eng), *Clin Orthop Relat Res,* no. 392, pp. 46-55, Nov 2001.

[210] C. K. Fitzpatrick, R. H. Kim, A. A. Ali, L. M. Smoger, and P. J. Rullkoetter, "Effects of resection thickness on mechanics of resurfaced patellae," *Journal of Biomechanics,* vol. 46, no. 9, pp. 1568-1575, 2013.

[211] C. K. Fitzpatrick and P. J. Rullkoetter, "Influence of patellofemoral articular geometry and material on mechanics of the unresurfaced patella," *Journal of Biomechanics,* vol. 45, no. 11, pp. 1909-1915, 2012.

[212] T. R. Abo-Alhol *et al.*, "Patellar mechanics during simulated kneeling in the natural and implanted knee."
[213] C. K. Fitzpatrick, M. A. Baldwin, C. W. Clary, A. Wright, P. J. Laz, and P. J. Rullkoetter, "Identifying alignment parameters affecting implanted patellofemoral mechanics," *Journal of Orthopaedic Research,* vol. 30, no. 7, pp. 1167-1175, 2012.
[214] A. Keshmiri *et al.*, "The influence of component alignment on patellar kinematics in total knee arthroplasty An in vivo study using a navigation system," *Acta Orthopaedica,* vol. 86, no. 4, pp. 444-450, 2015.
[215] P. S. Walker, "The design and pre-clinical evaluation of knee replacements for osteoarthritis," *Journal of Biomechanics,* vol. 48, no. 5, pp. 742-749, 2015.
[216] P. J. Rullkoetter, C. K. Fitzpatrick, and C. W. Clary, "How can we use computational modeling to improve total knee arthroplasty? Modeling stability and mobility in the implanted knee," *Journal of the American Academy of Orthopaedic Surgeons,* vol. 25, no. February, pp. S33-S39, 2017.
[217] M. A. Baldwin, C. W. Clary, C. K. Fitzpatrick, J. S. Deacy, L. P. Maletsky, and P. J. Rullkoetter, "Dynamic finite element knee simulation for evaluation of knee replacement mechanics," *J Biomech,* vol. 45, no. 3, pp. 474-483, 2012.
[218] E. Chen, R. E. Ellis, J. T. Bryant, and J. F. Rudan, "A computational model of postoperative knee kinematics," (in eng), *Med Image Anal,* vol. 5, no. 4, pp. 317-330, 2001.
[219] E. Otten, "Inverse and forward dynamics: models of multi-body systems," (in eng), *Philos Trans R Soc Lond B Biol Sci,* vol. 358, no. 1437, pp. 1493-500, Sep 29 2003.
[220] M. G. Pandy, "Computer modeling and simulation of human movement," *Annu Rev Biomed Eng,* vol. 3, pp. 245-273, 2001.
[221] T. R. Abo-Alhol *et al.*, "Patellar mechanics during simulated kneeling in the natural and implanted knee," *J Biomech,* vol. 47, no. 5, pp. 1045-51, Mar 21 2014.
[222] A. A. Ali, M. D. Harris, S. Shalhoub, L. P. Maletsky, P. J. Rullkoetter, and K. B. Shelburne, "Combined measurement and modeling of specimen-specific knee mechanics for healthy and ACL-deficient conditions," *Journal of Biomechanics,* vol. 57, pp. 117-124, 2017.
[223] T. M. Guess, G. Thiagarajan, M. Kia, and M. Mishra, "A subject specific multibody model of the knee with menisci," *Medical Engineering & Physics,* vol. 32, no. 5, pp. 505-515, 2010.
[224] M. Kazemi, Y. Dabiri, and L. P. Li, "Recent advances in computational mechanics of the human knee joint," vol. 2013, ed: Hindawi, 2013, pp. 718423-718423.
[225] K. Manal and T. S. Buchanan, "An Electromyogram-Driven Musculoskeletal Model of the Knee to Predict in Vivo Joint Contact Forces During Normal and Novel Gait Patterns," *Journal of Biomechanical Engineering,* vol. 135, no. 2, pp. 021014-021014, 2013.
[226] H. N. Beidokhti, D. Janssen, M. Khoshgoftar, A. Sprengers, E. Semih Perdahcioglu, and N. Verdonschot, "A comparison between dynamic implicit and explicit finite element simulations of the native knee joint," *Medical Engineering and Physics,* vol. 38, pp. 1123-1130, 2016.
[227] D. L. Robinson *et al.*, "Mechanical properties of normal and osteoarthritic human articular cartilage," 2016.
[228] J. Yao, P. D. Funkenbusch, J. Snibbe, M. Maloney, and A. L. Lerner, "Sensitivities of Medial Meniscal Motion and Deformation to Material Properties of Articular Cartilage, Meniscus and Meniscal Attachments Using Design of Experiments Methods," *Journal of Biomechanical Engineering,* vol. 128, no. 3, pp. 399-399, 2005.
[229] W. Mesfar and A. Shirazi-Adl, "Biomechanics of changes in ACL and PCL material properties or prestrains in flexion under muscle force-implications in ligament reconstruction," (in eng), *Comput Methods Biomech Biomed Engin,* vol. 9, no. 4, pp. 201-209, 2006.
[230] H. Atmaca, C. C. Kesemenli, K. Memişoğlu, A. Özkan, and Y. Celik, "Changes in the loading of tibial articular cartilage following medial meniscectomy: A finite element analysis study," *Knee Surgery, Sports Traumatology, Arthroscopy,* vol. 21, no. 12, pp. 2667-2673, 2013.

[231] E. Peña, B. Calvo, M. A. Martinez, D. Palanca, and M. Doblaré, "Why lateral meniscectomy is more dangerous than medial meniscectomy. A finite element study," *Journal of Orthopaedic Research,* vol. 24, no. 5, pp. 1001-1010, 2006.

[232] C. T. Arsene and B. Gabrys, "Probabilistic finite element predictions of the human lower limb model in total knee replacement," *Med Eng Phys,* vol. 35, no. 8, pp. 1116-1132, 2013.

[233] B. J. Fregly, S. A. Banks, D. D. D'Lima, and C. W. Colwell Jr, "Sensitivity of knee replacement contact calculations to kinematic measurement errors," (in eng), *J Orthop Res,* vol. 26, no. 9, pp. 1173-1179, 2008.

[234] J. Halloran, A. J. Petrella, and P. J. Rullkoetter, "Explicit finite element modelling of total knee replacement mechanics," *Journal of Biomechanics,* vol. 38, pp. 323-331, 2005.

[235] H. J. Lundberg, K. C. Foucher, T. P. Andriacchi, and M. A. Wimmer, "Direct comparison of measured and calculated total knee replacement force envelopes during walking in the presence of normal and abnormal gait patterns," *J Biomech,* vol. 45, no. 6, pp. 990-996, 2012.

[236] R. Willing and I. Y. Kim, "The development, calibration and validation of a numerical total knee replacement kinematics simulator considering laxity and unconstrained flexion motions," (in Eng), *Comput Methods Biomech Biomed Engin,* pp. 1-9, 2011.

[237] L. Blankevoort, J. H. Kuiper, R. Huiskes, and H. J. Grootenboer, "Articular contact in a three-dimensional model of the knee," *Journal of Biomechanics,* vol. 24, no. 11, pp. 1019-1031, 1991.

[238] D. L. Butler, M. D. Kay, and D. C. Stouffer, "Comparison of material properties in fascicle-bone units from human patellar tendon and knee ligaments," (in eng), *J Biomech,* vol. 19, no. 6, pp. 425-32, 1986.

[239] S. Martelli, R. E. Ellis, M. Marcacci, and S. Zaffagnini, "Total knee arthroplasty kinematics: Computer simulation and intraoperative evaluation," *Journal of Arthroplasty,* Article vol. 13, no. 2, pp. 145-155, 1998.

[240] A. Jilani, A. Shirazi-Adl, and M. Z. Bendjaballah, "Biomechanics of human tibio-femoral joint in axial rotation," *Knee,* Article vol. 4, no. 4, pp. 203-213, 1997.

[241] M. S. Hefzy and T. D. V. Cooke, "Review of knee models: 1996 update," *Applied Mechanics Reviews,* Article vol. 49, no. 10, pp. S187-S193, 1996.

[242] T. M. Guess and L. P. Maletsky, "Computational modelling of a total knee prosthetic loaded in a dynamic knee simulator," *Med Eng Phys,* vol. 27, no. 5, pp. 357-367, 2005.

[243] D. D. D'Lima, S. Patil, N. Steklov, and C. W. Colwell Jr, "An ABJS Best Paper: Dynamic intraoperative ligament balancing for total knee arthroplasty," (in eng), *Clinical Orthopaedics and Related Research,* vol. 463, pp. 208-212, 2007.

[244] H. Mizu-Uchi, C. W. Colwell, Jr., S. Fukagawa, S. Matsuda, Y. Iwamoto, and D. D. D'Lima, "The importance of bony impingement in restricting flexion after total knee arthroplasty: computer simulation model with clinical correlation," (in eng), *J Arthroplasty,* vol. 27, no. 9, pp. 1710-6, Oct 2012.

[245] W. M. Mihalko and J. L. Williams, "Computer modeling to predict effects of implant malpositioning during TKA," *Orthopedics,* vol. 33, no. 10 Suppl, pp. 71-75, 2010.

[246] C. W. Colwell Jr, P. C. Chen, and D. D'Lima, "Extensor malalignment arising from femoral component malrotation in knee arthroplasty: effect of rotating-bearing," (in eng), *Clin Biomech (Bristol, Avon),* vol. 26, no. 1, pp. 52-57, 2011.

[247] W. M. Mihalko, D. J. Conner, R. Benner, and J. L. Williams, "How does TKA kinematics vary with transverse plane alignment changes in a contemporary implant?," *Clin Orthop Relat Res,* vol. 470, no. 1, pp. 186-192, 2012.

[248] S. Okamoto, H. Mizu-Uchi, K. Okazaki, S. Hamai, H. Nakahara, and Y. Iwamoto, "Effect of Tibial Posterior Slope on Knee Kinematics, Quadriceps Force, and Patellofemoral Contact Force After Posterior-Stabilized Total Knee Arthroplasty," *The Journal of Arthroplasty,* vol. 30, pp. 1439-1443, 2015.

[249] S. Nakamura *et al.*, "Superior-inferior position of patellar component affects patellofemoral kinematics and contact forces in computer simulation," *Clinical Biomechanics,* vol. 45, pp. 19-24, 2017.
[250] R. Mootanah *et al.*, "Development and validation of a computational model of the knee joint for the evaluation of surgical treatments for osteoarthritis," *Comput Methods Biomech Biomed Engin,* vol. 17, no. 13, pp. 1502-17, 2014.
[251] J. A. Ewing *et al.*, "Estimating patient-specific soft-tissue properties in a TKA knee," *J Orthop Res,* vol. 34, no. 3, pp. 435-43, Mar 2016.
[252] M. Woiczinski, A. Steinbruck, P. Weber, P. E. Muller, V. Jansson, and C. Schroder, "Development and validation of a weight-bearing finite element model for total knee replacement," *Comput Methods Biomech Biomed Engin,* vol. 19, no. 10, pp. 1033-45, 2016.
[253] V. Vanheule *et al.*, "Evaluation of pre dicte d knee function for component malrotation in total knee arthroplasty," *Medical Engineering and Physics,* vol. 40, pp. 56-64, 2017.
[254] B. J. Fregly *et al.*, "Grand challenge competition to predict in vivo knee loads," (in eng), *J Orthop Res,* vol. 30, no. 4, pp. 503-513, 2012.
[255] P. Gerus *et al.*, "Subject-specific knee joint geometry improves predictions of medial tibiofemoral contact forces," (in eng), *J Biomech,* vol. 46, no. 16, pp. 2778-86, Nov 15 2013.
[256] S. Kuriyama, M. Ishikawa, S. Nakamura, M. Furu, H. Ito, and S. Matsuda, "Posterior tibial slope and femoral sizing affect posterior cruciate ligament tension in posterior cruciate-retaining total knee arthroplasty," (in eng), *Clin Biomech (Bristol, Avon),* vol. 30, no. 7, pp. 676-81, Aug 2015.
[257] G. Li, J. Gil, A. Kanamori, and S. Woo, "A validated three-dimensional computational model of a human knee joint," *TRANSACTIONS-AMERICAN SOCIETY OF MECHANICAL ENGINEERS JOURNAL OF BIOMECHANICAL ENGINEERING,* vol. 121, no. 6, pp. 657-662, 1999.
[258] L. Blankevoort and R. Huiskes, "Validation of a three-dimensional model of the knee," (in eng), *Journal of Biomechanics,* vol. 29, no. 7, pp. 955-961, 1996.
[259] T. L. Donahue, M. L. Hull, M. M. Rashid, and C. R. Jacobs, "A finite element model of the human knee joint for the study of tibio-femoral contact," (in eng), *J Biomech Eng,* vol. 124, no. 3, pp. 273-280, 2002.
[260] Y. Song, R. E. Debski, V. Musahl, M. Thomas, and S. L. Woo, "A three-dimensional finite element model of the human anterior cruciate ligament: a computational analysis with experimental validation," (in eng), *J Biomech,* vol. 37, no. 3, pp. 383-90, Mar 2004.
[261] M. Ishikawa, S. Kuriyama, H. Ito, M. Furu, S. Nakamura, and S. Matsuda, "Kinematic alignment produces near-normal knee motion but increases contact stress after total knee arthroplasty: A case study on a single implant design," 2015.
[262] J. M. Weiss *et al.*, "What functional activities are important to patients with knee replacements?," *Clinical Orthopaedics and Related Research,* vol. 404, pp. 172-188, 2002.
[263] S. M. Howell, K. Kuznik, M. L. Hull, and R. A. Siston, "Results of an initial experience with custom-fit positioning total knee arthroplasty in a series of 48 patients," *Orthopedics,* vol. 31, no. 9, pp. 857-863, 2008.
[264] R. Padua, E. Ceccarelli, R. Bondi, A. Campi, and L. Padua, "Range of motion correlates with patient perception of TKA outcome," (in eng), *Clin Orthop Relat Res,* vol. 460, pp. 174-7, Jul 2007.
[265] D. M. Fang, M. A. Ritter, and K. E. Davis, "Coronal alignment in total knee arthroplasty: just how important is it?," (in eng), *J Arthroplasty,* vol. 24, no. 6 Suppl, pp. 39-43, Sep 2009.
[266] J. M. Sikorski, "Alignment in total knee replacement," (in eng), *J Bone Joint Surg Br,* vol. 90, no. 9, pp. 1121-7, Sep 2008.
[267] S. Parratte, M. W. Pagnano, R. T. Trousdale, and D. J. Berry, "Effect of postoperative mechanical axis alignment on the fifteen-year survival of modern, cemented total knee replacements," *J Bone Joint Surg Am,* vol. 92, no. 12, pp. 2143-2149, 2010.

[268] S. M. Howell, S. J. Howell, and M. L. Hull, "Assessment of the radii of the medial and lateral femoral condyles in varus and valgus knees with osteoarthritis," (in eng), *J Bone Joint Surg Am,* vol. 92, no. 1, pp. 98-104, Jan 2010.

[269] R. J. D. Howell S M, Hull M L. , "Kinematic Alignment in Total Knee Arthroplasty. Definition,

History, Principle, Surgical Technique, and Results of an Alignment Option for TKA.," *Arthropaedia 2014;1:44-53.,* 2014.

[270] B. A. Klatt, N. Goyal, M. S. Austin, and W. J. Hozack, "Custom-fit total knee arthroplasty (OtisKnee) results in malalignment," *Journal of Arthroplasty,* vol. 23, no. 1, pp. 26-29, 2008.

[271] S. M. Howell, S. Papadopoulos, K. T. Kuznik, and M. L. Hull, "Accurate alignment and high function after kinematically aligned TKA performed with generic instruments," (in eng), *Knee Surg Sports Traumatol Arthrosc,* vol. 21, no. 10, pp. 2271-80, Oct 2013.

[272] T. M. Guess and L. P. Maletsky, "Computational modeling of a dynamic knee simulator for reproduction of knee loading," *J Biomech Eng,* vol. 127, no. 7, pp. 1216-1221, 2005.

[273] J. P. Halloran, A. J. Petrella, and P. J. Rullkoetter, "Explicit finite element modeling of total knee replacement mechanics," *J Biomech,* vol. 38, no. 2, pp. 323-331, 2005.

[274] J. P. Halloran, C. W. Clary, L. P. Maletsky, M. Taylor, A. J. Petrella, and P. J. Rullkoetter, "Verification of Predicted Knee Replacement Kinematics During Simulated Gait in the Kansas Knee Simulator," *Journal of Biomechanical Engineering,* vol. 132, no. 8, pp. 81010-81010, 2010.

[275] C. K. Fitzpatrick, R. D. Komistek, and P. J. Rullkoetter, "Developing simulations to reproduce in vivo fluoroscopy kinematics in total knee replacement patients," *J Biomech,* vol. 47, no. 10, pp. 2398-2405, 2014.

[276] S. Patil, C. W. Colwell Jr, K. A. Ezzet, and D. D. D'Lima, "Can normal knee kinematics be restored with unicompartmental knee replacement?," (in eng), *Journal of Bone and Joint Surgery [Am],* vol. 87, no. 2, pp. 332-338, 2005.

[277] W. a. S. G. Scott, "Insall and Scott Surgery of the Knee: Expert Consult (5th Edition)," *Elsevier Health Sciences,* 2011.

[278] K. H. Bloemker, T. M. Guess, L. Maletsky, and K. Dodd, "Computational knee ligament modeling using experimentally determined zero-load lengths," (in eng), *Open Biomed Eng J,* vol. 6, pp. 33-41, 2012.

[279] C. K. Fitzpatrick and P. J. Rullkoetter, "Estimating total knee replacement joint load ratios from kinematics," (in eng), *J Biomech,* vol. 47, no. 12, pp. 3003-11, Sep 22 2014.

[280] C. K. Fitzpatrick, M. A. Baldwin, C. W. Clary, L. P. Maletsky, and P. J. Rullkoetter, "Evaluating knee replacement mechanics during ADL with PID-controlled dynamic finite element analysis," (in eng), *Comput Methods Biomech Biomed Engin,* vol. 17, no. 4, pp. 360-9, 2014.

[281] D. Nam, K. M. Lin, S. M. Howell, and M. L. Hull, "Femoral bone and cartilage wear is predictable at 0 degrees and 90 degrees in the osteoarthritic knee treated with total knee arthroplasty," (in eng), *Knee Surg Sports Traumatol Arthrosc,* vol. 22, no. 12, pp. 2975-81, Dec 2014.

[282] H. M. Ji, J. Han, D. S. Jin, H. Seo, and Y. Y. Won, "Kinematically aligned TKA can align knee joint line to horizontal," (in eng), *Knee Surg Sports Traumatol Arthrosc,* vol. 24, no. 8, pp. 2436-41, Aug 2016.

[283] K. Kobayashi, M. Sakamoto, A. Hosseini, H. E. Rubash, and G. Li, "In-vivo patellar tendon kinematics during weight-bearing deep knee flexion," (in eng), *J Orthop Res,* vol. 30, no. 10, pp. 1596-603, Oct 2012.

[284] M. Abdel, S. Oussedik, S. Parratte, S. Lustig, and F. Haddad, "Coronal alignment in total knee replacement: historical review, contemporary analysis, and future direction," *Bone Joint J,* vol. 96, no. 7, pp. 857-862, 2014.

[285] A. S. Panni *et al.*, "Tibial internal rotation negatively affects clinical outcomes in total knee arthroplasty: a systematic review," *Knee Surgery, Sports Traumatology, Arthroscopy,* journal article vol. 26, no. 6, pp. 1636-1644, June 01 2018.

[286] Y.-H. Kim, J.-W. Park, J.-S. Kim, and S.-D. Park, "The relationship between the survival of total knee arthroplasty and postoperative coronal, sagittal and rotational alignment of knee prosthesis," *International Orthopaedics,* journal article vol. 38, no. 2, pp. 379-385, February 01 2014.

[287] K. Carroll, A. Patel, A. Carli, M. Cross, S. Jerabek, and D. Mayman, "DOES RESTORATION OF JOINT LINE OBLIQUITY, TIBIAL VARUS, AND CORONAL ALIGNMENT IMPROVE EARLY CLINICAL OUTCOMES IN TKA?," *Bone Joint J,* vol. 98, no. SUPP 9, pp. 27-27, 2016.

[288] J. Henckel *et al.*, "Very low-dose computed tomography for planning and outcome measurement in knee replacement," *Bone & Joint Journal,* vol. 88, no. 11, pp. 1513-1518, 2006.

[289] M. Hirschmann, P. Konala, F. Amsler, F. Iranpour, N. Friederich, and J. Cobb, "The position and orientation of total knee replacement components: a comparison of conventional radiographs, transverse 2D-CT slices and 3D-CT reconstruction," *J Bone Joint Surg Br,* vol. 93, no. 5, pp. 629-633, 2011.

[290] J. Bellemans, S. Banks, J. Victor, H. Vandenneucker, and A. Moemans, "Fluoroscopic analysis of the kinematics of deep flexion in total knee arthroplasty. Influence of posterior condylar offset," (in eng), *Journal of Bone and Joint Surgery [Br],* vol. 84, no. 1, pp. 50-53, 2002.

[291] A. Malviya, E. Lingard, D. Weir, and D. Deehan, "Predicting range of movement after knee replacement: the importance of posterior condylar offset and tibial slope," *Knee Surgery, Sports Traumatology, Arthroscopy,* vol. 17, no. 5, pp. 491-498, 2009.

[292] N. Clement, D. MacDonald, D. Hamilton, and R. Burnett, "Posterior condylar offset is an independent predictor of functional outcome after revision total knee arthroplasty," *Bone & joint research,* vol. 6, no. 3, pp. 172-178, 2017.

[293] J. W. Martin and L. A. Whiteside, "The influence of joint line position on knee stability after condylar knee arthroplasty," *Clinical orthopaedics and related research,* no. 259, pp. 146-156, 1990.

[294] P. F. Partington, J. Sawhney, C. H. Rorabeck, R. L. Barrack, and J. Moore, "Joint line restoration after revision total knee arthroplasty," *Clinical orthopaedics and related research,* no. 367, pp. 165-171, 1999.

[295] B. C. Bengs and R. D. Scott, "The effect of patellar thickness on intraoperative knee flexion and patellar tracking in total knee arthroplasty," *The Journal of arthroplasty,* vol. 21, no. 5, pp. 650-655, 2006.

[296] T. L. Petersen and G. A. Engh, "Radiographic assessment of knee alignment after total knee arthroplasty," *The Journal of arthroplasty,* vol. 3, no. 1, pp. 67-72, 1988.

[297] J. Petterwood, M. M. Dowsey, D. Rodda, and P. F. Choong, "The immediate post-operative radiograph is an unreliable measure of coronal plane alignment in total knee replacement," *Frontiers in surgery,* vol. 1, 2014.

[298] A. Park, J. B. Stambough, R. M. Nunley, R. L. Barrack, and D. Nam, "The inadequacy of short knee radiographs in evaluating coronal alignment after total knee arthroplasty," *The Journal of arthroplasty,* vol. 31, no. 4, pp. 878-882, 2016.

[299] T. Holme, J. Henckel, J. Cobb, and A. Hart, "Quantification of the difference between 3D CT and plain radiograph for measurement of the position of medial unicompartmental knee replacements," *The Knee,* vol. 18, no. 5, pp. 300-305, 2011.

[300] S. Chauhan, G. Clark, S. Lloyd, R. Scott, W. Breidahl, and J. Sikorski, "Computer-assisted total knee replacement a controlled cadaver study using a multi-parameter quantitative CT assessment of alignment (The Perth CT Protocol)," *Journal of Bone & Joint Surgery, British Volume,* vol. 86, no. 6, pp. 818-823, 2004.

[301] L. M. Jazrawi, L. Birdzell, F. J. Kummer, and P. E. Di Cesare, "The accuracy of computed tomography for determining femoral and tibial total knee arthroplasty component rotation," *The Journal of arthroplasty,* vol. 15, no. 6, pp. 761-766, 2000.

[302] G. Matziolis, D. Krocker, U. Weiss, S. Tohtz, and C. Perka, "A prospective, randomized study of computer-assisted and conventional total knee arthroplasty: three-dimensional evaluation of implant alignment and rotation," *JBJS,* vol. 89, no. 2, pp. 236-243, 2007.

[303] H. Mizu-Uchi, S. Matsuda, H. Miura, K. Okazaki, Y. Akasaki, and Y. Iwamoto, "The evaluation of post-operative alignment in total knee replacement using a CT-based navigation system," *Bone & Joint Journal,* vol. 90, no. 8, pp. 1025-1031, 2008.

[304] B. Konigsberg, R. Hess, C. Hartman, L. Smith, and K. L. Garvin, "Inter-and intraobserver reliability of two-dimensional CT scan for total knee arthroplasty component malrotation," *Clinical Orthopaedics and Related Research®,* vol. 472, no. 1, pp. 212-217, 2014.

[305] J. Victor, D. Van Doninck, L. Labey, B. Innocenti, P. M. Parizel, and J. Bellemans, "How precise can bony landmarks be determined on a CT scan of the knee?," *The Knee,* vol. 16, no. 5, pp. 358-65, 2009.

[306] J. G. Twiggs *et al.*, "Patient Variation Limits Use of Fixed References for Femoral Rotation Component Alignment in Total Knee Arthroplasty," *Journal of Arthroplasty,* vol. 33, no. 1, pp. 67-74, 2018.

[307] N. Saltybaeva, M. E. Jafari, M. Hupfer, and W. A. Kalender, "Estimates of effective dose for CT scans of the lower extremities," *Radiology,* vol. 273, no. 1, pp. 153-159, 2014.

[308] S. Walter, M. Eliasziw, and A. Donner, "Sample size and optimal designs for reliability studies," *Statistics in medicine,* vol. 17, no. 1, pp. 101-110, 1998.

[309] L. G. Portney and M. P. Watkins, *Foundations of clinical research: applications to practice*. Prentice Hall, 2000.

[310] R. B. Abu-Rajab, A. H. Deakin, M. Kandasami, J. McGlynn, F. Picard, and A. W. Kinninmonth, "Hip–Knee–Ankle Radiographs Are More Appropriate for Assessment of Post-Operative Mechanical Alignment of Total Knee Arthroplasties than Standard AP Knee Radiographs," *The Journal of arthroplasty,* vol. 30, no. 4, pp. 695-700, 2015.

[311] M. T. Hirschmann *et al.*, "A novel standardized algorithm for evaluating patients with painful total knee arthroplasty using combined single photon emission tomography and conventional computerized tomography," *Knee surgery, sports traumatology, arthroscopy,* vol. 18, no. 7, pp. 939-944, 2010.

[312] L. Hu, X. Xu, L. Wang, N. Guo, and F. Xie, "3D registration method based on scattered point cloud from B-model ultrasound image," in *International Conference on Innovative Optical Health Science*, 2017, vol. 10245, p. 102450C: International Society for Optics and Photonics.

[313] Y. Kim, K.-I. Kim, J. hyeok Choi, and K. Lee, "Novel methods for 3D postoperative analysis of total knee arthroplasty using 2D–3D image registration," *Clinical Biomechanics,* vol. 26, no. 4, pp. 384-391, 2011.

[314] T. J. Heyse, J. B. Stiehl, and C. O. Tibesku, "Measuring tibial component rotation of TKA in MRI: what is reproducible?," *The Knee,* vol. 22, no. 6, pp. 604-608, 2015.

[315] R. A. Siston, S. B. Goodman, J. J. Patel, S. L. Delp, and N. J. Giori, "The high variability of tibial rotational alignment in total knee arthroplasty," *Clinical Orthopaedics and Related Research,* no. 452, pp. 65-69, 2006.

[316] W. Wang, B. Yue, J. Wang, H. Bedair, H. Rubash, and G. Li, "Posterior Condyle Offset and Maximum Knee Flexion Following a Cruciate Retaining Total Knee Arthroplasty," *The journal of knee surgery,* 2018.

[317] R. M. Degen, J. Matz, M. G. Teeter, B. A. Lanting, J. L. Howard, and R. W. McCalden, "Does Posterior Condylar Offset Affect Clinical Results following Total Knee Arthroplasty?," *The journal of knee surgery,* 2017.

[318] A. van Houten, N. Kosse, M. Wessels, and A. Wymenga, "Measurement techniques to determine tibial rotation after total knee arthroplasty are less accurate than we think," *The Knee,* 2018.

[319] K. P. Valkering, S. J. Breugem, M. P. Van den Bekerom, W. E. Tuinebreijer, and R. C. van Geenen, "Effect of rotational alignment on outcome of total knee arthroplasty: A systematic

review of the literature and correlation analysis," *Acta orthopaedica,* vol. 86, no. 4, pp. 432-439, 2015.
[320] P.-J. Vandekerckhove, B. Lanting, J. Bellemans, J. Victor, and S. MacDonald, "The current role of coronal plane alignment in total knee arthroplasty in a preoperative varus aligned population: an evidence based review," *Acta Orthop Belg,* vol. 82, no. 1, pp. 129-142, 2016.
[321] H. Rasch, A. L. Falkowski, F. Forrer, J. Henckel, and M. T. Hirschmann, "4D-SPECT/CT in orthopaedics: a new method of combined quantitative volumetric 3D analysis of SPECT/CT tracer uptake and component position measurements in patients after total knee arthroplasty," *Skeletal radiology,* vol. 42, no. 9, pp. 1215-1223, 2013.
[322] A. Zeighami *et al.*, "Tibio-femoral joint contact in healthy and osteoarthritic knees during quasi-static squat: A bi-planar X-ray analysis," *Journal of biomechanics,* vol. 53, pp. 178-184, 2017.
[323] J. M. Scarvell, M. R. Pickering, and P. N. Smith, "New registration algorithm for determining 3D knee kinematics using CT and single-plane fluoroscopy with improved out-of-plane translation accuracy," *Journal of Orthopaedic Research,* vol. 28, no. 3, pp. 334-340, 2010.
[324] E. C. Rodriguez-Merchan, "Patient dissatisfaction after total knee arthroplasty for advanced painful osteoarthritis of the knee," *International Journal of Orthopaedics,* vol. 3, no. 2, pp. 519-524, 2016.
[325] R. B. Bourne, B. M. Chesworth, A. M. Davis, N. N. Mahomed, and K. D. Charron, "Patient satisfaction after total knee arthroplasty: who is satisfied and who is not?," *Clinical Orthopaedics and Related Research®,* vol. 468, no. 1, pp. 57-63, 2010.
[326] M. K. Harman, S. A. Banks, S. Kirschner, and J. Lützner, "Prosthesis alignment affects axial rotation motion after total knee replacement: a prospective in vivo study combining computed tomography and fluoroscopic evaluations," *BMC musculoskeletal disorders,* vol. 13, no. 1, p. 206, 2012.
[327] B. C. Carr and T. Goswami, "Knee implants–Review of models and biomechanics," *Materials & Design,* vol. 30, no. 2, pp. 398-413, 2009.
[328] F. W. Werner, D. C. Ayers, L. P. Maletsky, and P. J. Rullkoetter, "The effect of valgus/varus malalignment on load distribution in total knee replacements," *Journal of biomechanics,* vol. 38, no. 2, pp. 349-355, 2005.
[329] J. Bellemans, S. Banks, J. Victor, H. Vandenneucker, and A. Moemans, "Fluoroscopic analysis of the kinematics of deep flexion in total knee arthroplasty: influence of posterior condylar offset," *The Journal of bone and joint surgery. British volume,* vol. 84, no. 1, pp. 50-53, 2002.
[330] E. E. Hutter, J. F. Granger, M. D. Beal, and R. A. Siston, "Is there a gold standard for TKA tibial component rotational alignment?," *Clinical Orthopaedics and Related Research®,* vol. 471, no. 5, pp. 1646-1653, 2013.
[331] M. Dunbar, G. Richardson, and O. Robertsson, "I can't get no satisfaction after my total knee replacement," *Bone Joint J,* vol. 95, no. 11 Supple A, pp. 148-152, 2013.
[332] H. D. Clarke and J. G. Hentz, "Restoration of femoral anatomy in TKA with unisex and gender-specific components," *Clinical orthopaedics and related research,* vol. 466, no. 11, pp. 2711-2716, 2008.
[333] S. Shalhoub, F. Fitzwater, M. Dickinson, C. Clary, and L. Maletsky, "QUANTIFYING THE CHANGE IN TIBIOFEMORAL KINEMATICS BETWEEN PRIMARY AND REVISION TOTAL KNEE ARTHROPLASTY INSERTS," *Bone Joint J,* vol. 99, no. SUPP 5, pp. 145-145, 2017.
[334] B. M. Hillberry, "Simulating dynamic activities using a five-axis knee simulator," 2005.
[335] K. M. Varadarajan, R. E. Harry, T. Johnson, and G. Li, "Can in vitro systems capture the characteristic differences between the flexion–extension kinematics of the healthy and TKA knee?," *Medical engineering & physics,* vol. 31, no. 8, pp. 899-906, 2009.
[336] S. Patil, A. Bunn, W. D. Bugbee, C. W. Colwell, and D. D. D'Lima, "Patient-specific implants with custom cutting blocks better approximate natural knee kinematics than standard TKA without custom cutting blocks," *The Knee,* vol. 22, pp. 624-629, 2015.

[337] S. Nakamura, H. Ito, H. Yoshitomi, S. Kuriyama, R. D. Komistek, and S. Matsuda, "Analysis of the flexion gap on in vivo knee kinematics using fluoroscopy," *The Journal of arthroplasty,* vol. 30, no. 7, pp. 1237-1242, 2015.

[338] R. D. Komistek, T. R. Kane, M. Mahfouz, J. A. Ochoa, and D. A. Dennis, "Knee mechanics: a review of past and present techniques to determine in vivo loads," *Journal of biomechanics,* vol. 38, no. 2, pp. 215-228, 2005.

[339] H. Haider, P. Walker, J. DesJardins, and G. Blunn, "Effects of patient and surgical alignment variables on kinematics in TKR simulation under force-control," in *Wear of Articulating Surfaces: Understanding Joint Simulation*: ASTM International, 2006.

[340] S. Kuriyama, M. Ishikawa, S. Nakamura, M. Furu, H. Ito, and S. Matsuda, "No condylar lift-off occurs because of excessive lateral soft tissue laxity in neutrally aligned total knee arthroplasty: a computer simulation study," *Knee Surgery, Sports Traumatology, Arthroscopy,* vol. 24, no. 8, pp. 2517-2524, 2016.

[341] M. A. Baldwin, C. Clary, L. P. Maletsky, and P. J. Rullkoetter, "Verification of predicted specimen-specific natural and implanted patellofemoral kinematics during simulated deep knee bend," *Journal of Biomechanics,* vol. 42, no. 14, pp. 2341-2348, 2009.

[342] M. Kia *et al.*, "A Multibody Knee Model Corroborates Subject-Specific Experimental Measurements of Low Ligament Forces and Kinematic Coupling During Passive Flexion," *Journal of biomechanical engineering,* vol. 138, no. 5, p. 051010, 2016.

[343] V. Vanheule *et al.*, "Evaluation of predicted knee function for component malrotation in total knee arthroplasty," *Medical engineering & physics,* vol. 40, pp. 56-64, 2017.

[344] FDA, "Stryker Navigation Regulatory Approvals," FDAOct, 2016.

[345] W. Theodore *et al.*, "Variability in static alignment and kinematics for kinematically aligned TKA," (in eng), *Knee,* vol. 24, no. 4, pp. 733-744, Aug 2017.

[346] S. J. Piazza and S. L. Delp, "Three-dimensional dynamic simulation of total knee replacement motion during a step-up task," *Journal of biomechanical engineering,* vol. 123, no. 6, pp. 599-606, 2001.

[347] E. S. Grood and W. J. Suntay, "A joint coordinate system for the clinical description of three-dimensional motions: application to the knee," *Journal of biomechanical engineering,* vol. 105, p. 136, 1983.

[348] T. Bonner, W. Eardley, P. Patterson, and P. Gregg, "The effect of post-operative mechanical axis alignment on the survival of primary total knee replacements after a follow-up of 15 years," *The Journal of bone and joint surgery. British volume,* vol. 93, no. 9, pp. 1217-1222, 2011.

[349] C. K. Fitzpatrick, C. Maag, C. W. Clary, A. Metcalfe, J. Langhorn, and P. J. Rullkoetter, "Validation of a new computational 6-DOF knee simulator during dynamic activities," *J Biomech,* vol. 49, no. 14, pp. 3177-3184, Oct 03 2016.

[350] S. Pianigiani, D. Croce, M. D'Aiuto, W. Pascale, and B. Innocenti, "Sensitivity analysis of the material properties of different soft-tissues: implications for a subject-specific knee arthroplasty," (in eng), *Muscles Ligaments Tendons J,* vol. 7, no. 4, pp. 546-557, Oct-Dec 2017.

[351] K.-T. Kang, S.-H. Kim, J. Son, Y. H. Lee, and H.-J. Chun, "Computational model-based probabilistic analysis of in vivo material properties for ligament stiffness using the laxity test and computed tomography," *Journal of Materials Science: Materials in Medicine,* vol. 27, no. 12, p. 183, 2016.

[352] K.-T. Kang, S.-H. Kim, J. Son, Y. H. Lee, and Y.-G. Koh, "Validation of a computational knee joint model using an alignment method for the knee laxity test and computed tomography," *Bio-medical materials and engineering,* vol. 28, no. 4, pp. 417-429, 2017.

[353] R. E. Carey, L. Zheng, A. K. Aiyangar, C. D. Harner, and X. Zhang, "Subject-specific finite element modeling of the tibiofemoral joint based on CT, magnetic resonance imaging and dynamic stereo-radiography data in vivo," (in eng), *J Biomech Eng,* vol. 136, no. 4, Apr 2014.

[354] L. Bertozzi, R. Stagni, S. Fantozzi, and A. Cappello, "Knee model sensitivity to cruciate ligaments parameters: a stability simulation study for a living subject," *J Biomech,* vol. 40 Suppl 1, pp. S38-44, 2007.

[355] M. Kia *et al.*, "A Multibody Knee Model Corroborates Subject-Specific Experimental Measurements of Low Ligament Forces and Kinematic Coupling During Passive Flexion," (in eng), *J Biomech Eng,* vol. 138, no. 5, p. 051010, May 2016.

[356] C. R. Smith, M. F. Vignos, R. L. Lenhart, J. Kaiser, and D. G. Thelen, "The Influence of Component Alignment and Ligament Properties on Tibiofemoral Contact Forces in Total Knee Replacement," (in eng), *J Biomech Eng,* vol. 138, no. 2, p. 021017, Feb 2016.

[357] A. A. Ali *et al.*, "Validation of predicted patellofemoral mechanics in a finite element model of the healthy and cruciate-deficient knee," (in eng), *J Biomech,* vol. 49, no. 2, pp. 302-9, Jan 25 2016.

[358] Y. Matsuda, Y. Ishii, H. Noguchi, and R. Ishii, "Varus-valgus balance and range of movement after total knee arthroplasty," (in eng), *J Bone Joint Surg Br,* vol. 87, no. 6, pp. 804-8, Jun 2005.

[359] H. Sekiya, K. Takatoku, H. Takada, H. Sasanuma, and N. Sugimoto, "Postoperative lateral ligamentous laxity diminishes with time after TKA in the varus knee," (in eng), *Clin Orthop Relat Res,* vol. 467, no. 6, pp. 1582-6, Jun 2009.

[360] T. Tsukeoka and Y. Tsuneizumi, "Varus and valgus stress tests after total knee arthroplasty with and without anesthesia," (in eng), *Arch Orthop Trauma Surg,* vol. 136, no. 3, pp. 407-11, Mar 2016.

[361] J. C. Kupper, B. Loitz-Ramage, D. T. Corr, D. A. Hart, and J. L. Ronsky, "Measuring knee joint laxity: a review of applicable models and the need for new approaches to minimize variability," *Clin Biomech (Bristol, Avon),* vol. 22, no. 1, pp. 1-13, 2007.

[362] E. W. James, B. T. Williams, and R. F. LaPrade, "Stress radiography for the diagnosis of knee ligament injuries: a systematic review," (in eng), *Clin Orthop Relat Res,* vol. 472, no. 9, pp. 2644-57, Sep 2014.

[363] K. Jacobsen, "Stress radiographical measurement of the anteroposterior, medial and lateral stability of the knee joint," (in eng), *Acta Orthop Scand,* vol. 47, no. 3, pp. 335-4, Jun 1976.

[364] T. Jackman, R. F. LaPrade, T. Pontinen, and P. A. Lender, "Intraobserver and interobserver reliability of the kneeling technique of stress radiography for the evaluation of posterior knee laxity," (in eng), *Am J Sports Med,* vol. 36, no. 8, pp. 1571-6, Aug 2008.

[365] K. Okazaki *et al.*, "Asymmetry of mediolateral laxity of the normal knee," (in eng), *J Orthop Sci,* vol. 11, no. 3, pp. 264-6, May 2006.

[366] Y. Ishii, H. Noguchi, Y. Matsuda, H. Kiga, M. Takeda, and S. Toyabe, "Preoperative laxity in osteoarthritis patients undergoing total knee arthroplasty," (in eng), *Int Orthop,* vol. 33, no. 1, pp. 105-9, Feb 2009.

[367] M. S. Schulz, K. Russe, G. Lampakis, and M. J. Strobel, "Reliability of stress radiography for evaluation of posterior knee laxity," (in eng), *Am J Sports Med,* vol. 33, no. 4, pp. 502-6, Apr 2005.

[368] M. T. Hirschmann and W. Muller, "Complex function of the knee joint: the current understanding of the knee," (in eng), *Knee Surg Sports Traumatol Arthrosc,* vol. 23, no. 10, pp. 2780-8, Oct 2015.

[369] P. Markelj, D. Tomazevic, B. Likar, and F. Pernus, "A review of 3D/2D registration methods for image-guided interventions," *Med Image Anal,* vol. 16, no. 3, pp. 642-661, 2012.

[370] M. N. Haque, M. R. Pickering, A. Al Muhit, M. R. Frater, J. M. Scarvell, and P. N. Smith, "A fast and robust technique for 3D–2D registration of CT to single plane X-ray fluoroscopy," *Computer Methods in Biomechanics and Biomedical Engineering: Imaging & Visualization,* vol. 2, no. 2, pp. 76-89, 2014/04/03 2014.

[371] K. Matsuki, K. O. Matsuki, T. Kenmoku, S. Yamaguchi, T. Sasho, and S. A. Banks, "In vivo kinematics of early-stage osteoarthritic knees during pivot and squat activities," (in eng), *Gait Posture,* vol. 58, pp. 214-219, Oct 2017.

[372] R. D. Komistek, D. A. Dennis, and M. Mahfouz, "In vivo fluoroscopic analysis of the normal human knee," (in eng), *Clinical Orthopaedics and Related Research,* no. 410, pp. 69-81, 2003.
[373] T. A. Moro-oka *et al.*, "Dynamic activity dependence of in vivo normal knee kinematics," (in eng), *J Orthop Res,* vol. 26, no. 4, pp. 428-434, 2008.
[374] S. A. Banks and W. A. Hodge, "Accurate measurement of three-dimensional knee replacement kinematics using single-plane fluoroscopy," (in eng), *IEEE Trans Biomed Eng,* vol. 43, no. 6, pp. 638-49, Jun 1996.
[375] M. R. Mahfouz, W. A. Hoff, R. D. Komistek, and D. A. Dennis, "A robust method for registration of three-dimensional knee implant models to two-dimensional fluoroscopy images," (in eng), *IEEE Trans Med Imaging,* vol. 22, no. 12, pp. 1561-1574, 2003.
[376] S. Yamaguchi, K. Gamada, T. Sasho, H. Kato, M. Sonoda, and S. A. Banks, "In vivo kinematics of anterior cruciate ligament deficient knees during pivot and squat activities," (in Eng), *Clin Biomech (Bristol, Avon),* 2008.
[377] "<grood and suntay 1983 - A joint coordinate system for the clinical description of three dimensional motions.pdf>."
[378] P. SA, "ART KNEE Software - Instructions for Use," OmniLifeScience2014.
[379] G. M. Freisinger, L. C. Schmitt, A. B. Wanamaker, R. A. Siston, and A. M. W. Chaudhari, "Tibiofemoral Osteoarthritis and Varus-Valgus Laxity," (in eng), *J Knee Surg,* vol. 30, no. 5, pp. 440-451, Jun 2017.
[380] M. W. Creaby *et al.*, "Varus-valgus laxity and passive stiffness in medial knee osteoarthritis," (in eng), *Arthritis Care Res (Hoboken),* vol. 62, no. 9, pp. 1237-43, Sep 2010.
[381] L. Sharma *et al.*, "Laxity in healthy and osteoarthritic knees," (in eng), *Arthritis Rheum,* vol. 42, no. 5, pp. 861-70, May 1999.
[382] L. Q. Zhang, D. Xu, G. Wang, and R. W. Hendrix, "Muscle strength in knee varus and valgus," (in eng), *Med Sci Sports Exerc,* vol. 33, no. 7, pp. 1194-9, Jul 2001.
[383] F. M. Griffin, J. N. Insall, and G. R. Scuderi, "Accuracy of soft tissue balancing in total knee arthroplasty," (in eng), *J Arthroplasty,* vol. 15, no. 8, pp. 970-3, Dec 2000.
[384] B. P. Gladnick *et al.*, "Primary and coupled motions of the native knee in response to applied varus and valgus load," (in eng), *Knee,* vol. 23, no. 3, pp. 387-92, Jun 2016.
[385] T. Kobayashi, M. Suzuki, T. Sasho, K. Nakagawa, Y. Tsuneizumi, and K. Takahashi, "Lateral laxity in flexion increases the postoperative flexion angle in cruciate-retaining total knee arthroplasty," (in eng), *J Arthroplasty,* vol. 27, no. 2, pp. 260-5, Feb 2012.
[386] T. A. Moro-oka *et al.*, "Can magnetic resonance imaging-derived bone models be used for accurate motion measurement with single-plane three-dimensional shape registration?," (in eng), *J Orthop Res,* vol. 25, no. 7, pp. 867-72, Jul 2007.
[387] M. D. Harris *et al.*, "A Combined Experimental and Computational Approach to Subject-Specific Analysis of Knee Joint Laxity," *Journal of Biomechanical Engineering,* vol. 138, no. 8, pp. 081004-081004, 2016.
[388] J. D. Roth, S. M. Howell, and M. L. Hull, "Native knee laxities at 0, 45, and 90 of flexion and their relationship to the goal of the gap-balancing alignment method of total knee arthroplasty," *JBJS,* vol. 97, no. 20, pp. 1678-1684, 2015.
[389] J. M. Dorlot, M. Ait Ba Sidi, G. M. Tremblay, and G. Drouin, "Load elongation behavior of the canine anterior cruciate ligament," (in eng), *J Biomech Eng,* vol. 102, no. 3, p. 190, Aug 1980.
[390] J. Bellemans, H. Vandenneucker, J. Vanlauwe, and J. Victor, "The influence of coronal plane deformity on mediolateral ligament status: an observational study in varus knees," (in eng), *Knee Surg Sports Traumatol Arthrosc,* vol. 18, no. 2, pp. 152-6, Feb 2010.
[391] W. L.A., "TECHNIQUES FOR MANAGING FLEXION CONTRACTURES," *Orthopaedic Proceedings,* vol. 100-B, no. SUPP_10, pp. 128-128, 2018.
[392] K. Wong, G. Trudel, and O. Laneuville, "Noninflammatory Joint Contractures Arising from Immobility: Animal Models to Future Treatments," *BioMed Research International,* vol. 2015, p. 6, 2015, Art. no. 848290.

[393] K. M. Quapp and J. A. Weiss, "Material characterization of human medial collateral ligament," (in eng), *J Biomech Eng,* vol. 120, no. 6, pp. 757-63, Dec 1998.
[394] E. A. Morra, Rosca, M., Greenwald, J., Greenwald, A. S., "The Influence of Contemporary Knee Design on High Flexion II: A Kinematic Comparison with the Normal Knee," presented at the Orthopaedic Research Laboratories, 2009.
[395] A. Zavatsky, "A kinematic-freedom analysis of a flexed-knee-stance testing rig," *Journal of biomechanics,* vol. 30, no. 3, pp. 277-280, 1997.
[396] D. D. D'Lima, M. Trice, A. G. Urquhart, and C. W. Colwell Jr, "Comparison between the kinematics of fixed and rotating bearing knee prostheses," (in eng), *Clin Orthop Relat Res,* no. 380, pp. 151-157, 2000.
[397] K. T. Kang, S. H. Kim, J. Son, Y. H. Lee, and H. J. Chun, "Probabilistic Approach for Determining the Material Properties of Meniscal Attachments In Vivo Using Magnetic Resonance Imaging and a Finite Element Model," (in eng), *J Comput Biol,* vol. 22, no. 12, pp. 1097-107, Dec 2015.
[398] N. A. Morton, L. P. Maletsky, S. Pal, and P. J. Laz, "Effect of variability in anatomical landmark location on knee kinematic description," *J Orthop Res,* vol. 25, no. 9, pp. 1221-1230, 2007.
[399] P. N. Baker, S. Rushton, S. S. Jameson, M. Reed, P. Gregg, and D. J. Deechan, "Patient satisfaction with total knee replacement cannot be predicted from pre-operative variables alone," *The Bone and Joint Journal,* vol. 95, no. B, pp. 1359-65, 2013.
[400] P. C. Noble, M. A. Conditt, K. F. Cook, and K. B. Mathis, "The John Insall Award: Patient expectations affect satisfaction with total knee arthroplasty," *Clinical Orthopaedics and Related Research (1976-2007),* vol. 452, pp. 35-43, 2006.
[401] C. E. Scott, K. E. Bugler, N. D. Clement, D. MacDonald, C. R. Howie, and L. C. Biant, "Patient expectations of arthroplasty of the hip and knee," (in eng), *J Bone Joint Surg Br,* vol. 94, no. 7, pp. 974-81, Jul 2012.
[402] P. F. M. C. Michelle M. Dowsey, "Predictors of Pain and Function Following Total Joint Replacement, Arthroplasty," Available: https://www.intechopen.com/books/arthroplasty-update/predictors-of-pain-and-function-following-total-joint-replacement
[403] Y. Jiang, M. T. Sanchez-Santos, A. D. Judge, D. W. Murray, and N. K. Arden, "Predictors of Patient-Reported Pain and Functional Outcomes Over 10 Years After Primary Total Knee Arthroplasty: A Prospective Cohort Study," (in eng), *J Arthroplasty,* vol. 32, no. 1, pp. 92-100.e2, Jan 2017.
[404] C. E. Scott, C. R. Howie, D. MacDonald, and L. C. Biant, "Predicting dissatisfaction following total knee replacement: a prospective study of 1217 patients," (in eng), *J Bone Joint Surg Br,* vol. 92, no. 9, pp. 1253-8, Sep 2010.
[405] D. F. Hamilton *et al.*, "What determines patient satisfaction with surgery? A prospective cohort study of 4709 patients following total joint replacement," (in eng), *BMJ Open,* vol. 3, no. 4, 2013.
[406] S. Van Onsem, C. Van Der Straeten, N. Arnout, P. Deprez, G. Van Damme, and J. Victor, "A New Prediction Model for Patient Satisfaction After Total Knee Arthroplasty," (in eng), *J Arthroplasty,* vol. 31, no. 12, pp. 2660-2667.e1, Dec 2016.
[407] J. Blackburn, A. Qureshi, R. Amirfeyz, and G. Bannister, "Does preoperative anxiety and depression predict satisfaction after total knee replacement?," (in eng), *Knee,* vol. 19, no. 5, pp. 522-4, Oct 2012.
[408] T. Barlow, M. Dunbar, A. Sprowson, N. Parsons, and D. Griffin, "Development of an outcome prediction tool for patients considering a total knee replacement--the Knee Outcome Prediction Study (KOPS)," (in eng), *BMC Musculoskelet Disord,* vol. 15, p. 451, Dec 23 2014.
[409] E. Lungu, F. Desmeules, C. E. Dionne, É. L. Belzile, and P.-A. Vendittoli, "Prediction of poor outcomes six months following total knee arthroplasty in patients awaiting surgery," *BMC Musculoskeletal Disorders,* journal article vol. 15, no. 1, p. 299, September 08 2014.

[410] C. a. HHS, "NHE Fact Sheet," Center for Medicare & Medicaid Services2019, Available: https://www.cms.gov/research-statistics-data-and-systems/statistics-trends-and-reports/nationalhealthexpenddata/nhe-fact-sheet.html, Accessed on: Mar-2019.
[411] M. o. H.-P. D. MP, "Rising cost of Good Health," ed, 2014.
[412] OECD. (2018, March). *Health Spending*. Available: https://data.oecd.org/healthres/health-spending.htm
[413] A. I. o. H. a. Welfare, "Health Expenditure Australia 2015-16," 2017, Available: https://www.aihw.gov.au/getmedia/3a34cf2c-c715-43a8-be44-0cf53349fd9d/20592.pdf.aspx?inline=true.
[414] S. Pianigiani, L. Labey, W. Pascale, and B. Innocenti, "Knee kinetics and kinematics: What are the effects of TKA malconfigurations?," (in eng), *Knee Surg Sports Traumatol Arthrosc,* vol. 24, no. 8, pp. 2415-21, Aug 2016.
[415] R. C. Q. S. C. M. G. T. N. J. L. W. Theodore, "Reducing Kinematic Data Uncertainty During Mechanical Testing of Orthopaedic Implants: The Benefits and Pitfalls of Auxiliary Motion Capture Systems," in *Orthopaedic Research Society*, Austin, Texas, 2019.
[416] I.-I. M. D. R. Forum. (2019, March). *Medical device single audit program (MDSAP)*. Available: http://www.imdrf.org/workitems/wi-mdsap.asp
[417] ASME. (2019, March). *V&V 40 Verification and Validation in Computational Modelling of Medical Devices*. Available: https://cstools.asme.org/csconnect/CommitteePages.cfm?Committee=100108782
[418] Emergo. (2019, March). *MEDDEV 2.7.1 rev 4 and Clinical Evaluation Reports (CER) for Medical Devices*. Available: https://www.emergobyul.com/services/europe/clinical-evaluation-report